School of Earth and Planetary Sciences

Tectonostratigraphic Evolution of the Roebuck Basin and the northeast area of the Northern Carnarvon Basin, North West Shelf, Australia

Peng Chen

This thesis is presented for the Degree of

Doctor of Philosophy

of

Curtin University

September 2018

Declaration

To the best of my knowledge and belief this thesis contains no material previously published by any other person except where due acknowledgement has been made.

This thesis contains no material which has been accepted for the award of any other degree or diploma in any university.

Signature: 

Data: 18/09/2018

ABSTRACT

The Roebuck Basin and the northeast area of the Northern Carnarvon Basin remain the least explored and poorest understood area of the North West Shelf of Australia. This is due to the long standing perception of low prospectivity and the lack of data and research. Recently released high quality seismic data sets provide a good opportunity to reveal the tectonostratigraphic history of the area.

Detailed structural analysis suggests that the area was influenced by both northwest- and northeast- trending Palaeozoic structures, which are respectively related to the northwest-trending Devonian-Permian rift system and the northeast- to north- trending Carboniferous-Permian rift system. In the latest Permian, the study area experienced a period of uplift, erosion and volcanism, which led to the formation of the Bedout High and a prominent angular unconformity.

In the Triassic, several tectonic events took place, forming several types of structures. From older to younger, they include the development of lava-fed deltas, the formation of a bowl-shaped structure (a potential caldera), the development of a large population of northeast- and west-northwest- trending extensional faults and a period of differential uplift and erosion in the Norian.

The Early Jurassic is interpreted to be the rift initiation phase which led to the final India-Australia breakup. A large population of small and segmented faults were developed. They display two major strike components, north- and northwest- trending, which respectively reflect the extension direction of the Greater Indian rifting (east-directed) and the control of the underlying northwest- trending Palaeozoic structural fabrics associated with the Canning Basin. Simultaneously, northwest- trending linear uplift and erosion and a broad northwest-trending arch were formed, and are also attributable to the pre-existing northwest- trending structures. The rift initiation phase was followed by a period of tectonic quiescence in the Middle Jurassic.

The Late Jurassic-Early Cretaceous saw the climax of the rifting in the area, associated with the breakup of the Gondwanaland. The tectonic events that exerted influences in the area are mainly the drift of Argoland in the Oxfordian (northwest- directed, relative to present-day north) and the Greater India-Australia breakup in the Valanginian (east- directed). The extension associated with the two events, under the influences of the pre-existing structures, especially the large Palaeozoic rift structures, generated a complex extensional fault architecture, which consists of northeast-, north- and northwest trending faults. For each of strikes, a proportion terminate upward at the Oxfordian Unconformity, suggesting an Oxfordian age, while the rest sustained activities from the Oxfordian to the Valanginian. This

suggests the strong interaction between the extensions related to the two continental breakup events. In addition, several dome structures were formed simultaneously, and add more complexities to the rift processes.

Detailed seismic facies, 3D stratigraphic architecture and geomorphologic analyses were conducted for the Jurassic sedimentary succession, which resulted in the identification a large fluviodeltaic-related system. This depositional system consists of a tens of kilometres wide fluviodeltaic plain. Sediment input from a fluviodeltaic system formed a northwesterly progradational shelf-slope-basin clinoformal system. The early-stage deposition of this system was influenced by the rift initiation.

Several types of depositional elements were developed in association with this fluviodeltaic-related system, including fluvial channel belts, delta-scale subaqueous clinoforms, submarine channels and their associated gravity flow deposits, sands/mud filled slope gullies, and slump complexes.

The deposition of the fluviodeltaic-related system was terminated by rift tectonics during the Oxfordian-Valanginian. In the uplifted area, the upper part of the fluviodeltaic-related succession was significantly eroded, forming a peneplaned unconformity. The eroded sediments were transported through large submarine canyons and re-deposited in the adjacent marine-shale dominated grabens, forming gravity flow deposits.

ACKNOWLEDGEMENTS

The author thanks Geoscience Australia, CNOOC Australia and Quadrant Energy for providing the seismic data used in this study. China Scholarship Council and Curtin University are thanked for the grant of a PhD scholarship. Schlumberger is acknowledged for granting an education licence for Petrel software that was used for seismic interpretation. In particular, Peng Chen would like to thank Chris Elders (Curtin University) for supervising this project. Acknowledgements are also due to Jane Cunneen and Greg Smith (Curtin University), Malcolm MacNeil, Eujay McCartain and Robert Seggie (Woodside Energy), Ming-quan Liu and Quan-xiong Feng (CNOOC Australia), for their kind advice and discussions regarding some issues of this project. Special thanks are due to AAPG Bulletin reviewers Bruce Ainsworth (Chevron Australia), and Ángel Puga Bernabéu (Universidad de Granada), and Editor Barry Katz (Chevron), for their constructive comments and instructions on a manuscript that overlaps this study, which significantly improved the results of this study. Most importantly, Peng Chen would like to thank his families, especially his wife Nicole, for their unconditional support, without which this project can never be accomplished.

CONTENT

LIST OF FIGURES

LIST OF TABLES

1 INTRODUCTION

1.1 Location of Study Area

The North West Shelf of Australia is geographically located in the northwest of the Australia and covers a northeast-southwest trending elongate offshore region (Figure 1-1a). The area can been defined as a passive margin since India-Australia breakup in the Cretaceous. The North West Shelf consists of four sedimentary basins, which, from southwest to northeast, are the Northern Carnarvon Basin, Roebuck Basin, Browse Basin and Bonaparte Basin (Figure 1-1a). These four basins were widely referred as the Westralia Superbasin (AGSO Group, 1994). This study focuses particularly on the central area of the North West Shelf, which mainly covers the Roebuck Basin and the northeast area of the Northern Carnarvon Basin (Figure 1-1b).

1.2 Aims and Objectives

The North West Shelf is the most prolific hydrocarbon producing area in Australia. It is interesting that most of the discoveries, especially the most commercial ones, are concentrated in the south and central part of the Northern Carnarvon Basin, the Browse Basin and the Bonaparte Basin (Figure 1-1) (Longley et al., 2002). Exploration in the central area, including the Roebuck Basin and the northeast area of the Northern Carnarvon Basin, has been less successful, which led to the perception of low prospectivity in the area. Since 2014, several exploration breakthroughs have been made in the inboard part of the Roebuck Basin, including the Phoenix South and Roc discoveries (gas and condensate of limited economic value), and the Dorado discovery (171 million barrels of oil) (Molyneux et al., 2016; Carnarvon Petroleum Ltd, 2018). These discoveries started to reverse the long-standing low-prospectivity perception of the area. However, the fundamental understanding of the geology in the area remains limited, especially in the publically available domain.

The aim of this research is to study the tectonostratigraphic evolution (structural development and sedimentary infill processes) of the central area of the North West Shelf, including the Roebuck Basin and the northeast of the Northern Carnarvon Basin. Basin development prior to and coeval with the corresponding supercontinent breakup (pre-rift and syn-rift respectively) are covered. The objectives of this study can be summarized as harnessing available seismic and well data for the identification of the structural architecture, sedimentary facies and depositional elements that were formed in the foresaid geological time interval and discussing the findings and implications in terms of the way the basin was formed. Hopefully, a better understanding of the basin can help guide the prospecting and exploration for hydrocarbons in the area.

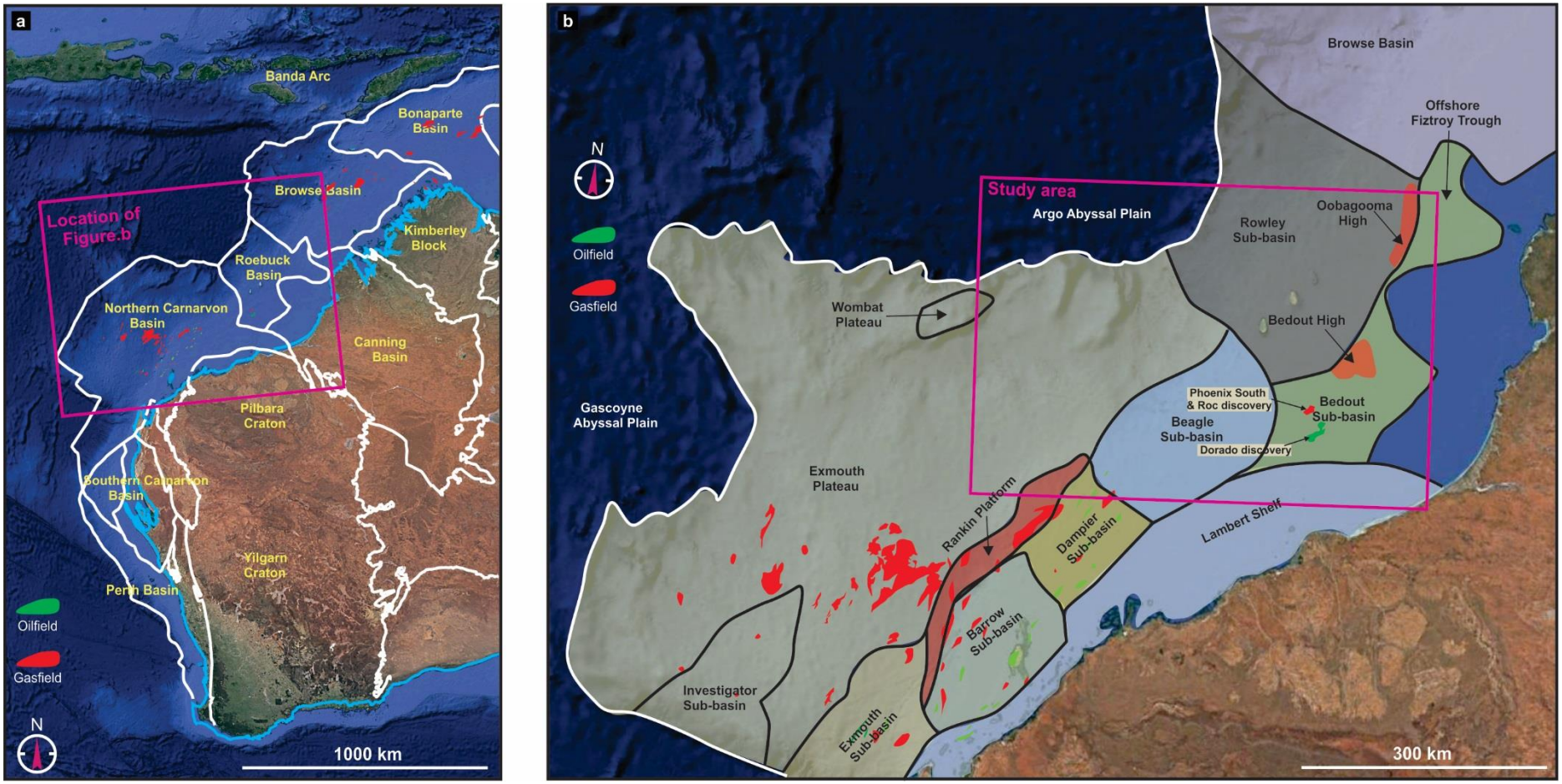

Figure 1-1. Maps showing major sedimentary basins of Western Australia (a), and basin subdivisions of the Northern Carnarvon Basin and Roebuck Basin (b). Maps compiled after Geoscience Australia (2013) and Totterdell et al. (2014).

1.3 Thesis Structure

This thesis consists of seven chapters, including the Introduction (Chapter 1). A detailed literature review is presented in Chapter 2, which summarizes the present understanding of the study area, regarding the basin subdivision and structural elements, basin development and stratigraphy. It is followed by a brief discussion of the gaps and/or debates in the understanding of the area, which lay the foundation for the objectives of this study. The data and methodology are described in Chapter 3. It is followed by the core portion of the thesis, Chapter 4, 5, 6 and 7, which present the results of the study. Chapter 4 comprises results of basin-scale interpretations, including the chronostratigraphic framework, basin geometry and stratigraphic architecture. Chapter 5 is focused on the structural architecture, which describes the details of structural elements in the three-dimensions and discusses their implications for the regional tectonic evolution and basin development. Three-dimensional (3D) stratigraphic architecture, sedimentary facies and geomorphology, together with their implications for understanding the sediment infill processes and regional stratigraphic architecture are presented in Chapter 6. Part of Chapter 6 is converted into a manuscript titled "Architecture, geomorphology, and sediment gravity flows of a Jurassic subaqueous clinoform system, northeast Exmouth Plateau, North West Shelf, Australia", which has been submitted to and accepted by the AAPG Bulletin, and the authors are Chen and Elders. All the original interpretation, idea construction, figure illustration and manuscript preparation are done by Chen, and Elders provides technical support, concept discussion and proof reading for the manuscript. After the submission, more interpretation was done and is included the Chapter 6. To integrate the results of structural architecture and depositional systems, a detailed evolutionary model is presented in Chapter 7, which serves as the summaries of this study. It is followed by sections that present conclusions and recommendations for future work.

2 GEOLOGICAL SETTINGS

2.1 Basin Subdivisions

The Roebuck Basin is divided into three major sub-basins, the Bedout Sub-basin in the south, the Offshore Fitzroy Trough in the northeast and the Rowley Sub-basin in the northwest (Figure 1-1b). Two basin highs are identified between these sub-basins. The Bedout High, is a circular pre-Mesozoic high that is located between the Rowley Sub-basin and the Bedout Sub-basin. The Oobagooma High is a fault controlled elongate pre-Mesozoic high that separates the Offshore Fitzroy Trough from the Rowley Sub-basin (Figure 1-1b). The Roebuck Basin is flanked by the Canning Basin to the southeast, which consists of a series of northwest- trending fault-bounded areas, e.g., Fitzroy Trough, Broome Platform and Willara Sub-basin.

The Northern Carnarvon Basin consists of four sub-basins in the inboard part that follow a northeast structural trend (Figure 1-1b). From southwest to northeast, they are the Exmouth Sub-basin, the Barrow Sub-basin, the Dampier Sub-basin and the Beagle Sub-basin. The extensive outboard area of the Northern Carnarvon Basin is named the Exmouth Plateau. It contains a small structural high in the north named the Wombat Plateau and a structural low in the south named the Investigator Sub-basin (Figure 1-1b). The Exmouth Plateau is separated from the Barrow and Dampier Sub-basin by a northeast-trending structural high named the Rankin Platform. The Lambert Shelf is located in the more landward area and is aligned with present coastline. It defines the landward high flanks of the Exmouth, Barrow, Dampier, Beagle and Bedout Sub-basin.

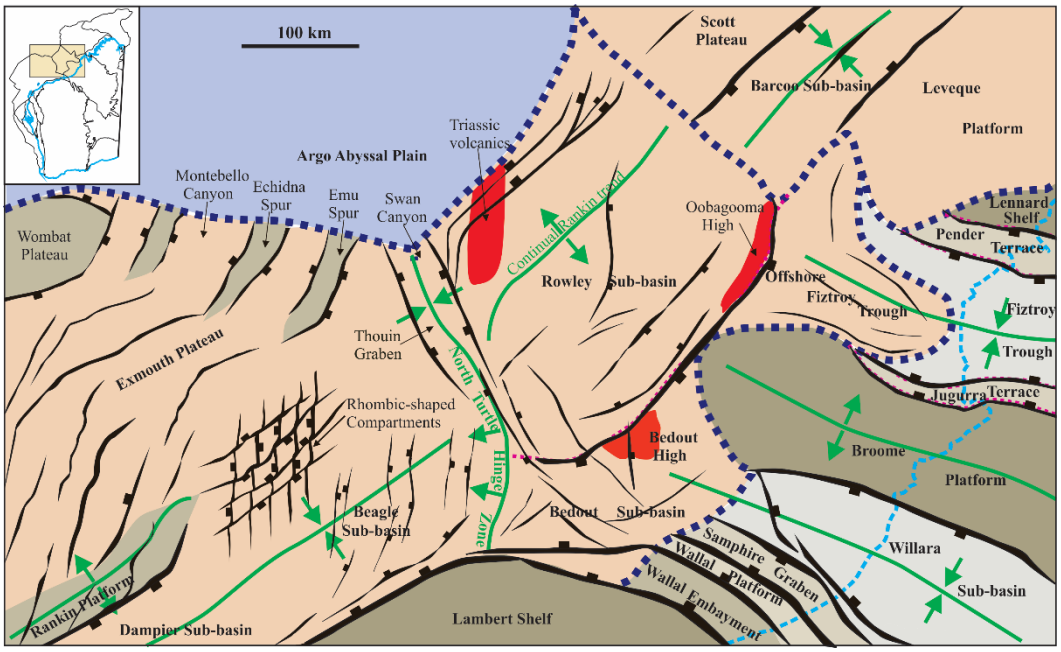

Figure 2-1. Structural elements of the Roebuck Basin and the adjacent areas of the Browse, Canning and Northern Carnarvon Basin. This map is compiled from a few publically available studies (AGSO Group, 1994; Hocking et al., 1994; Ramsay and Exon, 1994; Smith et al., 1999; Lech, 2013; McCormack and McClay, 2018) and represent the pre-existing understanding of the structural elements of the area.

2.2 Structural Elements

There are a limited number of publically available studies on structural elements of the Roebuck Basin and the northeast area of the Northern Carnarvon Basin. Early studies demonstrated that the Roebuck Basin is an offshore extension of the onshore Canning Basin and conjectured that the northwest- trending Palaeozoic structures of the Canning Basin are present in the offshore area (Wales and Forman, 1981; Horstman and Purcell, 1988) (Figure 2-1). 2D seismic based studies identified the major intra-basin highs and lows at shallow stratigraphic levels (Mesozoic-Present), which include the symmetric Bedout High, the seaward-thickening Rowley Sub-basin, and embayment-like Bedout Sub-basin (AGSO Group, 1994; Colwell and Stagg, 1994; Lipski, 1994; Ramsay and Exon, 1994). On the northern

Exmouth Plateau, large fault bounded structural highs (horsts) including the Wombat Plateau, Echidna Spur and Emu Spur, together with the intervening troughs (grabens) were identified (e.g., Swan Canyon, Montebello Canyon, noting that "canyon" is not appropriate terminology for them, because they are structural lows) (Figure 2-1) (Ramsay and Exon, 1994). Large faults that define these basin-scale structures were mapped to the maximum extent possible at this period of time. However, faults with less displacement were rarely mapped due to the limitation of the seismic quality and coverage, thus the structural trends in most of the study area were poorly understood. The most comprehensive study for the Roebuck Basin was conducted by Smith et al. (1999) after a better coverage of 2D seismic surveys. The major advances of this study include the identification a northeast- trending elongate fault-bounded structural high at the Palaeozoic level (Oobagooma High), which separates the Offshore Fitzroy Trough from the Rowley Sub-basin (Figure 2-1). The author deemed that the Oobagooma High and Bedout High form a northeast- trending structural element that truncates the northwest- trending Broome Platform. Smith et al. (1999) further confirmed the Swan Canyon is a north-northwest- trending graben separating the Rowley Sub-basin from the northeast Exmouth Plateau and named it as the Thouin Graben (Figure 2-1). He also interpreted the structural trend of the Thouin Graben to extend to the south where it forms a hinge zone (North Turtle Hinge Zone) which separates the Beagle Sub-basin from the Bedout Sub-basin. The interpretation of intra-sub-basin structures was conjectural because of the limitation of the 2D seismic data. In the Rowley Sub-basin, northeast- trending Mesozoic extensional faults were conjectured to be present, in accordance with the North Rankin structural trend (Stagg and Colwell, 1994; Smith, 1999). In the Bedout Sub-basin and the Offshore Fitzroy Trough, northwest- trending faults were interpreted, based on the northwest-trending Canning Basin structural elements (Smith et al., 1999). 3D seismic interpretation based studies only appeared recently, but significantly advanced the understanding of the structural elements. A population of north- trending Mesozoic rift-related extensional faults were identified in the central Beagle Sub-basin (Lech, 2013) and both north-trending and northeast-trending Mesozoic rift-related extensional faults were interpreted in the northern Beagle Sub-basin, cutting the area into rhombic-shaped compartments (McCormack and McClay, 2018) (Figure 2-1).

2.3 Regional Tectonic Evolution

The northwest area of Australia (including the present-day North West Shelf and onshore basins) was formed in multiple tectonic events during the Phanerozoic Eon (Yeates et al., 1987; Horstman and Purcell, 1988). The geological history of the area can be divided into two fundamental phases: 1) the pre-Mesozoic phase, which was only studied for a broad regional context and is still poorly understood for the North West Shelf, and 2) the Mesozoic phase,

representing the basin development phase that accumulated a thick sedimentary succession, which contains most of the prospective hydrocarbon intervals and thus has been extensively studied.

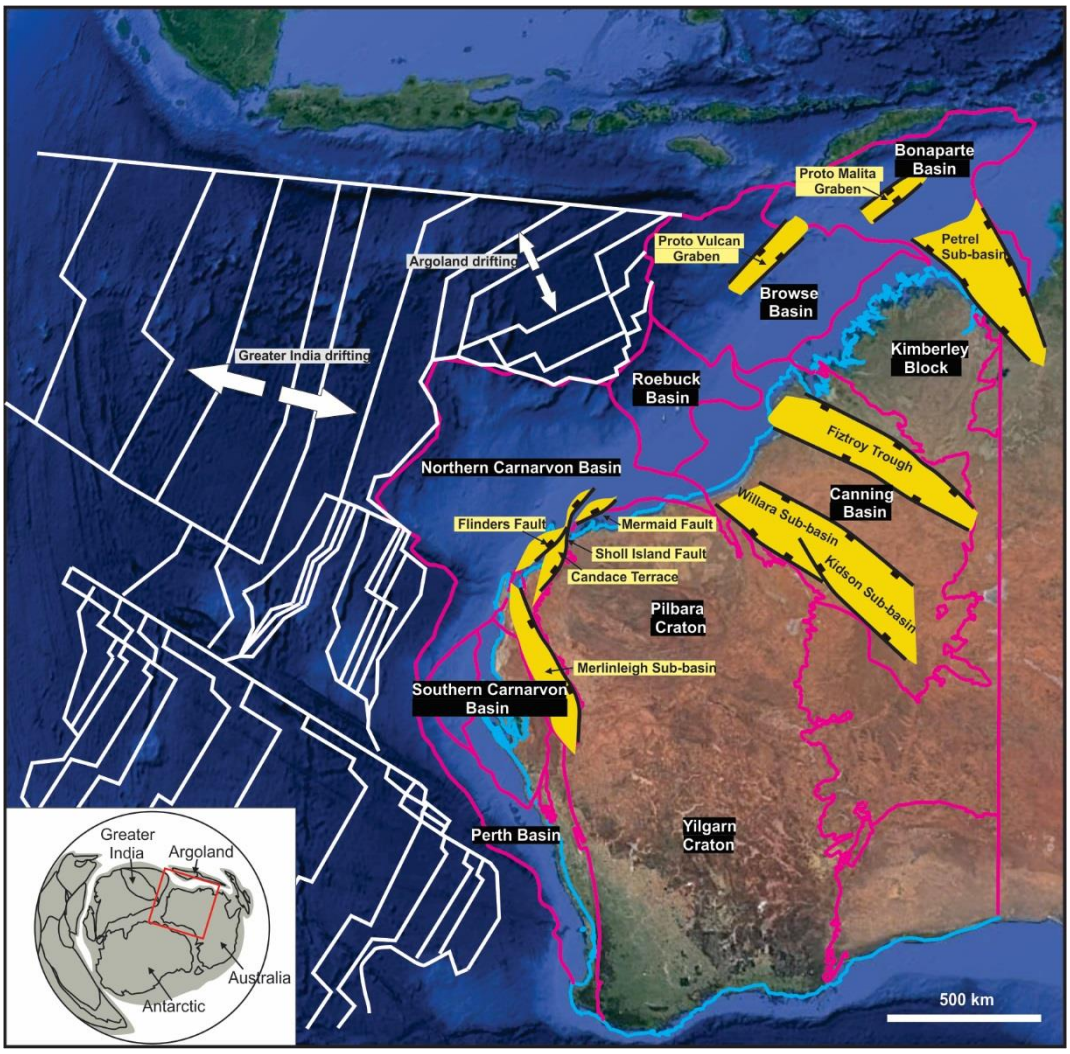

Figure 2-2. Map showing the location of the Western Australia relative to tectonic plates in the Oxfordian (bottom left) and the major Palaeozoic rift basins (yellow shading) in the adjacent areas of the Roebuck Basin, compiled after publically available studies (Bentley, 1988; Gunn, 1988; AGSO Group, 1994; Hocking et al., 1994; Struckmeyer et al., 1997; Iasky et al., 1998a; McHarg et al., 2018), and the reconstructed plate positions (constrained by sea-floor magnetic anomalies), compiled from Gibbons (2012).

2.3.1 Pre-Mesozoic Tectonic Evolution

Ordovician-Silurian

In the Ordovician-Silurian, Western Australia was in the interior of the Gondwanaland and a phase of extension in the early Ordovician led to the formation of intracratonic sags, including the Southern Carnarvon Basin, the Canning Basin and the Bonaparte Basin (Baillie et al., 1994). Marine clastic, carbonate and evaporitic facies dominated the deposition in these basins (Hocking, 2008; Nicoll et al., 2009).

Early Devonian

The Ordovician-Silurian deposition was terminated by the Prices Creek Movement in the Early Devonian (Kennard et al., 1994; Shaw et al., 1994). The Canning Basin area was uplifted and folded, and the Ordovician rocks were largely eroded during this phase.

Devonian-Early Carboniferous

The Devonian-Early Carboniferous saw the major Palaeozoic extensional phase that had an extensive influence on the northwest of Australia. This extension was northeast- directed and produced a series of northwest- trending basement fault-bounded grabens in the weakness zone formed in previous stretching. These grabens, including the Merlinleigh Sub-basin in the Southern Carnarvon Basin (Iasky et al., 1998a; Iasky et al., 1998b), the Fitzroy Trough in the Canning Basin (Hocking et al., 1994) and the Petrel Sub-basin in the Bonaparte Basin (Gunn, 1988) (Figure 2-2), represent different segments of a northwest- trending Palaeozoic rift system in the area (Middleton, 1991). Sediments deposited in this phase are characterized by carbonate reefs and terrestrial to marine sediments (Ercole et al., 2003; Hocking, 2008; Nicoll et al., 2009)

Middle (-Late) Carboniferous

In the Middle (-Late) Carboniferous, the northwest of Australia underwent another phase of uplift and erosion, which is demonstrated by a prominent coeval sedimentary gap in the Canning Basin (Baillie et al., 1994; Hocking, 2008). This tectonic event presumably inverted the pre-existing Devonian-Early Carboniferous rift-related structures. It is named the Meda Transpression, which led to the formation of coeval flower structures (Jackson et al., 1993; Shaw et al., 1994)

Late Carboniferous-Early Permian

The Devonian-Early Carboniferous rift system was rejuvenated in the Late Carboniferous-Early Permian. The Devonian-Early Carboniferous faults were widely reactivated and underwent prominent Late Carboniferous-Early Permian growth in the Southern Carnarvon Basin(Iasky et al., 1998a), Canning Basin (Shaw et al., 1994) and Petrel Sub-basin (Gunn, 1988; Gorter et al., 2005). Simultaneously, a northeast- (north-northeast-) trending rift system was developed in the present North West Shelf area. This rift system is mainly represented by the Sholl Island, Flinders and Mermaid Fault System, which separate the Northern Carnarvon Basin from the pre-Cambrian basement of the Pilbara Craton (Figure 2-2) (Bentley, 1988; Langhi and Borel, 2005; Elders et al., 2016; McGee et al., 2017). Northeast- trending Palaeozoic faults were also reported in the Browse Basin and outer Bonaparte Basin (e.g., Proto-Vulcan and Malita Graben) (AGSO Group, 1994; Struckmeyer et al., 1997). The two perpendicular rift systems (northwest- and northeast- trending) represent weakness zones within the interior of Gondwanaland (Harrowfield et al., 2005; Haig et al., 2014). The

northeast- trending rift system lay the foundation for the formation of the Westralia Superbasin in the Mesozoic and exerted a huge influence on the Mesozoic rift-related structural development (McHarg et al., 2018). Deposition of this phase is characterized by fluvial-marine sediments, with locally distributed glacial-influenced sediments (Hocking, 2008; Mory et al., 2008).

Late Permian

In the Late Permian, the foresaid rift systems ceased development. A set of fluvial to marine clastic deposits continued to conformably fill the Carboniferous-Early Permian rift basins (Hocking, 2008; McHarg et al., 2018). Deposition in the Roebuck Basin was interrupted by a period of uplift and volcanism in the latest Permian, which formed the Bedout High and Oobagooma High, and resulted in prominent erosion of the uplifted area (Smith et al., 1999). The genesis of the Bedout High has been widely debated because of its circular and symmetric geometry, and its origin as a meteorite impact structure was proposed (Gorter, 1996; Renne et al., 2004; Müller et al., 2005). However, the penetration of latest Permian (253 Ma) intrusive volcanic rocks in the borehole La Grange-1 suggests it more likely has an igneous origin (Nosiara and Groombridge, 1983). Moreover, the recognition of volcanic rocks of the similar age around the Roebuck Basin suggests an important volcanism during this period (Reeckmann and Mebberson, 1984).

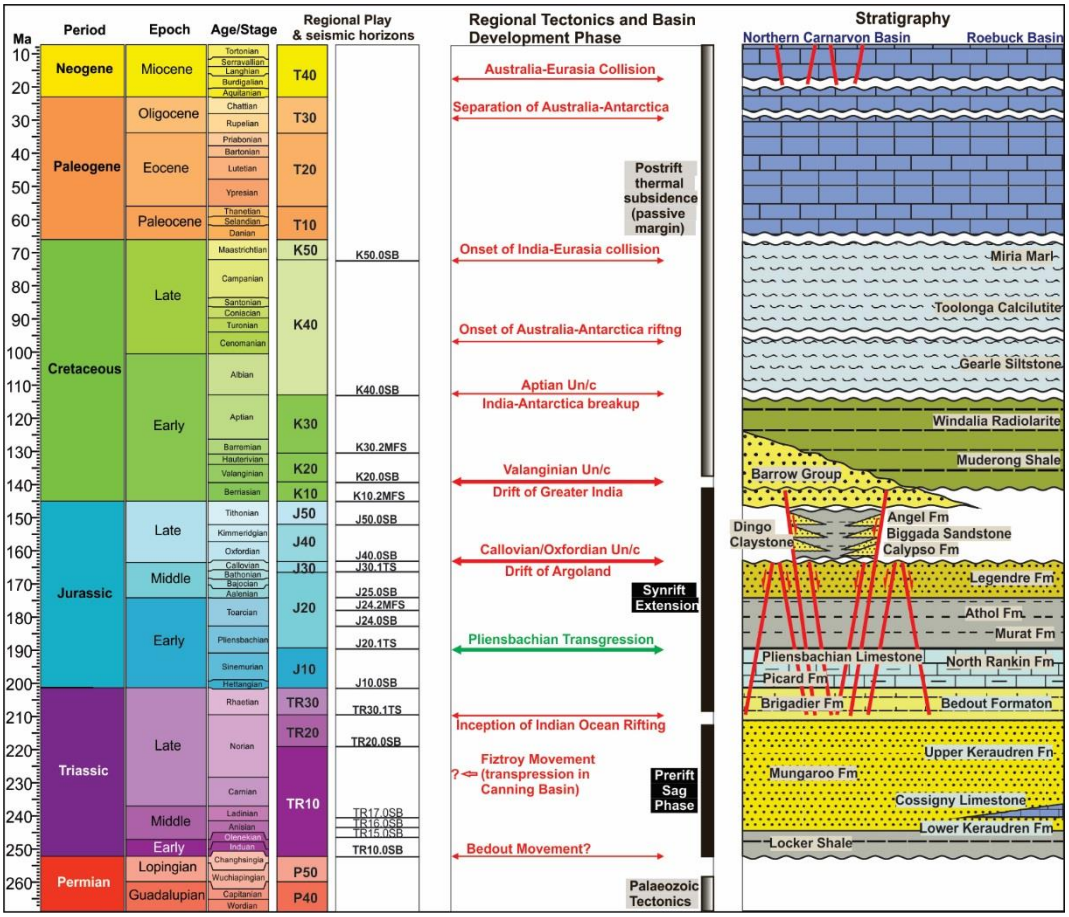

Figure 2-3. Mesozoic tectonostratigraphic evolution of the Northern Carnarvon Basin and the Roebuck Basin. Stratigraphy compiled from the Geoscience Australia (2014), regional plays and key horizons compiled from Marshall and Lang (2013) and the tectonic events compiled from a few publications (Forman et al., 1981; Smith et al., 1999; Longley et al., 2002; Keep et al., 2007; McCormack and McClay, 2013)

2.3.2 Mesozoic Tectonic Evolution

From the Triassic, the present-day North West Shelf started to differentiate significantly from the adjacent areas and has been filled with significant thickness of sediments, which formed the Westralia Superbasin (AGSO Group, 1994). Based on reported fault activities, the Mesozoic tectonic evolution can be divided into four major tectonic phases: 1) pre-rift sag phase, 2) syn-rift extension phase, 3) post-rift thermal subsidence (passive margin phase) (Figure 2-3).

Pre-rift sag phase (Early-Late Triassic)

The North West Shelf, in the Northern Carnarvon Basin at least, was widely believed to be tectonically quiet in the Triassic, because the Triassic sedimentary succession displays uniform thickness and shows little evidence of syn-sedimentary faulting (AGSO Group, 1994). In the Northern Carnarvon Basin, the Triassic sediments continued to fill the under-filled graben created by the Carboniferous-Permian rift, thus were controlled by the rift boundary

faults (McHarg et al., 2018). In other areas, the thickness of the Triassic succession show gradual variation from area to area along the North West Shelf, which was presumably controlled by the sag-like topography inherited from the Carboniferous-Early Permian rift. Sediments deposited during the Triassic are characterized by marine-fluviodeltaic facies.

Although faults with Triassic age are rarely reported on the Northern Carnarvon Basin, there is sufficient information to suggest the occurrence of the Triassic tectonic movements around the North West Shelf. In the onshore Canning Basin, the presence of a large sedimentary gap of the Middle Triassic-Early Jurassic age has been interpreted as a result of a prominent transpressional event named the Fitzroy Movement, which created a set of en-echelon faults and anticlines in the onshore Fitzroy Trough (Rattigan, 1967; Smith, 1968; Zhan and Mory, 2013). The exact timing of this event is poorly constrained due to the lack of preservation of syn-tectonic successions. Smith et al. (1999) interpreted three seismically unconformable horizons in the Roebuck basin, which were allocated Ladinian, Norian and Sinemurian/Plienbachian ages respectively. He concluded that these three unconformities represent three different episodes of the Fitzroy Movement. In the Browse Basin, a Norian compression-inversion tectonic event was interpreted to reactivate the Carboniferous-Permian rift structures and create new Triassic faults (Struckmeyer et al., 1998). Most recently, MacNeill et al. (2018) reported a large Early-Middle Triassic lava delta in the outer Rowley Sub-basin (Roebuck Basin) and suggested a triple junction was present in the area in the Early-Middle Triassic. The three failed arms overlap the onshore Fitzroy Trough, Barcoo-Caswell Sub-basin in the Browse Basin and northern edge of the Exmouth Plateau respectively. The clinoforms of the lava delta, however, were alternatively interpreted as a late Permian carbonate shelf edge system (Paschke et al., 2018). This indicates a lack of consensus on the understanding of the pre-rift basin genesis and stratigraphic framework.

Syn-rift extension phase (Late Triassic-Early Cretaceous)

The rift processes on the North West Shelf were associated with the opening of the Ceno-Tethys which initiated with the drift of the Lhasa Block in the Late Triassic (Norian), and lasted till the Early Cretaceous (Valanginian) on the North West Shelf (Figure 2-3) (Metcalfe, 1999; Longley et al., 2002; Metcalfe, 2013). Previous study has confirmed that the structural development on the North West Shelf was significantly influenced by the drifting of two continental fragments, including the drifting of the Argoland in the Callovian/Oxfordian (Gradstein and Ludden, 1992) and the breakup of Greater India-Australia in the Valanginian (Powell et al., 1988). Sea-floor magnetic anomalies constrain the movement directions of the two episodes of continent drifting, Argoland's northwest drift and Greater India's east- drift (relative to present day north) (Figure 2-2) (Fullerton et al., 1989; Gibbons et al., 2012).

The extension associated the two drift events reactivated the Palaeozoic structures and formed a series of northeasterly aligned Mesozoic grabens on the North West Shelf (e.g., Exmouth-Barrow-Dampier-Beagle Sub-basin, Vulcan-Malita Graben)(AGSO Group, 1994). In the Northern Carnarvon Basin, 3D seismic based studies suggest the extension associated with the rift processes are oblique to the Carboniferous-Permian rift structures, forming both northeast- and north- trending extensional faults (Jitmahantakul and McClay, 2013; Elders et al., 2016; Black et al., 2017). The dominance of the north- trending extensional faults suggests it was the east- directed India-Australia separation that exerted influences in the area (McHarg et al., 2018)(Figure 2-2). Detailed fault analysis suggests there were two distinct fault development phases in the Northern Carnarvon Basin: Late Triassic-Middle Jurassic (Norian-Callovian/Oxfordian) and Late Jurassic-Early Cretaceous (Oxfordian-Valanginian) (McCormack and McClay, 2013). At the northeast end of the North West Shelf (Bonaparte Basin), however, 3D seismic based studies suggest that northeast- or east-northeast- trending faults are the dominant rift-related faults and north- trending faults, if they exist, are very few in number (Frankowicz and McClay, 2010; Saqab and Bourget, 2015). This may suggests the syn-rift process in the northeast end was largely controlled by the northwest- directed Argoland-Australia separation (Figure 2-2). However, there are few studies that well constrain the timing of rift-related fault growth on the northeast end of the North West Shelf, because the reported faults have no syn-kinematic succession preserved, which is largely due to strong erosion (Saqab and Bourget, 2015). Sediments deposited from the Late Triassic-Early Cretaceous are mainly characterized by fluviodeltaic-marine facies.

Post-rift subsidence (passive margin) phase (Early Cretaceous-Present)

The North West Shelf underwent post-rift thermal subsidence and became a passive margin after the Greater India-Australia breakup in the Valanginian. Deposition during this phase is characterized by a succession of fine-grained clastic to carbonate facies. In the post-rift phase, a few far-field tectonic events took places, including drifting of India-Antarctic in the Aptian, breakup of Australia-Antarctic during the Late Cretaceous-Oligocene and the collision of Australia-Eurasia since the Miocene (Figure 2-3). The syn-rift structures were extensively reactivated during Australia-Eurasia collision (Keep et al., 2000; Keep et al., 2007; Saqab and Bourget, 2015).

2.4 Stratigraphy

A detailed Mesozoic chronostratigraphy of the study area is summarized below based on the publically available studies. The regional plays and key stratigraphic boundaries compiled by Marshall and Lang (2013) are used for a better understanding of the regional stratigraphic framework (Figure 2-3).

2.4.1 Pre-rift Stratigraphy

The lowermost part of the Triassic succession is a unit of marine shale (Locker Shale, TR10.0SB-TR15.0SB) (Figure 2-3), which is widely present on the North West Shelf (Longley et al., 2002). The marine shale-dominated sediments gradually switched into fluviodeltaic facies, which formed the sand-rich Mungaroo Formation (TR15.0SB-TR30.1TS) in the Northern Carnarvon Basin. In the Roebuck Basin, however, the equivalent fluviodeltaic system was named the Keraudren Formation, which is divided into the lower and upper sub-units separated by a thin layer of carbonate (Cossigny Limestone, TR16.0SB-TR17.0SB)(Molyneux et al., 2016)(Figure 2-3). Passing upward, the Mungaroo Formation changes into finer-grained siliciclastic sediments dominated by the Brigadier Formation (TR30.1TS-J10.0SB)(Adamson et al., 2013).

2.4.2 Syn-rift Stratigraphy

The onset of syn-rift started with the deposition of the Brigadier Formation and is marked by a regional transgressive surface (TR30.1TS) (Figure 2-3). This transgression increased the carbonate content within the Brigadier Formation (TR30.1TS-J10.0SB) and led to the formation of the carbonate-dominated North Rankin Formation (J10.0SB-J20.1TS) (Adamson et al., 2013; Gartrell et al., 2016). In a few locations, pure limestones are identified and named the Picard Formation and the Pliensbachian Limestone. Carbonate deposition was terminated by a regional flooding event in the Pliensbachian (J20.1TS) (Figure 2-3). Following that, a large volume of fluviodeltaic sediments were input into the Roebuck Basin and the Northern Carnarvon Basin, forming the Legendre Delta. The Legendre Delta consists of the shale-dominated Murat-Athol Formation (J20.1TS- J25.0SB) and the sand-dominated Legendre Formation (J25.0SB -J40.0SB). The base of the Legendre Formation is interpreted as J25.0SB because it is located within the C.turbatus zone (J24.2MFS-J26.0SB, Marshall and Lang, 2013) in the Huntsman-1 (Sturrock, 2007). The accumulation of the Legendre Delta was terminated during Argoland drifting in the Oxfordian (J40.0SB). Since then, most of the areas on the North West Shelf underwent a period of non-deposition and erosion from the Oxfordian to the Valanginian (J4.0SB-K20.0SB). However, in the Barrow-Dampier-Beagle Sub-basins, a package of gravity flow deposits, e.g., turbidites and debrites that are incorporated into marine shale were developed (Dupuy, Biggada, Angel and Dingo Formation) (Figure 2-3) (Vincent and Tilbury, 1988; Osborne, 1994; Longley et al., 2002). Simultaneously, a large volume of sands were poured into the south of the Northern Carnarvon Basin, forming the Barrow Group since the earliest Cretaceous (K10.2MFS). The accumulation of the Barrow Group lasted into the post-rift phase (K30 play).

2.4.3 Post-rift Stratigraphy

The post-rift succession is characterized by a set of clastic to carbonate-rich siliciclastic sediments (from older to younger, they include Muderong Shale, Windalia Radiolarite, Gearle Siltstone, Toolonga Calcilutite and Miria Marl) in the Cretaceous (K20-K50 play) and carbonate-dominated deposits from the Palaeogene to present day (after T10 play) (Figure 2-3).

2.5 Discussion

According to the literature review above, a few research gaps have been identified with respects to the tectonostratigraphic evolution of the Roebuck Basin and the northeast area of the Northern Carnarvon Basin.

1) The North West Shelf has undergone multi-phase tectonic evolution and its present basin architecture and structural style had taken shape up until the Greater India-Australia breakup in the Early Cretaceous. 3D seismic based studies in the Northern Carnarvon Basin, Browse Basin and the Bonaparte Basin have revealed the 3D structural architectures of the southwest and northeast ends of the North West Shelf, which shed light on rifting processes associated with continental breakup. However, in the central area of the North West Shelf, particularly the Roebuck Basin and the northeast part of the Northern Carnarvon Basin, 3D structural architecture are poorly understood, which is a consequence of the lack of data and research due to the perception of low prospectivity.

2) Argoland drifted from the North West Shelf in a northwesterly direction in the Oxfordian. The relationship between the extension generated by Argoland rifting and the structural style, especially the structural grain, has rarely been discussed. The Roebuck Basin is situated closest to the nucleation zone of the Argoland rifting, and the interpretation of the 3D structural architecture may provide a better understanding of the influences of the Argoland Rifting on the structural development.

3) Recent studies have started to reverse the perception of the tectonic quiescence in the Triassic, by the identification of volcanism and faulting in the Triassic. However, the Triassic structural development, for most of the area across the North West Shelf, remains enigmatic.

4) The weakness zones formed by rift tectonics in the Palaeozoic exerted huge influences on the development of the Mesozoic rift-related extensional structures. The Roebuck Basin is located at the intersection of two orthogonal rift systems, the northwest- trending Devonian-Permian rift system of the Canning Basin and the northeast-north- trending Carboniferous-Permian rift system of the North West Shelf. It remains a question whether the Palaeozoic rift

structures extends into the Roebuck Basin and if so, how they influenced the Mesozoic rift-related structural development.

5) From the perspective of depositional systems, the lack of the 3D seismic based studies have hindered the understanding of three dimensional stratigraphic architecture, sedimentary facies and geomorphology, which are of great significance for revealing the interaction of tectonics, sea-level fluctuations and sediment infill.

A few 3D seismic surveys acquired in the study area became publically available recently, which has provided research opportunities in narrowing the foresaid research gaps and facilitating the understanding of the tectonostratigraphic evolution of the central area of the North West Shelf.

3 DATA AND METHODOLOGY

This chapter presents a brief description of the data and methodology utilized in this study.

3.1 Data

This study utilized a number of 2D and 3D seismic surveys. The 2D seismic surveys provide a good coverage of the study area (Figure 3-1). The density, image depth and quality vary from survey to survey, which has previously led to the relatively low-degree of consistency and confidence of the interpretation of geological bodies and/or boundaries. Therefore, 2D seismic data were only used to establish a coarse basin-scale chronostratigraphic framework and the geometry of the major depocentres and basin highs (Chapter 4).

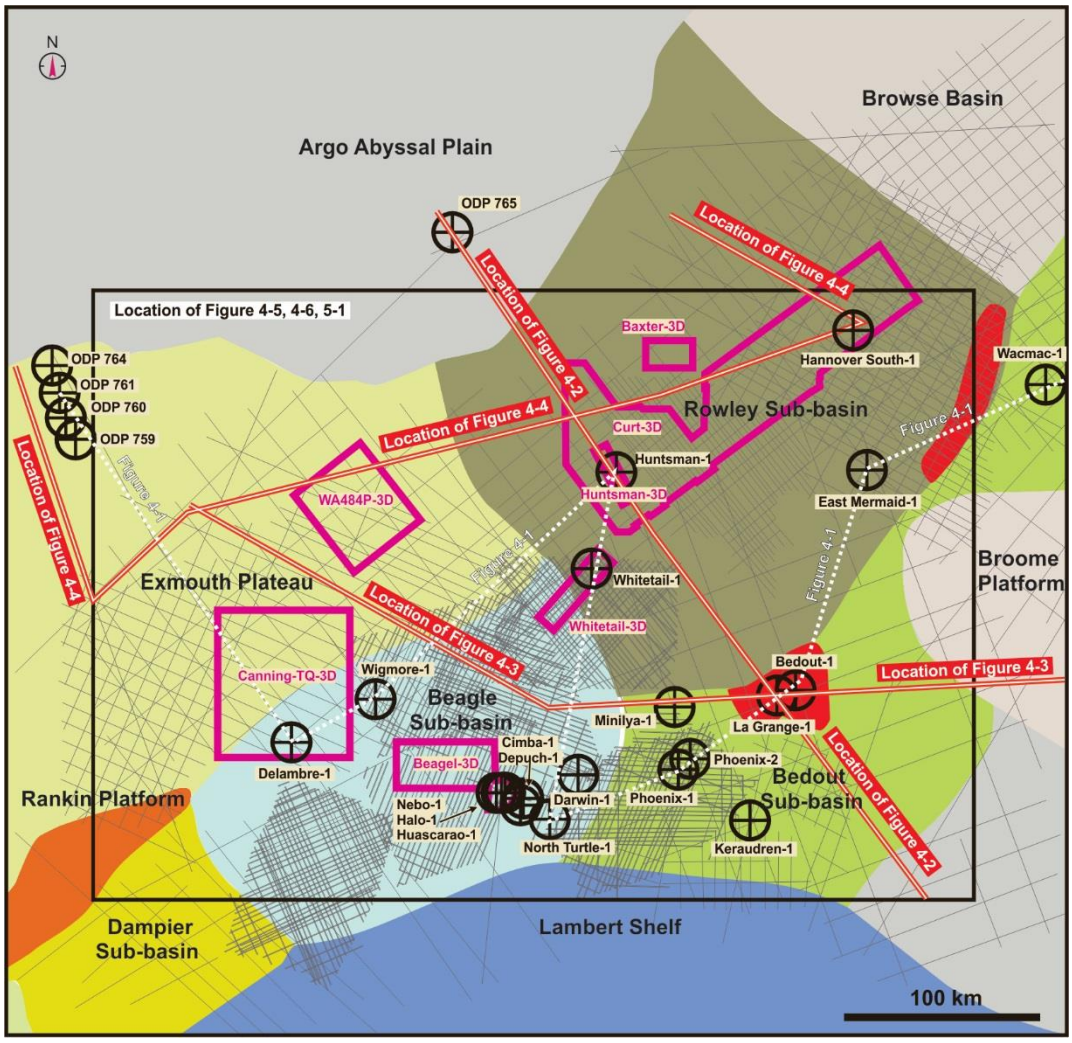

Figure 3-1. Data overview map showing the locations of the 2D and 3D seismic surveys, wells and key figures in Chapter 4.

3D seismic data sets are the core of the study. There are seven 3D seismic data sets used this study, including the Beagle-3D and Canning-TQ-3D in the Beagle Sub-basin, WA484P-3D on the northeast Exmouth Plateau, Whitetail-3D, Huntsman-3D, Curt-3D and Baxter-3D in

the Rowley Sub-basin (Figure 3-1). The details of these data sets are summarized in Table 1. These seven data sets are generally used for the interpretation of the structural architecture (Chapter 5). Only Curt-3D and WA484P-3D are used for the interpretation of the depositional system and sedimentary facies (Chapter 6).

The seismic interpretation are calibrated by the available wells in the study area (Figure 3-1), which provide age controls on the key seismic succession boundaries (see Chapter 4 for details) and lithological constraints on seismic facies (see Chapter 6 for details).

3.2 Methodology

Conventional seismic interpretation were conducted for both 2D and 3D seismic data sets, including horizon and fault interpretation. For the 2D seismic data sets, emphases are put on the interpretation of the horizons that are recognizable across the study area, e.g., regional unconformities and surfaces of sequence stratigraphic significance. Two-way travel-time structure maps and isochron maps are made based on the basin-wide horizons. This provides a general understanding of the stratigraphic framework, basin geometry and architecture (Chapter 4). 2D seismic data are also used to map the Palaeozoic faults and anomalous Mesozoic geological bodies (e.g., dome structures in Chapter 5) that are not covered by 3D seismic data. For 3D seismic data sets, more survey-specific seismic horizons are interpreted under the basin-scale stratigraphic framework established by 2D seismic interpretation. These survey-restricted horizons, with or without well control, in conjunction with seismic attribute analysis, are used for the analysis of the 3D structural architecture (Chapter 5) and the 3D sedimentary facies and depositional system (Chapter 6).

Seismic attributes are widely used in this study, in the form of section profiles, surfaces and time slices. The results presented in this study comprise: 1) variance, a trace to trace difference attribute (opposite to similarity or coherency) that can highlight geological fabrics, e.g., faults, channels, and sedimentary contacts; 2) Root Mean Squre (RMS) amplitude, which emphasizes the acoustic impedance change within a specified interval; 3) maximum magnitude, which illustrates the variation of the maximum amplitude within a specified interval; 4) edge-detection attribute, which is similar to variance and highlights geological relief.

Time depth conversions are not conducted in this study because of the lack of a consistent velocity model across such a large area. Seismic sections shown in this paper are in two-way-travel time (TWT) vertical domain. TWT structure maps and isochron maps used in this paper do not represent real depth and thickness but are an effective way of showing relative depth and thickness change.

Table 3-1. Summary of 3D seismic surveys used in this study

Survey name	Area	Inline trend/ numbers/ spacing	Xline trend/ numbers/ spacing	Record length	Sampling rate	Quality
Beagle-3D	71.63 km × 38.05 km	E-W/ 3044/ 12.5 m	N-S/ 5730/ 12.5 m	5596 ms	4 ms	Good quality for the Upper Jurassic-present stratigraphy (from seafloor-2.5 second TWT); Relative poor quality below 2.5 second TWT
Canning-TQ-3D	74.04 km × 84.86 km	N-S/ 4628/ 16 m	E-W/ 6789/ 12.5 m	6004 ms	4 ms	High quality for the Jurassic-present stratigraphy (from seafloor to 4.5 second TWT); Poor quality for the Triassic and older stratigraphy (below 4.5 second TWT)
Whitetail-3D	10.95 km × 51.94 km	NE-SW/ 730/ 15 m	NW-SE/ 4155/ 12.5	5996 ms	4 ms	High quality for the Cretaceous and younger stratigraphy (above 2.5 second TWT); Poor quality for Jurassic and older stratigraphy (below 2.5 second TWT); Strong artefact due to seafloor canyons.
WA484P-3D	51.25 km × 44.50 km	NW-SE / 1780 / 25 m	NE-SW/ 4099/ 12.5 m	9214 ms	2 ms	High quality for the Jurassic-present stratigraphy (from seafloor to 6.0 second TWT); Poor quality for the Triassic and older stratigraphy (below 6.0 second TWT
Huntsman-3D	8.1 km × 34.25 km	NW-SE/ 270/ 30 m	NE-SW/ 2740/ 12.5 m	6000 ms	4 ms	High quality for the Upper Triassic and younger stratigraphy (above 4.5 second TWT); Low quality for the Middle Triassic and older stratigraphy (below 4.5 second TWT)
Curt-3D	100.28 km × 265.1 km	NE-SW/ 8022/ 12.5 m	NW-SE/ 21208/ 12.5 m	9000 ms	4 ms	High quality for the Triassic and younger stratigraphy (above 5.5 second TWT); Poor quality for the Lower Triassic and older stratigraphy (Below 5.5 second TWT); Partially influenced by seafloor canyons.
Baxter-3D	31.1 km × 53.83 km	E-W/ 2478/ 12.5 m	N-S/ 4306/ 12.5 m	8250 ms	2 ms	High quality for the Upper Triassic and younger stratigraphy (above 5.5 second TWT); Low quality for the Middle Triassic and older stratigraphy (below 5.5 second TWT)

4 BASIN GEOMETRY AND FRAMEWORK

This Chapter is focused on the basin-scale chronostratigraphic framework and the basin geometry and architecture, based on the correlation of the available borehole stratigraphy and the interpretation of the available 2D seismic profiles.

4.1 Seismostratigraphic Framework

The seismostratigraphic framework for the Triassic-Early Cretaceous sedimentary succession is present based on well correlation (Figure 4-1) and 2D seismic interpretation (Figure 4-4 to 4-6). The targeted succession corresponds to the pre-rift sag phase and the syn-rift extension phase in the Northern Carnarvon Basin (Figure 2-3). However, the results of the structural analysis and sedimentary facies analysis in this study (see Chapter 5&6 for details) suggest that the structural evolution is slightly different from the structural development phases recognized in the literature. To avoid the confusion between the structural evolution derived from the literature and the results of this study, the seismostratigraphic framework is presented purely based on ages, regardless of their tectonic significance (e.g., pre-rift and syn-rift). Simple age abbreviations are used for the horizon nomenclature (e.g., JP=Pliensbachian). The key stratigraphic horizons of Marshall and Lang (2013) are listed for comparison where available.

Palaeozoic

The Palaeozoic succession is seismically poorly imaged in most of the study area due to the thick Mesozoic sedimentary cover. In the uplifted inboard area (e.g., Bedout High), the upper part of Palaeozoic succession is interpreted (Figure 4-2, 4-3, and 4-4). A prominent seismic event is identified within the succession. It marks the top boundary of a set of Palaeozoic fault growth wedges, which is conjectured to correspond to the Carboniferous-Early Permian rift (Figure 4-3). Therefore this horizon is interpreted to be end of rift unconformity (early Permian in age), thus named EP. On the Exmouth Plateau, this Early Permian event (EP) is characterized by a set of high-amplitude reflections and no rift structures can be interpreted beneath it (Figure 4-4). The base of the Palaeozoic succession is poorly defined on the seismic and an arbitrary horizon that marks the bottom of layered seismic packages is interpreted as basement (B). The only well that penetrated into the pre-Triassic succession is on the Bedout High, where the Palaeozoic sedimentary succession is missing and igneous intrusive rocks are present, which is interpreted as a result of magma upwelling in the latest Permian (Figure 4-1). The upper part of the Palaeozoic succession was largely eroded around the Bedout High, forming a prominent unconformity (T [TR10.0SB]) (Figure 4-2, 4-3). In the Rowley Sub-basin, a package of discordant and wavy high-amplitude reflections are present right below

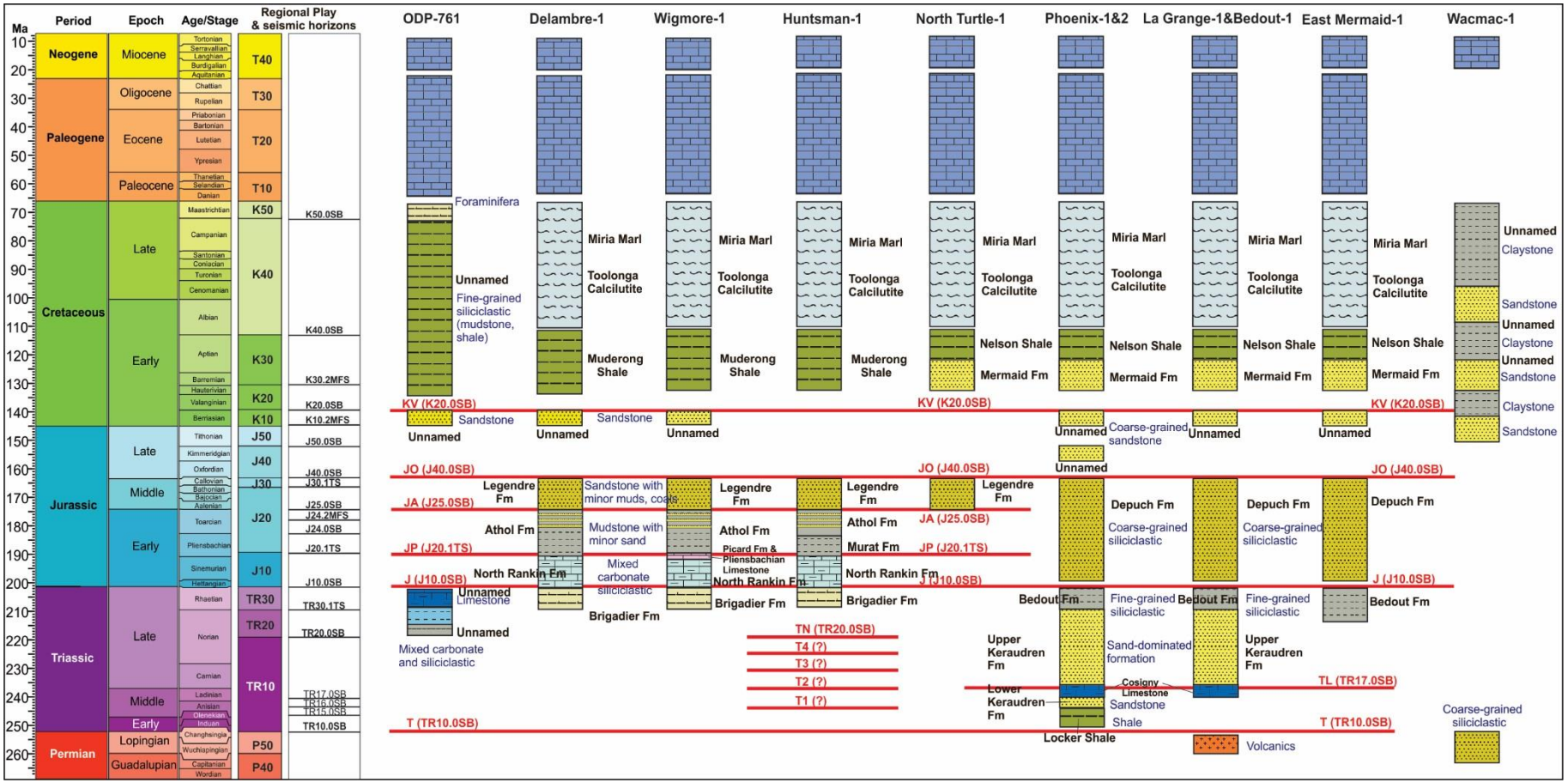

Figure 4-1. Chronostratigraphy of the northeast area of the Northern Carnarvon Basin and the Roebuck Basin (compiled from well completion reports) and key seismic horizons interpreted in this study. The regional play and seismic horizons by Marshall and Lang (2013) are listed for comparison. The locations of the wells are shown in Figure 3-1.

the base of Triassic (T [TR10.0SB]) and similar seismic package is present in the middle of the Palaeozoic succession in the Bedout Sub-basin (Figure 4-2).

Triassic

The Triassic succession (T-J) was only drilled in the Bedout Sub-basin and on the Bedout High. It comprises, from base to top, the Locker Shale, the Lower Keraudren Formation, the Cossigny Limestone, the Upper Keraudren Formation and the Bedout Formation (Figure 4-1). The Cossigny Limestone is characterized by high-amplitude reflections, which form a very strong seismic marker in the inboard area (TL [TR17.0SB]) (Figure 4-2, 4-3). However, it becomes inconspicuous outboard, e.g., the Rowley Sub-basin, Beagle Sub-basin and the Exmouth Plateau. The boundary between the Upper Keraudren Formation and the Bedout Formation is a conformable high-amplitude reflection in the Bedout Sub-basin. The exact age of Bedout Formation is not well constrained, and it presumably started with TR30.1TS and ended in the earliest Jurassic. In the Beagle and Rowley Sub-basin, the Bedout Formation equivalent succession is named as Brigadier Formation, consistent with the lithostratigraphic terminology for the Northern Carnarvon Basin (Figure 4-1). The available wells with stratigraphic ages did not penetrate the bottom of the Brigadier Formation (TR30.1TS) in the outboard part of the basin. However, seismically, an unconformity, which is characterized by truncation of the folded underlying succession, is interpreted to be present in the Rowley Sub-basin (TN) (Figure 4-2, 4-4). The Hannover South-1 penetrated this horizon, but detailed stratigraphic data is not yet available to the public. The released biostratigraphic data in the Hannover South-1 suggests that TN is located below the A.reducta, H.balmei and W.listeri zones and overlaps S.speciosus and R.wigginsii zones (Figure 4-4), and according to stratigraphic framework by Marshall and Lang (2013), it more likely corresponds to the TR20.0SB. Besides, the remarkable uplift and erosion associated with the TN surface is consistent with the regional uplift and erosion in the TR20.0SB, which is interpreted as the major phase of the Fitzroy Movement (Smith et al., 1999; Marshall and Lang, 2013). This Norian horizon (TN) is observable on the Exmouth Plateau, but is not associated with obvious erosion. Below the Norian Unconformity (TN) in the Rowley Sub-basin, a few Triassic horizons have been interpreted, which, from older to younger, are named T1-T4, due to the lack of the age control (Figure 4-1, 4-2). Among those, T4 horizon is seemingly an unconformity that is associated with differential erosion.

Jurassic

The Jurassic succession comprises by the Depuch Formation in the Bedout Sub-basin and consists of the North Rankin Formation, Murat Formation, Athol Formation and Legendre Formation in the Beagle Sub-basin and the Rowley Sub-basin (Figure 4-1). Seismically, the

base of the Jurassic succession (J [J10.0SB]) was poorly defined in the outboard, due to weak lithological contrast between the Brigadier Formation and the North Rankin Formation. However, it can be interpreted from the wells in the Bedout Sub-basin where there is a sedimentary gap between the Bedout and the Depuch Formations (Figure 4-1). The most prominent seismic marker within the succession is a Pliensbachian downlapping surface (JP), corresponding to the J20.1TS, which separates the shale-dominated Murat-Athol Formation from the underlying carbonate-dominated North Rankin Formation. This flooding event (JP [J20.1TS]) is only resolved in the outboard area (the Rowley Sub-basin and Exmouth Plateau) (Figure 4-1, 4-2, 4-3, 4-4). Another horizon that is picked within the Jurassic succession is the boundary between the Athol Formation and the Legendre Formation (JA), which is interpreted to be the J25.0SB (Figure 4-1). However, it is only picked in the Rowley Sub-basin due to the lack of confidence correlating to other areas (Figure 4-2, 4-4). The top of the Jurassic succession in most of the study area is an angular unconformity that corresponds to a sedimentary gap from Oxfordian to Valanginian (JO-KV) (J40.0SB-K20.0SB) (Figure 4-1). However, the Oxfordian unconformity (JO [J40.0SB]) and the Valanginian unconformity (KV [K20.0SB]) can be separated in the Bedout Sub-basin and localized grabens in the outboard area (see Chapter 5&6 for details).

Cretaceous

For the Cretaceous succession, the Valanginian unconformity (KV [K20.0SB]) is the only horizon interpreted. The only potential Cretaceous sediments below the Valanginian unconformity (KV [K20.0SB]) in the study area are the sand-dominated succession bounded between the Oxfordian unconformity (JO) and the Valanginian unconformity (KV), which was encountered in most of the wells (Figure 4-1). Because the wells in the study area were drilled on the horst structures and rotated footwall blocks, the sequence intersected by wells is very thin, which led to the poor definition of this succession. The stratigraphic framework for the succession that was formed after the Valanginian has not been investigated.

4.2 Basin Geometry and Architecture

The study area displays different basin geometry at different stratigraphic levels and the stratigraphic architecture changes from area to area. This section is mainly focused on the geometry and stratigraphic architecture of the major basin highs and depocentres. The major extensional faults are briefly introduced with the basin architecture, to set up the basin-scale context for detailed structural architecture in the Chapter 5.

Bedout High

The southeast of the study area has the thinnest Mesozoic sedimentary covers (T-KV) as a consequence of the controls by the pre-Mesozoic highs including the Broome Platform, the

Bedout High and the Lambert Shelf. The Bedout High is an asymmetrical circular high mainly at the pre-Triassic stratigraphic level but exerted a control on the Triassic stratigraphic architecture (Figure 4-2, 4-5a-c, 4-6a). It is covered by approximately 1.0 second TWT thick Triassic-Early Cretaceous succession (T-KV) that are thickening away from the Bedout High (Figure 4-2, 4-3). The Lower Triassic Locker Shale and Lower Keraudren Formation is missing on the crest of the Bedout High but is present on the adjacent flanks. The Bedout High was most likely formed prior to the Locker Shale deposition because 1) the intrusive volcanic rock has a latest Permian age (Nosiara and Groombridge, 1983) and 2) the Locker Shale and Lower Keraudren Formation show subtle onlapping on the flanks of the Bedout High. The Middle-Upper Triassic Cossigny Limestone and Upper Keraudren Formation (TL-TN) formed a thin cover (-0.2 second TWT) that thickens away from the Bedout High (Figure 4-2). On top of that, the Bedout Formation and the lower part of the Depuch Formation formed the Upper Triassic-Lower Jurassic succession (TN-JP) (-0.3 second TWT in thickness). It slightly thickens away from the Bedout High, suggesting minor influences of the Bedout High. The Lower-Middle Jurassic Depuch Formation (JP-JO) formed a thicker succession which is approximately 0.5 second TWT thick and shows little control by the Bedout High (Figure 4-2). The structures interpreted around the Bedout High are characterized by a few north- and northeast- trending faults mainly at the Palaeozoic level (Figure 4-3, 4-6c).

Bedout Sub-basin and Beagle Sub-basin

The Bedout High and the Lambert Shelf together confine the Bedout Sub-basin, which expressed as a westerly dipping narrow embayment at the base Triassic level (T) and is flanked by the deeper and wider Beagle Sub-basin to the west (Figure 4-5a). The two sub-basins are separated from each other by the North Turtle Hinge Zone, which is a broad and gentle anticline at the pre-Valanginian stratigraphic level (Figure 4-3). It seemingly controlled the thickness of the Triassic-Lower Jurassic succession (T-JP) (Figure 4-6a). In these two sub-basins, the westerly steepening embayment-like palaeo-topography exerted influences on the Mesozoic stratigraphic architecture (Figure 4-5). The Triassic-Lower Jurassic (T-JP) succession, which consists of the Locker Shale, the Lower Keraudren Formation, the Cossigny Limestone, the Upper Keraudren Formation, the Bedout Formation and the lowermost part of the Depuch Formation shows a westerly thickening sedimentary wedge (from 0 second TWT close to the Broome Platform to >7.0 second TWT in the Beagle Sub-basin) (Figure 4-3, 4-6a). The Jurassic-Lower Cretaceous succession (JP-KV) is around 0.5 second TWT thick in the Bedout Sub-basin and 2.0 second TWT thick in the Beagle Sub-basin but was not controlled by the embayment geometry (Figure 4-6b). The structures in the two sub-basins consist of a large population of north- trending listric Mesozoic rift-related faults that are

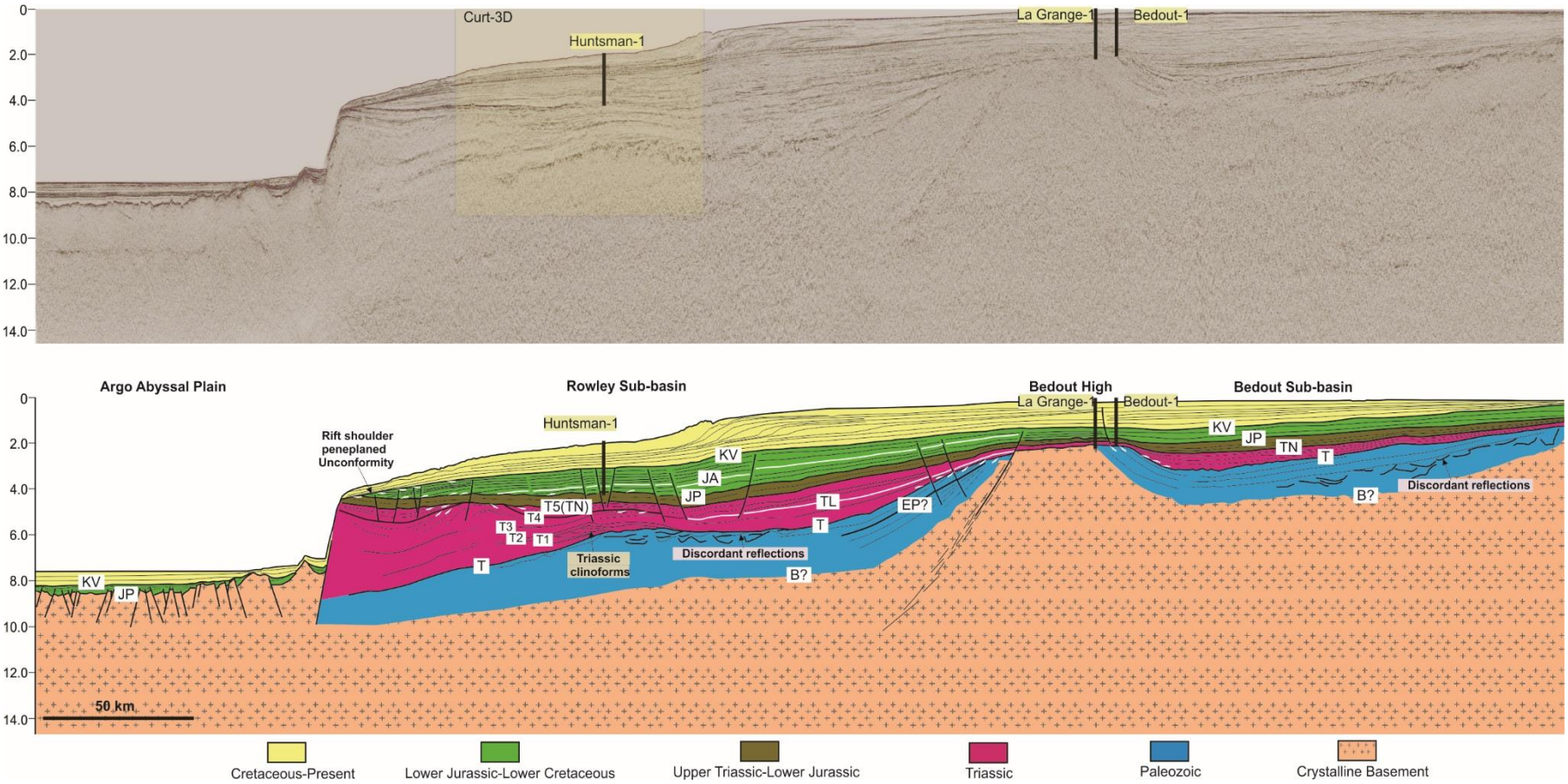

Figure 4-2. Regional seismic profile and its interpretation, showing the basin architecture across Bedout Sub-basin, Bedout High, Rowley Sub-basin and Argo Abyssal Plain (see Figure 3-1 for location). KV=Valanginian Unconformity, JA=Aalenian, JP= Pliensbachian Unconformity, TN=Norian Unconformity, TL=Ladinian, T=Base Triassic Unconformity, EP=Early Permian, B=basement.

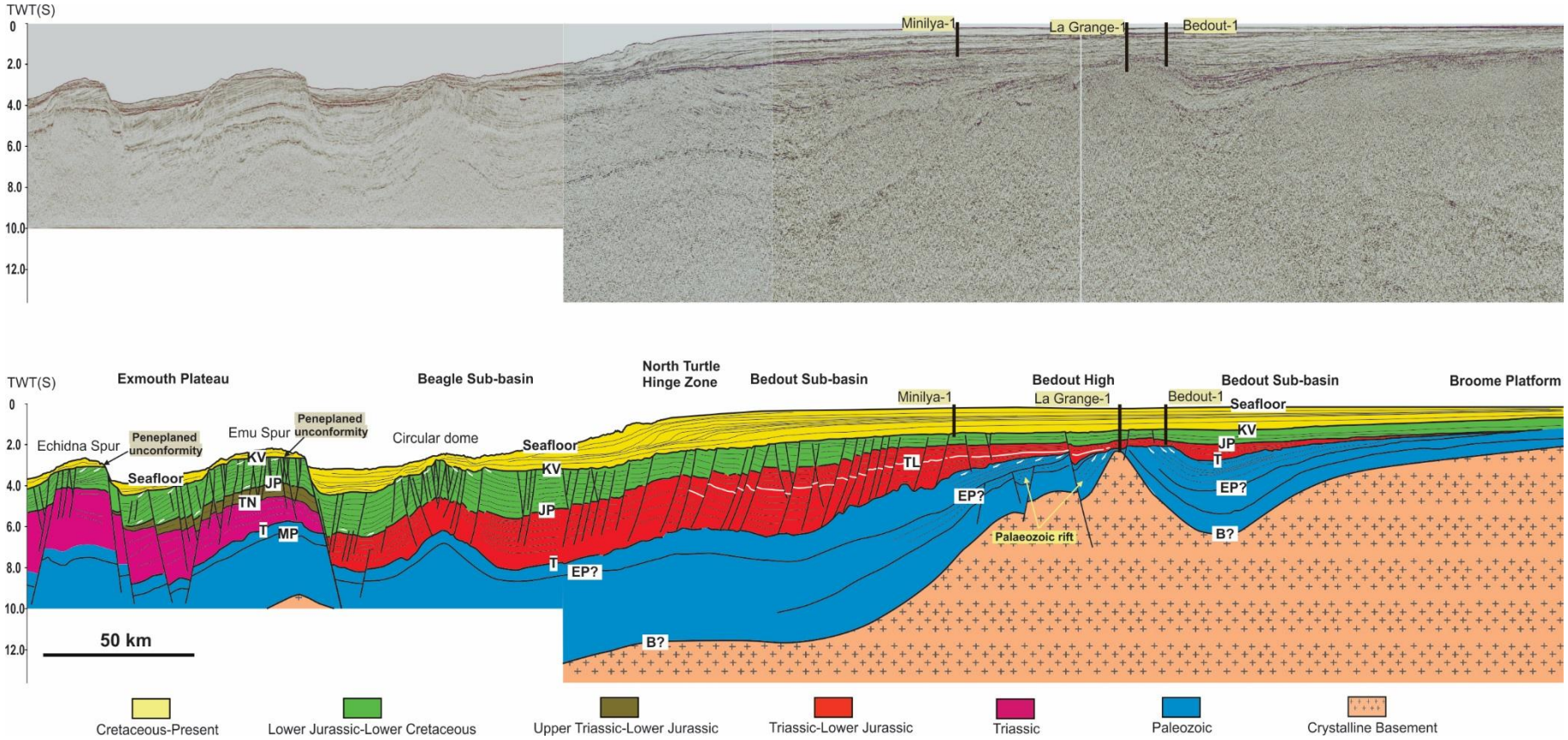

Figure 4-3. Composite seismic profile and its interpretation, showing the basin architecture across Broome Platform, Bedout Sub-basin, Bedout High, Beagle Sub-basin and Exmouth Plateau (see Figure for location). KV=Valanginian Unconf4-5ormity, JP= Pliensbachian Unconformity, TN=Norian Unconformity, TL=Ladinian Unconformity, T=Base Triassic Unconformity, EP=Early Permian, B=basement

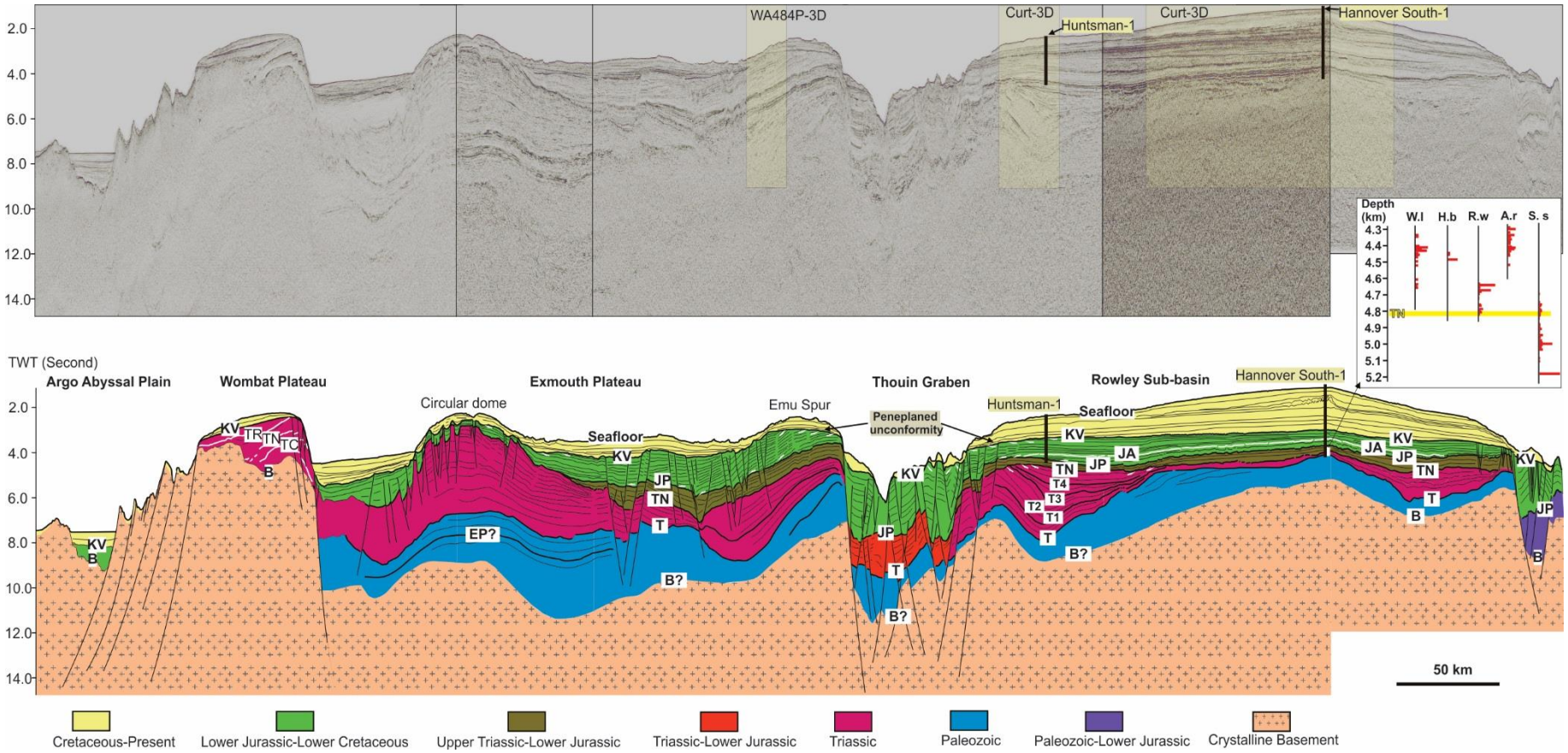

Figure 4-4. Composite seismic profile and its interpretation, showing the basin architecture across Rowley Sub-basin, Thouin Graben, Exmouth Plateau, Wombat Plateau and Argo Abyssal Plain (see Figure for location), and biostratigraphic constraints on the age of TN horizon. KV=Valanginian Unconformity, JP= Pliensbachian Unconformity, TN=Norian Unconformity, TL=Ladinian Unconformity, T=Base Triassic Unconformity, MP=Mid-Permian Unconformity, B=basement, W.l=W.listeri, H.b=H.balmei, R.w=R.wigginsii, A.r=A.reducta, S.s=S.speciousus.

detached into the lowermost of the Triassic succession (Figure 4-3, 4-6c). In the north part of the Beagle Sub-basin, close to the Exmouth Plateau, rift-related faults are present in both northeast- and north- trends, forming rhombic-shaped fault blocks.

Rowley Sub-basin

The Rowley Sub-basin is a northeast- trending elongate depocentre located in the northeast of the study area. It generally deepens towards the northwest at the base of Triassic horizon (T) (Figure 4-2, 4-5a). The Triassic succession (T-TN), which is equivalent to the Locker Shale, Keraudren Formation and Bedout Formation thins from the Broome Platform (<0.5 second TWT in thickness) to the outer Rowley Sub-basin (>4.5 second TWT in thickness) (Figure 4-2). Within the Triassic succession, irregular structures such as large clinoforms and circular structure are observed, which have become the debate topics recently (see Chapter 5 for details). On top of that, the Upper Triassic-Lower Jurassic Brigadier and North Rankin Formation (TN-JP) formed a consistent sedimentary sheet (0.3-0.5 second TWT in thickness). The Jurassic Murat, Athol and Legendre Formation (JP-KV) was deposited as gradually northwesterly thickening sedimentary wedges. However, the upper part of this succession in the outboard area close to present continental-oceanic crust boundary (COB) was significantly eroded as a result of the rift-shoulder uplift, forming a northwesterly thinning trend (Figure 4-2, Figure 4-6b). In the Rowley Sub-basin, a large population of Mesozoic rift-related extensional faults are interpreted with northwest-, north- and northeast- trends (Figure 4-6c).

Exmouth Plateau

On the northeast Exmouth Plateau, a few circular to elongate dome structures are present at the Triassic-Jurassic stratigraphic level, which partitioned the northeast Exmouth Plateau into highs and lows of varied geometries (Figure 4-5a-e). The elongate domes, which include the Emu Spur and Echidna Spur, are bounded by basement involved faults. The circular domes are not associated with basement faults, suggesting a different formation mechanism for them (Figure 4-3, 4-4). These dome structures are interpreted to be formed during the rift processes in the Oxfordian-Valanginian (JO-KV) (see Chapter 5 for details), thus had little syn-sedimentary controls on the stratigraphic architecture of pre-Oxfordian succession (T-JO). The southwest and central Exmouth Plateau is confirmed to have up to 6 km thick Triassic succession (AGSO Group, 1994). This study suggests the northeast Exmouth Plateau also has a thick Triassic succession (T-TN) that is equivalent to the Locker Shale and Mungaroo Formation. This succession is approximately 4.0 second TWT in thickness in the southwest of the study area and thins to less than 1.0 second TWT in thickness close to the Thouin Graben (Figure 4-4). Passing upward, the Upper Triassic-Lower Jurassic succession (Brigadier and North Rankin Formation, TN-JP) displays southwesterly thinning wedge,

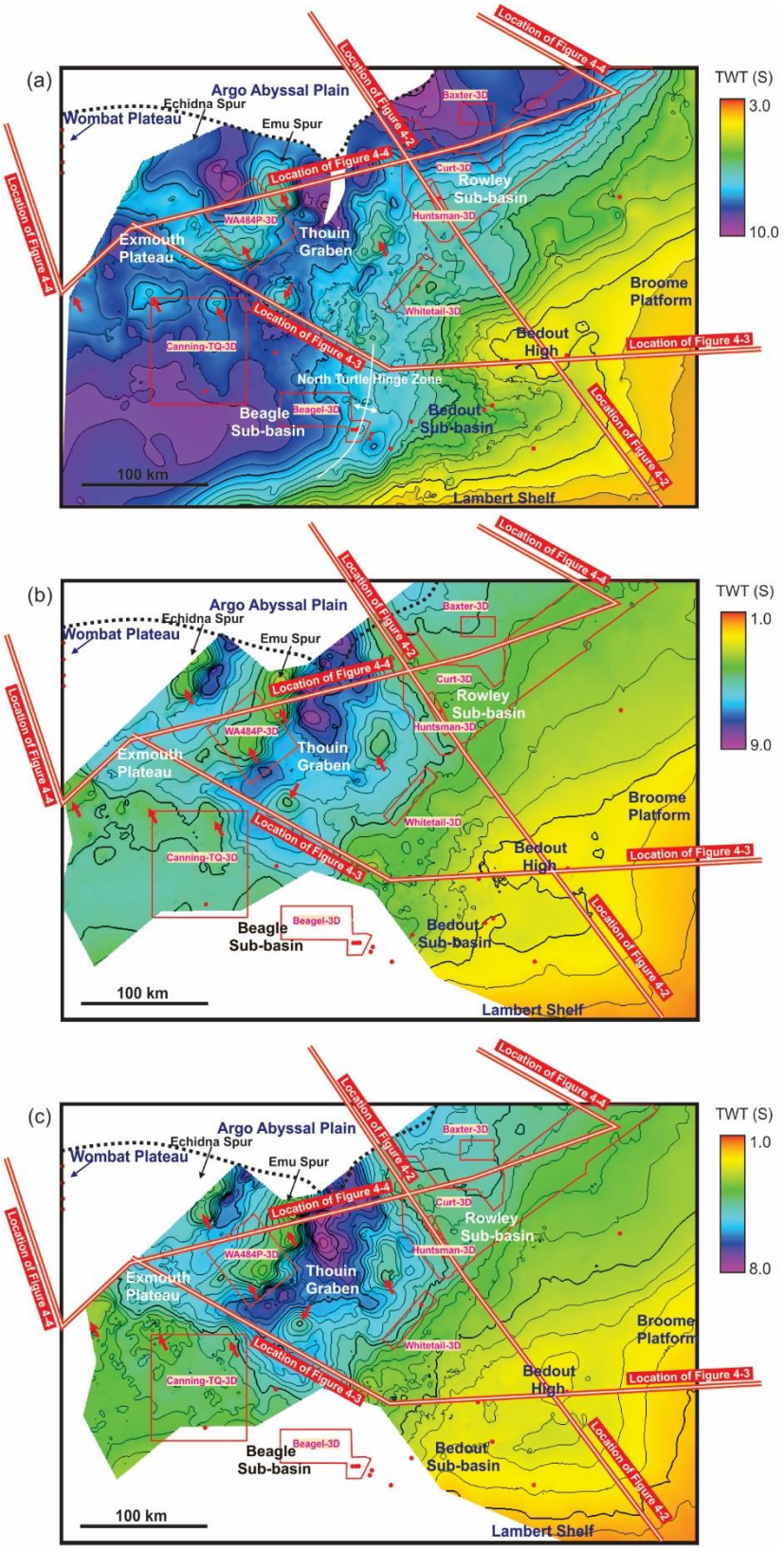

Figure 4-5. Two-way traveltime (TWT) structure maps showing basin geometry and architecture for a) Base of Triassic (T), b) Ladinian surface (TL) in the inboard and T4 in the outboard, c) Norian Surface (TN), d) Pliensbachian surface (JP), e) Aalenian surface (JA) and f) Valanginian Unconformity (KV) (see Figure 3-1 for the map location). The red polygons show the locations of 3D seismic data sets. Red dots represent well locations. Red arrows point to dome structures/uplifts. Locations for Figure 4-2, 4-3 and 4-4 are labelled.

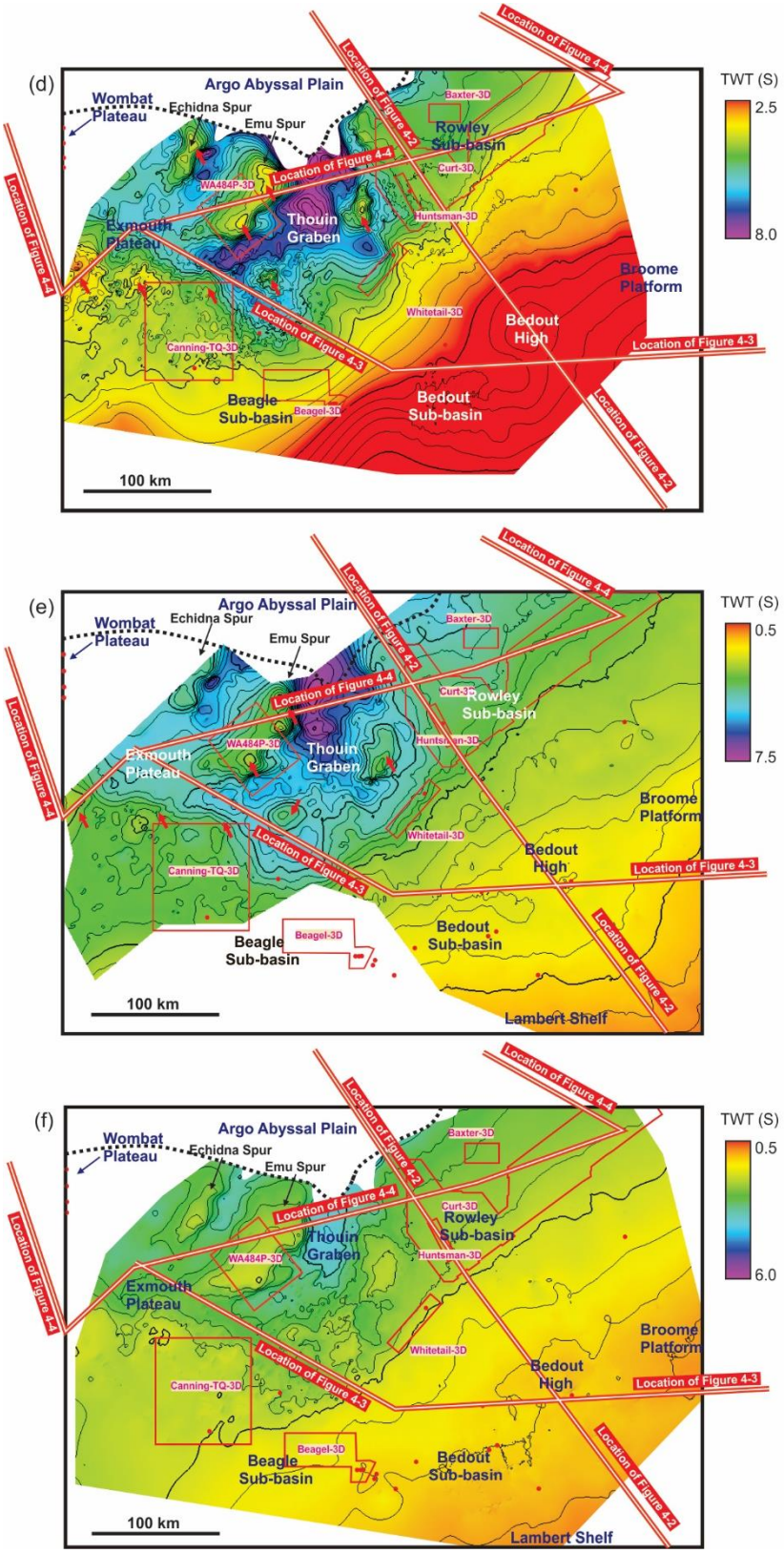

Figure 4-5. Continued

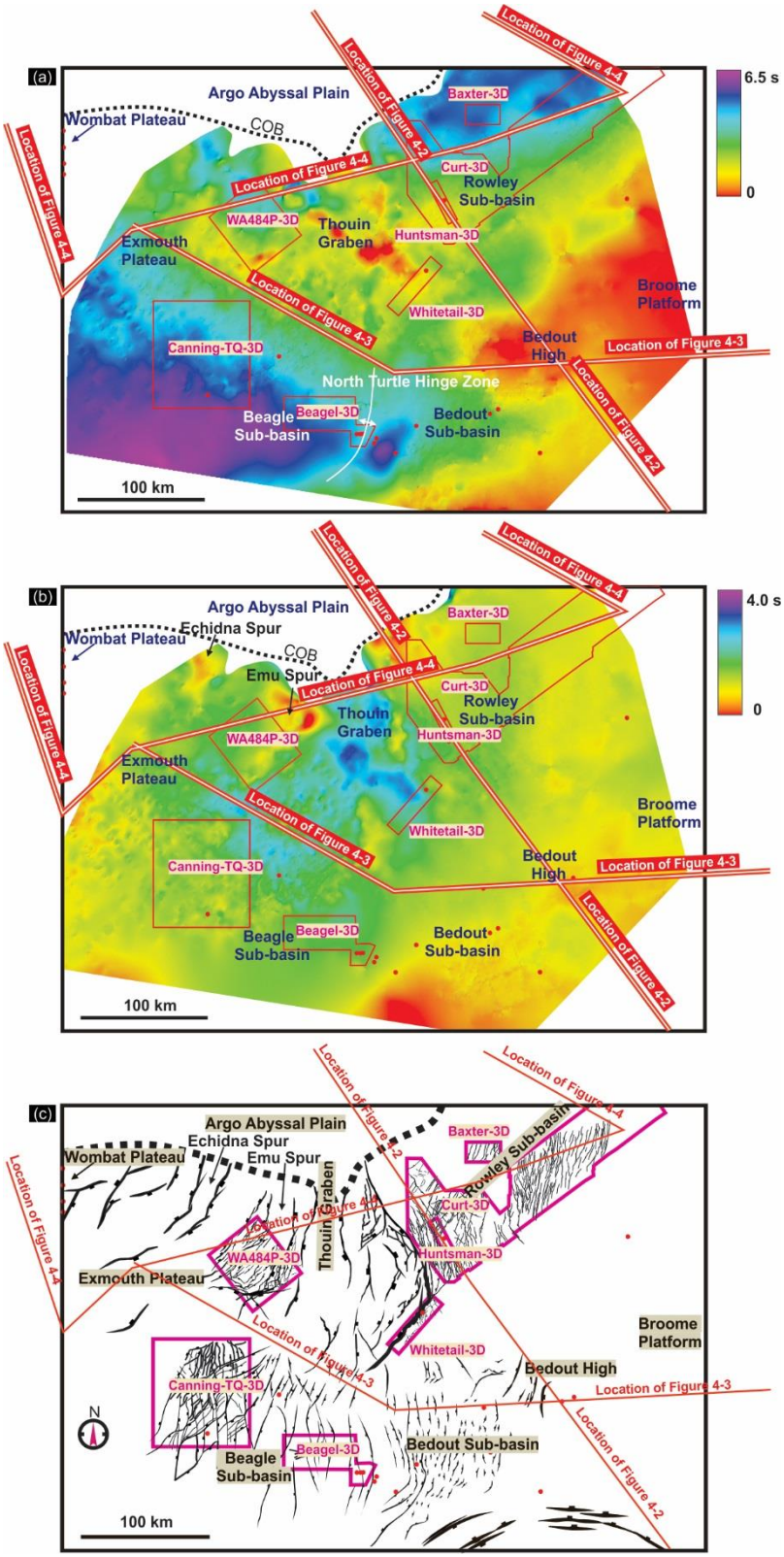

Figure 4-6. Isochron maps of the Traissic-Lower Jurassic Succession (T-JP) (a) and Lower Jurassic-Lower Cretaceous (JP-KV) (b) showing the major depocenters in Triassic and Jurassic respectively and map showing the major extensional faults interpreted in the study area (c). See Figure 3-1 for the map locations. The red polygons show the locations of 3D seismic data sets. Red dots represent well locations. Locations for Figure 4-2, 4-3 and 4-4 are labelled. The details of fault architecture are addressed in Chapter 5.

which is approximately 0.5 second TWT thick on the northeast limit of the Exmouth Plateau and pinches out towards the southwest (Figure 4-4). The Jurassic Murat, Athol and Legendre Formation formed a thick sedimentary cover (JP-KV) on the northeast Exmouth Plateau. The upper part of the Jurassic succession (JP-KV) was subject to the differential erosion associated with the formation of the dome structures (Figure 4-4). The northeast Exmouth Plateau is structurally dominated by a large number of northeast- trending rift-related extensional faults (Figure 4-6c).

Thouin Graben

The Thouin Graben is interpreted to be a graben that was bounded by northwest- to north-trending faults, which were formed in association with the rift processes during the Oxfordian-Valanginian. The relatively poor image of the seismic reflections hindered the interpretation of its geometry and internal stratigraphic architecture. It is conjectured to consist of a thin succession of Triassic-Lower Jurassic sediments (T-JP) (less than 1.0 second TWT). However, it hosts the thickest (over 3.0 second TWT) Jurassic-Lower Cretaceous succession (JP-KV) (Figure 4-4, 4-6b). On the flanks of the Thouin Graben, the upper part of the Jurassic-Lower Cretaceous succession (JP-KV) was significantly eroded, which is interpreted to be a result of rift shoulder uplift processes associated with the formation of Thouin Graben (Figure 4-4).

4.3 Discussion

The basin geometry and architecture indicate a few interesting findings:

1) Two major Triassic depocentres were present, the Bedout-Beagle Sub-basin in the south and the Rowley Sub-basin in the north. They were separated by a wide northwest- trending high in the central area, including northeast Exmouth Plateau, Thouin Graben, southern end of the Rowley Sub-basin and the Bedout High (Figure 4-6a). From the stratigraphic geometry, this high was seemingly formed in association with the Fitzroy Movement, represented by the Norian unconformity (TN) (Figure 4-4). The northwest trend of this highland suggests it was likely associated with the Canning Basin structure fabrics. The nature of the Fitzroy Movement has still to be resolved.

2) The basin high and low arrangement was reversed and the major depocentre shifted to the proximity of the Thouin Graben during the rift tectonics (Oxfordian-Valanginian), which is demonstrated by a much thicker Jurassic-Lower Cretaceous succession (JP-KV) in the Thouin Graben than the northeast Exmouth Plateau and the Rowley Sub-basin (Figure 4-4). This thickness difference was mainly associated with the strong erosion of the flanks of the Thouin Graben during the rift processes in the Oxfordian-Valanginian. The thickness map suggests that the Thouin Graben is mainly northwest-north- trending, whereas in the Northern Carnarvon Basin, basin-scale rift-related grabens were aligned in a northeast direction

(Exmouth, Barrow, Dampier and Beagle Sub-basin). This suggests strong variations in the rift processes across the North West Shelf.

3) The circular dome structures present anomalous structural elements, compared to the other parts of the North West Shelf. Their formation mechanism and influences on the structural architecture in the surrounding area are interesting research topics and will be discussed later.

The basin geometry and architecture of the Roebuck Basin and the adjacent northeast area of the Northern Carnarvon Basin show many differences to their counterparts, which indicate the uniqueness and complexity of the study area.

5 STRUCTURAL ARCHITECTURE

2D and 3D seismic interpretation has revealed different types of structures, mainly extensional faults and dome structures/basement highs. This Chapter presents a detailed description of the three-dimensional structural architecture in the study area. Emphases are put on the geometries, styles, architecture of the structural elements, and their geometric relationship with the host stratigraphy. These results are discussed with respects to the timing and kinematics of the formation of the structural elements and their implications for regional tectonics.

This study has identified a large population of extensional faults that have different ages and trends. They are divided into four different fault groups based on the principal time period of their formation. From older to younger, they are the Palaeozoic faults (Fault Group 1), Triassic faults (Fault Group 2), Early (-Middle) Jurassic faults (Fault Group 3) and (Middle?)-Late Jurassic and (Middle?) Late Jurassic-Early Cretaceous faults (Fault Group 4) (Figure 5-1). It is noteworthy that the geological time attached to this fault classification represents only the most important fault propagation period for each group and does not cover the whole time span of each fault's development. For example, the Triassic faults (FG 2) mean faults that were primarily formed in the Triassic. They may or may not have been inherited from the Palaeozoic faults (FG 1) and/or reactivated in the subsequent tectonics that were responsible for the formation of the Jurassic-Cretaceous faults (FG 3&4). Also, the faults in the same group were not necessarily formed at exactly the same time, which is largely due to the resolution of the stratigraphic correlations and the variabilities of the tectonics inherent in such a large area.

In addition to extensional faults, which are typical structural elements for rift-related basins or passive margins, several dome structures and one bowl-shaped structure have been identified (Figure 5-1). These irregular structures represent anomalous features of a passive margin derived from continental breakup and indicate the complexities of structural development of the study area.

5.1 Palaeozoic Faults (Fault Group 1)

The Palaeozoic faults are represented by rift structures interpreted from the Palaeozoic succession in the uplifted inboard area where Mesozoic sedimentary cover is thin, including the Lambert Shelf and the Bedout High (Figure 5-1). Due to the lack of 3D seismic coverage, the interpretation of the Palaeozoic faults is based on 2D seismic sections.

On the southern flank of the Bedout Sub-basin, several east-striking, north-dipping faults show clear Palaeozoic growth (presumably Carboniferous- Early Permian) and form a series

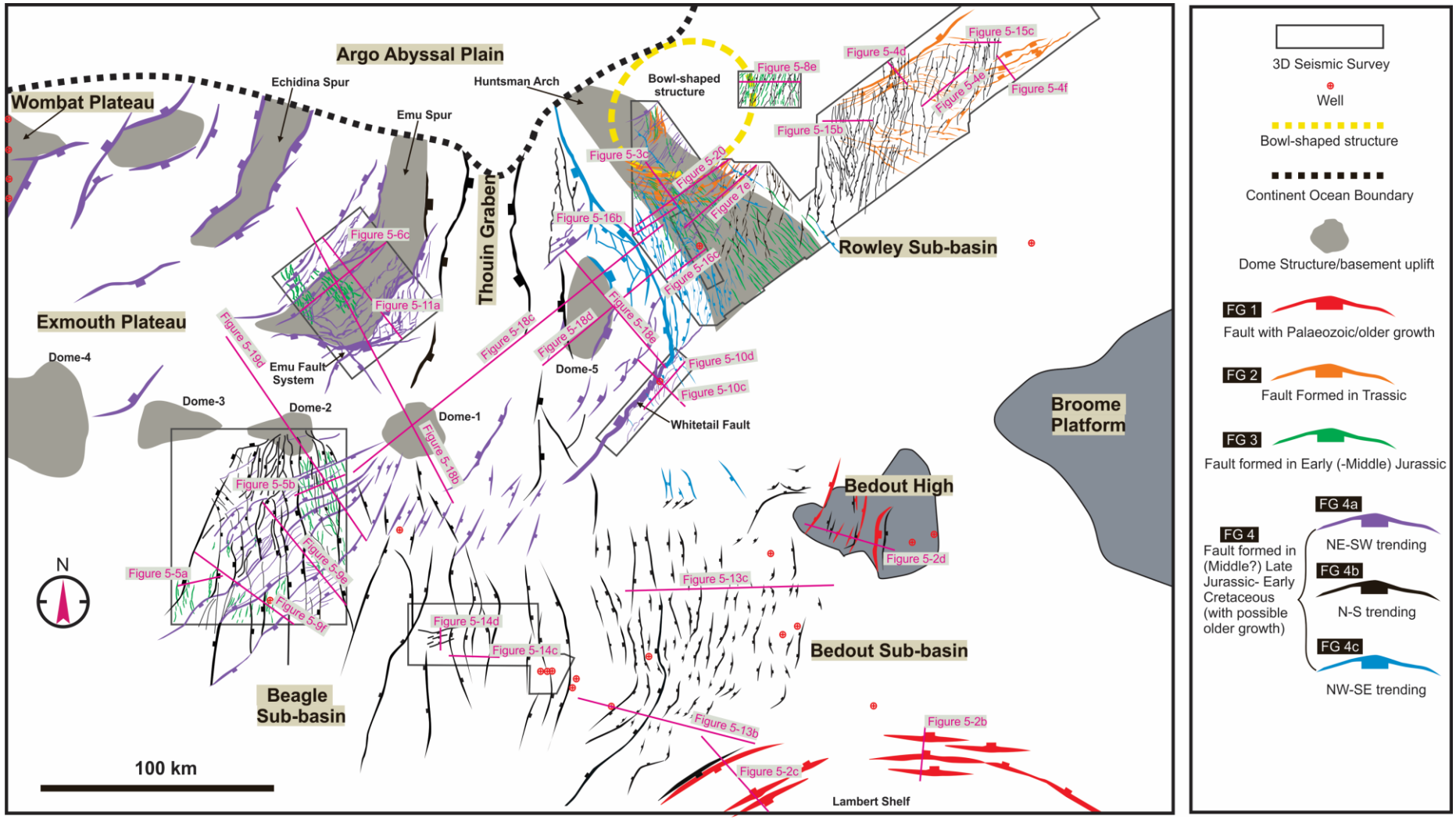
Argo Abyssal Plain
Wombat Plateau
Echidina Spur
Emu Spur
Huntsman Arch
Bowl-shaped structure
Thouin Graben
Rowley Sub-basin
Exmouth Plateau
Dome-4
Dome-3
Dome-2
Dome-1
Dome-5
Emu Fault System
Whitetail Fault
Broome Platform
Bedout High
Bedout Sub-basin
Beagle Sub-basin
Lambert Shelf
N
100 km
Figure 5-1a
Figure 5-1b
Figure 5-1c
Figure 5-1d
Figure 5-1e
Figure 5-1f
Figure 5-1g
Figure 5-2b
Figure 5-2c
Figure 5-2d
Figure 5-3c
Figure 5-4c
Figure 5-4e
Figure 5-4f
Figure 5-5a
Figure 5-5b
Figure 5-6c
Figure 5-7e
Figure 5-8e
Figure 5-10c
Figure 5-10d
Figure 5-11a
Figure 5-13b
Figure 5-13c
Figure 5-14c
Figure 5-14d
Figure 5-15b
Figure 5-15c
Figure 5-16b
Figure 5-16c
Figure 5-16d
Figure 5-18c
Figure 5-18d
Figure 5-19d
Figure 5-20
3D Seismic Survey
Well
Bowl-shaped structure
Continent Ocean Boundary
Dome Structure/basement uplift
FG 1
Fault with Palaeozoic/older growth
FG 2
Fault Formed in Trassic
FG 3
Fault formed in Early (-Middle) Jurassic
FG 4
Fault formed in (Middle?) Late Jurassic- Early Cretaceous (with possible older growth)
FG 4a
NE-SW trending
FG 4b
N-S trending
FG 4c
NW-SE trending

of "downstepping" to the north terraces at the Palaeozoic stratigraphic level (Figure 5-2a, b). The majority of these faults terminate upward at the Early-Permian Unconformity (EP). A few propagated into the Mesozoic succession due to the subsequent structural reactivation.

Further to the southwest, along the edge of Lambert Shelf, the Palaeozoic faults are mainly northeast- trending. Faults dipping both landwards and basinwards form large-scale graben and horst structures (~ 40 km wide) (Figure 5-2c). The Carboniferous-Early Permian succession in the graben thickens towards the graben boundary faults, suggesting the same fault development period. The graben-boundary faults cut into the Mesozoic succession, which represent reactivation during the subsequent Mesozoic tectonics, and new Mesozoic faults were developed within the grabens (Figure 5-2c).

On the Bedout High, the Palaeozoic faults are approximately north-northeast-striking according to 2D seismic data interpretation (Figure 5-2a). Graben, half-graben and westerly down stepping terraces are present at the Palaeozoic stratigraphic level (C-EP). The half-graben boundary fault was reactivated in subsequent tectonic events and propagated into the Mesozoic and Cenozoic succession.

Due to the scarcity of seismic coverage and limited data quality, detailed fault geometry and style of the Palaeozoic faults are unknown. Also, because of the uncertainty associated with the horizon ages, the timing of the development of these faults remains uncertain.

5.2 Triassic Faults (Fault Group 2)

In the Rowley Sub-basin (based on Curt-3D), a large number of faults were interpreted to be developed in the Triassic (FG 2) below the regionally recognizable Norian unconformity (TN). These Triassic faults are characterized by complex trends, with northeast-, west-northwest- and east- as the most common strike components (Figure 5-1). Four Triassic horizons (T1-T4) were interpreted in the Rowley Sub-basin below the Norian unconformity (TN), to help understand the development of these Triassic faults.

In the southwestern part of Rowley Sub-basin, a group of east-west trending, south-dipping domino-style extensional Triassic faults formed a series of half-grabens (ca. ~ 1km wide and ~20 km long) at the Triassic

Figure 5- 1. Map showing all the structural elements interpreted in the study area, with the locations of the 3D seismic surveys and wells. Extensional faults are widely interpreted and are divided into different groups, which are faults with Palaeozoic and older growth (red, Fault Group 1), faults formed in the Triassic (orange, Fault Group 2), faults formed in the Early (-Middle) Jurassic (Green, Fault Group 3), and faults formed in (Middle?) Late Jurassic-Early Cretaceous (northeast- trending [purple, Fault Group 4a], north- trending [black, Fault Group 4b] and northwest- trending [blue, Fault Group 4c]). Several basement highs and uplifted areas are identified (grey). A circular bowl-shaped structure is interpreted in the outboard of the Rowley Sub-basin. The locations of the seismic sections in this chapter are labelled.

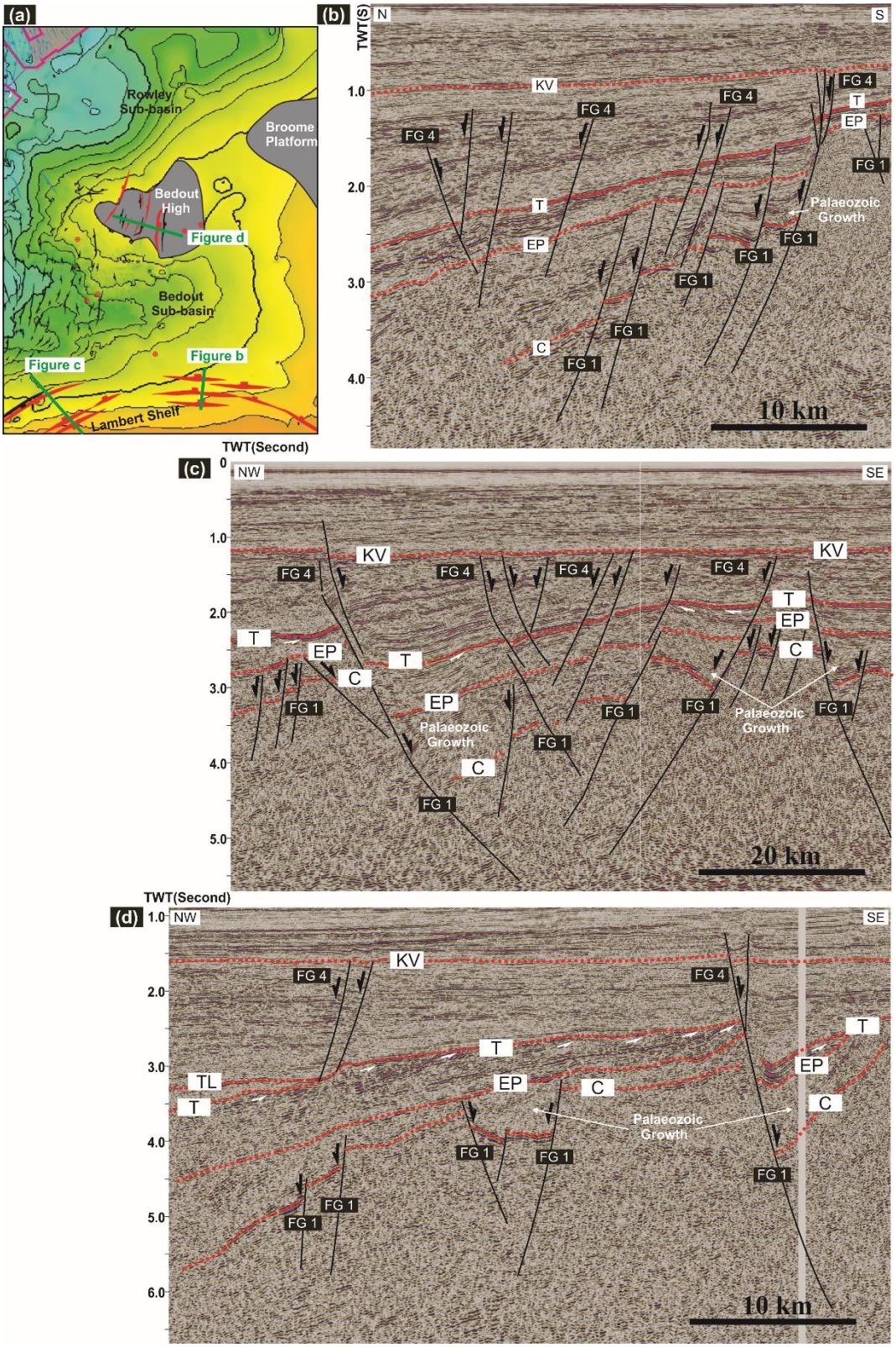

Figure 5-2. a) Two-way travel-time structure map of the base of Triassic horizon (T) of the Bedout Sub-basin and the adjacent area with Palaeozoic faults (red, Fault Group 1) and (Middle?)Late Jurassic-Early Cretaceous faults (black, Fault Group 4b); Seismic profiles with interpretation showing the Palaeozoic faults on the southern flank of the Bedout Sub-basin (b), the edge of the Lambert Shelf (c) and the Bedout High (d). EP=Early Permian unconformity, C= conjectured Carboniferous horizon.

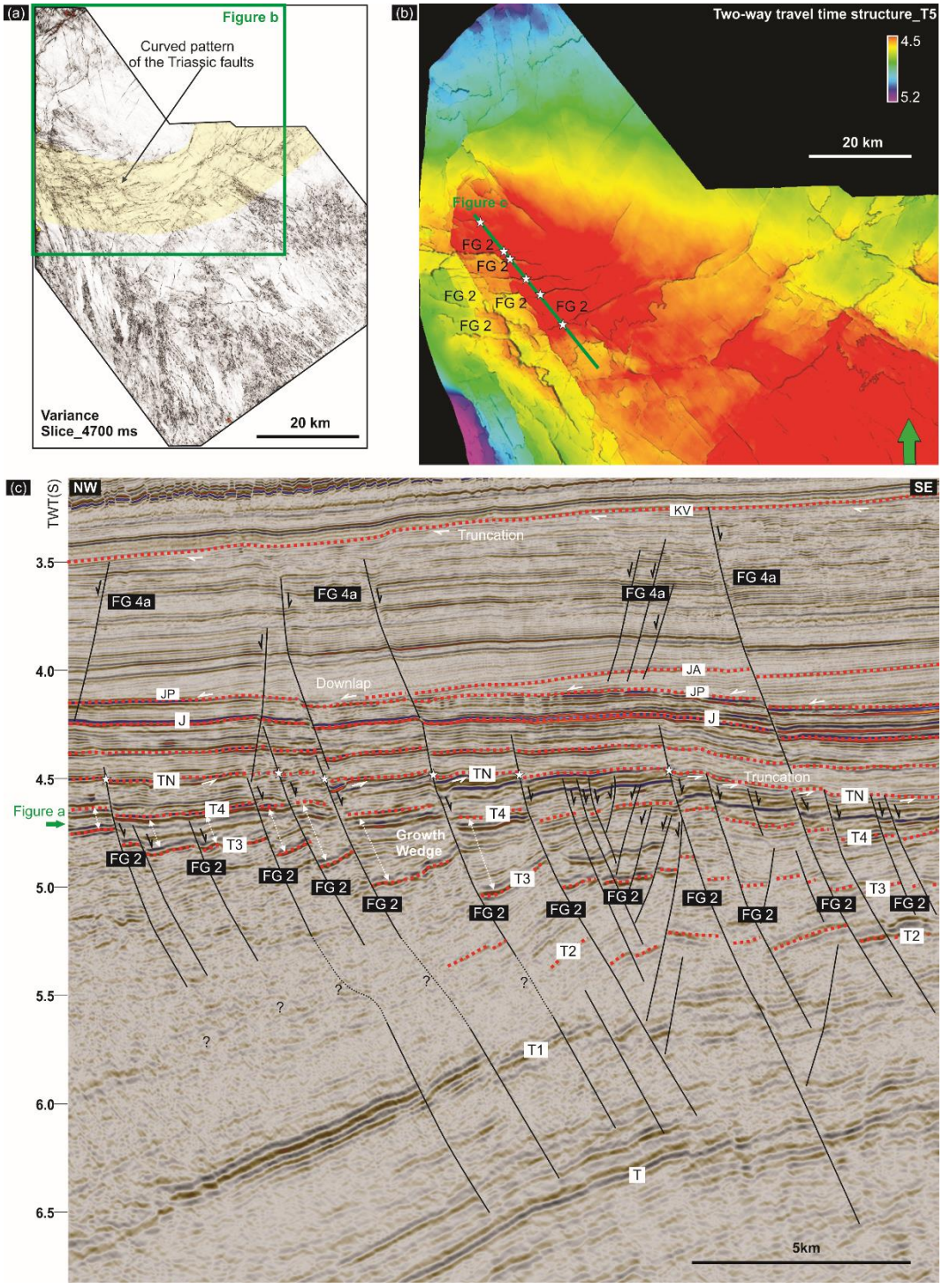

Figure 5-3. Variance slice at 4700 ms (a), two-way travel-time structure map of the Norian horizon (TN) (b) and a representative seismic section with detailed interpretation (c) showing the Triassic fault (Fault Group 2) architecture in the southwest Rowley Sub-basin

stratigraphic level (Figure 5-3). The Triassic succession (T3-T4) on the hanging-walls are rotated and divergent towards the controlling fault, which suggests a prominent stage of fault growth in this period. The T4 horizon, which shows little fault controlled rotation, represents the top boundary of the fault growth wedge, and thus marks the end of the Triassic extension. The overlying T4-TN succession also exhibits an obvious but lower-magnitude thickness

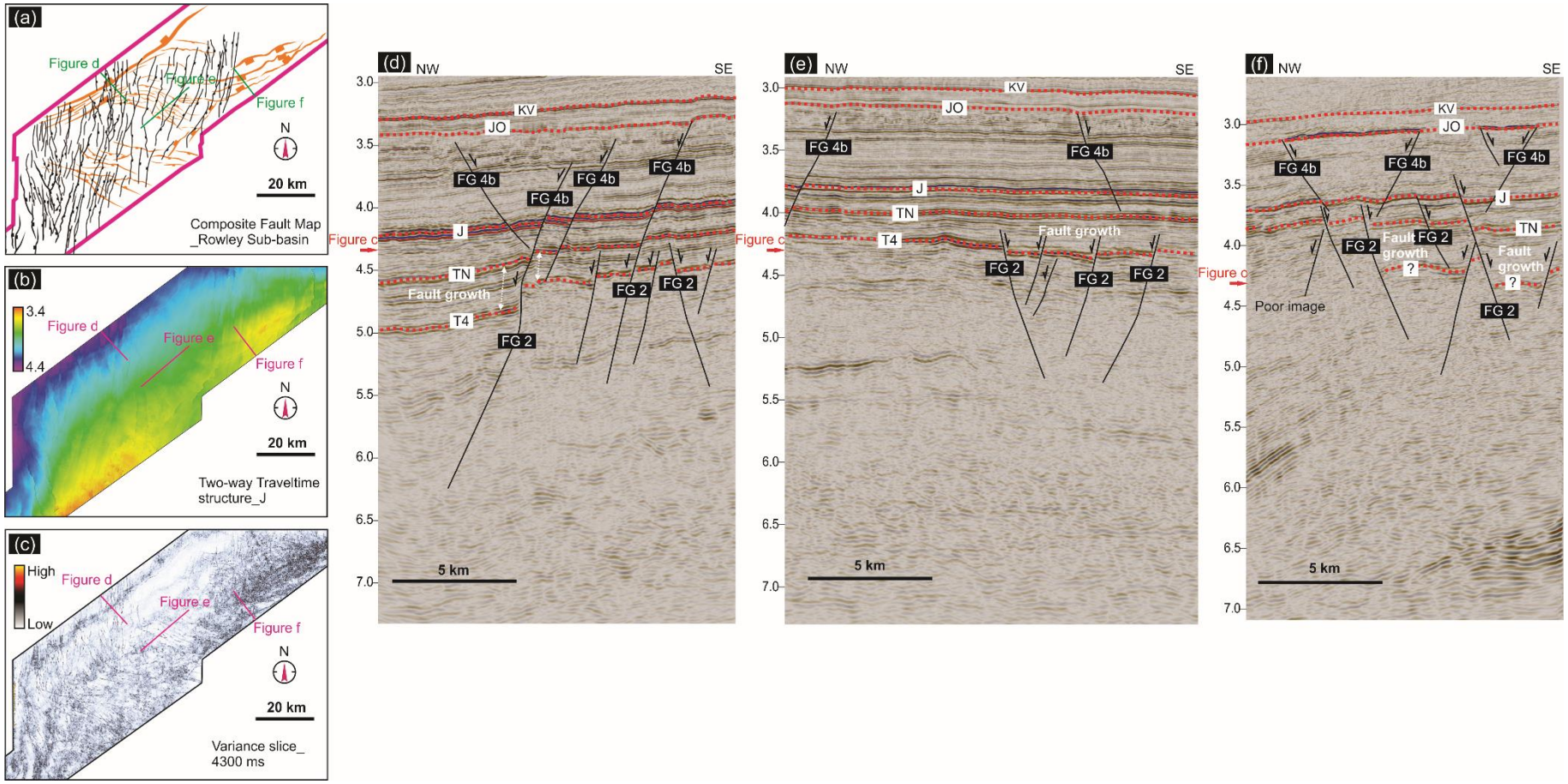

Figure 5-4. a) Composite fault map interpreted from the northeast part of Curt-3D in the Rowley Sub-basin (Triassic faults [Fault Group 2] in orange, ~Oxfordian faults [Fault Group 4b] in black); b) Two-way travel-time structure map of the Base of Jurassic (J); c) Variance slice at 4300 ms; d, e, f) Seismic sections showing the Triassic faults in the northeast Rowley Sub-basin.

change across these faults (relative to the T3-T4 succession). The reflections are parallel, suggesting limited syn-sedimentary fault growth during this phase. The Triassic faults (FG 2) terminate upward at the prominent Norian angular unconformity (TN) (Figure 5-3c). This suggests that the tectonic event associated with the Fitzroy Movement reactivated these Triassic faults and caused the differential erosion. A few Triassic faults (Fault Group 2) propagated upward into the TN-J succession due to subsequent reactivation. Downward, due to the poor quality of seismic image below T3, fault trajectories are difficult to interpret. However, a normal displacement component is observed on at the T1 horizon, suggesting these faults cut at least into the lower part of the Triassic succession (Figure 5-3c). A high-quality variance slice through the syn-kinematic succession shows that the area affected by the Triassic faults is characterized by a high density of fault segments (Figure 5-3a). The fault strikes change from east-west trending in the west of the area to northeast-southwest trending in the east, forming a concave-outboard curved fault zone. This curved fault pattern is interpreted to be controlled by a pre-existing bowl-shaped structure (see Chapter 5.6.4 for details).

In the northeast area of the Rowley Sub-basin, the Triassic faults (FG 2) consist of a set of west-northwest- trending faults that are soft linked with two sets of northeast-trending faults (Figure 5-4a). The upper tips of these faults are mainly located in the T4-TN succession, which shows obvious thickness change across these faults (Figure 5-4d, e, f). This suggests a phase of growth (T4-TN) for these Triassic faults. Due to the poor imaging below T4, it is difficult to know whether these faults have pre-T4 growth. A few northeast-trending Triassic faults propagated upward into the Jurassic succession, suggesting a reactivation in the Jurassic extension (Figure 5-4b, d, f).

5.3 Early (-Middle) Jurassic Faults (Fault Group 3)

Fault Group 3 comprises a large population of Early (-Middle) Jurassic faults that are characterized by minor displacement (~ 20 ms) and length (~ 10 km). They are interpreted in the Beagle Sub-basin (Canning TQ-3D), northeast Exmouth Plateau (WA484P-3D) and Rowley Sub-basin (Curt-3D, Baxter-3D). They display varied strikes (north-, northwest-), and their ages are presumably different from area to area (from Early Jurassic to Middle Jurassic).

In the Beagle Sub-basin, a group of north-trending faults (FG 3) are interpreted to cut the Triassic-Lower Jurassic succession. They show planar geometry, within their upper tips mainly located right above the Pliensbachian horizon (JP) (Figure 5-5a, b). These faults are relatively small and segmented (normally 5-10 km in length) and have very subtle displacement (~20 ms). There are no evident growth wedges associated with the Early Jurassic faults (Figure 5-5a, b). On a variance map of the Pliensbachian horizon (JP), the Early Jurassic

faults are distinguished from the large scale Late Jurassic-Early Cretaceous faults by their small-scale and segmented nature (Figure 5-5d). The majority of the Early Jurassic faults were presumably reactivated during subsequent rift tectonics and developed into larger north-trending (Middle?)-Late Jurassic and (Middle?) Late Jurassic-Early Cretaceous faults (see Chapter 5.4).

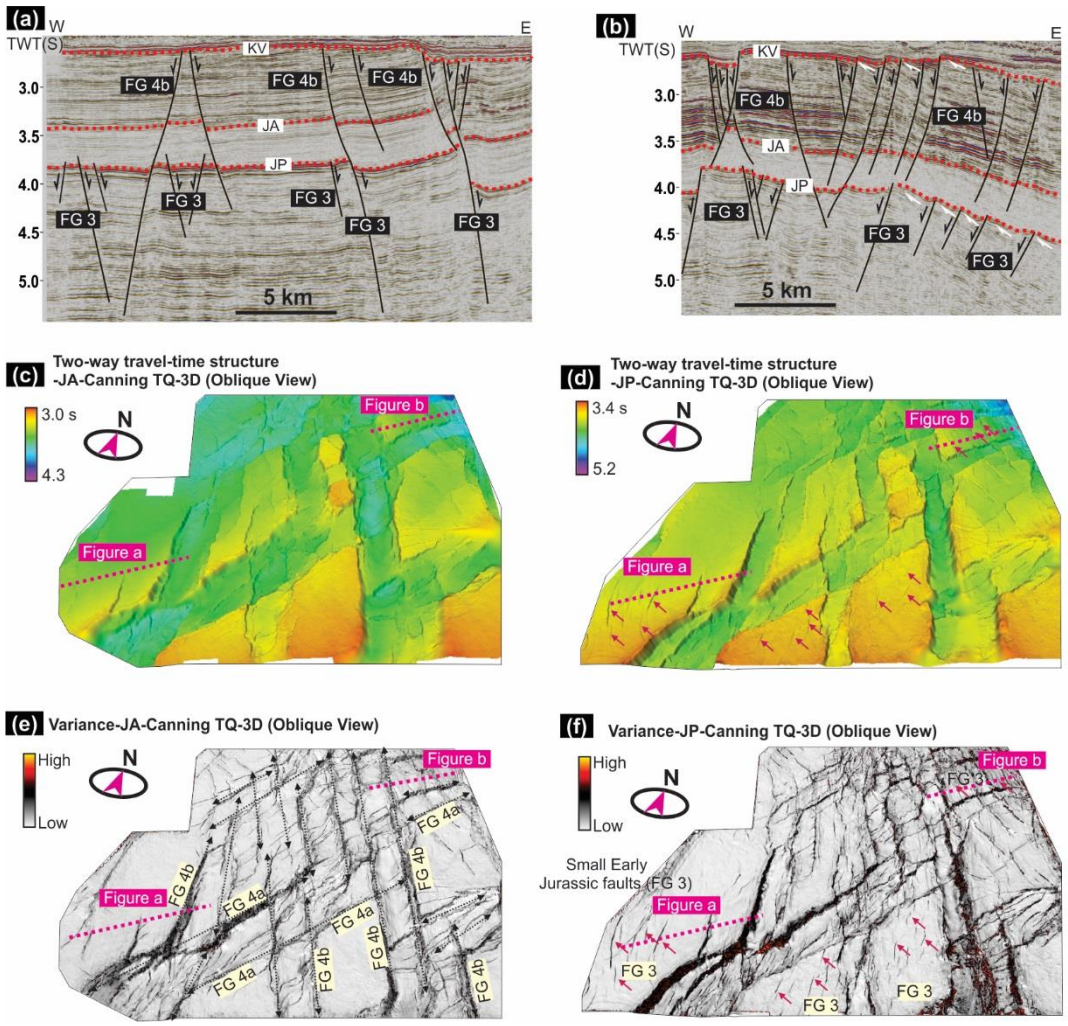

Figure 5-5. Seismic sections with interpretations (a, b), two-way travel-time structure maps (oblique view) (JA [c], JP [d]) and variance maps (oblique view) (JA [e], JP [f]) of the Canning-TQ-3D seismic survey showing the fault architecture in the northern Beagle Sub-basin. The area is cut into rhombic-shaped compartments by the northeast- trending (Fault Group 4a) and north- trending (Fault Group 4b) ~Oxfordian and Oxfordian-Valanginian faults (details are shown in Figure 5-9). A set of the north- trending Early Jurassic faults are interpreted to cut the Lower Jurassic-Triassic stratigraphy (Fault Group 3, red arrows).

On northeast Exmouth Plateau, the Early Jurassic faults (FG 3) strike northwesterly and are interestingly aligned with two northwest- trending corridors (Figure 5-6a, b). They range from approximately 2 to 6 km in length with displacements up to 20 ms (Figure 5-6c). The Early Jurassic faults in this area are slightly listric, with their tips terminated upward at the Pliensbachian horizon (JP) or located in the succession from J to JP. There is no growth wedge associated with them. These faults are interpreted to be formed in the period represented by the Pliensbachian horizon (JP). The Pliensbachian horizon is a Maximum Flooding Surface

and represents a highly condensed succession that may have a long time span (Early-Middle Jurassic) on the northeast Exmouth Plateau (see Chapter 6 for details). Thus, the age of these faults can only be constrained to Early-Middle Jurassic.

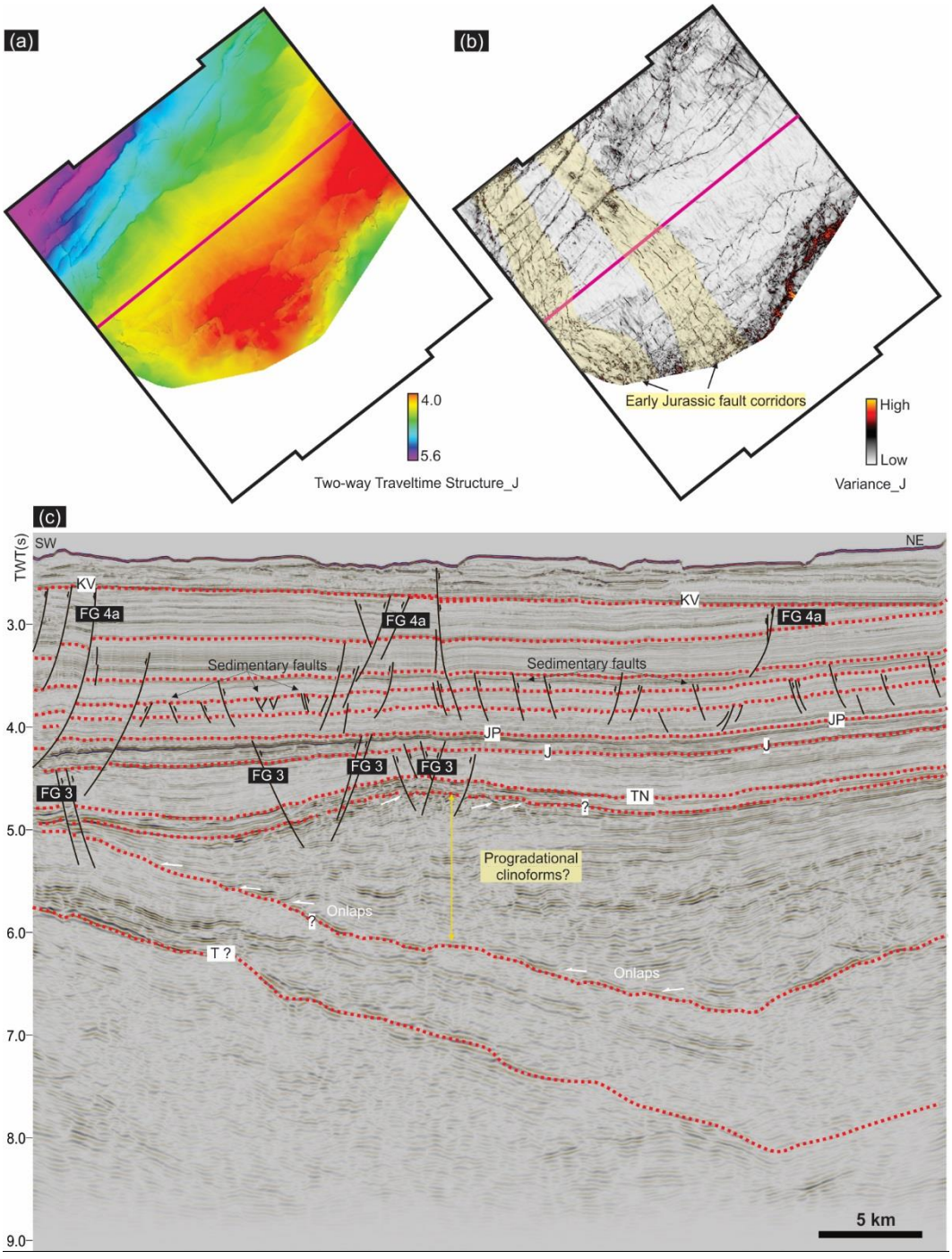

Figure 5-6. Two-way travel-time structure (a) and variance (b) of the Base of Jurassic surface map, and a representative northeast-southwest trending seismic section of the WA484P-3D seismic survey (c), showing the stratigraphic and structural architecture on the northeast Exmouth Plateau. A set of northwest- trending Early Jurassic faults (Fault Group 3) are aligned with two northwest- trending corridors. A group of small listric sedimentary faults are interpreted in the Jurassic succession.

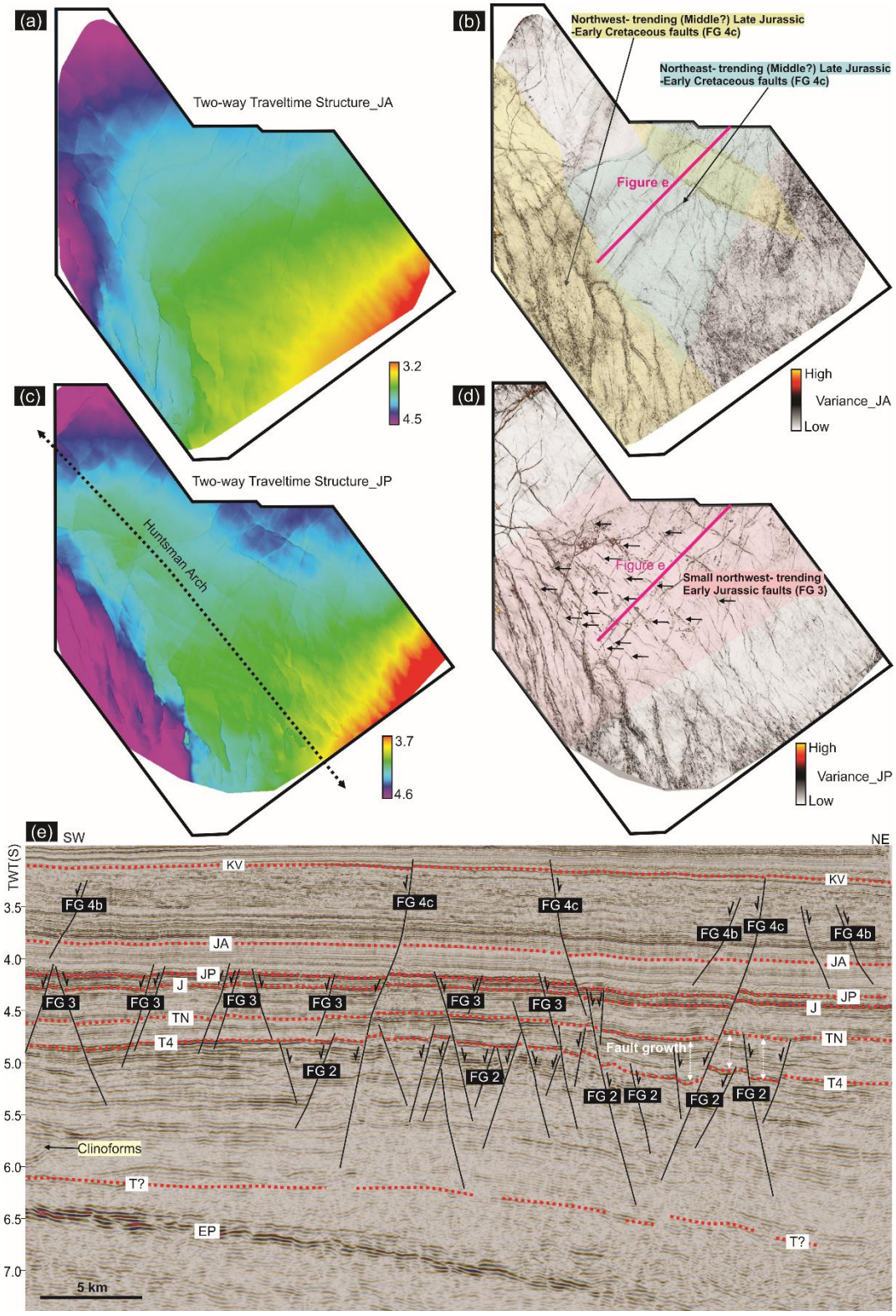

Figure 5-7. Surface maps of the Aalenian horizon (JA) (a, two-way travel-time structure; b, variance) and the Plienbachian horizon (JP) (c, two-way travel-time structure; d, variance) and a representative seismic section with interpretation (e) showing the structural architecture in the southwest part of the Rowley Sub-basin. The maps show the larger northeast- (FG 4a), northwest- (FG-4b) trending (Middle?) Late Jurassic-Early Cretaceous faults, and highly segmented Early Jurassic faults (FG 3). Triassic faults (FG 2) are interpreted on the seismic section. EP=Early Permian. See Figure 4-1 for the age of other horizons.

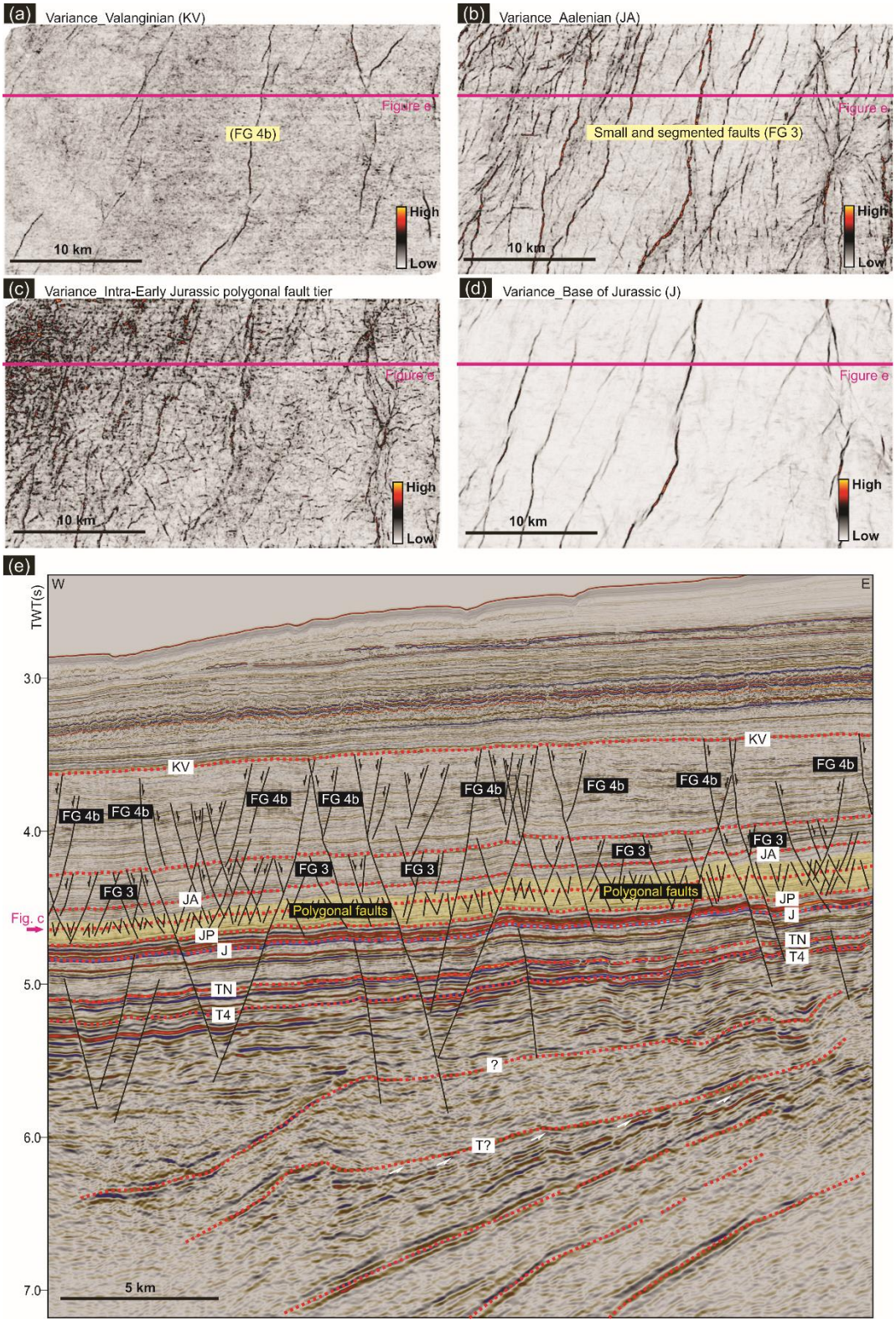

Figure 5-8. Variance map of the Valanginian (a), Aalenian (b), an intra-Early Jurassic horizon (c) and the base of Jurassic (d), and a representative east-west trending seismic section (with interpretation) of the Baxter-3D survey, showing the structural architecture in the outboard area of the Rowley Sub-basin. They illustrate the large north- trending (Middle?) Late Jurassic-Early Cretaceous faults (FG 4b), smaller segmented Middle Jurassic faults (FG 3) and a set of Early Jurassic polygonal faults. See Figure 5-1 for seismic section location.

In the southern part of Rowley Sub-basin, the Early Jurassic faults (Fault Group 3) are northwest- trending and show strong alignment with the northwest- trending Huntsman Arch

(Figure 5-7). They are highly segmented with average length of 5-10 km (Figure 5-7d). They have a planar geometry and cut the Lower Jurassic-Triassic succession with displacement up to 30 ms (Figure 5-7e). Most of them have their upper tips located right above the Pliensbachian horizon (JP). Downward, these Early Jurassic faults are detached at various Triassic stratigraphic levels.

In the outer area of Rowley Sub-basin (Baxter-3D), a population of north-trending faults are interpreted to cut the Lower-Middle Jurassic succession (FG 3) (Figure 5-8). They are characterized by highly dense fault segments that extend to ~10 km in length with a displacement up to 20 ms (Figure 5-8b, e). No growth wedges are associated with these segmented north- trending Jurassic faults (FG 3). The majority have their upper tips terminating at a horizon in the Middle Jurassic succession (Figure 5-8e), suggesting they have a Middle Jurassic age, which distinguishes them from the Early Jurassic faults in this Fault Group.

In the northeast part of the Rowley Sub-basin (northeast of Curt-3D), interestingly, no Early-Middle Jurassic faults are interpreted.

5.4 (Middle?)-Late Jurassic and Late Jurassic-Early Cretaceous Faults (Fault Group 4)

The structural deformation in the study area is dominated by the extensional faults that were formed in association with continental breakups during the Late Jurassic-Early Cretaceous. Detailed 3D seismic interpretation revealed a highly complex rift-related fault architecture, which is comprised of northeast-southwest (FG 4a), north-south (FG 4b) and northwest-southeast (FG 4c) trending faults (Figure 5-1). For each of the sub-group (4a, 4b, 4c), a proportion of faults terminate upward at the Oxfordian Unconformity and the rest terminate upward at the Valanginian unconformity, in areas where the two unconformities (JO and KV) can both be interpreted. However, for most of the study area, these faults terminate upward at the unconformity that represents a sedimentary gap of Oxfordian-Valanginian. The growth of the faults that terminate at the Oxfordian Unconformity where it can be distinguished from the Valanginian Unconformity clearly ended in the Oxfordian (early part of the Late Jurassic). However, whether they have Middle Jurassic growth remains unclear because of strong erosion of the upper part of the Middle Jurassic succession. In the following description, ~Oxfordian faults refer to the faults terminating at the Oxfordian Unconformity and Oxfordian-Valanginian faults refer to the faults that terminate at the Valanginian Unconformity and display growth during the period of Oxfordian-Valanginian. For areas where the two unconformities cannot be distinguished, faults could have ~Oxfordian and/or Oxfordian-Valanginian ages, and thus are named (Middle?) Late Jurassic-Early Cretaceous

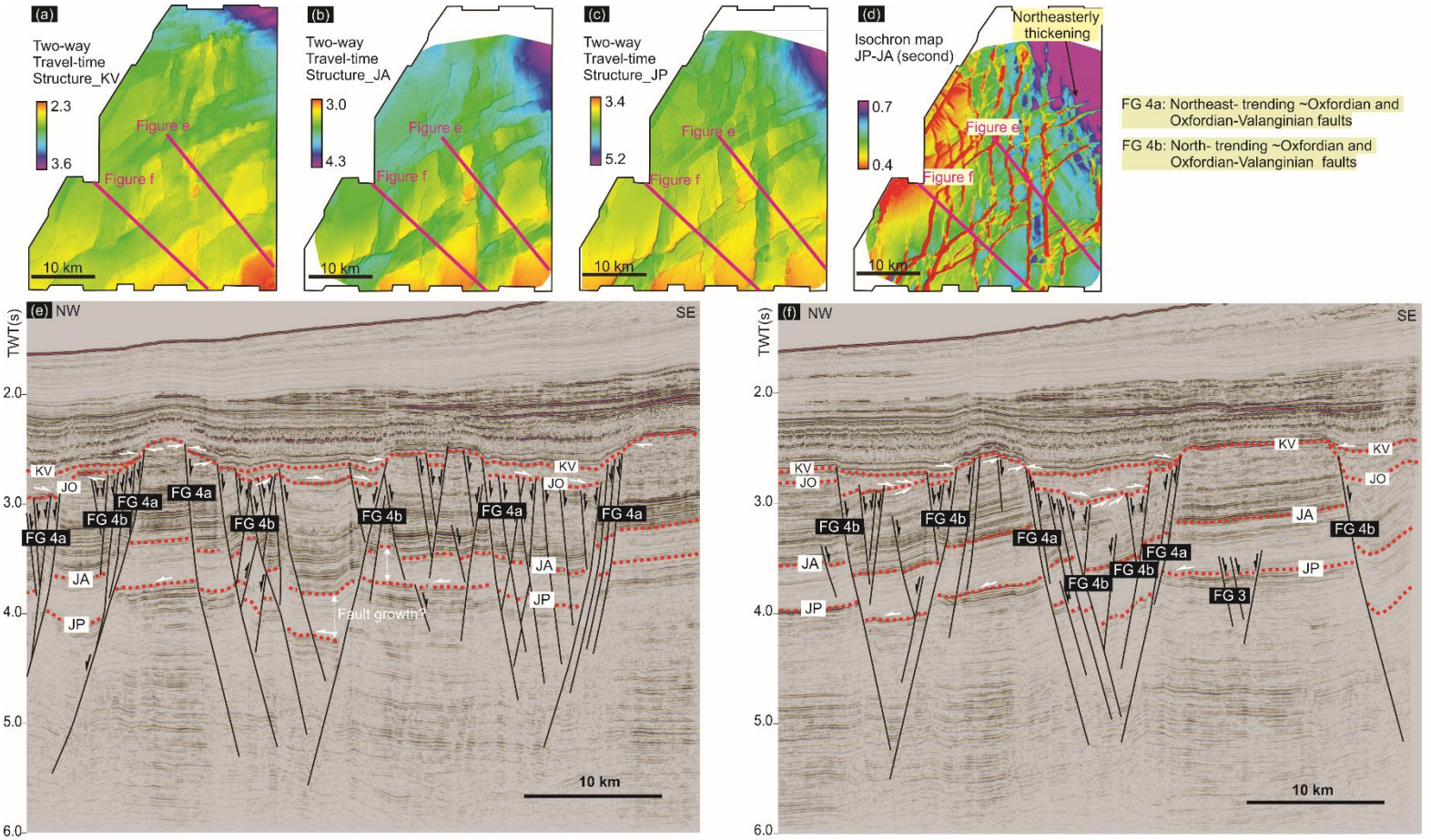

Figure 5-9. Two-way travel-time structure map of the Valanginian (a), Aalenian (b) and Plienbachian (c) and two representative seismic sections with detailed interpretation (c, d) of the Canning-TQ-3D survey, showing the structural architecture in the northern Beagle Sub-basin. The northeast- trending (FG 4a) and north- trending (FG 4b) ~Oxfordian and Oxfordian-Valanginian faults cut the area into rhombic-shaped compartments. See Figure 5-1 for the locations.

faults. It is noteworthy that faults in this group, though mainly attributed to the continental drift during the Oxfordian-Valanginian, may be inherited from or at least influenced by the previously mentioned older faults (FG 1, 2, 3). Some of them were reactivated during subsequent post-rift tectonics.

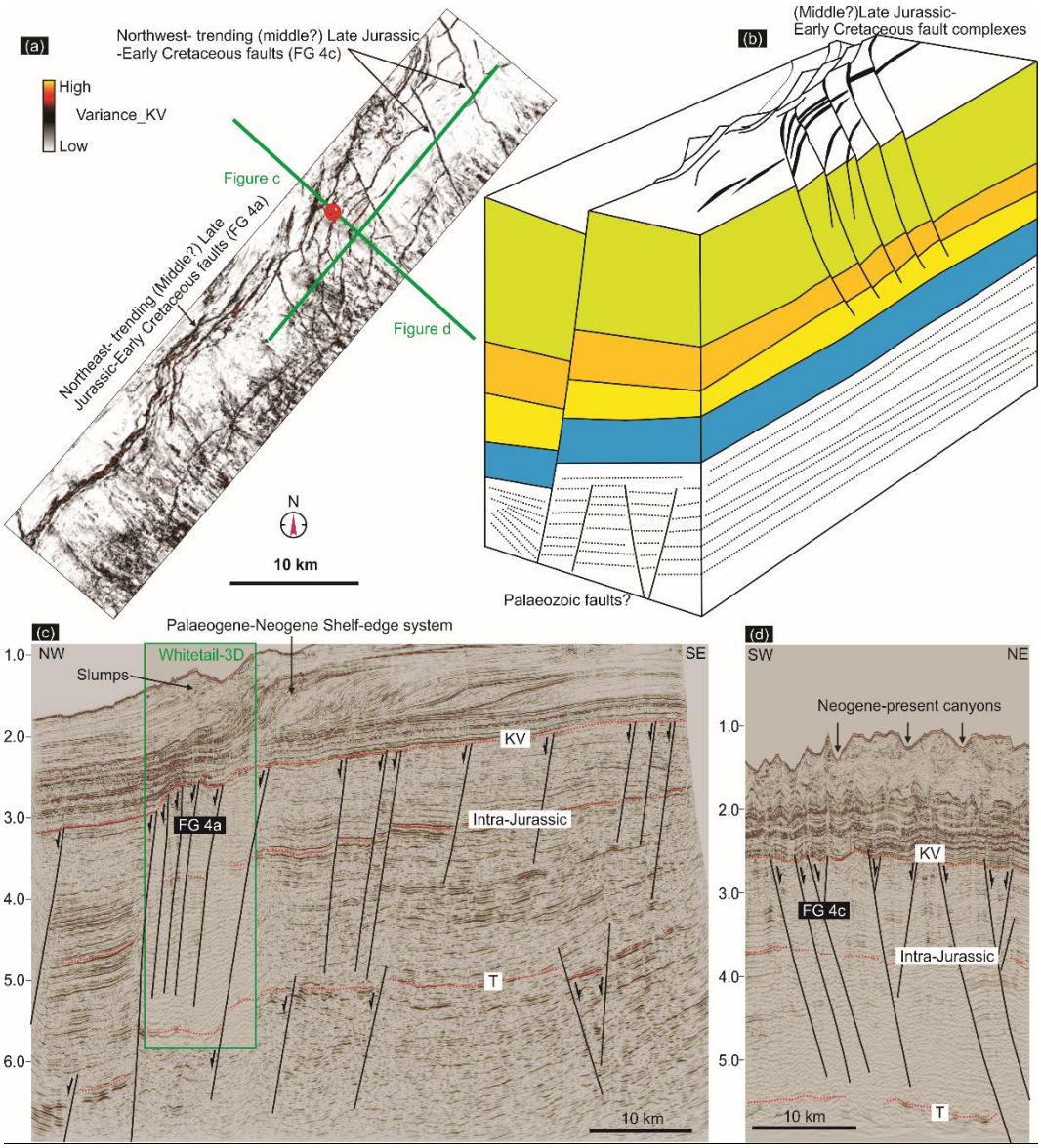

Figure 5-10. Variance map of the Valanginian Unconformity of the Whitetail-3D seismic survey (a), a three-dimensional schematic cartoon block (b) and two representative seismic sections with interpretation (c, d), showing a large fault damage zone (Whitetail Fault) formed by northeast- trending (Middle?)Late Jurassic-Early Cretaceous faults (FG 4a), which are linked with a group of northwest- trending Late Jurassic-Early Cretaceous faults (FG 4b). See Figure 5-1 for section locations.

5.4.1 Northeast-southwest trending faults (Fault Group 4a)

Northeast-southwest trending (Middle?)-Late Jurassic and (Middle?) Late Jurassic-Early Cretaceous faults (FG 4a) are identified in Beagle Sub-basin, northeast Exmouth Plateau and Rowley Sub-basin. They display planar or slightly listric geometry and cut the Lower

Cretaceous-Triassic succession with their upper tips terminating at either Oxfordian unconformity (JO) or the Valanginian Unconformity (KV).

The Beagle Sub-basin (Canning-TQ-3D survey area) was cut into rhombic-shaped compartments by the northeast- trending (FG 4a) and the north- trending (FG 4b) ~Oxfordian and Oxfordian-Valanginian faults (Figure 5-5c, d, 5-9a-d). Putting aside the north- trending faults (FG 4b), the northeast- trending faults (FG 4a) form northeast- oriented horst and graben structures. The grabens are ca. 5 km wide and extend tens of kilometres along strike. These northeast- trending faults display slightly listric geometry and cut the Triassic-Lower Jurassic succession (Figure 5-9e, f). The majority of the northeast- trending faults have their upper tips terminating at the Oxfordian Unconformity (JO). However, the graben boundary faults terminate upward at the Valanginian Unconformity (KV) and show growth during the Oxfordian-Valanginian, which controlled the simultaneously deposited syn-rift succession (Figure 5-9e, f). Downlaps on the Oxfordian Unconformity (JO) and onlaps against the fault scarps are widely associated with the syn-kinematic succession.

In the Whitetail-3D area, a set of overlapping northeast- trending, northwest- dipping (Middle?) Late Jurassic-Early Cretaceous faults (FG 4a) bundled together and formed a sinuous fault zone (Figure 5-10). This zone separates the Bedout Sub-basin from the Thouin Graben (Figure 5-1) and also controlled the location of the post-rift (Palaeogene-Neogene) carbonate shelf-slope transition (Figure 5-10c). Because of the artefacts of the complex post-rift carbonate architecture, the imaging of the Jurassic-Triassic succession in the Whitetail-3D seismic survey is poor quality. However, it is clear on the 2D seismic section that these northeast- trending faults are detached into the Palaeozoic succession (below T, Figure 5-10c). A few older faults, presumably with a Palaeozoic-Triassic age, are also present in the area. This may suggest the northeast- trending sinuous fault zone represents reactivated Palaeozoic structures.

On northeast Exmouth Plateau (WA484P-3D), northeast-southwest trending faults (FG 4a) are the dominant structural elements (Figure 5-11). They form three large-scale structural elements, the Thouin Graben in the southeast, the Central Horst in the middle and the Northern Slope to the northwest. These faults on the Central Horst terminate upward at a peneplained unconformity that represents a sedimentary hiatus from Oxfordian-Valanginian. There is no syn-extension sediment recorded on the Central Horst (Figure 5-11a). The Emu Fault System, which separates the Thouin Graben from the Central Horst, is a fault complex comprised of northeast-trending faults, with minor north- and northwest-trending faults. Several mini grabens and half-grabens are present on the Northern Slope (Figure 5-11b, c, d), within which syn-extension successions were deposited during the Oxfordian-Valanginian, which suggests that these northeast- trending faults were at least active during the same period (see Chapter

6 for details of the seismic facies and geomorphology of the syn-extension succession [Oxfordian-Valanginian] in the area).

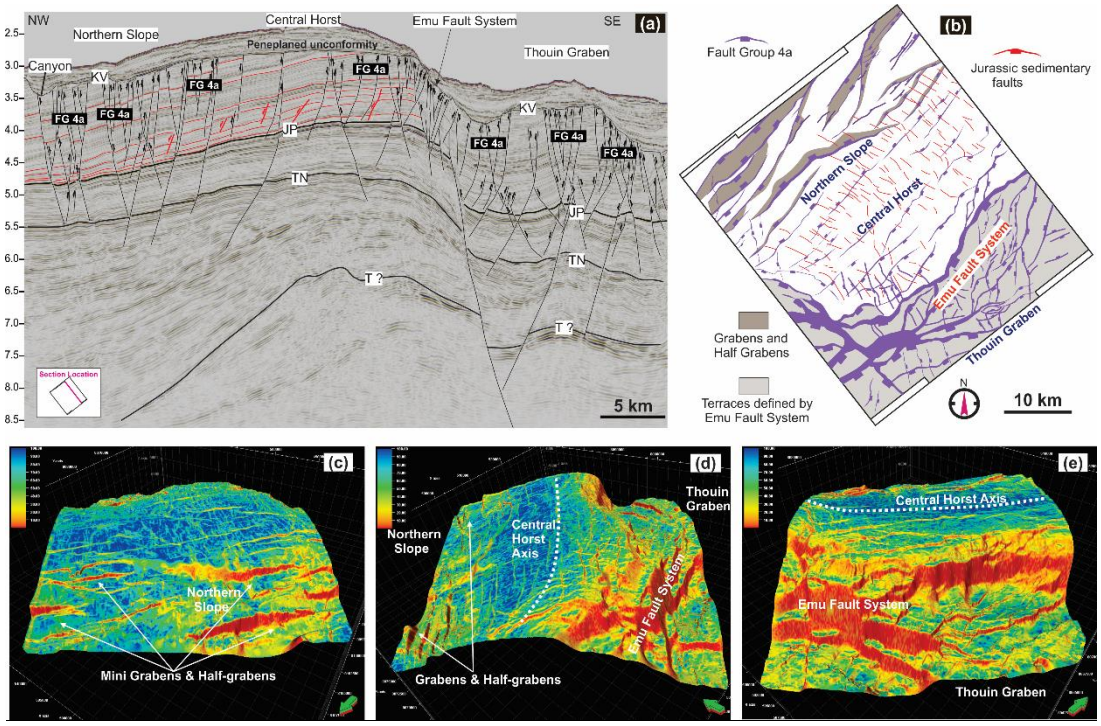

Figure 5-11. A representative seismic section through the WA484P-3D seismic survey with detailed interpretation showing structural and stratigraphic architecture (a); Detailed interpretation of fault architecture of WA484P-3D seismic survey area with schematic fault displacement profile (b); Oblique views of Edge-detection attribute map of the Pliensbachian Maximum Flooding Surface (JP-MFS)(c, d, e). A large population of northeast- trending (Middle?) Late Jurassic-Early Cretaceous faults (black, FG 4a) are interpreted. They define a northeast- trending horst (the Central Horst) in the middle, and the Thouin Graben to the southeast and a northwesterly dipping slope to the north (the Northern Slope). A set of small northwest- trending Jurassic faults are interpreted as sedimentary faults (red).

In the Rowley-Sub-basin, northeast-southwest trending faults (FG 4a) only account for a small proportion of the (Middle?) Late Jurassic-Early Cretaceous faults (FG 4) (Figure 5-1, 5-7b, d). They are mainly present in the southern part of Rowley Sub-basin and are characterized by fault segments that are ca. 5-10 kilometre long. In cross section, the faults mainly cut the Jurassic-Triassic succession (Figure 5-3c). The majority of the faults have their upper tips at the major unconformity that records Oxfordian-Valanginian sedimentary hiatus. The northeast- trending faults in the Rowley Sub-basin are not associated with syn-kinematic succession. This is likely due to 1) the corresponding extensional event is either weaker or shorter in the Rowley-basin; 2) the southern part of the Rowley Sub-basin received limited syn-tectonic succession (JO-KV)(see Chapter 6 for details). Detailed fault displacement analysis suggests the northeast- trending (Middle?) Late Jurassic-Early Cretaceous faults are characterized by a single displacement peak along strike and down dip with the maximum displacement located in the centre of the faults plane (Figure 5-12). This suggests these faults had grown radially from a central point in a consistent stress field with little influences of pre-existing structures.

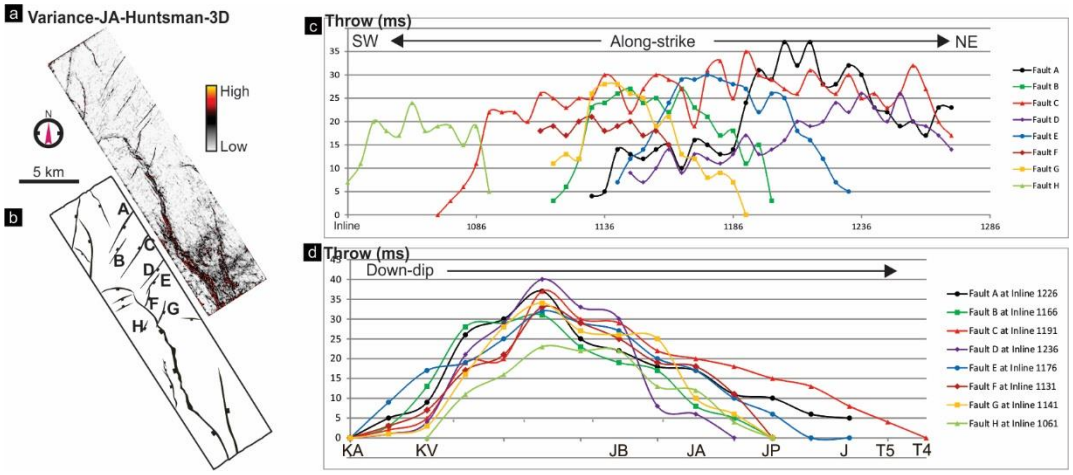

Figure 5-12. Variance map (a) and the fault map (b) of the Valanginian Unconformity (KV) of the Huntsman-3D seismic survey, along-strike (c) and down-dip (d) displacement analysis of the northeast- trending (Middle?) Late Jurassic-Early Cretaceous faults (FG 4a) in the southwest Rowley Sub-basin.

5.4.2 North-south trending faults (Fault Group 4b)

The north-trending faults (FG 4b) are the most dominant faults in the study area. They are widely interpreted in the Bedout, Beagle, and Rowley Sub-basin (Figure 5-1). Faults in this group show planar to slightly listric geometry and cut the Lower Cretaceous-Triassic succession. They mostly terminate upward at the major unconformities associated with the rift tectonics during the Oxfordian-Valanginian (JO-KV).

In the Bedout Sub-basin, the north-trending extensional faults (FG 4b) are evidently detached into a package of low-amplitude reflections, which are interpreted to correspond to the Locker Shale (Figure 5-13). The majority of the north-trending faults are west dipping, which is attributed to the westerly deepening detachment. At the location where detachment dip is greatest, large-scale rollover anticlines are developed in association with the detachment faults (Figure 5-13b). A set of synthetic and antithetic subsidiary faults are developed in association with the rollover anticline and form a graben system on the crest of the anticline. These crestal faults, similar to most of the north- trending faults in the area, terminate upward at the Oxfordian Unconformity (JO), suggesting a ~Oxfordian age. A few, e.g., the faults that control the rollover anticline, were active in the period from Oxfordian-Valanginian (JO-KV), which is demonstrated by the thickness change of the syn-tectonic succession (JO-KV) (Figure 5-13b). It is interesting that some of the faults in the Bedout Sub-basin also exhibit growth packages in the pre-Oxfordian succession. The Middle-Upper Triassic succession (TL-J) displays significant thickness change across these faults, which suggests a Triassic growth (Figure 5-13b). The Lower-middle Jurassic succession (J-JO) also shows prominent thickness change, which is likely to be attributed to 1) fault growth in the Middle Jurassic (pre-Oxfordian) and 2) differential erosion associated with the Oxfordian tectonics. Several faults display Early Triassic growth, demonstrated by fault-controlled thickness change of the

Lower Triassic succession (T-TL) (Figure 5-12c). The fact that they are detached into the Palaeozoic succession (below T) suggests the likelihood of the reactivation of pre-existing Palaeozoic faults (FG 1).

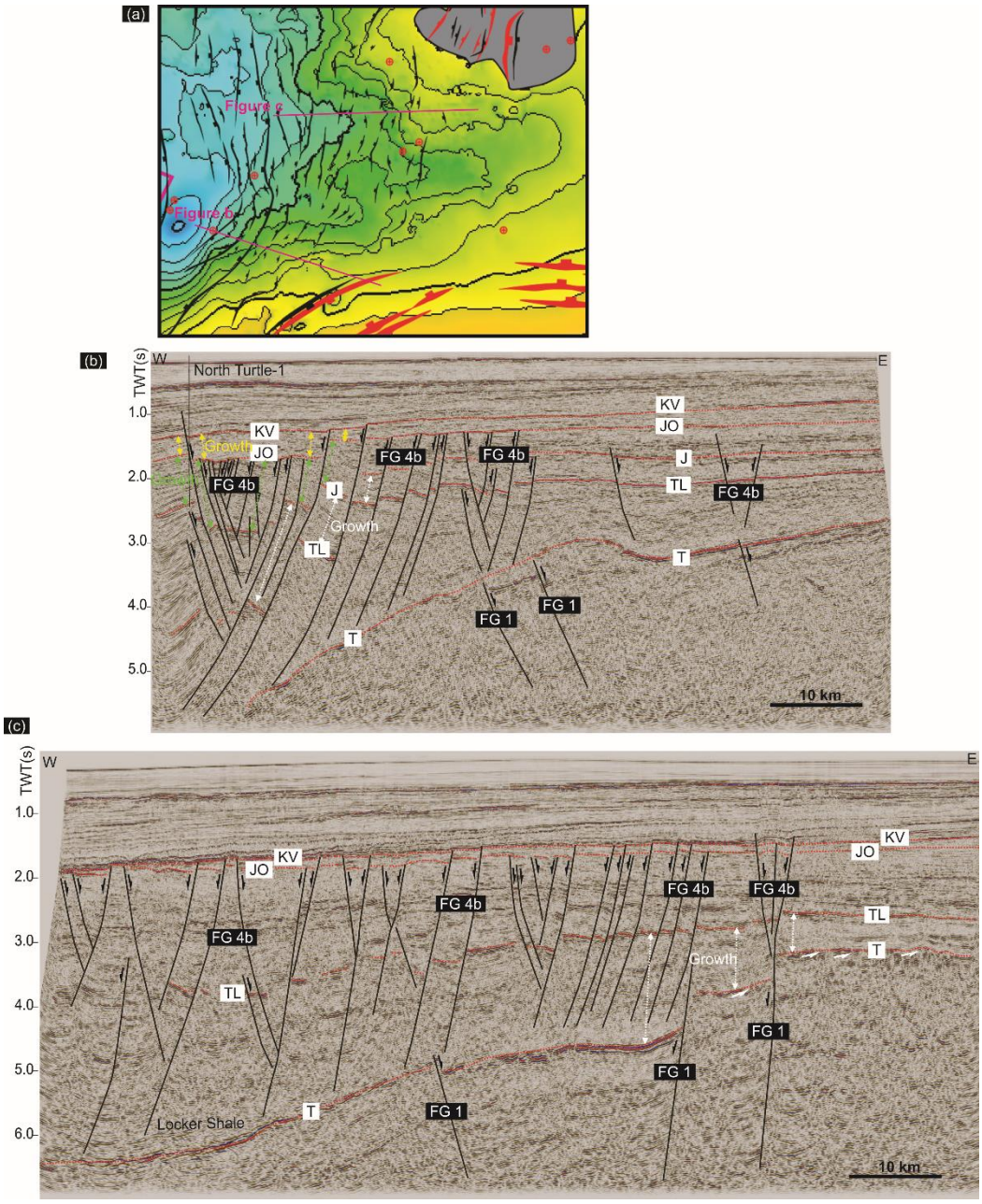

Figure 5-13. a) Two-way travel-time structure map of the base of Triassic horizon of the Bedout Sub-basin, with faults interpreted in the area; b, c) two east-west trending seismic sections (with interpretation) showing the architecture of the north- trending ~Oxfordian and Oxfordian-Valanginian faults (FG 4b). The interpretation suggests that the faults have a long growth history from the Triassic to the Early Cretaceous, which differ from the faults in the outboard area. See Figure 5-1 for the locations of the sections.

In the Beagle-3D survey area, the Locker Shale equivalent succession (detachment) is less steeply dipping (Figure 4-5a). More north- trending faults (FG 4b) dip landwards compared with the Bedout Sub-basin, and large-scale (tens of kilometres wide) north- trending horst-graben structures are formed (Figure 5-14). Similar to faults in the Bedout Sub-basin, the

majority of the north- trending faults terminate upward at the Oxfordian Unconformity (~Oxfordian faults), with graben boundary faults propagating into the Lower Cretaceous succession and terminating at the Valanginian Unconformity (Oxfordian-Valanginian faults). The syn-tectonic succession (JO-KV) shows fault controlled thickness variation. However, the pre-Oxfordian growth package is difficult to identify due to the data quality.

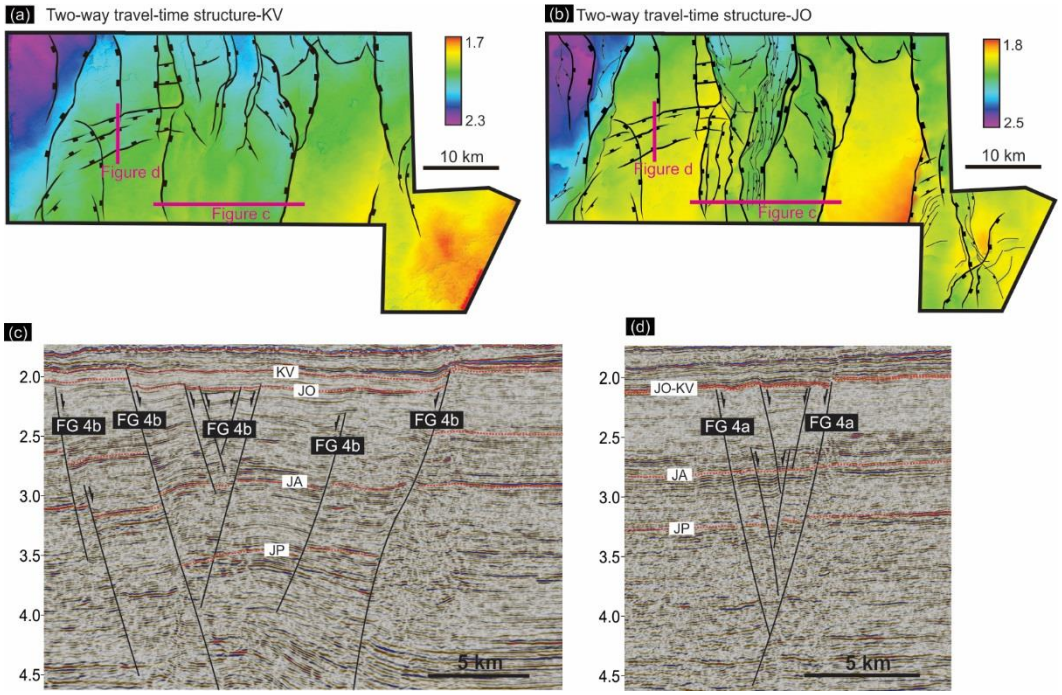

Figure 5-14. Two-way travel-time structure map of the Valanginian (a) and Oxfordian (b), and two representative seismic sections (c, d) of the Beagle-3D seismic survey, showing the architecture of the northeast- trending (FG 4a) and north- trending (FG 4b) ~Oxfordian and Oxfordian-Valanginian faults in the Beagle Sub-basin. See Figure 5-1 for locations.

Further to the west, in the Canning TQ-3D survey area, the north-trending faults (FG 4b), together with the northeast- trending faults (FG 4a) formed rhombic-shaped compartments (Figure 5-9a-d). Some north- trending faults in the area show Oxfordian-Valanginian growth (Oxfordian-Valanginian faults) and the rest terminate upward at the Oxfordian Unconformity with no clear growth packages (~Oxfordian faults) (Figure 5-9e, f). The Lower Jurassic succession (JP-JA), which is characterized by low-amplitude reflections, also shows a minor thickness change across these north- trending faults (Figure 5-9e, f). This Early Jurassic growth presumably corresponds to the formation of the north- trending Early Jurassic faults (FG 3) in the area (Figure 5-5).

In the Rowley Sub-basin, north-trending extensional faults (FG 4b) are well developed (Figure 5-1, 5-15a). In the outer area (Baxter 3D), they cut the Jurassic-Triassic succession with their tips terminating at a major unconformity that represents a hiatus of Oxfordian-Valanginian (Figure 5-8). In the inner Curt-3D survey area, where the syn-tectonic succession (JO-KV) is preserved, the upper tips of the north-trending faults (FG 4b) are located in the Cretaceous

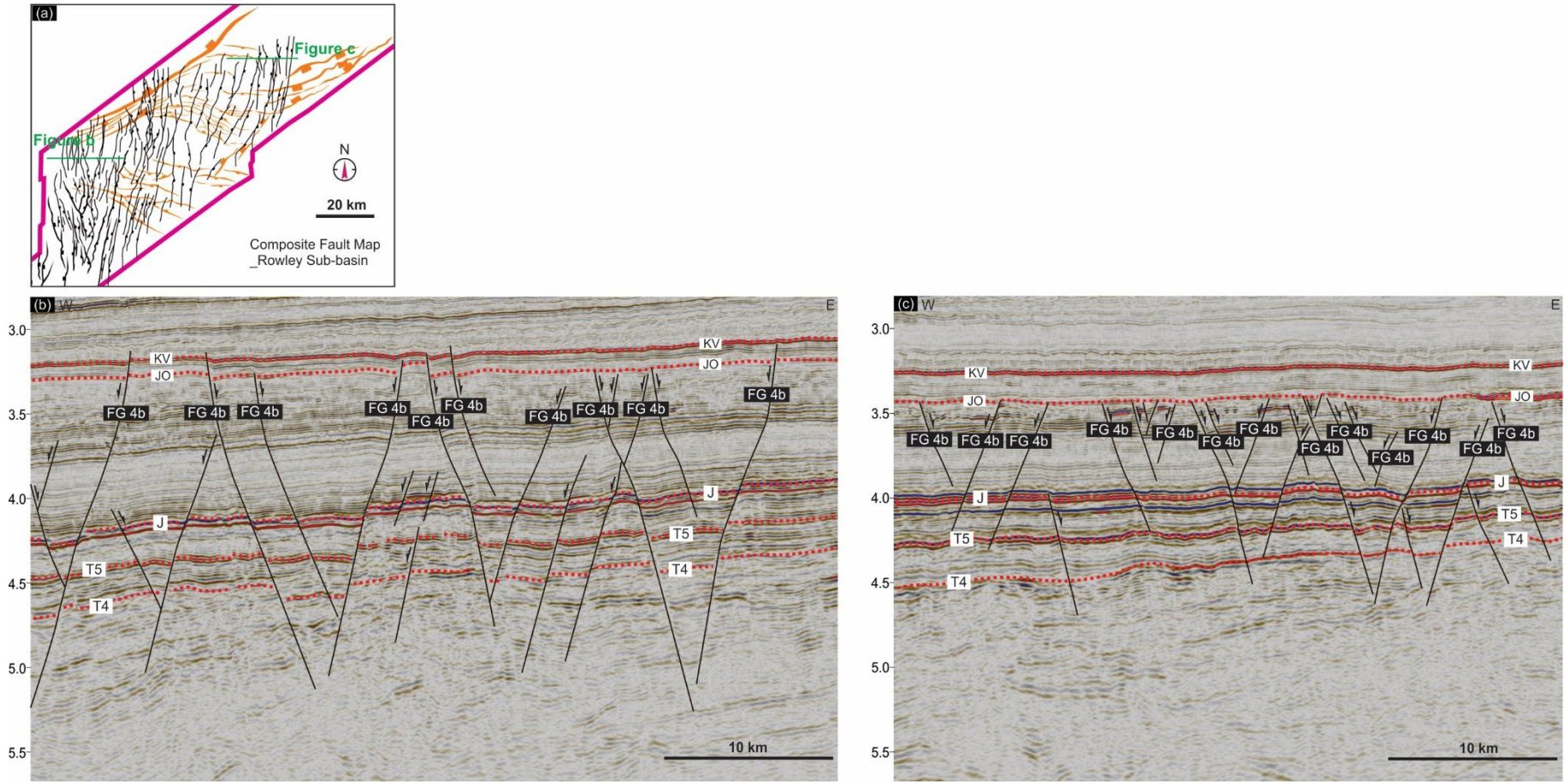

Figure 5-15. Composite fault map of the Rowley Sub-basin (Triassic faults [FG 2] in orange, ~Oxfordian and Oxfordian-Valanginian faults [FG 4b] in black) (a) and two east-west trending seismic sections of the Curt-3D seismic survey (b, c), showing the architecture of north- trending ~Oxfordian and Oxfordian-Valanginian faults (FG 4b) in the Rowley Sub-basin. See Figure 5-1 for locations.

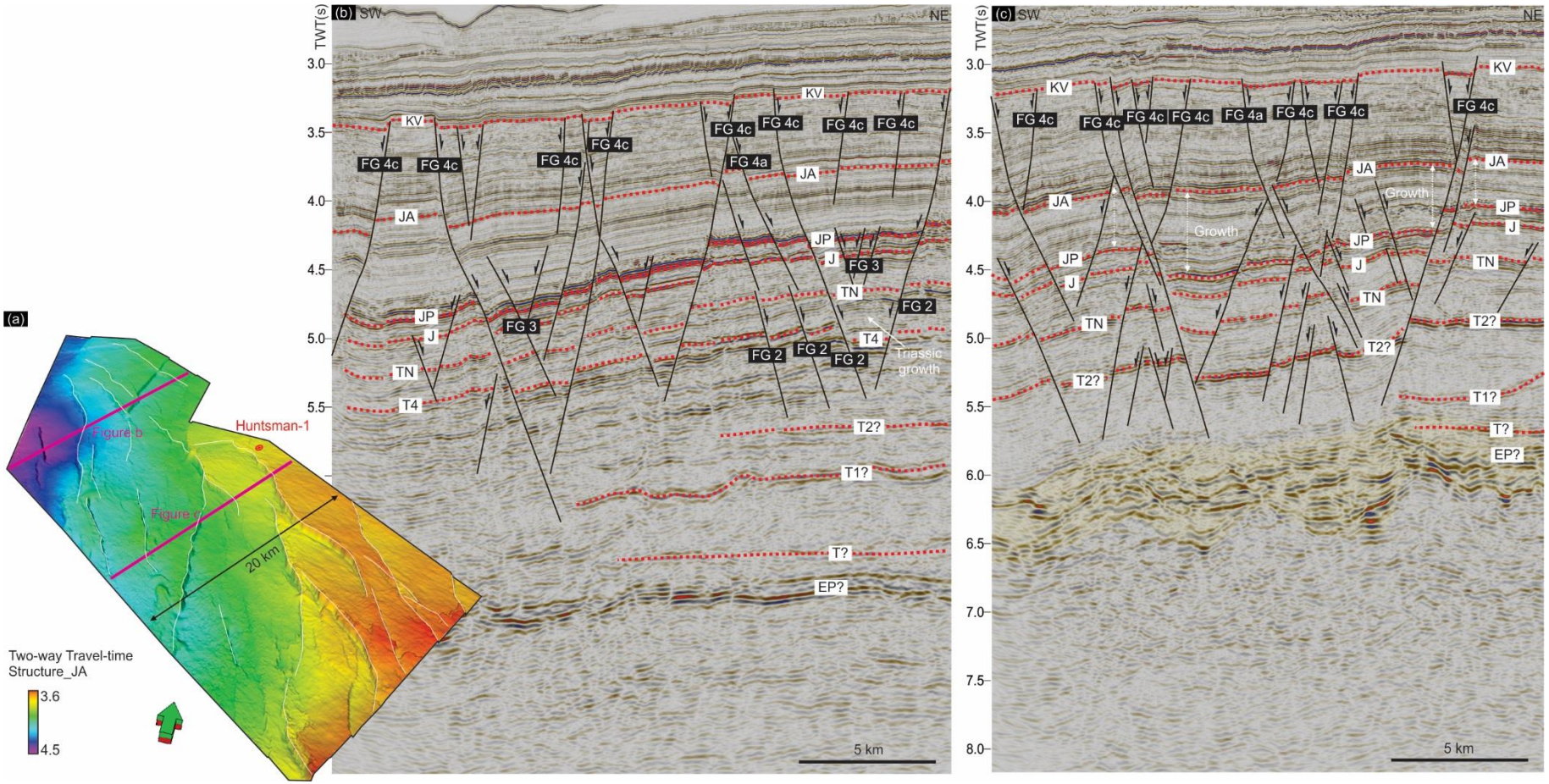

Figure 5-16. a) Two-way travel-time structure map (oblique view) of the Aalenian surface (JA) of the southwest part of Curt-3D seismic survey; b, c) two northeast- trending seismic sections with detailed interpretation showing the architecture of the northwest- trending (Middle?) Late Jurassic-Early Cretaceous faults (FG 4c) in the area.

succession in the southwest area (Oxfordian-Valanginian faults, Figure 5-15b) and at the Oxfordian Unconformity in the northeast area (~Oxfordian faults, Figure 5-15c). This suggests the development of the north- trending faults (FG 4b) lasted from (Middle?) Late Jurassic to the Cretaceous in the southwest Rowley Sub-basin but was restricted to the (Middle?) Late Jurassic in the northeast Rowley Sub-basin.

5.4.3 Northwest-southeast trending faults (Fault Group 4c)

In the southwest Rowley Sub-basin, a large population of northwest- trending (Middle?) Late Jurassic-Early Cretaceous faults are present (FG 4c, Figure 5-1, 5-7, 5-16a). The majority of the faults in this group terminate upward at the major unconformity that represents the Oxfordian-Valanginian hiatus and are detached downward into the Triassic succession (Figure 5-16b, c). A few cut into the Cretaceous succession, which indicates a post-rift reactivation. The fault planes show listric geometry in the upper part and planar geometry in the lower part. A few of them show clear Early Jurassic growth, which is demonstrated by fault controlled thickness change of the Lower Jurassic succession (JP-JA) (Figure 5-16c). This Early Jurassic fault growth likely corresponds to the formation of the northwest- trending Early Jurassic faults (FG 3) and the northwest- trending Huntsman Arch (see Chapter 5.6.3 for details) in the area.

Detailed fault analysis was conducted for one of the northwest- trending (Middle?)-Late Jurassic and (Middle?) Late Jurassic-Early Cretaceous faults (FG 4c) in the southwest Rowley Sub-basin (Figure 5-17). On the major unconformity that represents Oxfordian-Valanginian sedimentary hiatus (KV), this fault displays a sinuous trajectory and consists of multiple along-strike listric fault segments that are laterally connected. Antithetic subsidiary faults are coupled with each of the fault segments, forming a series of depocentres in an en-echelon pattern (Figure 5-17a-d). Along-strike fault displacement is characterized by multiple maximum and mimimum points, which correspond to the segment central points and linkage points respectively (Figure 5-17e). On the deeper stratigraphic levels (JA, JP), this fault consists of only two large segments (Figure 5-17f-i). The inconsistency of the along-strike displacement distribution at different stratigraphic levels suggests that this faults was formed by multi-phase extension. It could initiate as two large segments and subsequently evolved into smaller segments under an oblique extension. Alternatively it could initially nucleate as several smaller segments that were subsequently linked together to form two larger segments under further extension. Down-dip displacement was measured at the location of each segment centre (along-strike displacement maximal points). It is characterized by two down-dip displacement peaks, which are located at middle Jurassic stratigraphic level (JB) and the Lower Jurassic stratigraphic level (around JP) respectively (Figure 5-17j). This double-peak down-dip displacement distribution has two implications: 1) the fault has at least two phases

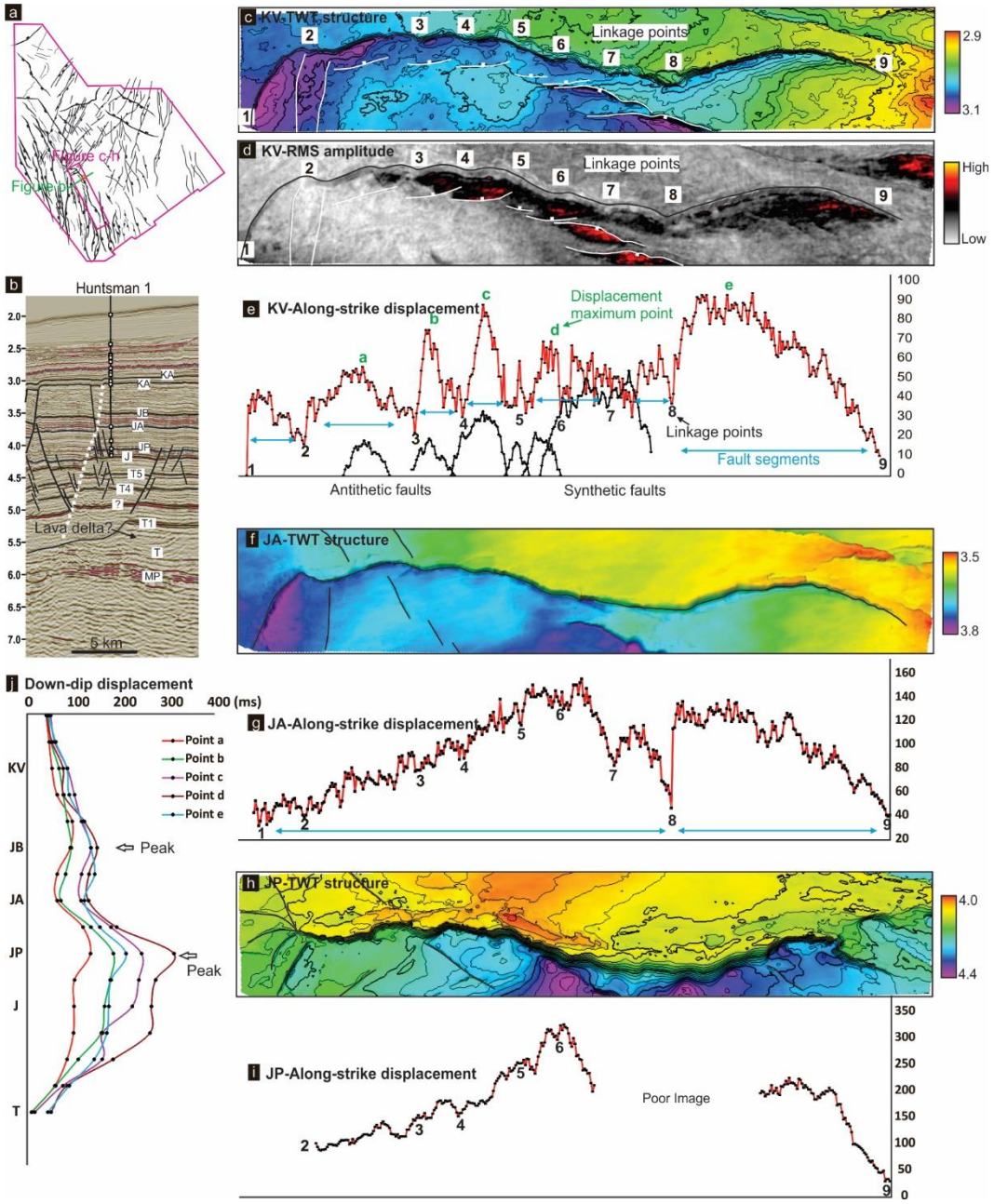

Figure 5-17. Detailed analysis of a representative (Middle?) Late Jurassic-Early Cretaceous faults (FG 4c) in the southwest Rowley Sub-basin. a) Map showing the fault location; b) A seismic section with interpretation showing the northwest- trending fault architecture (FG 4c, the white dashed line represents the selected fault for displacement analysis); c-i) Detailed analysis of the along-strike segmentation and linkages of selected northwest-trending fault and its subsidiary antithetic and synthetic faults at the Valanginian Unconformity (KV) (c, two-way travel-time structure map; d, RMS amplitude map; e, along-strike displacement [throw in ms] distribution), the Aalenian horizon (JA) (f, two-way travel-time structure map; g, along-strike displacement [throw in ms] distribution) and the Pliensbachian horizon (JP) (h, two-way travel-time structure map; i, along-strike displacement [throw in ms] distribution); j) down-dip displacement distribution of the selected fault measured at the central points of the each segment. JB=Bajacian

of growth, which is consistent with the along-strike displacement distribution; 2) there is a ductile layer to decouple the second-phase extension from the fault segments formed in the first-phase extension. This is because if no mechanically weak layer absorbs the second-phase extension as a detachment, the displacement created in the second-phase extension accumulates directly on the faults formed in the first-phase extension, which results in single-

peak down-dip displacement profile. The Lower Jurassic shale-dominated succession (JP-JA, see Chapter 6 for details) is interpreted as the decoupling ductile layer.

5.5 Non-tectonic faults

Two types of faults are interpreted to be formed by non-tectonic related processes, which include a large population of Early Jurassic polygonal faults on the outer Rowley Sub-basin and a group of northwest- trending Early-Middle Jurassic faults on the northeast Exmouth Plateau.

In the outer Rowley Sub-basin (Baxter-3D), a large number of polygonal faults (~2 km in length) are present in the Lower Jurassic succession (JP-JA) (Figure 5-8c, e). Polygonal fault systems have been widely interpreted in fine-grained sedimentary succession and are mostly attributed to syneresis, compaction, density inversion and overpressure release (Watterson et al., 2000; Cartwright et al., 2003; Goulty, 2008; Davies and Ireland, 2011). The polygonal fault bearing layer consists of a set of low-amplitude reflections, which correspond to the shale-dominated Murat-Athol Formation. The scale (length and vertical height) of these faults decreases from the east to west, consistent with the westerly thinning of the host layer. This suggests the polygonal fault system is a layer-bound system, thus is not formed in tectonic-related processes.

On the northeast Exmouth Plateau, a group of northwest- trending segmented faults are present in a succession of mud-dominated shelf slope sediments deposited in the Early-Middle Jurassic (see Chapter 6 for the details of the sedimentary facies). These faults have listric geometry with displacement up to 20 ms and length up to 5 km (Figure 5-6c). The fault strike is aligned with the slope-deepening direction, and their heights decrease northwesterly with the thinning of the host slope succession (Figure 5-11a, b), which suggests they are a layer-bound system. They are only associated with the slope succession and not present in the basin facies, suggesting they were formed by a slope-related process. Due to the lack of analogues, the genesis of these faults is unclear.

5.6 Dome Structures and Uplift

In the study area, several domes (circular high areas) and elongate uplifts have been identified, mainly on the 2D seismic data. These irregular structures are concentrated in the outboard area, mainly in the northern Beagle Sub-basin and on the northeast Exmouth Plateau (Figure 5-1).

5.6.1 Circular domes

There are four circular domes identified in the study area (Dome 1-4, Figure 5-1, 5-18a). They are generally characterized by symmetrical anticlines of the pre-Valanginian succession on

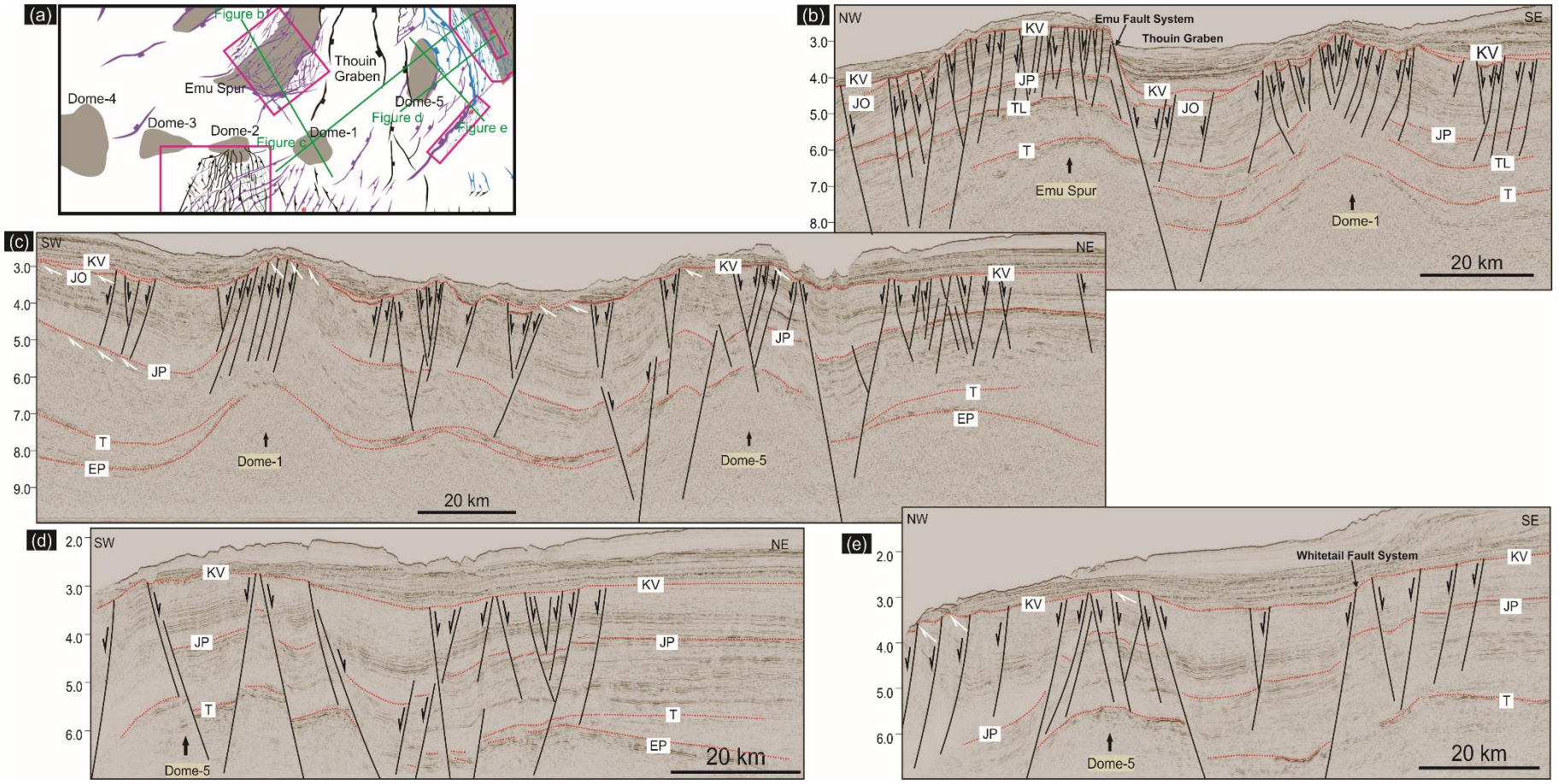

Figure 5-18. Structural element map (a) and seismic sections (b, c, d, e) showing the major dome structures and elongate highs of the northern Beagle Sub-basin, northeast Exmouth Plateau and flank of the Thouin Graben.

section views (Figure 5-18b, c) and listric extensional faults on the crest of the domes. The dome associated faults terminate upward at the major unconformity associated with the rift tectonics during the Oxfordian-Valanginian (JO-KV). The crests of the domes were significantly eroded, and the syn-tectonic succession (JO-KV) were deposited in the crestal fault controlled mini graben and half-graben system. The crestal faults associated with the Dome-1 have symmetrical assembly pattern on the northwest- trending seismic section (Figure 5-18b) and dip towards the west on northeast- trending seismic sections (Figure 5-18c). Downward, they are detached in the Triassic-Lower Jurassic succession. Dome-1 was recently investigated in a 3D seismic based study (data set is not available to public), which show the dome influenced area is dominated by northeast- and north- trending faults, with minor faults of other trends, forming a complex radial pattern (O'Halloran et al., 2018).

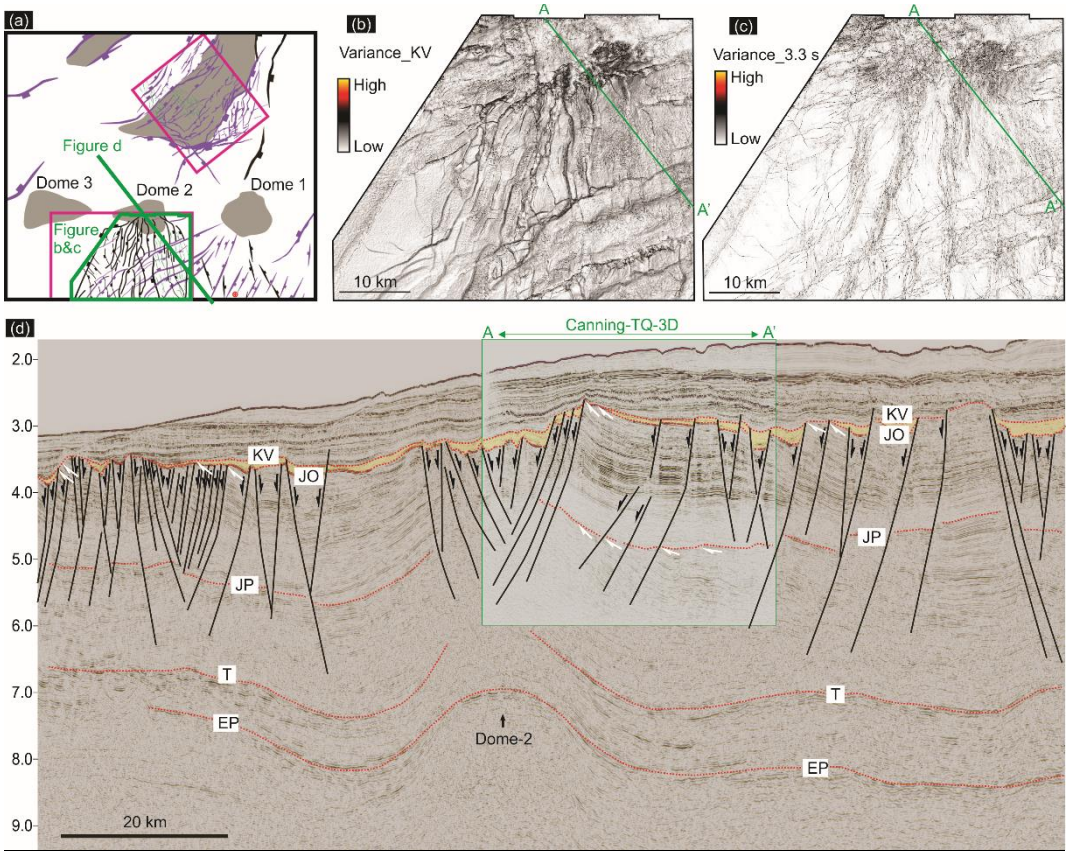

Figure 5-19. Structural element map of the northern Beagle Sub-basin and northeast Exmouth Plateau (a), variance map of the Valanginian Unconformity (KV) (b) and variance time slice at 3.3 s (TWT) (c) and a northwest-trending seismic section with interpretation (e) of the north part of the Canning-TQ-3D survey, showing the dome structures and the architecture of the associated faults.

The Canning-TQ-3D seismic survey covers the southern part of one of the circular domes (Dome 2, Figures 5-1, 5-19a-c). This dome shows similar symmetrical crestal faulting (comparing to Dome-1) on the section profile (Figure 5-19d) except that a larger crestal mini-basin is developed and hosts a thicker syn-tectonic succession (JO-KV). A high-quality variance map of the Valanginian Unconformity (KV) revealed that the dome-influenced area is characterized by a large population of small fault segments with a radial pattern (Figure 5-

19b, c). The crestal mini-basin is a circular low area and is interpreted as a result of crestal collapse during the dome withdrawal. The interaction of these radial faults with the northeast-trending (FG 4a) and north- trending (FG 4b) fault groups forms a very intense and complex deformation zone (Figure 5-19).

5.6.2 Fault controlled highs/uplifts

Several uplifted highs are interpreted to be bounded/controlled by the (Middle?) Late Jurassic-Early Cretaceous extensional faults (FG 4) (e.g., Dome 5, Emu Spur, Figure 5-18). They differ from the circular domes due to their elongate shapes and boundary faults that are detached into the Palaeozoic succession and separate them from the surrounding low areas (e.g., Dome-5, Figure 5-18b-e). From this perspective, they are more likely horst structures. The crests of these elongate highs were significantly eroded during rift tectonics (JO-KV), suggesting they were primarily formed during this period. The faulted pre-Oxfordian succession on the flanks of the Dome-5 dips away from the dome apex and does not display fault controlled rotation, which suggests the boundary faults formation is likely to postdate the uplift. The pre-Oxfordian succession on the Emu Spur, is northwest- dipping (Figure 5-11a, 5-18b), which can be interpreted as footwall uplift and tilt related to the formation of the Emu Fault System.

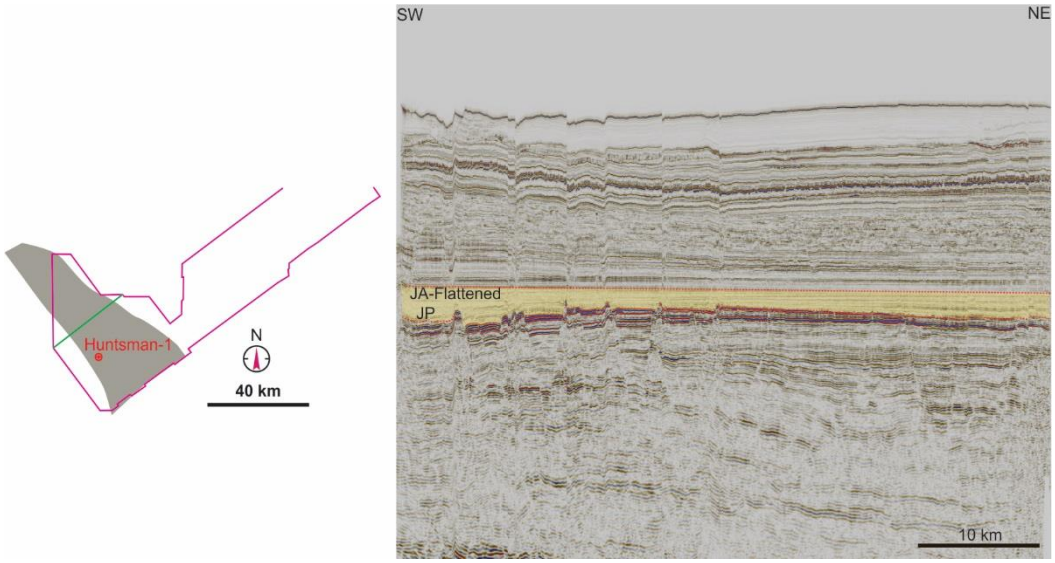

Figure 5-20. A northeast- trending seismic section flattened on the Aalenian horizon (JA) showing the thickness of the Lower Jurassic succession (JP-JA) was controlled by the northwest- striking Huntsman Arch.

5.6.3 Huntsman Arch

The Huntsman Arch is a broad northwest- plunging fold identified in the Rowley Sub-basin (Figure 5-1). It is interpreted to be formed during the Early Jurassic from the Pliensbachian (JP) to the Aalenian (JA), which is demonstrated by the stratigraphic thickening away from the Arch axis (Figure 5-20, see Chapter 6 for details of stratigraphy architecture). The

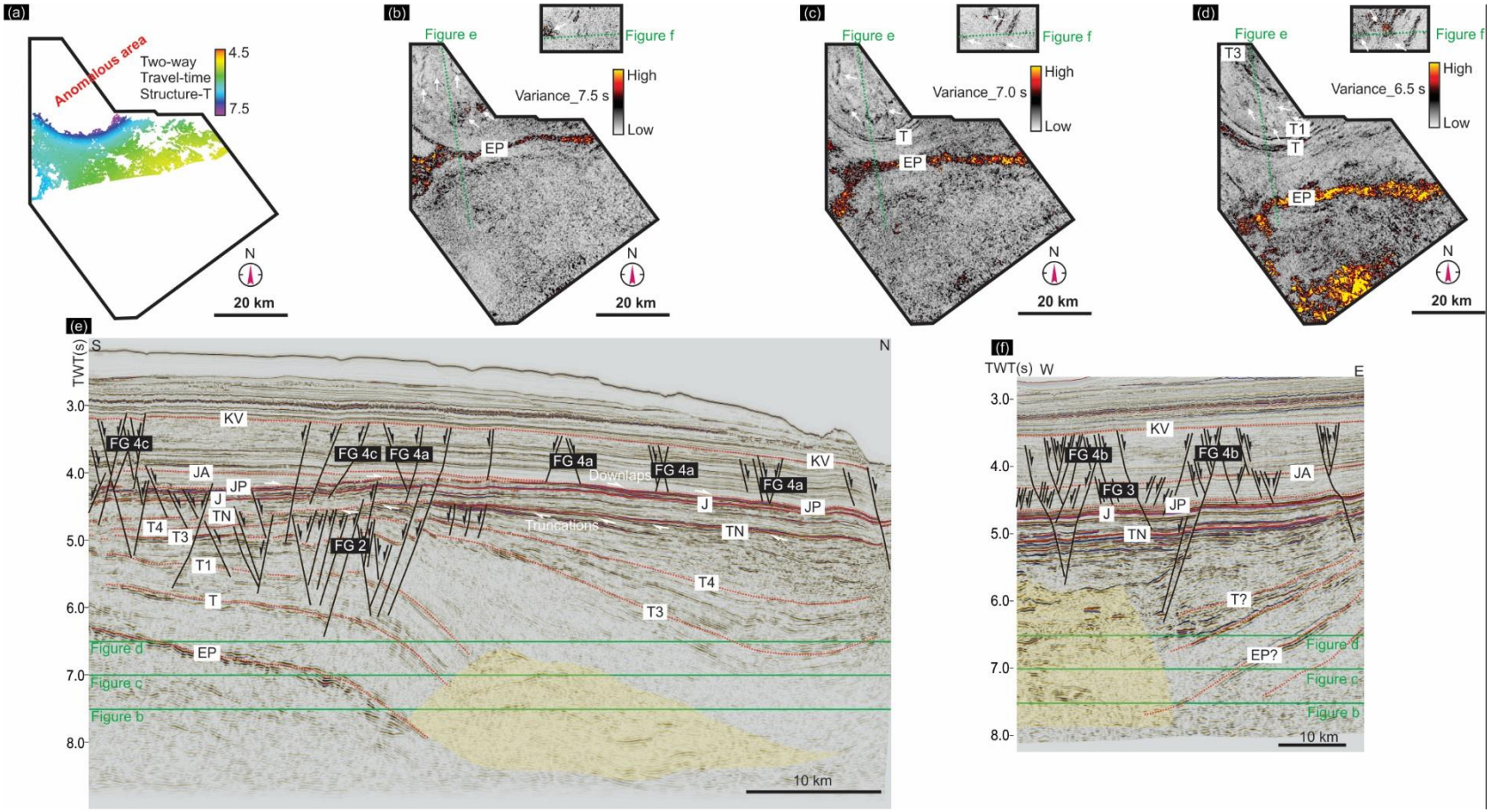

Figure 5-21. Two-way travel-time structure map of the base of Triassic (a), variance slice map at 7.5 s (b), 7.0 s (c), 6.5 s (d) TWT of the southwest part of the Curt-3D and Baxter-3D seismic survey and two seismic sections with interpretation (e, f), showing the architecture of a circular bowl-shaped structure

northwest- trending Early Jurassic faults (Fault Group 3) in the area are interpreted to be formed in the same time interval (JP-JA). However, whether they are genetically related to the Huntsman Arch is still unknown.

5.6.4 Circular bowl-shaped structure

In the southern part of the outer Rowley Sub-basin, a circular anomalous structure is interpreted at the Triassic stratigraphic level. The Curt-3D seismic survey covers a small portion of the structure (Figure 5-1, 5-21). Laterally, the structure extends to the Baxter-3D survey area. The layers influenced by this structure (e.g., EP-T1) dramatically deepens toward the north in the Curt-3D survey area and to the west in the Baxter-3D area, forming a bowl-like geometry (Figure 5-21). From the stratigraphic geometry, the subsidence of "bowl" floor is likely to occur in the time from T1 to T3, which is demonstrated by the dramatic thickness change of the coeval succession. A package of anomalous reflections, which is characterized by disorganized low-amplitude reflections incorporating discordant and cross-cutting high-amplitude reflections, are developed in the central low area (Figure 5-21e, f). High-quality variance slices through the structure revealed that these high-amplitude reflections form ring-like or rounded morphology (Figure 5-19b, c, d). Due to the limitation of the seismic data quality, the internal architecture of this structure, and its boundary with the surrounding stratigraphy is poorly defined.

5.7 Discussion

In this section, we will discuss the implications of the structure architecture for understanding the tectonic evolution of the Roebuck Basin as well as the North West Shelf. Emphasis is laid on the kinematic evolution of the extensional faults and their suggestions for the timing and directions of the key tectonic events. The potential mechanisms for the irregular structures (e.g., domes, bowl-shaped structures), are also briefly discussed.

Palaeozoic tectonics

The identification of extensional faults with Palaeozoic growth (FG 1) indicates the study area was under the influence of Palaeozoic tectonics. The tectonic events that are observable around the northwest margin of Australia include 1) northeast- directed extension that form the Southern Carnarvon Basin, Onshore Canning Basin and the Petrel Sub-basin; 2) northwest- directed extensions that lay the structural foundation of the Westralia Superbasin. The rifts formed under these two perpendicular stress fields were interpreted as the interior rift system of the Gondwanaland (Figure 5-22) (Harrowfield et al., 2005; Haig et al., 2014). The Roebuck Basin is located in the overlapping zone of the two Palaeozoic structural domains (Canning Basin and Westralia Superbasin). The two structural grains are demonstrated by the northeast- and northwest- trending anomalous gravity lineations (Figure

5-23). The Palaeozoic faults interpreted in this study shows both northeast- and northwest-trends on the southern flank of the Bedout Sub-basin and northeast- trend on the Bedout High (Figure 5-1, 5-2a), and match with the gravity anomalies. Therefore, the two orthogonal fault strikes are likely to represent the structural grains of the two rift systems of the interior Gondwanaland in the Palaeozoic. Due to the poor constraints of the horizon ages, the timing of the formation of the two sets of Palaeozoic domains are unknown.

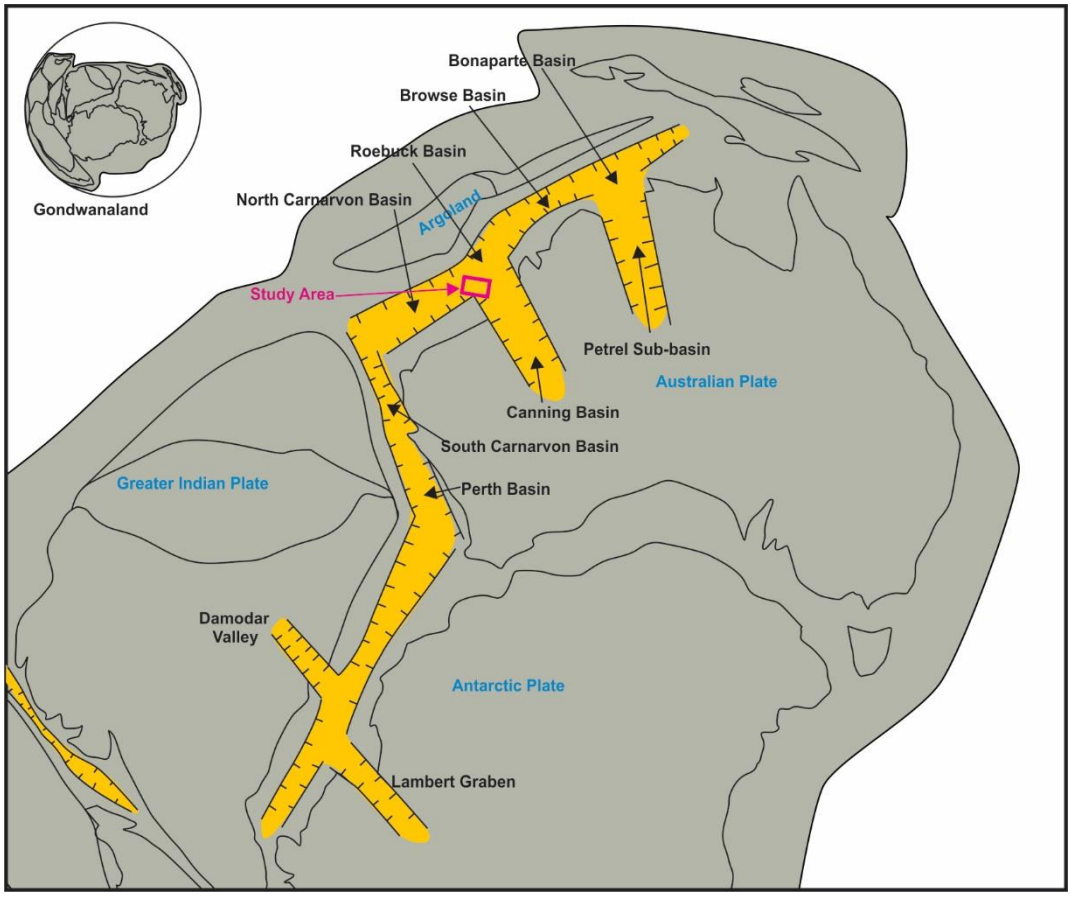

Figure 5-22. East Gondwanaland interior rift system in the Palaeozoic, after Harrowfield et al., 2005 and Haig et al., 2016.

Latest Permian Tectonics

The latest Permian Bedout Movement was proposed by Wales and Forman (1981) and cited subsequently in couple of publications (Horstman and Purcell, 1988; Colwell and Stagg, 1994; Smith, 1999), to explain the formation of the Bedout High and compressional structures in the Fitzroy Trough. The evident erosion associated with the Base of the Triassic unconformity (T) around the Bedout High (Figure 5-2d, 5-13c), the southern flank of the Bedout Sub-basin (Figure 5-2c) and in the outer Rowley Sub-basin (Figure 5-8e), are presumably linked to this event. In the outboard area, the Permian succession (EP-T) seemingly thins from both northeast and southwest towards the Thouin Graben (Figure 5-18c, d), which may indicate an uplift event in the latest Permian-earliest Triassic. This succession contains a package of

disorganized high-amplitude reflections that appear to form alternating synclines and anticlines (Figure 4-2, 5-16c). However, similar and equivalent seismic packages on the North West Shelf are interpreted as glaciation influenced deposits (Langhi and Borel, 2005; Al-Hinaai and Redfern, 2014). Due to the data limitation, it is difficult to clarify the genesis of this package and its relationship with the latest Permian-earliest Triassic Movement.

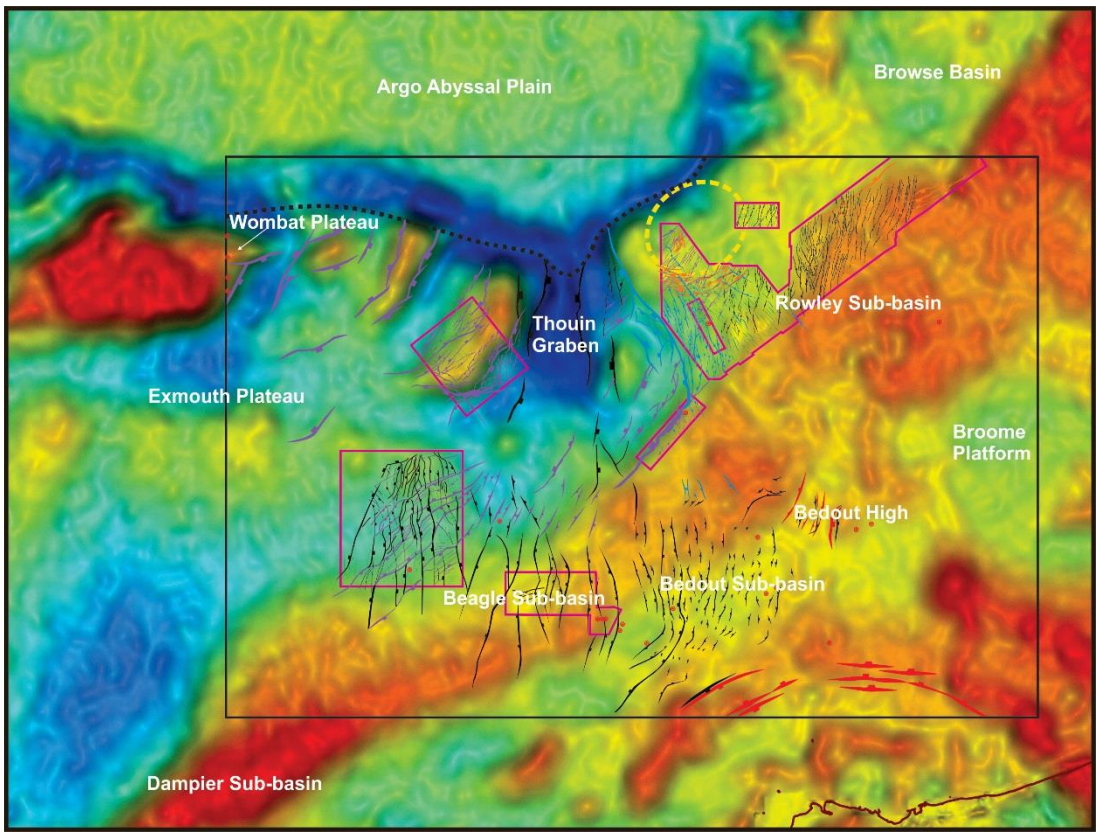

Figure 5-23. Structural element map superimposed on the gravity anomaly map (Bouguer gravity [onshore] and free-air gravity [offshore], GSWA Open-File Geophysical Database), showing the controls of the large northwest- and northeast- trending basement structural fabrics on the architectures of the extensional faults.

Triassic tectonics

The Triassic tectonic history is also poorly understood. The Triassic sedimentary succession is widely interpreted as a result of passive infill of a series of sag basins aligned with the Westralia Superbasin. The interpretation of the circular structure and extensional Triassic faults in the Rowley Sub-basin suggests significant tectonic events in the study area.

The lower part of the Triassic succession in the Rowley Sub-basin contains a set of clinoforms that are interpreted as an Early-Middle Triassic lava-flow delta (T-T1) (Figure 4-2) (MacNeill et al., 2018). Similar progradational clinoforms can be seen within the Triassic succession on the northeast Exmouth Plateau (Figure 5-6). However, the age of the clinoform system on the northeast Exmouth Plateau is not well constrained. It is conjectured that the clinoforms on the northeast Exmouth Plateau are likely to have the same lava-flow genesis.

The genesis of the circular bowl-shaped structure remains mysterious. The bowl-shaped geometry of the wall and the central peak on the floor resemble impact craters (Figure 5-21). However, elevated edges (rims), ejected materials and radial structures in the surrounding area, which are normally associated with the impact structures, are yet to be identified. Moreover, the ring-like and rounded high-amplitude bodies associated with the central material are difficult to explain. Given that this circular structure overlaps a magnetically strong area, it is likely a large Triassic caldera and these ring-like and rounded high-amplitude bodies could represent igneous intrusions. Whether it is genetically related to the previously mentioned lava flows is unknown. However, the formation of the bowl-shaped structure (T1-T3) seems to postdate the lava flows (T-T1). It is noteworthy that only a small piece of this structure is imaged in the dataset, and its geometry and architecture in the more outboard area are poorly constrained.

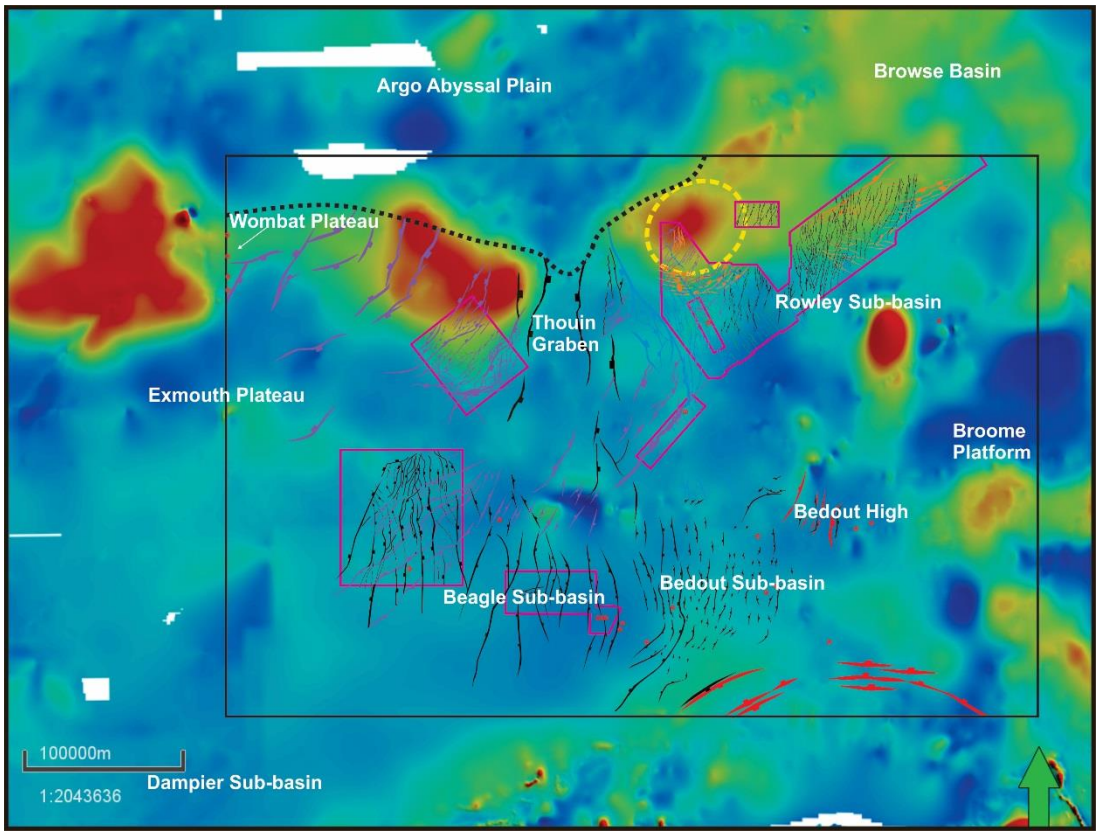

Figure 5-24. Structural element map superimposed on the airborne magnetic anomaly map (GSWA Open-File Geophysical Database) showing the potential presence of igneous bodies.

The interpretation of the extensional Triassic faults (FG 3) suggests the study area underwent significant extensional tectonics in the Triassic. The stratigraphic geometry suggests the Triassic faults underwent a major development phase in T3-T4 and were reactivated during the Norian Fitzroy Movement (TN) (Figure 5-3, 5-4). In the northeast Rowley Sub-basin, the northeast- trending Triassic faults appear to be the more dominant faults, given that their displacement and scale are greater than the north-northwest- trending Triassic faults (Figure

5-4). The distribution of the two sets of obliquely trending Triassic faults can be formed by 1) a strong northwest- directed extension event with minor influence of underlying northwest-trending Palaeozoic structures or 2) a weak northeast- directed extension with strong influence of underlying northeast- trending Palaeozoic faults. Both scenarios are possible because both the northwest- trending Canning Basin fabrics and the northeast- trending Palaeozoic fabris (Westralia Superbasin) are likely present in the area (Figure 5-22). The northeast- trending Triassic faults show strong alignment with a northeast gravity lineation (Figure 5-23), which may suggest the controls of the northeast- trending basement fabrics in the area. In the southern area, the Triassic faults nucleate around the circular bowl-shaped structure (Figure 5-1). The stratigraphic geometry suggests the formation of the bowl-shaped structure (T1-T3) pre-dated the formation of the Triassic faults (T3-TN) (Figure 5-3, 5-21). The circular structure, if it represents a caldera, should be mechanically harder than the surrounding sedimentary layers. The geometries and locations of the Triassic faults in the sedimentary layers that were developed around the circular structure, reflects the controls of this hard geological body on the subsequent extension. This provides a good explanation for the curved planform pattern of the Triassic faults (FG 2).

The Bedout Sub-basin also saw fault development in the Triassic. The north- trending listric faults show clear growth in the Triassic (Figure 5-13b). Given the north- trend and significantly greater displacement on these faults compared to the Triassic faults in the Rowley Sub-basin, they may suggest a different tectonic history in the Triassic. The faults in the Bedout Sub-basin mainly dip towards the west and the Triassic sedimentary succession thickens towards the west, which is attributed to the western steepening and tilting of the sub-basin. Linking the sub-basin embayment-like morphology, the listric fault geometry and the fluviodeltaic (Keraudren Formation) depositional background, there is high likelihood that the Triassic faults in the Bedout Sub-basin were, at least partially, a result of gravity tectonics. Besides, the pre-existing Palaeozoic faults (FG 1) were reactivated in the Triassic (Figure 5-13c).

In summary, the study area went through several phases of tectonics. From earlier to later, they are 1) the development of lava flows (T-T1), 2) a tectonic event characterized by the formation of the bowl-shaped structure (potential caldera?) (T1-T3), 3) a major extensional event in the period from T3-T4, 4) differential uplift and erosion in the Norian (Fitzroy Movement?), 5) gravity tectonics in the westerly deepening Bedout Sub-basin (through the Triassic?).

Early (-Middle) Jurassic tectonics

The rifting phase in the Northern Carnarvon Basin initiated from the Late Triassic and lasted until the Valanginian in the Early Cretaceous, which is demonstrated by the syn-extensional wedge-shaped strata deposited from the Late Triassic- Early Cretaceous (McCormack and McClay, 2013; Black et al., 2017). However, faults interpreted in the study area are not associated with Late Triassic growth, except the previously mentioned Triassic faults in the Bedout Sub-basin (potential gravity driven growth). It shows high variability in the timing of rifting along the North West Shelf. The interpretation of the highly segmented Early (Middle) Jurassic faults (FG 3) indicate a minor phase of tectonics in the Early (Middle) Jurassic. They show different trends in different sub-basins (Figure 5-1), including north- trending in the Beagle Sub-basin (Figure 5-5) and outer Rowley Sub-basin (Figure 5-8), and northwest-trending on the Exmouth Plateau (Figure 5-6) and in the southwest Rowley Sub-basin (Figure 5-7). In the sub-basins where these Early (-Middle) Jurassic faults are present, a set of larger faults (FG 4), which have the same strikes, were developed during the subsequent rift breakup. This suggests these Early (-Middle) Jurassic faults (FG 2) are precursor faults which finally developed into the large (Middle?)-Late Jurassic and (Middle?)Late Jurassic - Early Cretaceous faults (FG 4) and may represent the initial inception of the rifting in the area.

The Huntsman Arch (Figure 5-20) is another Early Jurassic structure. Its northwest trend is consistent with the Early Jurassic faults (FG 3) in the area (Figure 5-7). The timing of the both can only be constrained to the period between the Pliensbachian (JP) and the Aalendian (JA). The lack of unconformities in the area can be because 1) the magnitude of this tectonic event is weak and 2) unconformities, if they exist, are normally hard to resolve seismically in the highly condensed Early Jurassic deepwater succession in the Rowley Sub-basin (see Chapter 6 for details of sedimentary facies). The only Lower Jurassic unconformity observed is in the northern Beagle Sub-basin (northeast part of the Canning TQ-3D), where obvious truncation is associated with a tectonic movement in the Pliensbachian (Figure 5-5b, 5-19d). The tectonic event significantly uplifted the Canning-TQ-3D area and created more accommodation towards the Thouin Graben, which is demonstrated by the northeasterly thickening Lower Jurassic succession (Figure 5-10d). This thickness change trend, together with the northwest-trending Early Jurassic faults (FG 3) in the Rowley Sub-basin and on the northeast Exmouth Plateau, and the northwest- trending Huntsman Arch, strongly indicate a northeast- directed linear tectonic event and/or the influence of the underlying northwest- trending Palaeozoic fabrics associated with the Canning Basin.

(Middle?)Late Jurassic-Early Cretaceous tectonics

The Late Jurassic-Early Cretaceous (Oxfordian-Valanginian), potentially including the Middle Jurassic, saw the climax of the rifting in the study area as the majority of the structural elements were formed during this period. The extensional faults formed during this period

(FG 4) display high complexity, which is characterized by the co-existence of the northeast- (FG 4a), north- (FG 4b), and northwest- (FG 4c) trending faults. The controls of the underlying structures, particularly the two sets of perpendicular Palaeozoic structural domain (Figure 5-22), and the two temporally contiguous rift events that have different extensional direction (Argo rifting and Greater Indian rifting) (Figure 2-2) are the principal controls of the complex fault architecture.

From the boarder context, north- (north-northeast-) trending extensional faults are the predominant rift associated faults in the Northern Carnarvon Basin and are normally attributed to the Greater Indian rifting, which was in a relatively east-west (east-southeast-) direction (McCormack and McClay, 2013; Black et al., 2017). The north- trending faults (FG 4b) identified in the study area, normal to the extensional direction associated with the Greater Indian rifting, are most likely to be formed as a consequence of the Greater Indian rifting. The relationship between the north- trending faults (FG 4b) and the seismic stratigraphy suggests that the some of them were developed in the ~Oxfordian and some have longer activities during Oxfordian-Valanginian, e.g., in the Bedout Sub-basin (Figure 5-13), Beagle Sub-basin (Figure 5-9) and the southwest part of Rowley Sub-basin (Figure 5-15b). In the northeast Rowley Sub-basin, the majority of north- trending faults were exclusively formed in the in the ~Oxfordian (Figure 5-15c).

The northeast- trending faults (FG 4a) in the Beagle Sub-basin (Figure 5-9), northeast Exmouth Plateau (Figure 5-11) and Rowley Sub-basin (Figure 5-3c) are also interpreted to have the same age components, ~Oxfordian and Oxfordian-Valanginian. There are two potential factors that potentially contribute to their formation: 1) the controls of large pre-existing northeast- trending structures and 2) the northwest- directed extensional stress field associated with the Argo Rifting. In the Northern Carnarvon Basin, large northeast- trending Palaeozoic faults are interpreted to be present, and therefore, the northeast- trending Mesozoic faults were interpreted as a reactivation of the underlying structures (Jitmahantakul and McClay, 2013). These northeast- trending Palaeozoic faults are interpreted to extend to the study area and may have controlled the formation of the northeast- trending Mesozoic rift-related faults (FG 4a). The northeast- trending Whitetail fault system is probably a good example of the control of underlying structural fabrics (Figure 5-10). The control of pre-existing structures, through theoretically plausible, is difficult to be applied to the areas (e.g., northeast Exmouth Plateau, Figure 5-11) where the northeast- trending Mesozoic rift-related faults are the dominant structures and northwest- trending Palaeozoic faults were not developed. The Argo Rifting, which resulted in the Argoland separation from the Australia in a relative NW-SE direction (Figure 2-2), is more likely the main cause for at least the ~Oxfordian faults, especially on the northeast Exmouth Plateau. In the Rowley Sub-basin, the

northeast- trending faults (FG 4a) are only present in the southwest flank, close to the Thouin Graben, suggesting that the northwest- directed extensional stress field, if it existed, had limited influence in the northeast Rowley Sub-basin. In the Beagle Sub-basin, the northeast-trending (FG 4a) were developed simultaneously with the north- trending (FG 4b), and a certain proportion were active during the Oxfordian-Valanginian (Figure 5-9). This suggests that, these northeast- trending structures, if they were primarily formed in the stress fields produced by the Argo Rifting, had been reactivated in the subsequent extension associated with the Greater Indian Rifting.

The northwest- trending (Middle?) Late Jurassic-Early Cretaceous faults (FG 4c) in the southwest flank of the Rowley Sub-basin are oblique to the directions of both the Argo rifting and the Greater Indian rifting, thus representing an oblique extension on pre-existing structures. Northwest- trending Palaeozoic faults are yet to be interpreted in the Rowley Sub-basin, but the presence of the northwest- trending Early Jurassic faults (FG 3) and the northwest- trending Huntsman Arch certainly implied the influences of some pre-existing northwest- trending structures (Figure 5-1). The northwest- trending linear gravity anomalies, which stretch from the Canning Basin into the offshore area, may reflect the northwest-trending Palaeozoic and older structures in the area (Figure 5-23). The northwest- trending the (Middle?) Late Jurassic-Early Cretaceous faults (FG 4c) show strong along-strike segmentation and consist of both northwest- and north- trending segments (Figure 5-16a), suggesting the east-west directed extension associated with Greater Indian rifting was the principal force for the reactivation of the pre-existing northwest- trending structures.

The formation of the dome structures add more complexities to rift processes of the study area. While O'Halloran et al. (2018) suggested that the Tres Hombres structure (Dome-1 in this study) was active in the Late Triassic through the Jurassic, the principal growth of domes were interpreted to be in the same period (Oxfordian-Valanginian) as the extensional faults. The crestal faults associated with the circular domes (Dome 1-4) are symmetric on the section view and radial in the plan view (Figure 5-18, 5-19), suggesting they represent the intrinsic features of the doming processes and were not formed by linear extension. Given that igneous activities are normally associated with the rift processes, these domes are likely due to the upwelling of the magma, which is demonstrated by the greater gravity anomalies (Figure 5-23). The normal faults and mini-basin on the crest, then, were formed as a result of the withdrawn of the magma. The elongate dome (Dome-5), which is close to both northeast- and northwest- trending linear gravity anomalies (Figure 5-23), was likely influenced by the Palaeozoic structures. It was subsequently cut by the large rift-related faults, forming the elongate planform geometry. Simultaneously, the Emu Spur and several large-scale horst structures were formed on the Exmouth Plaetau (Figure 5-11, 5-23). From seismic profiles,

they appear to be thin-skin extensional horst-graben structures. However, the regional mapping suggests that Emu Spur is seemingly comprised by two dome-like segments (Figure 4-5) and the gravity map suggests they are also controlled anomalies at the lower crust and/or mantle level (Figure 5-23).

This study has suggested that rift-related extensional faults were mainly developed during the (Middle?) Late Jurassic-Early Cretaceous. However, the north- (FG 4b) and northwest- (FG 4c) trending extensional faults have a minor Early (-Middle) Jurassic growth phase, which corresponds to the formation of the north- and northwest- trending small and segmented Early (-Middle) Jurassic faults (FG 3). The strike components of the Early (Middle?) Jurassic faults reflect both the initial inception of the east- directed Greater Indian rifting and the influences of the underlying northwest- trending structures. The rift-related faults became inactive for a certain period of time in the Middle Jurassic prior to the Oxfordian. Subsequently, the extension associated with the northwest- directed Argoland drift presumably formed the northeast- trending in the ~Oxfordian faults (FG 4a), e.g., on the northeast Exmouth Plateau, and the Oxfordian-Valanginian activities of northeast- trending faults (FG 4a) can be attributed to the Greater Indian Rifting. Similarly, the north- trending Oxfordian-Valanginian faults (FG 4b) are attributed to the east-west directed Greater Indian rifting. However, a certain proportion of them were exclusively formed in the in the ~Oxfordian, suggesting the control of the Argo rifting. The formation of the northwest- trending Late Jurassic-Early Cretaceous faults (FG 4c) are also likely attributable to the Greater India rifting but are strongly controlled by the pre-existing northwest- trending Palaeozoic structural fabrics. Therefore, this study suggests that the rift-related extensional faults in the area were a result of the controls of the two contiguous drift events (Argoland and Greater India) and the pre-existing structures.

6 DEPOSITIONAL SYSTEM: FACIES, ARCHITECTURE AND GEOMORPHOLOGY

From the Pliensbachian (JP), a large fluviodeltaic system (Legendre Delta) started to develop in the Roebuck Basin and adjacent areas (Bradshaw et al., 1988; Bradshaw et al., 1998; Longley et al., 2002). It is interpreted to be derived from the present day onshore area and prograded towards the northwest (Figure 6-1a). The accumulation of this fluviodeltaic system was terminated by the drifting of Argoland in the Oxfordian (Figure 6-1b) and the upper part of the succession was significantly eroded during the previously discussed rift tectonics in Oxfordian-Valanginian (JO-KV).

The succession of this fluviodeltaic-related system contains a coarsening-upward siliciclastic succession, which is 1569 m thick in Huntsman 1 (Sturrock, 2007) and 2563 m in Wigmore 1 (Fisher, 2003) (Figure 6-1, 6-2). The lower part of the succession is the Lower Jurassic Murat Formation, which consists of a claystone dominated succession, interbedded with minor sandstone, calcilutite and calcarenite. Passing upward to the shale-dominated Athol Formation, the proportion of calcilutite and calcarenite is reduced, whereas, the proportion of sandstone slightly increases. The upper part, the middle Jurassic Legendre Formation, is mainly made up of thick sandstone, with common lithic and coal fragments. The Murat and Athol Formation were interpreted as prodelta facies and the Legendre Formation was interpreted as delta-plain to delta-front facies (Fisher, 2003; Sturrock, 2007). The stacking pattern represents a typical progradational deltaic succession. It is underlain by the carbonate dominated North Rankin Formation and is truncated by a major unconformity representing a sedimentary hiatus from Oxfordian to Valanginian (JO-KV) (Figure 6-2).

The basin architecture has shown that the bulk of this sedimentary system was deposited and/or preserved in the outboard part of the study area, including the northeast Exmouth Plateau, the Thouin Graben, and the Rowley Sub-basin (Figure 4-6b). Due to the lack of 3D seismic data and the perception of low prospectivity of this succession, the internal stratigraphic architecture and sedimentary facies of the system has been rarely investigated in publically available studies.

Detailed interpretation was conducted for the southern part of the Curt-3D survey in the Rowley Sub-basin and the WA484P-3D survey on the northeast Exmouth Plateau (Figure 6-1). Both data sets exhibit high-quality imaging for the Jurassic and younger succession and thus provide an opportunity to investigate the detailed 3D stratigraphic architecture, sedimentary facies and geomorphology of the fluviodeltaic-related succession.

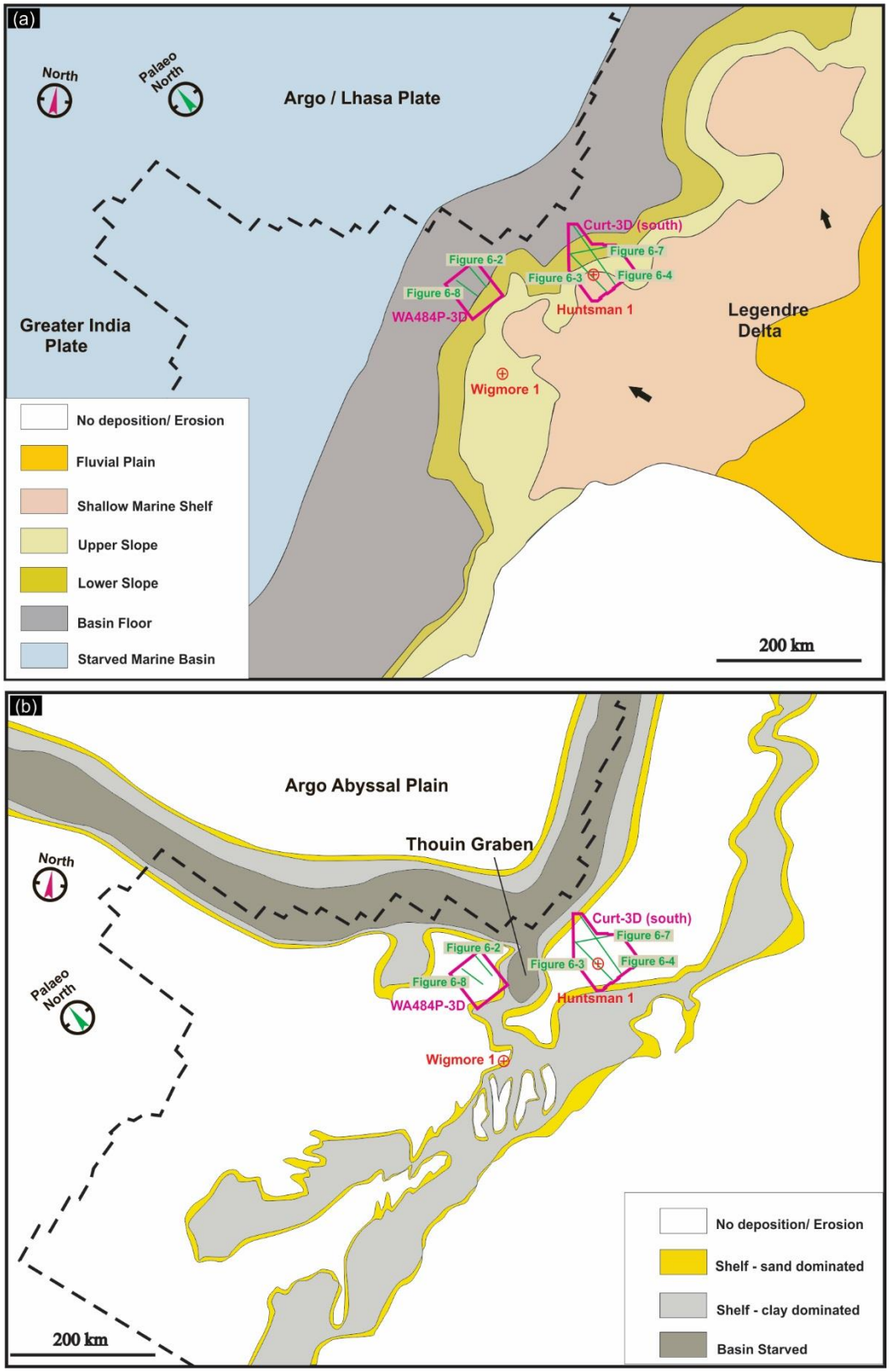

Figure 6-1. Maps showing the paleogeography of Pliensbachian (a) and Oxfordian (b), which respectively marks the onset of the fluviodeltaic system (the Legendre Delta, black arrows show the progradation direction) and the termination of deposition due to rift tectonics in the central North West Shelf. The maps are compiled from Longley et al. (2002).

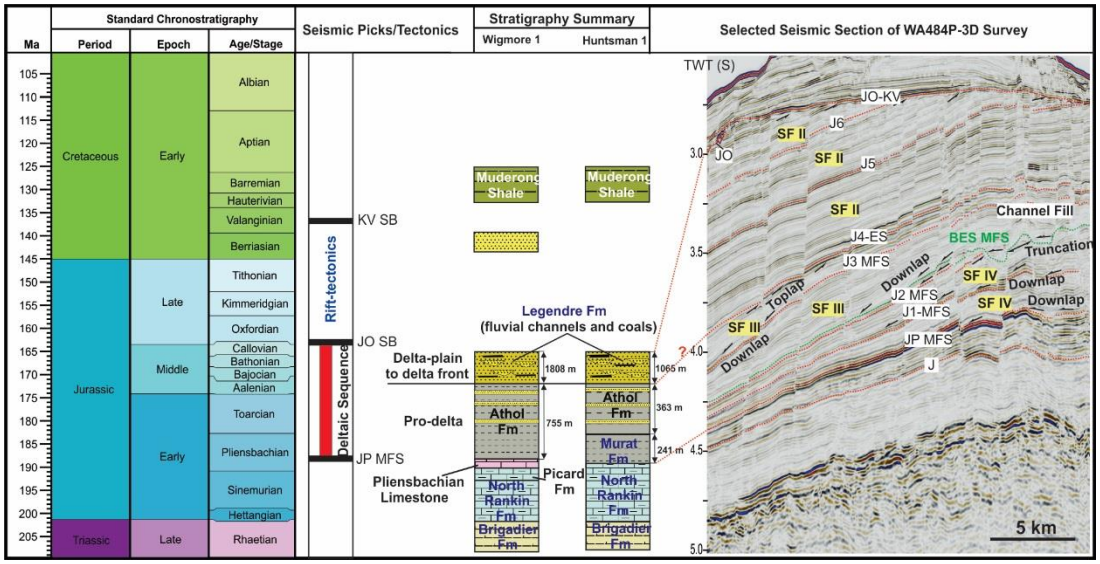

Figure 6-2. A representative NW-SE seismic section of WA484P-3D survey, showing seismostartigraphy and seismic facies of the Jurassic fluviodeltaic-related succession. J1-6 represent six Jurassic surfaces from older to younger, BES=Channelized basal Erosional Surface, MFS=Maximum Flooding Surface, ES=Erosional Surface, SF II= shelf, SF III=slope, SF IV=basin floor. See Figure 6-1 for location.

This chapter comprises three sub-sections. Chapter 6.1 presents the results of the seismic facies analysis, which is used to identify the major sedimentary facies (e.g., fluviodeltaic plain) and the associated depositional elements (e.g., fluvial channel belts). Chapter 6.2 introduces detailed three dimensional seismic stratigraphic architecture, which is based on isochron maps of different seismic units defined within the succession. The lateral variation in thickness of these seismic units are integrated with the seismic facies, which sheds lights on the lateral change of the depositional environments. Also, comparing the thickness and the seismic facies of different chronostratigraphic units provides insights into the dynamic evolution of the depositional environments. Chapter 6.3 presents seismic geomorphology, which investigates the plan view of the mappable components, geometry and morphology of the sedimentary facies and their associated depositional elements. In Chapter 6.4, the results of the seismic facies, stratigraphic architecture and geomorphology are discussed with respects to regional depositional system evolution, the governing processes of the key depositional elements, the interaction between structural evolution and sediment infilling, and the significance of sequence stratigraphy (relative sea-level and sediment supply).

Survey-specific seismic horizons are present in this chapter, the age of which are poorly constrained. They include four Lower Jurassic horizons (from older to younger named LJ1-LJ4) and five Middle Jurassic horizons (from older to younger named MJ1-MJ5) interpreted in the Curt-3D, and six Jurassic horizons (from older to younger, named J1-J6) interpreted in the WA484P-3D. The details of these horizons are introduced along with the related seismic facies, stratigraphic architecture and geomorphology. In this chapter, where needed, converted depth and/or thickness is given based on a constant velocity (Vp=3150 m/s, based on

velocities for the Jurassic succession of 3100 m/s in Huntsman-1 and 3165 m/s in Wigmore-1), for the convenience of comprehending the approximate scales of geological and geomorphological features.

6.1 Seismic Facies Classification

This section presents detailed descriptions of the seismic facies identified in the fluviodeltaic-related succession (Murat, Athol and Legendre Formations) (JP-JO) and the syn-tectonic succession (JO-KV) from the two 3D seismic surveys mentioned above. Particularly, emphases are placed on the seismic characteristics, including reflection geometries, strengths and stacking patterns. Two types of seismic facies are defined: 1) primary seismic facies, which are used to describe a set of reflections that show similar internal geometries, amplitude and stacking patterns and extend over a large area (up to tens of kilometres across the margin), and 2) secondary seismic facies, which are normally used for a single reflection/unconformity or a set of reflections that are restricted to a small area (less than several kilometres).

Five primary seismic facies are identified: fluviodeltaic plain (SF I), marine shelf (SF II), slope (SF III), basin floor (SF IV) and carbonate shelf-ramp facies (SF V). Eleven secondary seismic facies (SF V-XVI) have been identified which represent the depositional elements that are either incorporated in or associated with the primary seismic facies. The interpretation of the sedimentary facies and/or depositional elements these seismic facies represent are a result of integration of seismic facies (in this section), stratigraphic architecture (Section 6.2) and seismic geomorphology (Section 6.3). The latter two address the detailed stratigraphic contexts and plan-view morphology of the seismic facies, which provide important constraints on sedimentary facies/environment. This section describes only seismic facies, but sedimentary meanings are attached to each of the facies, in order to give readers an indication of what they represent and to avoid confusion between different seismic facies that show similarities.

6.1.1 Seismic Facies I (SF I): fluviodeltaic plain

Seismic facies I is characterized by parallel, discontinuous, medium-high amplitude reflections. It dominates the upper part of the Legendre Formation in the Rowley Sub-basin (SF I, Figure 6-3a, b). In Huntsman-1, the corresponding succession consists of thick sandstones, with coal fragments (Figure 6-3c). Detailed seismic geomorphology analysis indicates that its high internal heterogeneity is due to the presence of fluvial channel belts and their associated sedimentary facies (see Seismic Geomorphology section for details). It is interpreted as undifferentiated fluvial to deltaic plain environment.

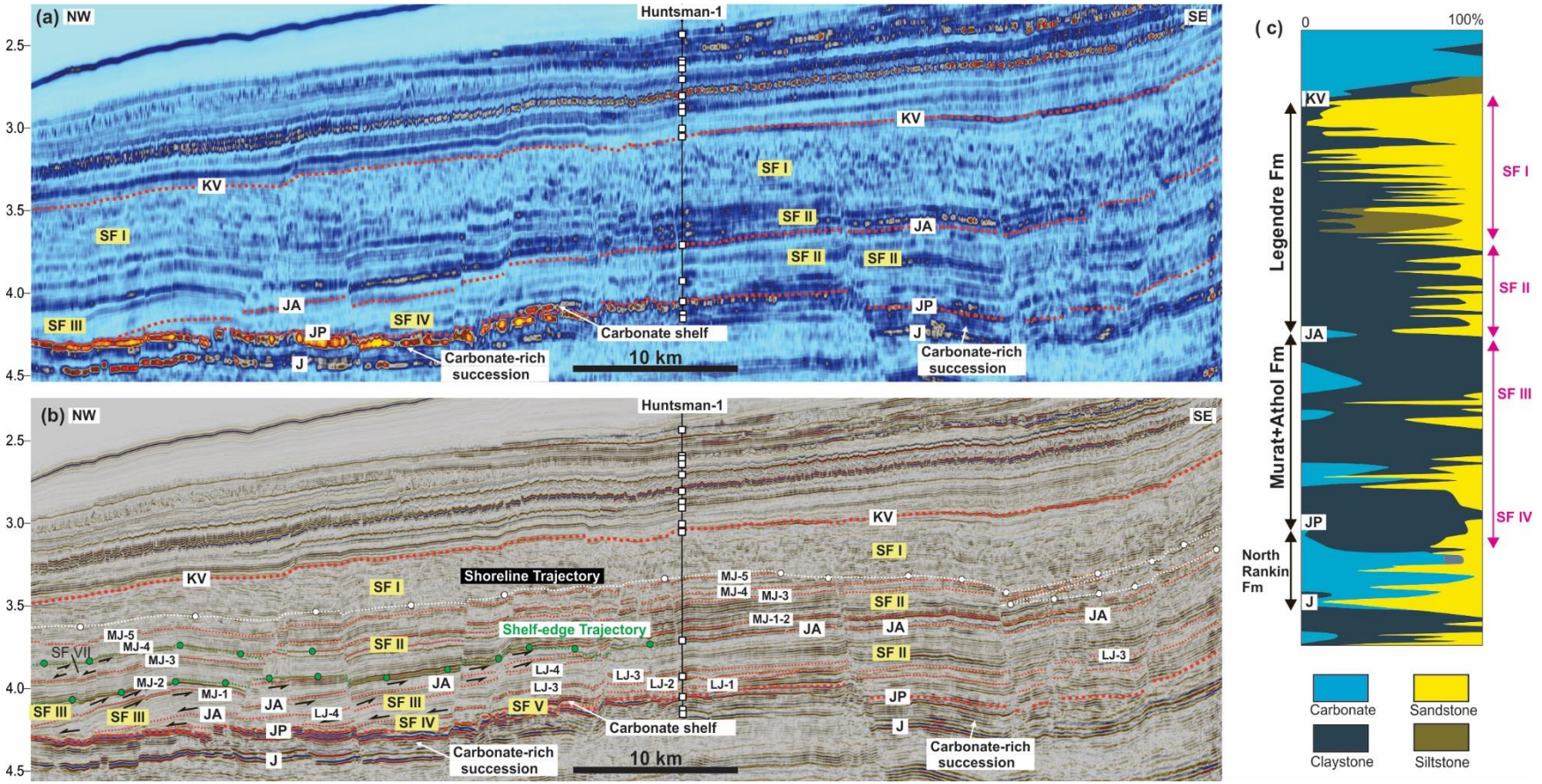

Figure 6-3. A representative NW-SE section (a, RMS amplitude; b, seismic) of Curt-3D with Huntsman-1 well intersection (c, wellsite lithology logging), showing the major surfaces (J= Base Jurassic, JP=Pliensbachian Maximum Flooding Surface, JA=Aalenian Erosional Surface, KV=Valanginian Unconformity, LJ1-4 represent four Lower Jurassic surfaces from older to younger, MJ1-5 represent five Middle Jurassic surfaces from older to younger), primary seismic facies between JP and KV (SF I: fluviodeltaic plain; SF II: shelf; SF III=slope; SF IV=basin floor, SF V= carbonate shelf-ramp) and the approximate trajectories of shoreline (white dots and dashed line) and shelf-edge (green dots and dashed line). See Figure 6-1 for location

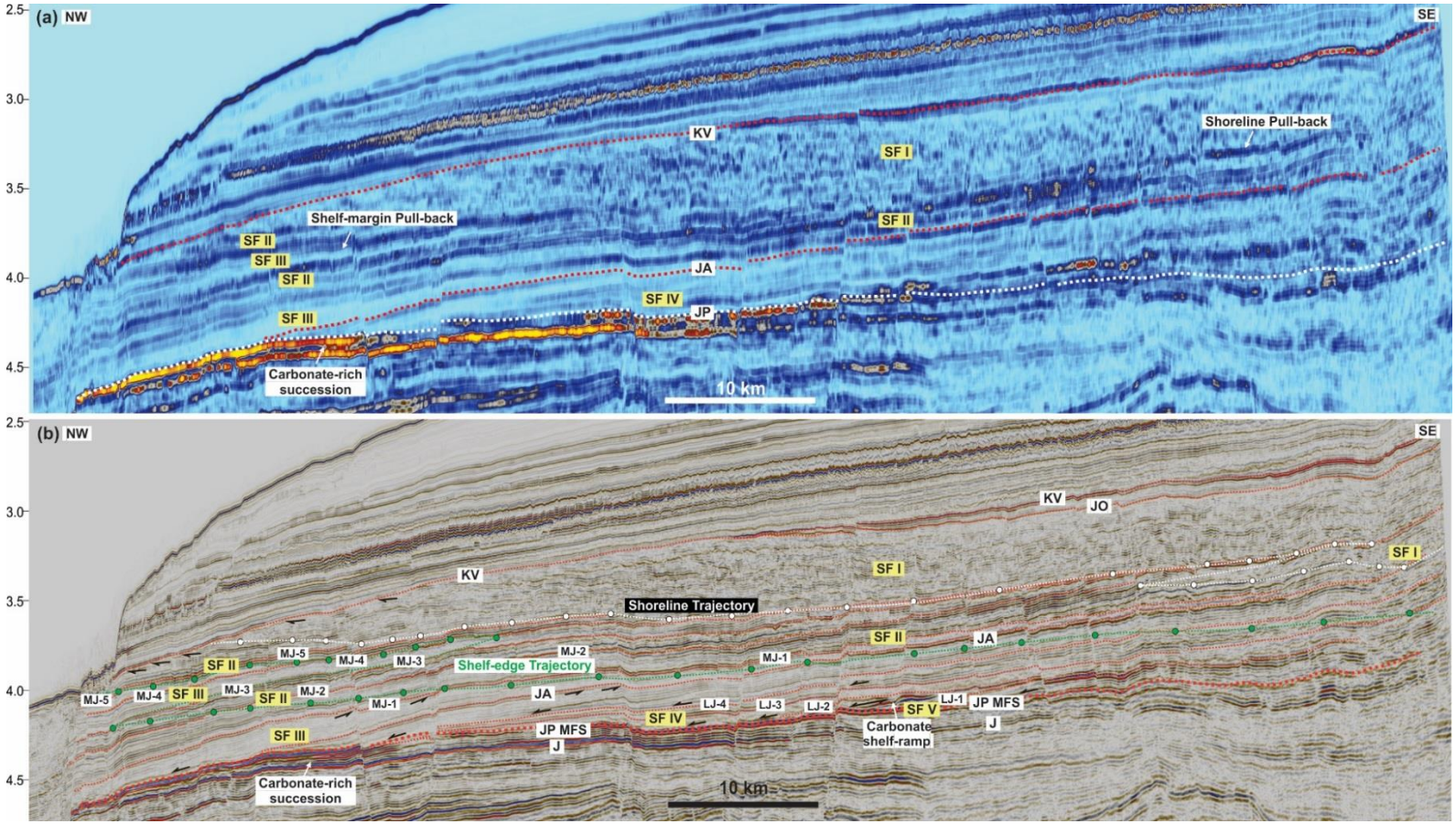

Figure 6-4. A representative NW-SE section (a, RMS amplitude; b, seismic) of Curt-3D with Huntsman-1 well intersection (c, wellsite lithology logging), showing the major surfaces (J= Base Jurassic, JP=Pliensbachian Maximum Flooding Surface, JA=Aalenian Erosional Surface, KV=Valanginian Unconformity, LJ1-4 represent four Lower Jurassic surfaces from older to younger, MJ1-5 represent five Middle Jurassic surfaces from older to younger), primary seismic facies between JP and KV (SF I: fluviodeltaic plain; SF II: shelf; SF III=slope; SF IV=basin floor, SF V= carbonate shelf-ramp) and the approximate trajectories of shoreline (white dots and dashed line) and shelf-edge (green dots and dashed line). See Figure 6-1 for location.

6.1.2 Seismic Facies II-III-IV: shelf-slope-basin system

Large-scale clinoforms were identified within the lower part of the fluviodeltaic-related succession (corresponding to the Athol and Murat Formation) in the two sub-basins (Figure 6-2, 6-3). These clinoforms consists of, 1) topsets that are parallel, continuous, medium to high-amplitude reflections that are parallel with the base of the fluviodeltaic-related succession (JP MFS) (Seismic Facies II); 2) foresets that are continuous, sigmoidal, medium to low-amplitude northwest-dipping clinoforms (Seismic Facies III); 3) bottom sets that are sub-parallel, medium to low-amplitude reflections, which dip and pinch out towards the northwest (Seismic Facies IV). The clinoforms have a vertical scale of hundreds of meters height and tens of kilometres width and are interpreted as a shelf-margin clinoform system (see discussion for details). From the perspective of depositional environments, Seismic Facies II (SF II) represents sediments deposited on the marine shelf between the shoreline and the shelf break; Seismic Facies III (SF III) and Seismic Facies IV (SF IV) correspond to deposits on the shelf break slope and basin floor respectively.

6.1.3 Seismic Facies V: carbonate shelf-ramp

A set of sigmoidal to oblique high-amplitude reflections were identified in the lowermost part of the Jurassic fluviodeltaic-related succession (from LJ-1 to LJ-2) in the Rowley Sub-basin. They have a vertical scale of approx. 150 meters height, 5-8 km width with < 2° maximum dip (Figure 6-3, 6-4). They downlap the Pliensbachian Maximum Flooding Surface (JP MFS) and show progradation towards northwest. Inboard, they are toplapped by the high-amplitude reflection of LJ2. The corresponding sediments around LJ2 in the Huntsman-1 indicate carbonate rocks that are incorporated in the mud-dominated Murat Formation (Figure 6-3c). Given its high-amplitude nature and the well constraints on lithology, the sigmoidal reflection set is interpreted as carbonate shelf-ramp system (Seismic Facies V).

6.1.4 Seismic Facies VI: fluvial channel belts

Seismic Facies V is a secondary facies that is exclusively associated with the fluviodeltaic plain facies (SF I) in the Rowley Sub-basin (Curt-3D). It refers to the channelized surfaces with infills that show little amplitude contrast with the surrounding sediments, which makes them very difficult to recognize on the seismic section (Figure 6-5a). However, time / horizontal slices of seismic attribute revealed the presence of the channels (see Section 6.3 for details).

6.1.5 Seismic Facies VII: delta-scale subaqueous clinoforms

A set of fine-scale clinoforms (60-80 meters high, 1-2 kilometers wide) (Seismic Facies VII) were identified within the succession that corresponds to Legendre Formation in the Rowley

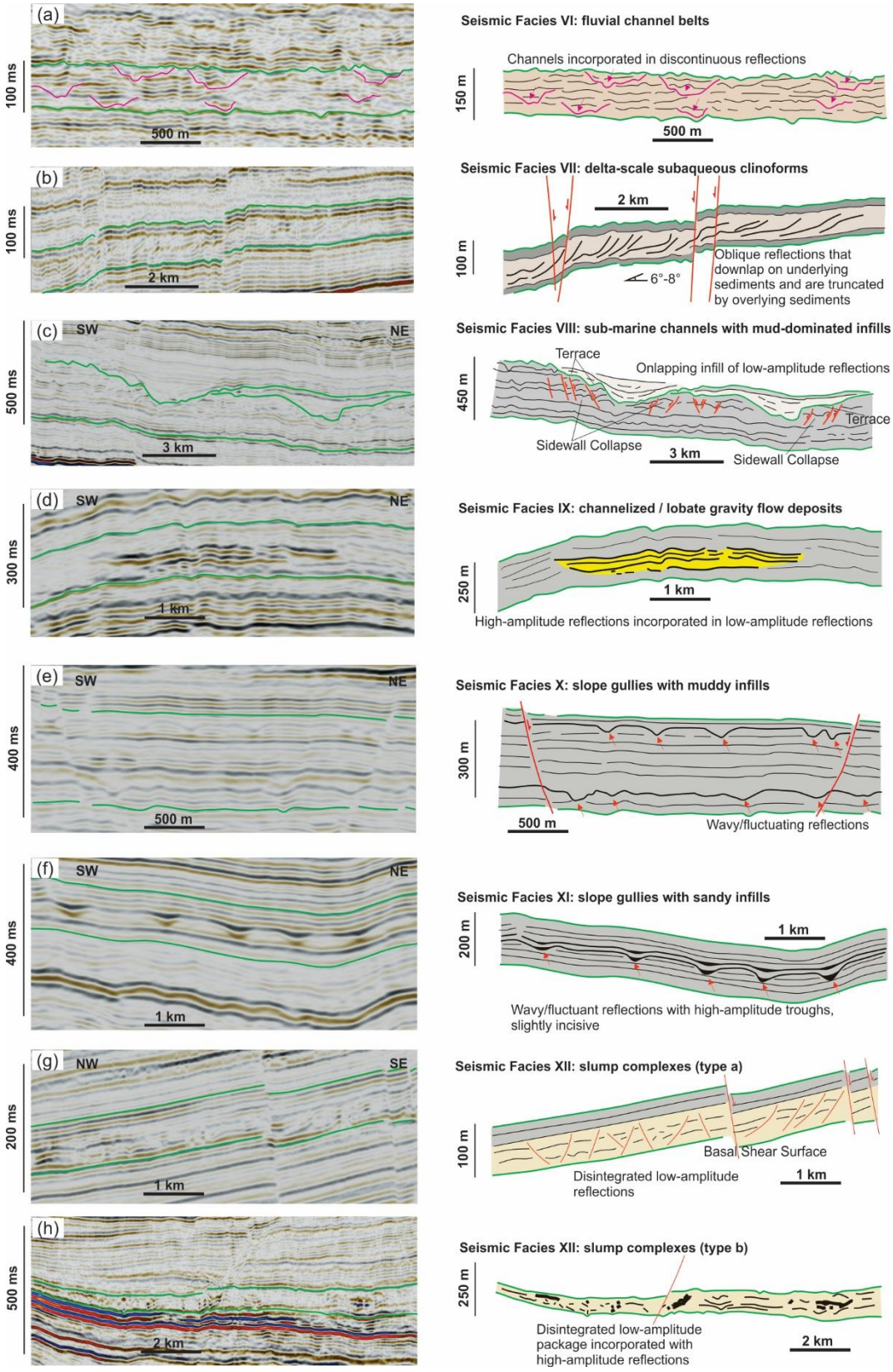

Figure 6-5. Representative seismic sections from Curt-3D and WA484P-3D seismic surveys showing secondary seismic facies identified for the Lower-Middle Jurassic fluviodeltaic related succession (JP-JO), and their interpretation. The metric vertical scales are based on an average velocity 3150 m/s of the succession.

Sub-basin (Curt-3D)(Figure 6-5b). The reflections of Seismic Facies VII (SF VII) show low amplitude and oblique geometries (6°-8° dips). They are toplapped upward by overlying

parallel reflections (shelf facies, SF II), thus clinoform topsets are absent. The reflections downlap the underlying shelf-slope facies (SF III, IV). The clinoforms have greatest dips in the centre, which decreases both basinward and landward until gradually transitioning into parallel reflections. Seismic Facies VII is interpreted as set of fine-scale subaqueous clinoforms (relative to the previously mentioned shelf-slope-basin clinoforms) developed in the proximity of the shelf-slope transition. They are equivalent to delta-scale subaqueous clinoforms (Patruno et al., 2015b).

6.1.6 Seismic Facies VIII: submarine channels with mud-dominated infills

Seismic Facies VIII (SF VIII) is associated with erosional channelized surfaces that incise up to 200 ms TWT (315 m [1033 ft]) in the underlying sediments (Figure 6-5c) and are present in the lower part of fluviodeltaic-related succession on the northeast Exmouth Plateau (WA484P-3D). It is associated with the slope facies (SF III), which presumably corresponds to the Murat and Athol Formation. The channelized surfaces are infilled / downlapped by a prograding low-amplitude slope succession (Figure 6-2). Seismic characteristics suggest the channel infills are softer than the background sediments. They are interpreted as submarine channels developed at the slope that were buried by a prograding mud-prone slope succession.

6.1.7 Seismic Facies IX: channelized to lobate gravity flow deposits

Seismic Facies IX is characterized by channelized to lobate high-amplitude reflections that are slightly incised into the underlying sediments in the northeast Exmouth Plateau (WA484P-3D) (Figure 6-5d). They represent the downslope counterparts of the submarine channels on the slope (SF VIII). Seismic characteristics suggest they are harder than the background sediments. Seismic Facies IX is mainly associated with the slope to basin facies (SF III, IV), and is interpreted as sand-rich gravity flow deposits in submarine channels and terminal fans on the slope and basin floor.

6.1.8 Seismic Facies X: slope gullies with mud infills

Seismic Facies X is characterized by wavy reflections, which define a large number of gullies (troughs) that are approximately 300m [984 ft] wide and 20 ms TWT (32 m [105 ft]) deep (Figure 6-5e). They are only identified in the northeast Exmouth Plateau (WA484P-3D). The gullies show low-amplitude infills. Seismic Facies X (SF X) are exclusively associated with slope facies (SF III), which suggest that they were formed as a result of slope processes.

6.1.9 Seismic Facies XI: slope gullies with sand infills

Seismic Facies XI is characterized by similar type of gullies as Seismic Facies X except that they are characterized by high-amplitude infills (Figure 6-5f). Seismic Facies XI (SF XI) are

also associated with the clinoform front sets (SF III), which suggest that they are formed as a result of slope process.

6.1.10 Seismic Facies XII: slump complex

Seismic Facies XII consists of disrupted reflections along a basal shear surface that are interpreted as slump complex. On northeast Exmouth Plateau (WA484P-3D), slumps are generally 30-50 ms TWT (47-79 m) thick and are associated with the parallel shelf facies (SF I). Internally, the reflections are moderately disintegrated and show low-medium amplitude similar to the surrounding reflections (Figure 6-5g). In Rowley Sub-basin (Curt-3D), the slumps are only observed in the distal area and associated with the slope-basin facies (SF III-IV). It consists of highly disintegrated low-amplitude reflections containing isolated high-amplitude segments (Figure 6-5h).

6.1.11 Seismic Facies XIII: syn-tectonic canyons with variable infills

On the northeast Exmouth Plateau (WA484P-3D), the unconformity at the top of the Legendre Formation (JO-KV) is characterized by several highly incised canyons that are up to 4 km wide and 400 ms TWT (630 m) deep (Figure 6-6a). The basal erosive surfaces are infilled by oblique to sub-parallel reflections that show variable amplitudes. Seismic Facies XIII is interpreted as syn-tectonic canyons with variable post-tectonic infills.

6.1.12 Seismic Facies XIV: canyon-derived gravity flow deposits

Seismic Facies XIV is characterized by very high amplitude reflections aggrading in a zigzag style that are incorporated into low-amplitude to transparent packages in a fault bounded graben on the northeast Exmouth Plateau (WA484P-3D) (Figure 6-6b, details see Chapter 6.3). It is interpreted as syn-tectonic canyon-derived gravity flow deposits in a marine shale dominated graben.

6.1.13 Seismic Facies XV: syn-tectonic fan

Seismic Facies XV is made up of alternating high- and low- amplitude reflections, which are discontinuous but generally show as clinoforms (Figure 6-6c). They are confined between the Oxfordian Unconformity (JO) and the Valanginian Unconformity (KV) on the northeast Exmouth Plateau. Seismic Facies XV is interpreted as a syn-tectonic fan lobe.

6.1.14 Sesimic Facies XVI: fault bounded high-amplitude sheet-like bodies

In the southwest of Rowley Sub-basin, the syn-tectonic succession (JO-KV) is absent or highly condensed, if they are present. The unconformity (JO-KV) at the top of the Legendre Formation is characterized by uniform high-amplitude reflections that are only present in grabens or half-grabens (Figure 6-6d). Seismic characteristics suggest it is harder than the

underlying sediments. Seismic Facies XVI is interpreted as syn-tectonic sheet-like bodies, and their genesis remains unclear.

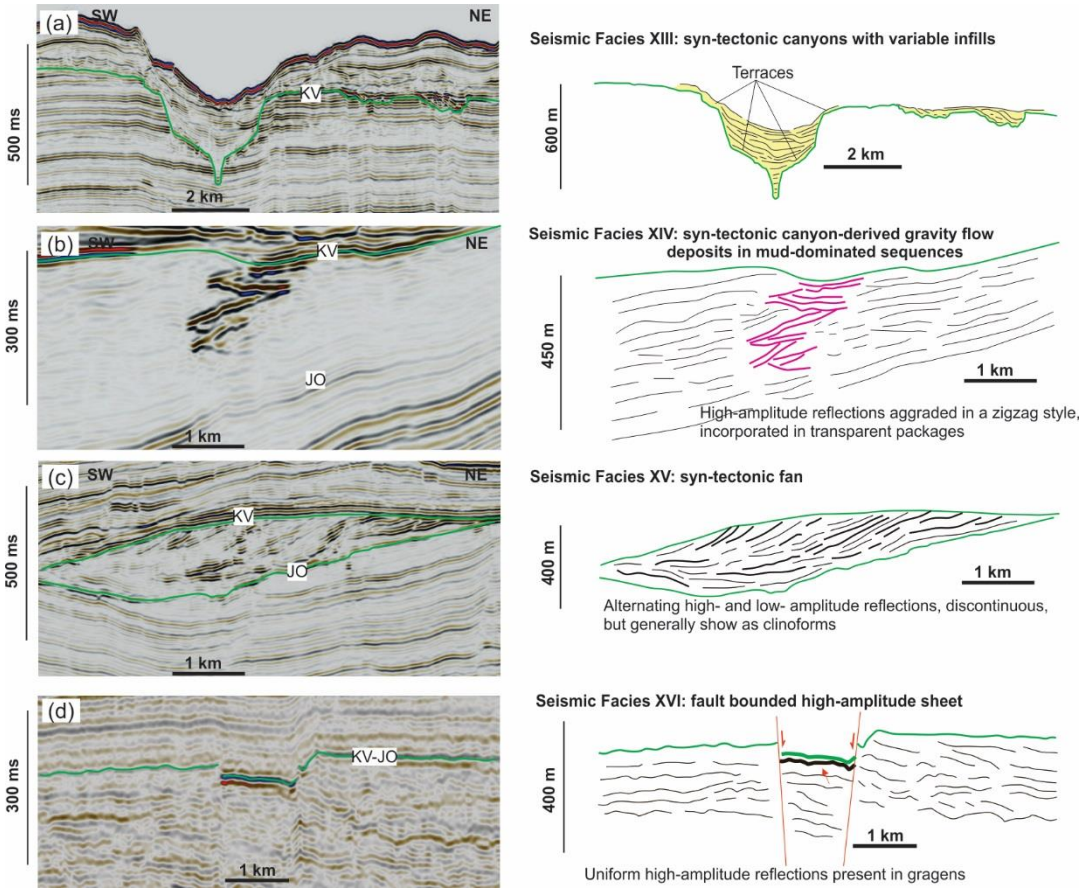

Figure 6-6. Representative seismic sections from Curt-3D and WA484P-3D seismic surveys showing secondary seismic facies identified for the syn-tectonic succession (JO-KV), and their interpretation.

The seismic facies defined above summarizes the major facies for the succession between Pliensbachian Maximum Flooding Surface (JP) and Valanginian Unconformity (KV). SF I-V revealed the genetically related depositional environment within a large fluviodeltaic system from subaerial to subaqueous, and SF VI-XII summarized these localized depositional elements within the system. SF XIII-XVI represent the elements that were formed during active rifting, thus representing a genetically different depositional system. The Lower Jurassic succession (J-JP), which is characterized by high-amplitude reflections (Figure 6-3, 6-4) and corresponds to the carbonate dominated succession (North Rankin Formation), is not included as a seismic facies in this classification scheme.

6.2 3D SEISMIC STRATIGRAPHIC ARCHITECTURE

Isochron maps (Figure 6-9, 6-10, 6-11) are constructed for a series of seismic stratigraphic units that are defined by regional surfaces and survey-restricted surfaces. The spatial variation of these seismic units, together with the primary seismic facies defined in Section 6.1, enable

investigation of the internal stratigraphic architecture, which, in turn, provides constraints on the interpretation of seismic/sedimentary facies.

Due to the chaotic nature of some of the seismic facies (e.g., fluviodeltaic plain), poor imaging caused by shallow feature artefacts and/or strong structural deformation (e.g., large fault displacement), some of the horizons are only picked for a small proportion of the survey areas. For instance, for the WA484P-3D survey area, the detailed stratigraphic correlation that is conducted on the Central Horst and Northern Slope does not extend into the Thouin Graben because of the intense structural deformation of the Emu Fault System; for the Curt-3D survey area, horizon interpretation are difficult to extend into the fluviodeltaic plain facies (SF I) and the artefact-influenced southeast area.

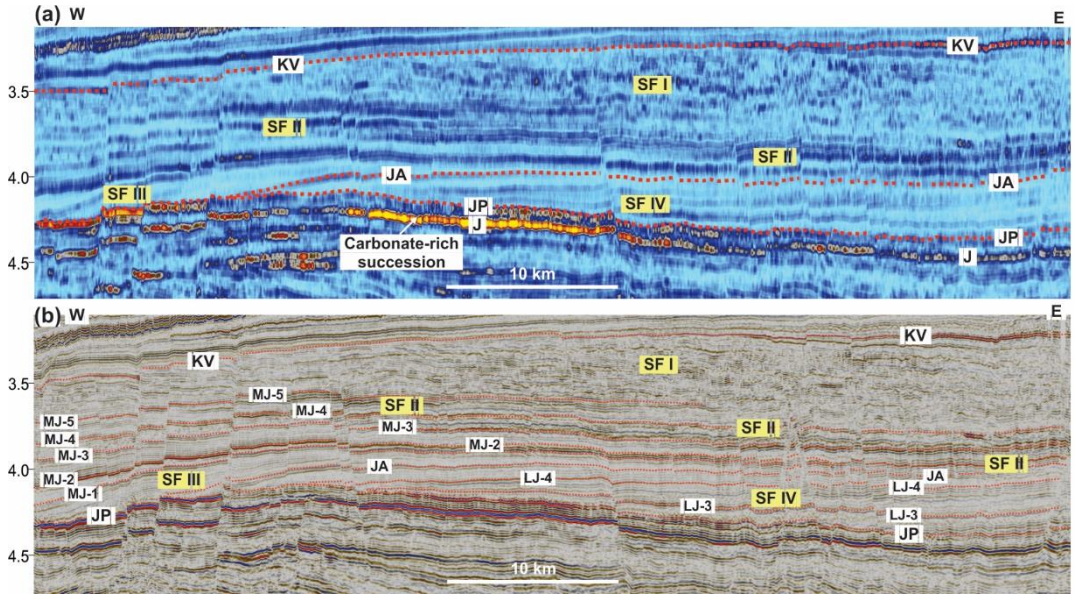

Figure 6-7. A representative NW-SE section (a, RMS amplitude; b, seismic) of Curt-3D with Huntsman-1 well intersection (c, wellsite lithology logging), showing the major surfaces (J= Base Jurassic, JP=Pliensbachian Maximum Flooding Surface, JA=Aalenian Erosional Surface, KV=Valanginian Unconformity, LJ1-4 represent four Lower Jurassic surfaces from older to younger, MJ1-5 represent five Middle Jurassic surfaces from older to younger), primary seismic facies between JP and KV (SF I: fluviodeltaic plain; SF II: shelf; SF III=slope; SF IV=basin floor, SF V= carbonate shelf-ramp). See Figure 6-1 for location.

The major focus of this section is on the internal stratigraphic architecture of the Lower-Middle Jurassic fluviodeltaic-related depositional system (JP-JO) and the subsequent syn-tectonic depositional system (JO-KV). However, the Lower Jurassic carbonate-rich system (J-JP) is also briefly covered.

6.2.1 Lower Jurassic mixed carbonate-siliciclastic system (J-JP)

In both the Rowley Sub-basin and northeast Exmouth Plateau, the lowermost part of the Jurassic succession (J-JP) consists of a set of parallel, continuous, high-amplitude reflections, which corresponds to the carbonate-rich North Rankin Formation (e.g., Figure 6-2, 6-3, 6-7, 6-8). In the Rowley Sub-basin (Curt-3D), the isochron map of this carbonate-rich succession

(J-JP) thins from more than 160 ms (252 m) in the southeast to less than 20 ms (31.5 m) in the northwest (Figure 6-9g). It also thins from southwest to northeast which is seemingly controlled by the pre-existing basin-scale northwest- trending high (Figure 4-6a). On the

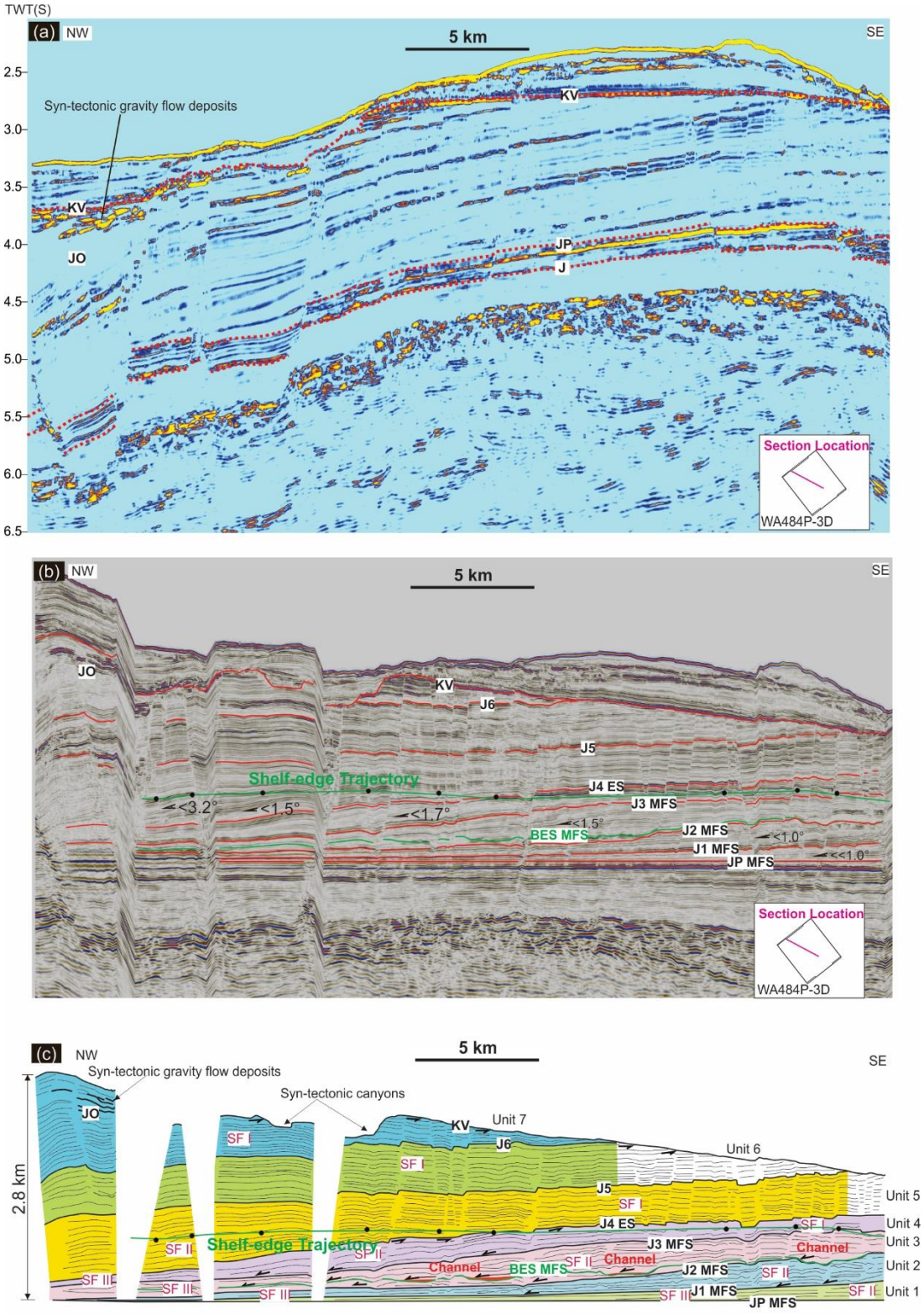

Figure 6-8. A representative NW-SE trending section of the WA484P-3D seismic survey, a) RMS amplitude, b) seismic flattened on the Pliensbachian Maximum Flooding Surface (JP), 3) detailed interpretation, showing spatial and temporal stratigraphic architecture of the shelf-slope-basin system. SF II = shelf facies, SF III = slope

facies, SF IV= basin floor facies; J1-6 represent six horizons in Jurassic from older to younger; BES=channelized basal erosive surface, MFS=Maximum Flooding Surface, ES=erosive surface. See Figure 6-1 for location.

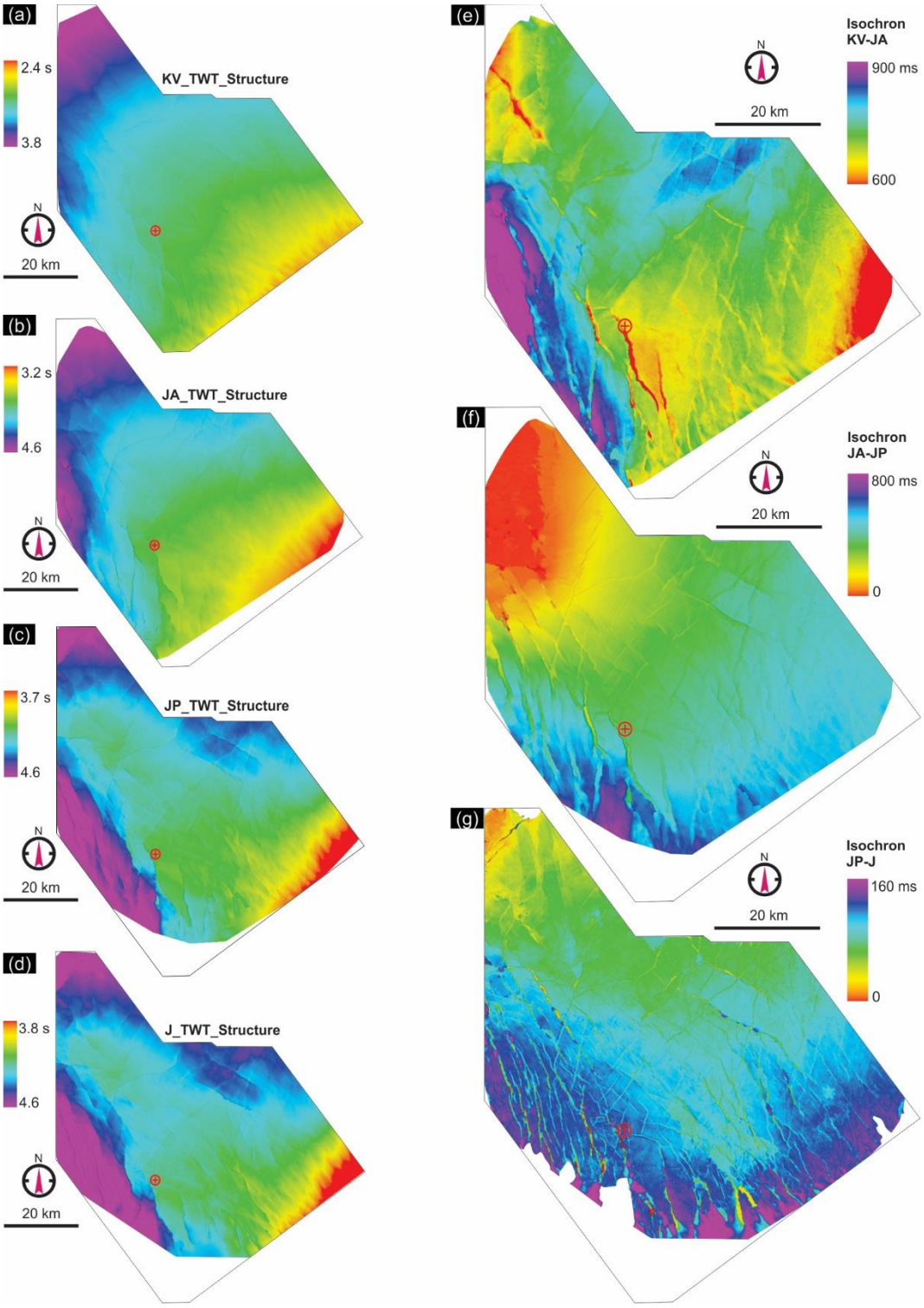

Figure 6-9. Two-way traveltime (TWT) structure map (Curt-3D) of, a) Valangnian Unconformity (KV), b) Aalenian Unconformity (JA), c) Pliensbachain Maximum Flooding Surface (JP) and d) Base Jurassic Unconformity (J). Isochron map of, e) Legendre Formation (JA-KV), f) Murat and Athol Formation (JP-JA) and g) North Rankin Formation (J-JP).

northeast Exmouth Plateau, this succession is around 200 ms (315 m) thick on the central horst and thins slightly northwesterly (Figure 6-2).

6.2.2 Lower-Middle Jurassic fluviodeltaic related system (JP-JO)

For the Lower-Middle Jurassic fluviodeltaic-related succession (JP-JO), it is difficult to establish a single chronostratigraphic framework between the Rowley Sub-basin and the northeast Exmouth Plateau because the Curt-3D and WA484P-3D seismic surveys are situated on opposite flanks of the Thouin Graben, and the Legendre Delta is highly progradational. The Rowley Sub-basin and northeast Exmouth Plateau are addressed separately in terms of the stratigraphic architecture of the Lower-Middle Jurassic fluviodeltaic related succession (JP-JO)

Rowley Sub-basin

In Rowley Sub-basin, the Aalenian horizon (JA) divides the fluviodeltaic-related succession into the shale dominated lower part (Murat + Athol Formation) and the sand dominated upper part (Legendre Formation) (Figure 6-3). The lower part generally thins toward the northwest, which reflects the northwesterly progradation of the system. It was also influenced by the northwest- trending Huntsman Arch, which is demonstrated by the presence of arch-like topography at the Pliensbachian horizon (JP) and the concave-outboard contours of the isochron map of the Lower Jurassic succession (JP-JA) (Figure 6-9c, d, f). The thickness of the Middle Jurassic succession (JA-JO) was predominantly controlled by the differential erosion associated with rift tectonics during the Oxfordian-Valanginian. The thickest part is located at southwest limit of the area (approx. 0.9 second TWT [1420 m]), which is controlled by northwest- trending (Middle?)Late Jurassic-Early Cretaceous faults (Fault Group 4c) (Figure 6-9e). The thinnest areas (approx. 0.6 second TWT [980 m]) are separately located at the northwest limit of the survey area and in the proximity to the Huntsman-1 well (Figure 6-9e). The former was due to the strong erosion of the rift shoulder and the latter was controlled the differential uplift and erosion related to the formation of the northwest- trending faults (Fault Group 4c).

A series of seismic units are defined on the basis of the interpretation of horizons LJ1-LJ4 (LJ=Lower Jurassic) and MJ1-MJ5 (MJ=Middle Jurassic). The stratigraphic architecture of these seismic units (isochron maps and internal facies distribution), together with stratigraphic significance of these survey-restricted horizons (termination patterns) are described as follows:

Unit i (JP - LJ1): the lowermost part of the fluviodeltaic succession is comprised of a northwesterly thinning wedge that downlaps on the Pliensbachian Maximum Flooding Surface (JP) and is bounded by a high-amplitude reflection at the top (LJ1) (Figure 6-3b, 6-4b). This seismic unit is over 200 ms (315 m) thick in the southeast and pinches out at the proximity of the Huntsman-1 (Figure 6-10). Internally it is characterized by the sub-parallel

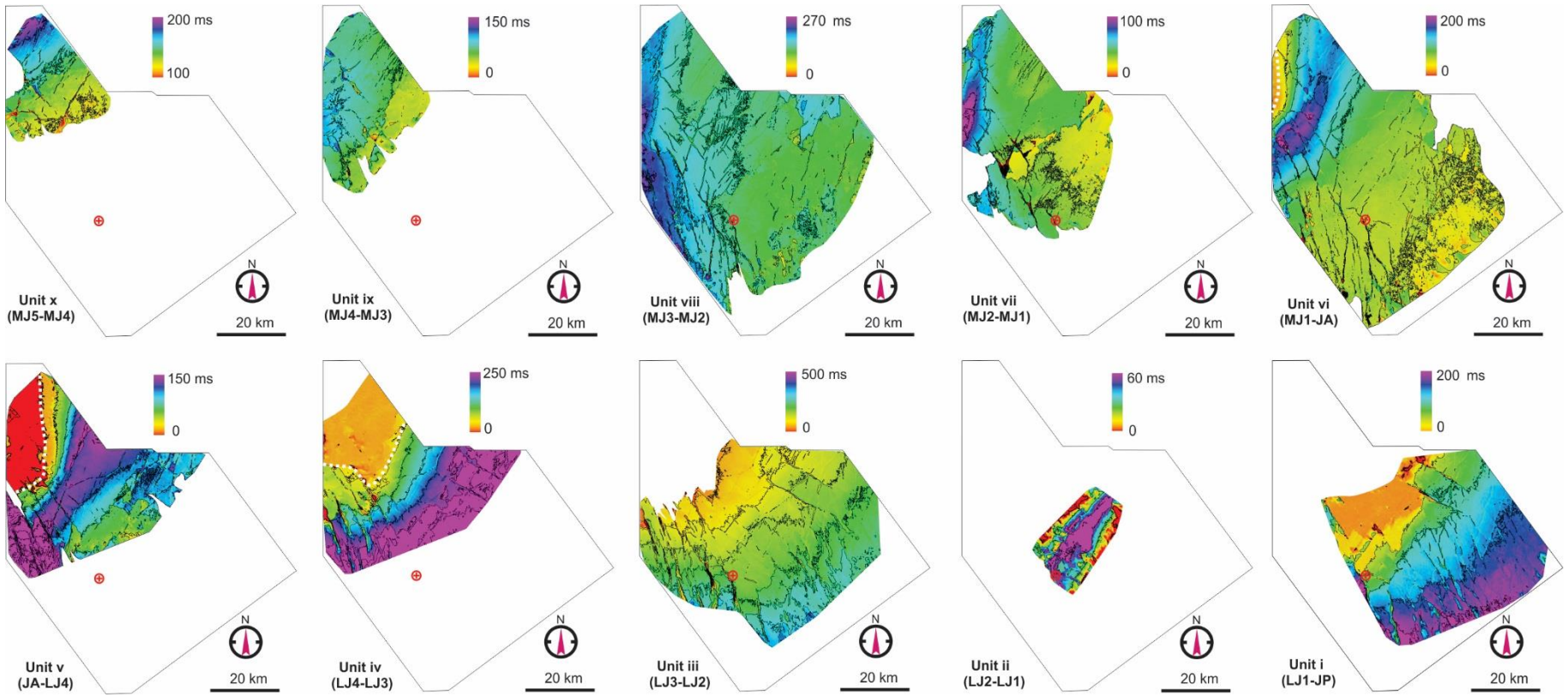

Figure 6-10. Isochron maps of seismic units defined within the Lower-Middle Jurassic fluviodeltaic-related succession (Murat, Athol and Legendre Formation) in the Rowley Sub-basin (Curt-3D), showing the stratigraphic architecture. The Unit i (LJ1-JP) show a northwesterly thinning sedimentary wedge; Unit ii (LJ1-2) represent a carbonate shelf-ramp system; Unit iii (LJ2-3) and iv (LJ3-4) represent northwesterly thinning wedges; Unit v (LJ4-JA), vi (JA-MJ1), vii (MJ1-2) and viii (MJ2-3) exhibit depocenters which represent the sigmoidal slope facies (Note the depocenters were migrating towards the northwest and their orientation changes from northeast to north-northeast); Unit ix (MJ3-4) and x(MJ4-5) show slightly northwesterly thickening wedges that represent the transition from shelf to basin facies.

low-amplitude basin facies (SF IV). Unit I (JP-LJ1) is interpreted as a fine-grain siliciclastic succession deposited from the lower slope to basin floor.

Unit ii (LJ1-LJ2): at the distal end of LJ1 developed a set of oblique high-amplitude clinoforms that are 150 m high, 5-8 km wide, with < 2° maximum dip (SF V) (Figure 6-4b). They downlap on the Pliensbachain Maximum Flooding Surface (JP) and are toplapped a high-amplitude reflection (LJ2). In plan view, Unit ii (LJ1-LJ2) shows a northeasterly trending elongate depocenter (60 ms [95 m] maximum thickness) and thins towards both northwest and southeast (Figure 6-10). The correlative high-amplitude reflection (LJ2) in Huntsman-1 is formed by tight dolomites with calcilutite. Unit ii (LJ1-LJ2) is interpreted to represent a carbonate shelf-ramp system, which is associated with a temporal transgression and/or sediment waning that started from LJ1.

Unit iii (LJ2-LJ3) and *Unit iv (LJ3-LJ4)*: these two units are both characterized by northwest-thinning sedimentary wedges (Figure 6-3, 6-3, 6-7). In the proximal area, they consist of parallel medium-high amplitude reflections (shelf facies, SF II) and gradually change into sub-parallel low-amplitude reflections (basin facies, SF IV) towards northwest. The facies distribution within these units are consistent with the northwesterly thinning trend (both two units are approx. 300 ms TWT [472.5 m] in the southeast and pinch out towards northwest) (Figure 6-10). Both of the two seismic units show isochron contours that are concave outboard, suggesting the control of the northwest- trending Huntsman Arch. Downlapping is observed associated with LJ3 and LJ4 in the distal area (Figure 6-3, 6-4), suggesting they are a maximum flooding surface.

Unit v (LJ4-JA): the upper part of Lower Jurassic succession is comprised by a unit that thins both to the northwest and southeast with a northeast trending elongate central depocentre (Figure 6-10). This thickness change is consistent with the lateral change of primary seismic facies. Clinoformal foresets (slope facies, SF III) are the thickest in the centre, and rapidly pinchs out toward northwest because of downlapping on the underlying Pliensbachian maximum flooding surface (JP MFS). They are flanked by the much broader and thinner topsets (shelf facies, SF II) to the southeast (Figure 6-3, 6-4). The depocentre widens towards both northeast and southwest with the narrowest part situated on the Huntsman Arch (Figure 6-10), which was a result of the control of the Huntsman Arch. On the western flank of the arch, this unit shows fault controlled thickness variation, which is consistent with the activities of the northwest- trending rift-related faults during this period (demonstrated in Figure 5-16). The top boundary of this unit (JA) is characterized by truncation on the shelf-slope transition (Figure 6-3, 6-4, 6-7), which is indicative of strong sediment bypass. In the basin, it is downlapped by the overlying sediments (Figure 6-3, 6-4), suggesting it is also a maximum flooding surface.

Unit vi (JA-MJ1) and *vii (MJ1-MJ2)*: these two units comprise the lower part of middle Jurassic Legendre Formation (Figure 6-3). Both units show the same sedimentary thinning trend as Unit v (LJ4-JA), with a tabular shelf facies (SF II) in the southeast and the thickest elongate depocentres (slope facies [SF III]) in the centre, which rapidly pinchs out towards the northwest (Figure 6-10). However, the orientation of the depocentre axes changes to north-northwest (Unit vi) and then to north-south (Unit vii). The contours still show concave-outboard geometry but have much gentler curvature compared with the underlying Unit v (LJ4-JA). Given that no coeval structural activity is interpreted, the two units are interpreted as the result of progressive sediment draping on the topography created by the underlying northwest- trending Huntsman Arch. The depocentres shift progressively towards the northwest, which shows the shelf-slope-basin clinoformal system is northwesterly progradational. Truncation is also associated with the boundary (MJ1) in the proximity of shelf-slope transition, suggesting strong sediment bypass (Figure 6-3, 6-4).

Unit viii (MJ2-MJ3): passing upward, the north-south trending depocentre (slope facies [SF III]) continues shifting to the northwest, only leaving a small proportion inside the Curt-3D survey area (Figure 6-10). A northwest- trending elongate depocentre is present in the southwest limit of the survey area and is interpreted as the result of the rejuvenation of northwest- trending Huntsman Arch. Most of the area was dominated by a uniformly thick succession that consists of the shelf facies (SF II). In the southeast area, the fluviodeltaic plain facies (SF I) is present due to the northwesterly progradation of the system (Figure 6-3, 6-4).

The Unit ix (MJ3-MJ4): it consists of a slightly northwesterly thickening succession (Figure 6-10). The low-amplitude slope facies (SF III) pulled back landwards during this period, which is consistent with the pullback of the fluviodeltaic plain facies (SF I) in the southeast area (Figure 6-3, 6-4). A set of small scale of clinoforms (delta-scale subaqueous clinoforms, SF VII) are observed within this succession at the shelf-slope transition area (see Chapter 6.3 for details).

Unit x (MJ4-MJ5): it contains a depocentre which represents the slope facies (SF III) outboard. It changes into the shelf-facies (SF II) in the central area and fluvial facies (SF I) in the southeast (Figure 6-4, 6-10). The depocentre is only partially revealed by the Curt-3D survey and is likely to be northeast-southwest trending, which differs from the orientation of the underlying shelf-slope system.

Passing upward, horizons are difficult to be interpreted because the disorganized fluviodeltaic plain facies (SF I) has occupied the whole survey area (Figure 6-3, 6-4, 6-7).

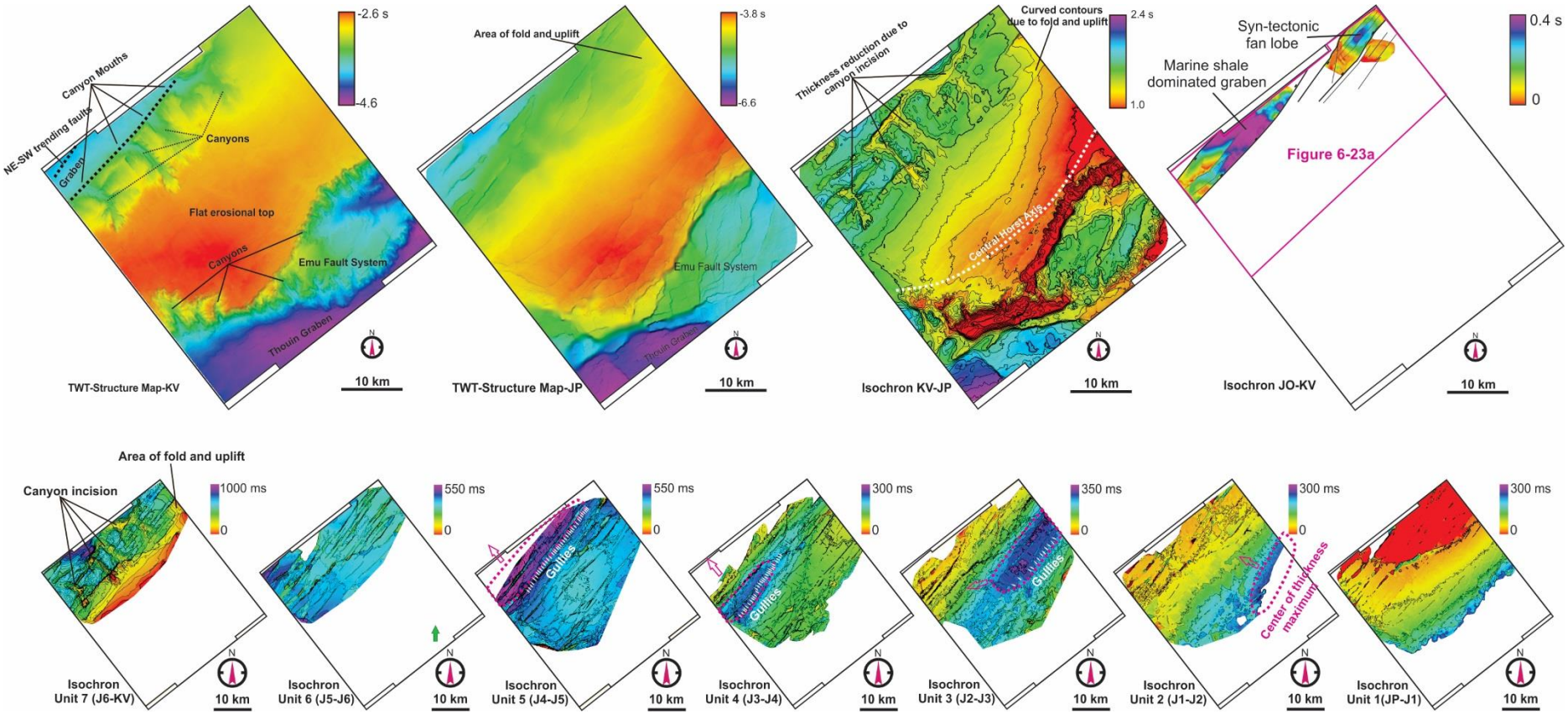

Figure 6-11. Two-way-time structure maps of Pliensbachian Maximum Flooding Surface (JP-MFS), Valanginian Unconformity (KV) and isochron map of the Jurassic fluviodeltaic- related succession (JP-KV) and syn-tectonic succession (JO-KV) (upper); Isochron maps of the seven seismic units defined within the succession, showing a constantly northwesterly progradational shelf-slope-basin clinoform system (below)

Northeast Exmouth Plateau

On the northeast Exmouth Plateau, detailed interpretation of this succession was only conducted on the Central Horst and the Northern Slope, due to the lack of accuracy of horizon correlation across the Emu Fault System and the intense structural deformation in the Thouin Graben (Figure 5-11). Six Jurassic horizons (J1-J6, from old to young, Figure 6-2, 6-8) are interpreted within this survey. Among these survey restricted horizons, J1-J3 are downlapping surfaces (MFS), and J4 is an erosive surface (ES). In addition, channelized basal erosive surfaces (BES) and the correlative reflections are picked in order to investigate the geometry and geomorphology of the channels that are identified from the succession. They are also downlapped by overlying sediments and thus represent maximum flooding surfaces (BES MFS). The internal stratigraphic architecture of this succession on the northeast Exmouth Plateau is described as follows:

Unit 1 (JP-J1) and *Unit 2 (J1-J2)*: these two seismic units comprised the lowermost part of the fluviodeltaic-related succession and are dominated by clinoform bottom sets (basin facies, SF IV, Figure 6-2, 6-8). Both units thin towards the northwest (Figure 6-11). The bounding surfaces of these units show downlapping in the distal area and are maximum flooding surfaces (MFS).

Unit 3 (J2-J3) and *Unit 4 (J3-J4)*: the middle part of the succession, Unit 3 (J2-J3) and Unit 4 (J3-J4) thin both to the northwest and southeast with a central depocentre (Figure 6-11). This thickness change is consistent with the lateral change of the primary seismic facies. Clinoformal foresets (slope facies, SF II) are thickest in the middle and are flanked by thinner top sets (shelf facies, SF I) to the southeast and bottom sets (basin facies, SF III) to the northwest (Figure 6-2, 6-8). Similar to the underlying seismic units, they are also bounded by maximum flooding surfaces (J3-MFS). The top of Unit 4 is truncated by J4 ES on the Northern Slope.

Unit 5 (J4-J5): it is generally thickening from the Central Horst (400 ms TWT [630 m]) to the Northern Slope (550 ms TWT [866 m], Figure 6-11). It consists of clinoformal topsets (shelf facies, SF I) on the central horst with front sets (SF II) to the northwest (Figure 6-2, 6-8).

Unit 6 (J5-J6) and *Unit 7 (J6-KV)*: the uppermost part of the succession, Unit 6 (J5-J6) and Unit 7 (J6-KV), is generally composed of parallel clinoform topsets (SF I, Figure 6-2, 6-8). The slope-basin facies (SF III-IV) has completely shifted outside the WA484P-3D survey area. The thickness of Unit 6 is relatively constant (Figure 6-11). The upper part of Unit 7 was significantly eroded due to canyon incision and tectonic erosion in Late Jurassic-Early Cretaceous (Figure 6-8, 6-11).

The erosion caused by rift tectonics during Oxfordian-Valanginian is better demonstrated by the isochron between the top and bottom boundaries, KV and JP MFS, respectively (Figure 6-11). The thinnest part of the succession (500 ms TWT [788 m]) is located along the axis of the Central Horst. Thickness increases drastically across the Emu Fault System into the Thouin Graben, where up to 2 s TWT (3150 m) of the succession are preserved. This suggests that approximately 2360 m of the succession has been eroded from the Central Horst. To the northwest, thickness gradually increases to 1.6 s TWT (2520 m) from the central horst. The incised canyons in the northern slope have caused around 300 ms TWT (473 m) erosion.

The depocentres (clinoform foresets) of the Units 1-4 shift progressively from southeast towards the northwest, which shows a constant basinward progradation of the shelf-slope system (Figure 6-11). The northeast Exmouth Plateau (WA484P-3D) was dominated, from earlier to later, by deep marine basin, shelf slope and marine shelf respectively and was significantly influenced by erosion during the subsequent rift event.

6.2.3 Late Jurassic-Early Cretaceous syn-tectonic system (JO-KV)

In Rowley Sub-basin, the syn-tectonic succession shows a west- thinning wedge, which is 130 ms (205 m) thick in the east and pinchs out around the Huntsman-1 (Figure 6-12a). It is characterized by parallel continuous low-amplitude reflections that are seemingly conformable with the underlying succession. The syn-tectonic succession (JO-KV) is cut by the northwest- trending (Middle?)Late Jurassic-Early Cretaceous faults (FG 4c) but shows no clear fault-controlled thickness variation (Figure 6-12c).

On northeast Exmouth Plateau, strong erosion formed a flat peneplaned unconformity (JO-KV) on the central horst (Figure 6-2) and the syn-tectonic succession (JO-KV) is interpreted to be present in two fault controlled mini-grabens on the Northern Slope, which are defined by northeast trending extensional faults (FG 4a) (Figure 6-11). In both grabens, this succession has a maximum thickness of over 400 ms (630 m) and thins towards both northeast and southwest, which is controlled by the along-strike displacement variation of the faults. The previously mentioned syn-tectonic seismic facies, including the canyon derived gravity flow deposits (SF XIV) and syn-tectonic fan lobe (SF XV), are hosted in the two grabens (see Chapter 6-3 for details).

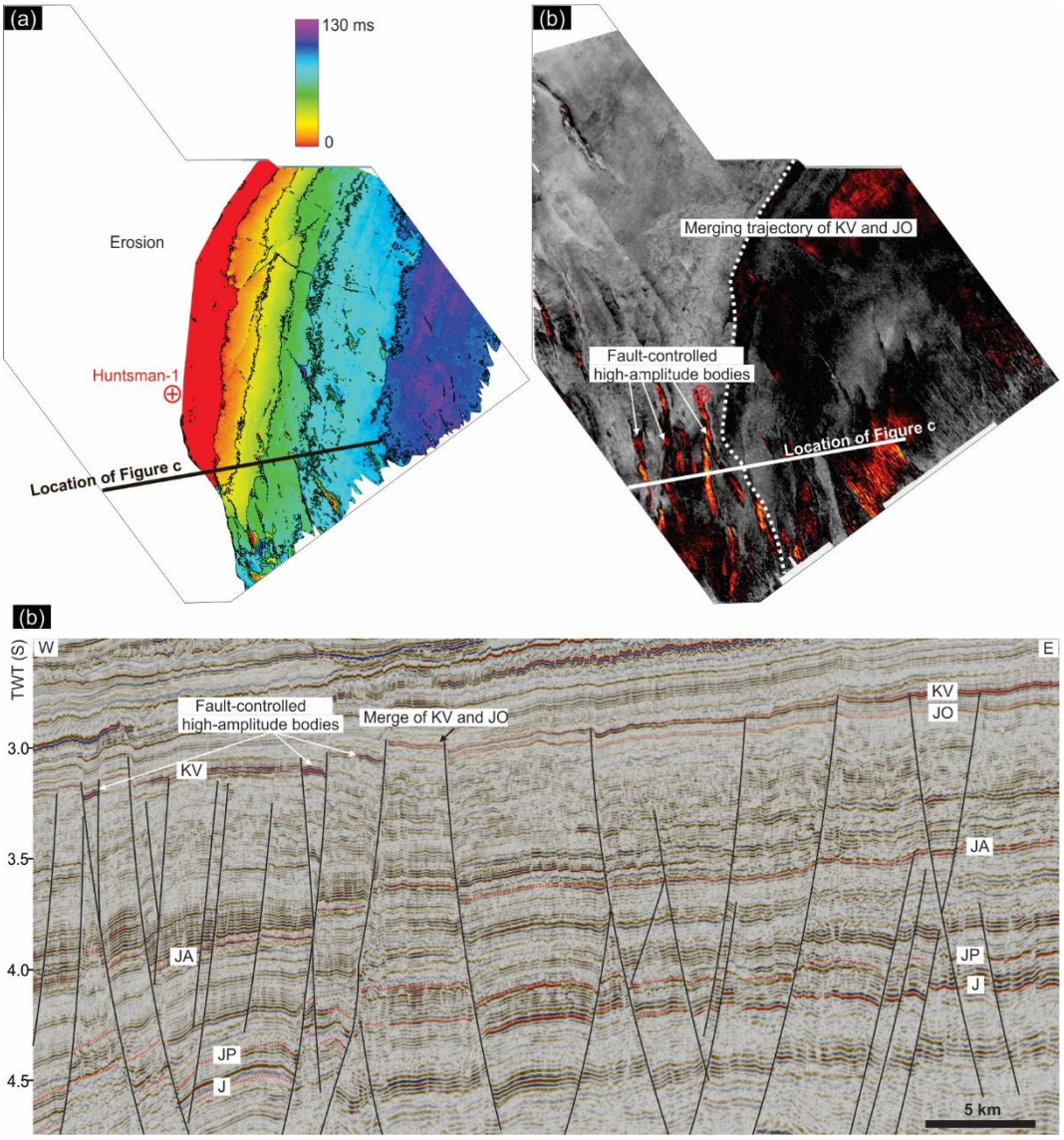

Figure 6-12. a) Isochron map of syntectonic succession (JO-KV) in the Rowley Sub-basin (Curt-3D), showing a westerly thinning sedimentary wedge with little fault control; b) Windowed RMS amplitude map of Valanginian Unconformity (KV) showing fault-controlled high-amplitude areas; c) A seismic section showing the high-amplitude anomalies of the Valanginian Unconformity (KV). Note these high-amplitude anomalies show more fault control in the western area where the Valanginian Unconformity (KV) and Oxfordian Unconformity (JO) merge together.

6.3 SEISMIC GEOMORPHOLOGY OF KEY DEPOSITIONAL ELEMENTS

This section is focused on the geomorphology of the key depositional systems and their associated depositional elements, which are defined by the seismic facies (Chapter 6.1). In particular, seismic attributes are used to reveal the mappable components, geometry and morphology of these depositional elements. The results are integrated with the seismic facies characteristics and three-dimensional stratigraphic architecture, in order to gain a comprehensive understanding of the sedimentary processes.

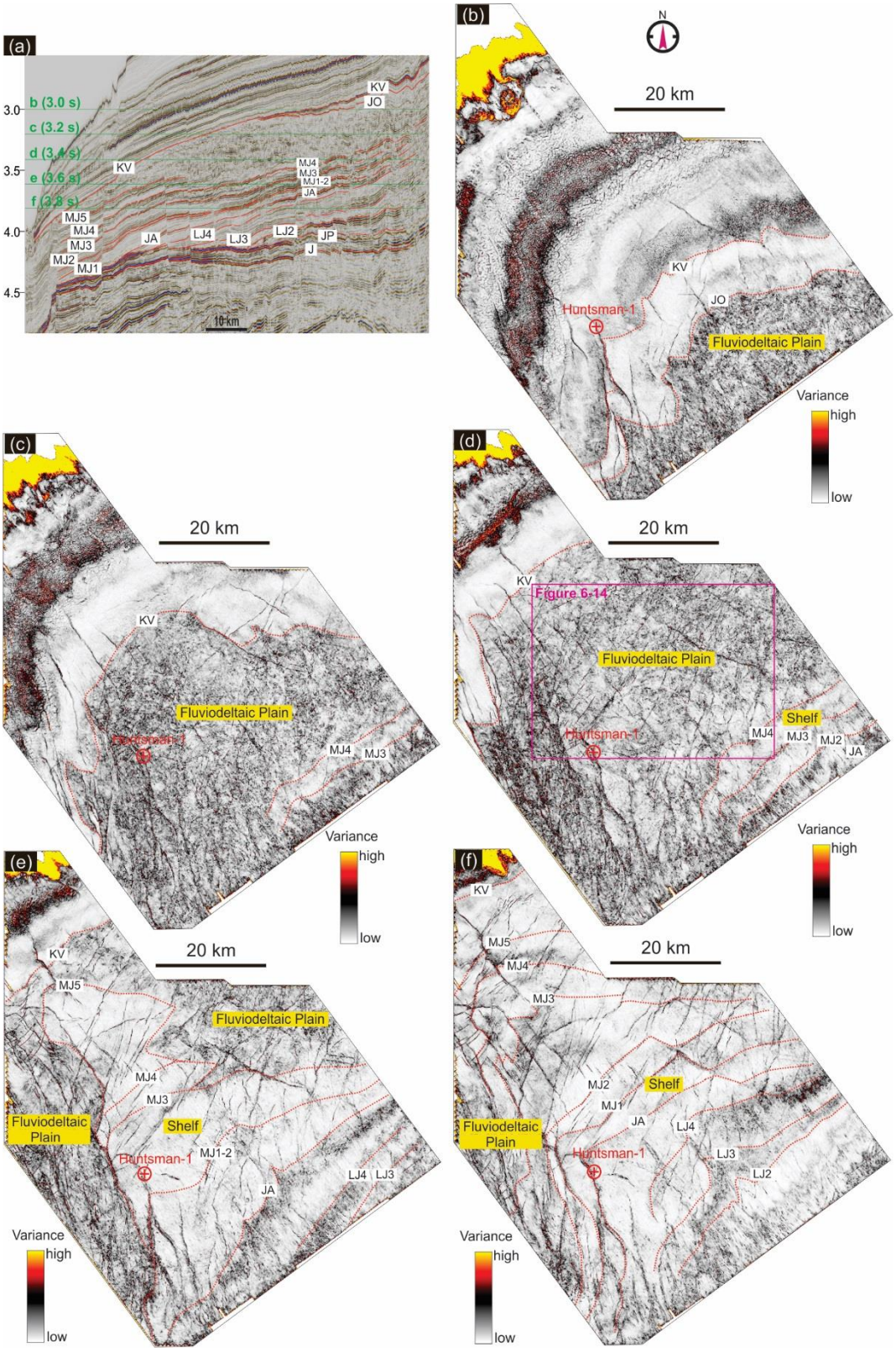

Figure 6-13. A representative northwest-southeast trending seismic section of the Curt-3D survey with the interpreted horizons (a), time slices of variance at 3.0 s (b), 3.2 s (c), 3.4 s (d), 3.6 s (e), 3.8 s (f), showing the geomorphological characteristics of fluviodeltaic plain facies (SF I) and shelf facies (SF II). The intersection trajectory between horizons and time slices are illustrated in red lines. J = Base Jurassic Unconformity, JP=Pliensbachian, JA=Aalenian, JO= Oxfordian, KV=Valanginian, LJ1-4 represent four Lower Jurassic horizons from older to younger, MJ1-5 represent five Middle Jurassic horizons from older to younger.

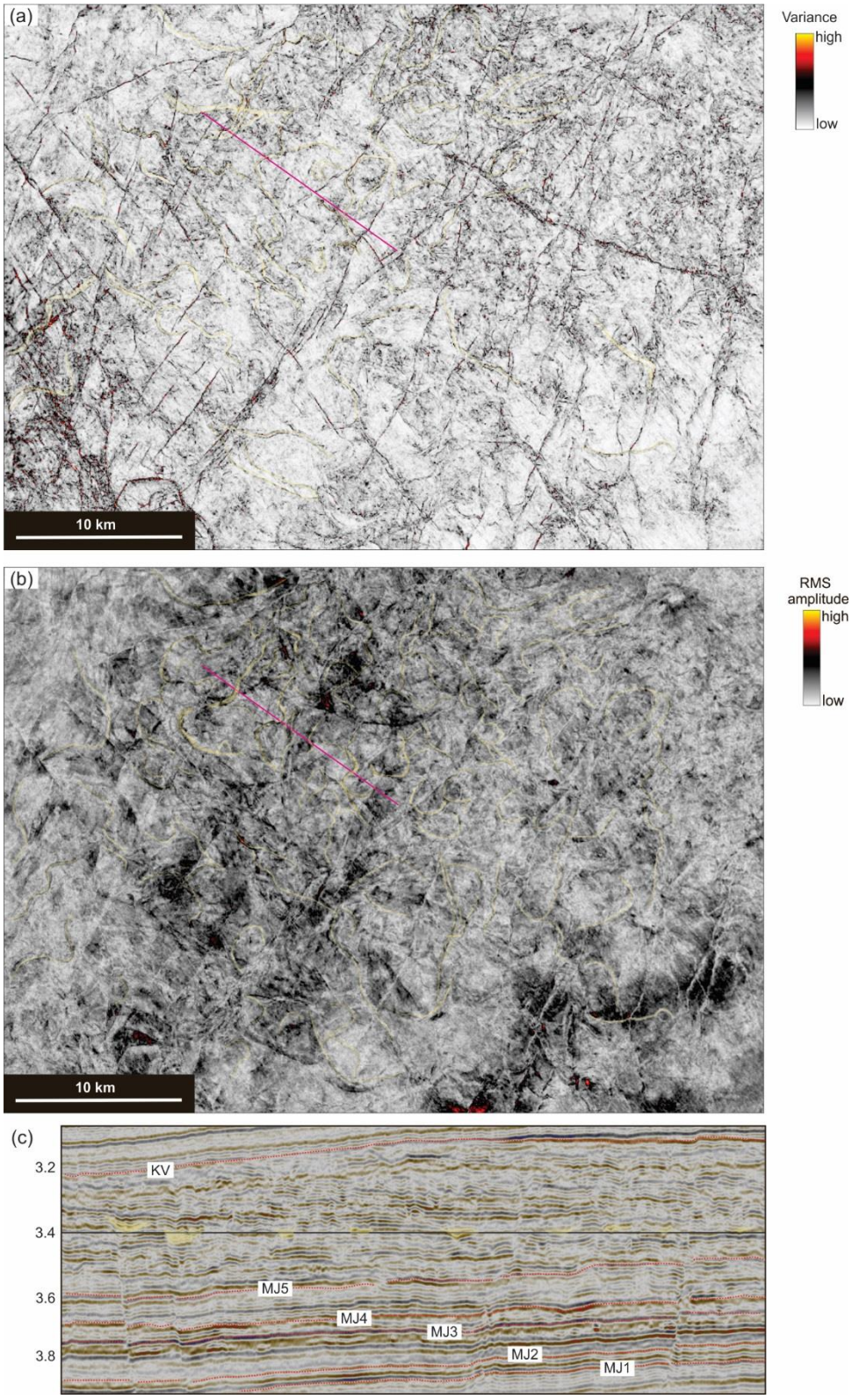

Figure 6-14. Time slice (a, variance; b, RMS amplitude) at 3.4 second of Curt-3D showing the geomorphological characteristics of the fluviodeltaic plain, and a seismic section (c) showing the disorganized seismic facies is due to a large amount of channels.

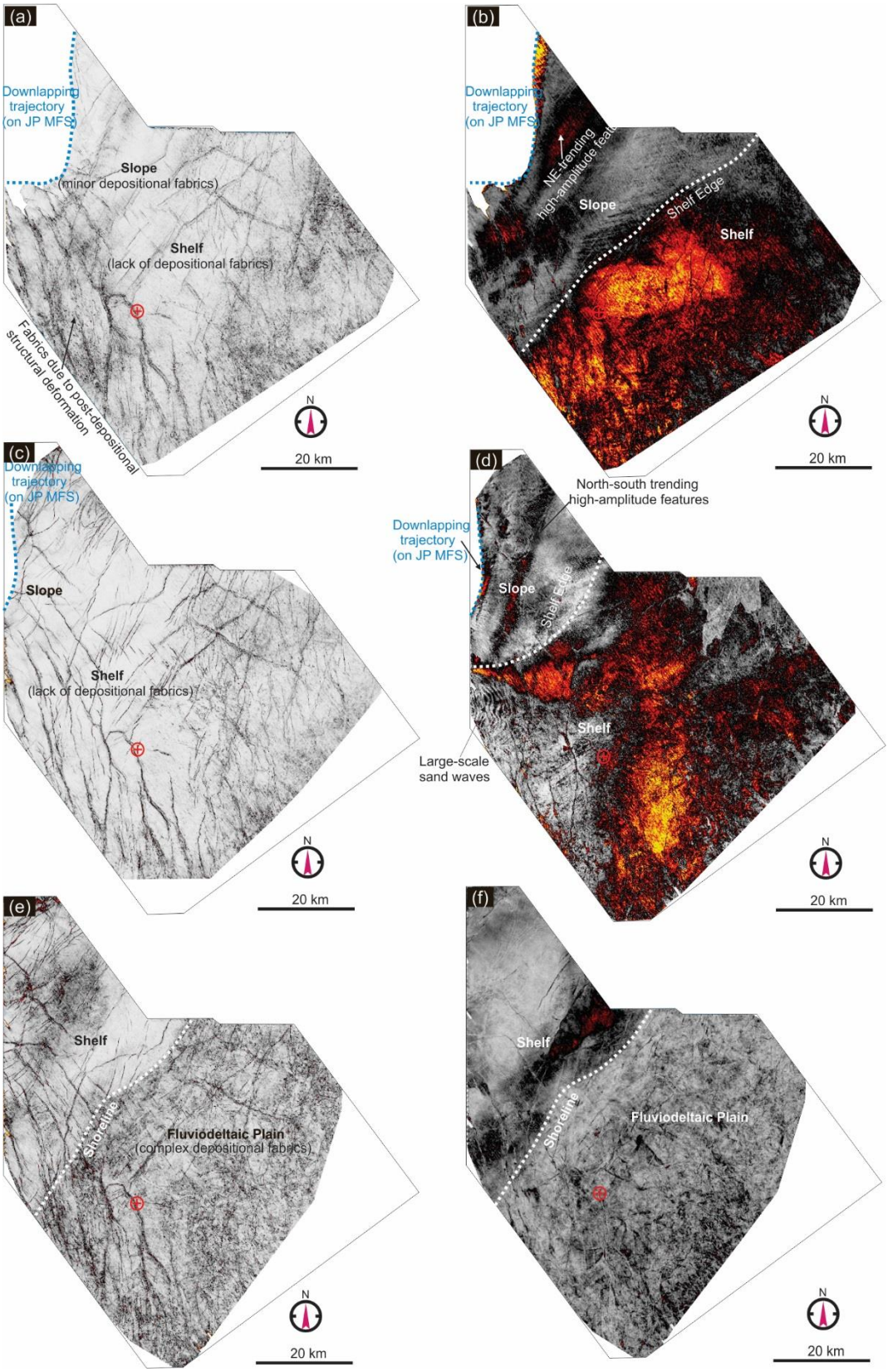

Figure 6-15. Seismic attributes maps of selected horizons, Aalenian (JA) (a, variance; b, RMS amplitude), MJ1 (c, variance; d, RMS amplitude) and 60 ms above MJ3 (e, variance; f, RMS amplitude), showing the geomorphological characteristics of the major primary seismic facies. The shelf is dominated by high RMS amplitude; the slope is dominated by low RMS amplitude area with elongate high-amplitude belts; the fluviodeltaic plain is generally low-amplitude, high variance area containing numerous channels.

6.3.1 Fluviodeltaic Plain & Fluvial Channel Belts

Fluviodeltaic plain (SF I) is the major sedimentary facies revealed from the upper part of the Legendre Formation in the Rowley Sub-basin (Curt-3D) and is characterized by a large amount of chaotic fabrics on the variance time slices, differing from the shelf facies (SF II), which shows minor and/or parallel fabrics (Figure 6-13). The chaotic fabrics consist of numerous channels that are usually less than 1 km wide and a few tens of milliseconds deep (tens of meters)(Figure 6-14). The channels mostly have low-amplitude infills which shows little amplitude contrast with the surrounding sediments, making it difficult to interpret them in cross section. They generally have high sinuosity (meandering channels) and their flow directions vary, suggesting they were formed in an environment with little stream gradient. High-amplitude patches are randomly distributed between the channels (Figure 6-14b).

6.3.2 Shelf-slope-basin: sand/mud belts

The subaqueous counterpart of the fluviodeltaic plain is the shelf-slope-basin system. Both variance and RMS amplitude are extracted at several stratigraphic levels to reveal the geomorphological features of the system. The shelf is characterized by large high-amplitude patches that extend across the entire shelf in the Aalenian (Figure 6-15a, b), blocky high-amplitude patches that occupied part of shelf at MJ1 (Figure 6-15c, d) and a narrow high-amplitude belt that is immediately adjacent to the fluviodeltaic plain at 60 ms below MJ3 (Figure 6-15e, f). These shelves are normally fabrics-free, especially in the outboard part, which is consistent with the fact deposition on shelf is usually laterally uniform. At MJ1, large sand waves that have a northwest orientation, are present. This suggests a northeast wave direction, which is parallel or slightly oblique to the east-northeast- dipping slope (Figure 6-15d). For the slopes investigated, there is normally little fabric on the variance maps, and elongate high-amplitude belts that are parallel/sub-parallel to slope, are observed (Figure 6-15b, d).

6.3.3 Delta-scale Subaqueous Clinoforms

Delta-scale subaqueous clinoforms are identified in Unit ix (MJ3-MJ4) in the northwest area of the Rowley Sub-basin (Curt 3D) where the Unit ix (MJ3-MJ4) shows slight northwesterly thinning which is interpreted to be a result of shelf slope transition (Figure 6-4, 6-10). Therefore these clinoforms are developed close to shelf-slope transition. High-quality variance map intersecting the clinoforms shows half-circle fabrics that are concave inboard (Figure 6-16b, c). This rules out gravity-driven slumps/landslides which normally show downslope listric geometry (concave outboard geometry). The fabrics only exerted an influence in an area of approximately 30 km × 20 km, suggesting they are not the primary controlling factor of northwesterly thinning of Unit ix (MJ3-MJ4). The adjacent southeast

area is characterized by fewer sedimentary fabrics and higher-amplitude shelf. The clinoforms mainly consists of low-amplitude reflections, in which several high-amplitude reflections are incorporated. In plan view they show as elongate patches in alignment with the curved fabrics (Figure 6-16c, d).

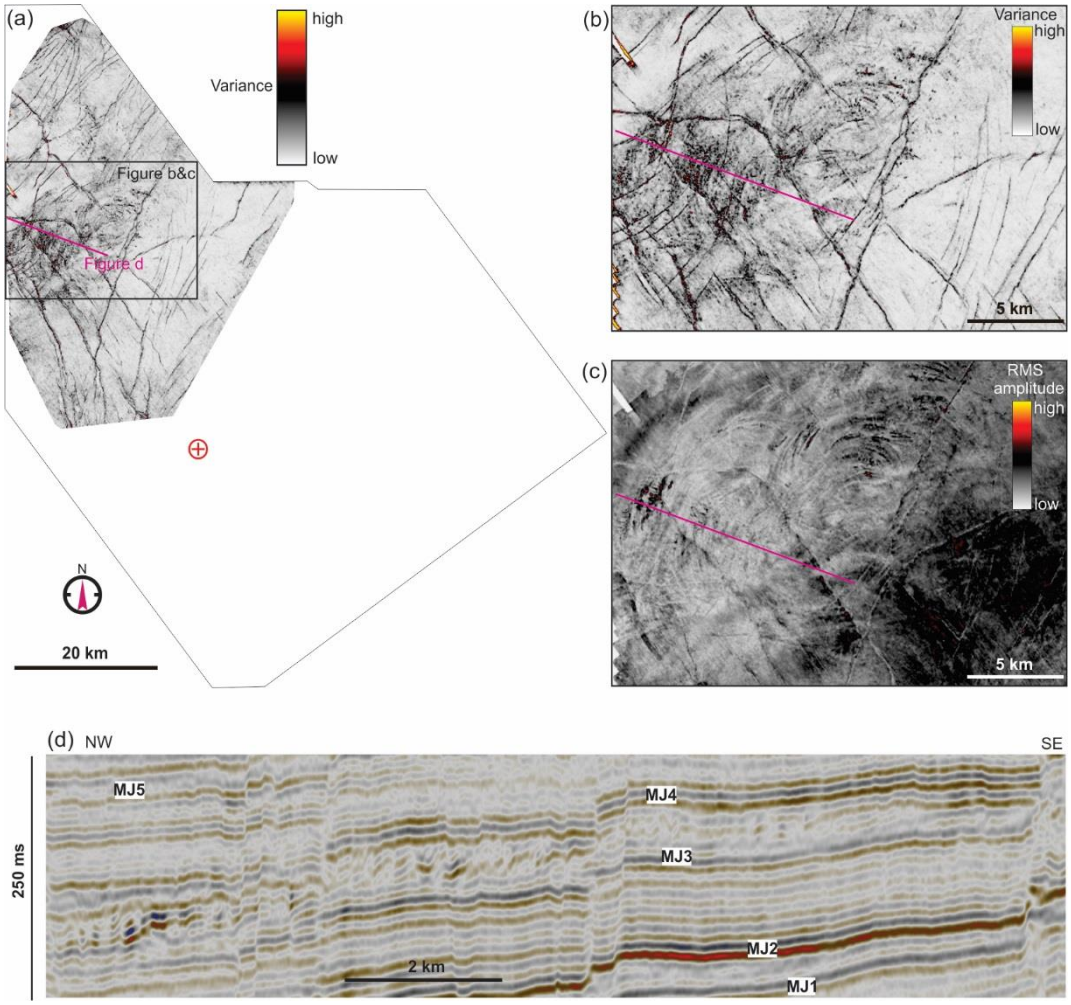

Figure 6-16. Seismic attribute map of 20 ms below MJ4 (a, variance; b, variance; c, RMS amplitude) and a seismic section (d) showing the geomorphology and facies characteristics of the subaqueous clinoforms. The clinoforms exhibit half-circle fabrics that are concave inboard. Several Late Jurassic-Early Cretaceous faults present as concave-outboard fabrics on plan view.

6.3.4 Sub-marine Channels

Submarine channels are only recognized on northeast Exmouth Plateau (WA484P-3D). They are present within the clinoform front-bottom sets (SF III & IV) in the lower part of the succession (Unit 2 [J1-J2], 3 [J3-J4]) (Figure 6-2, 6-8), which indicates that they are subaqueous channels developed on the slope to the basin floor. Three major segments with distinct characteristics are recognized: (1) the upslope segment, which is situated at the slope (Figure 6-17a, b, c) , is characterized by low-sinuosity, highly erosive surfaces that incise up to 200 ms TWT (315 m) into the underlying sediments (SF VIII). They are buried by parallel, oblique, and mounded low-amplitude mud-dominated sediments associated with the

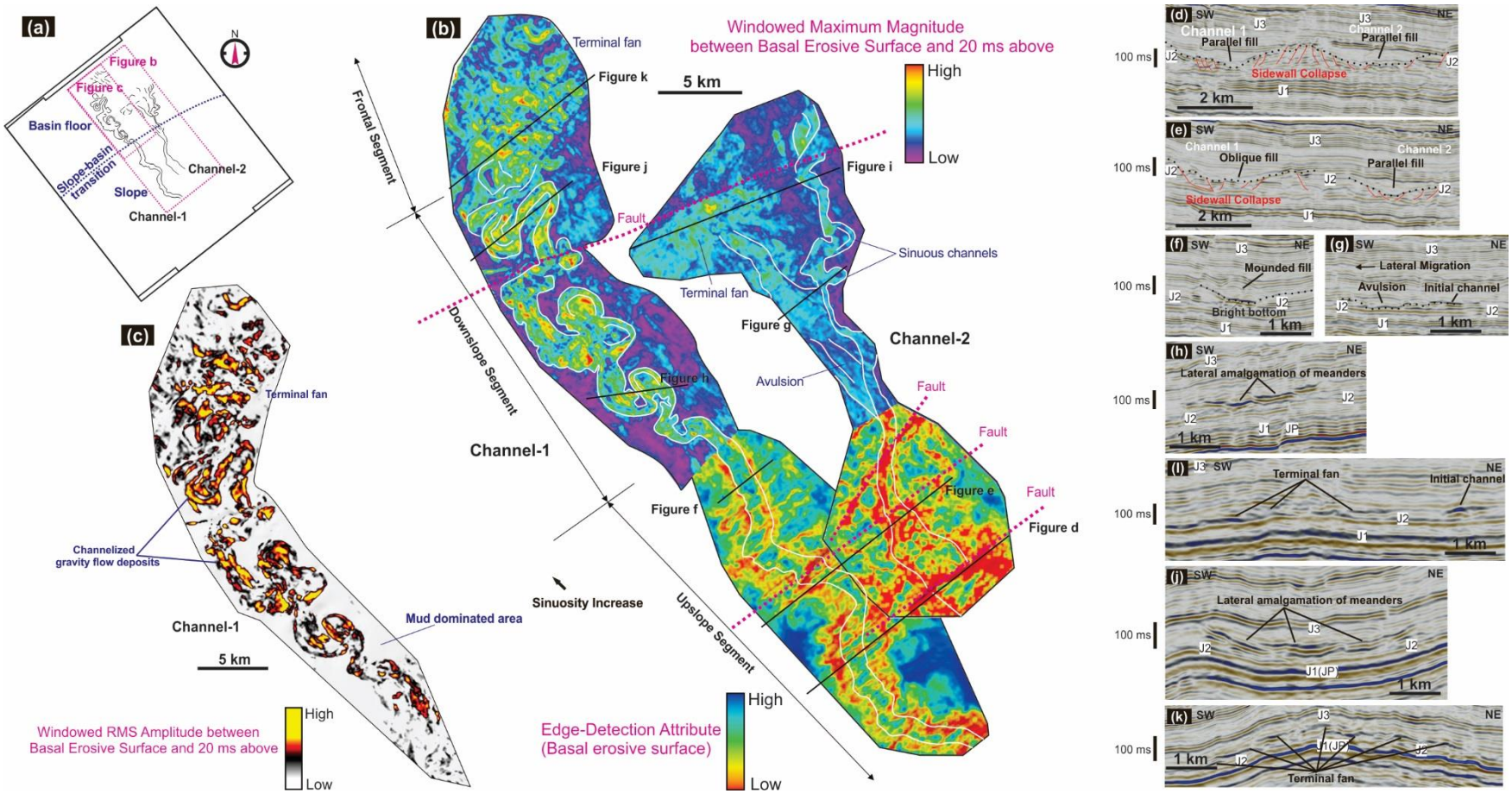

Figure 6-17. Location of two submarine channels identified in the succession (a); Edge-Detection Attribute, windowed Maximum Magnitude and windowed RMS Amplitude maps showing the three-dimensional geomorphology of the channels (b, c), and selected sections showing the architecture of different channel segments (d-k). Note that Edge-Detection Attribute was only used for the upslope segment of the channels which is filled with mud-dominated sediments and cannot be depicted by amplitude-based attributes.

progradation of Unit 3 (Slope Facies, SF III) (Figure 6-2, 6-8b, 6-17 d, e, f); (2) the downslope segment, located in slope to basin floor transition, consists of high-sinuosity, less erosive surfaces that are infilled with high-amplitude gravity flow deposits (SF IX) (Figure 6-17a, b , c, f, g, h, j); (3) the frontal segment, which is characterized by lobate basin floor fans (SF IX) (Figure 6-17a, b, c, i, k). Side-wall collapse features are commonly seen in the upslope segments of the channels (Figure 6-17d, e). The downslope segment of the Channel 2 shows the development of an avulsion, which is characterized by a sinuous channel with a north-northwest flow direction changing to a straight northwesterly flowing channel with a terminal fan (Figure 6-17b, g). Channel 1 was developed slightly later than Channel 2 based on erosive relationships and the reflection geometries of the infills (Figure 6-17e) and has northwest flow direction (Figure 6-17b).

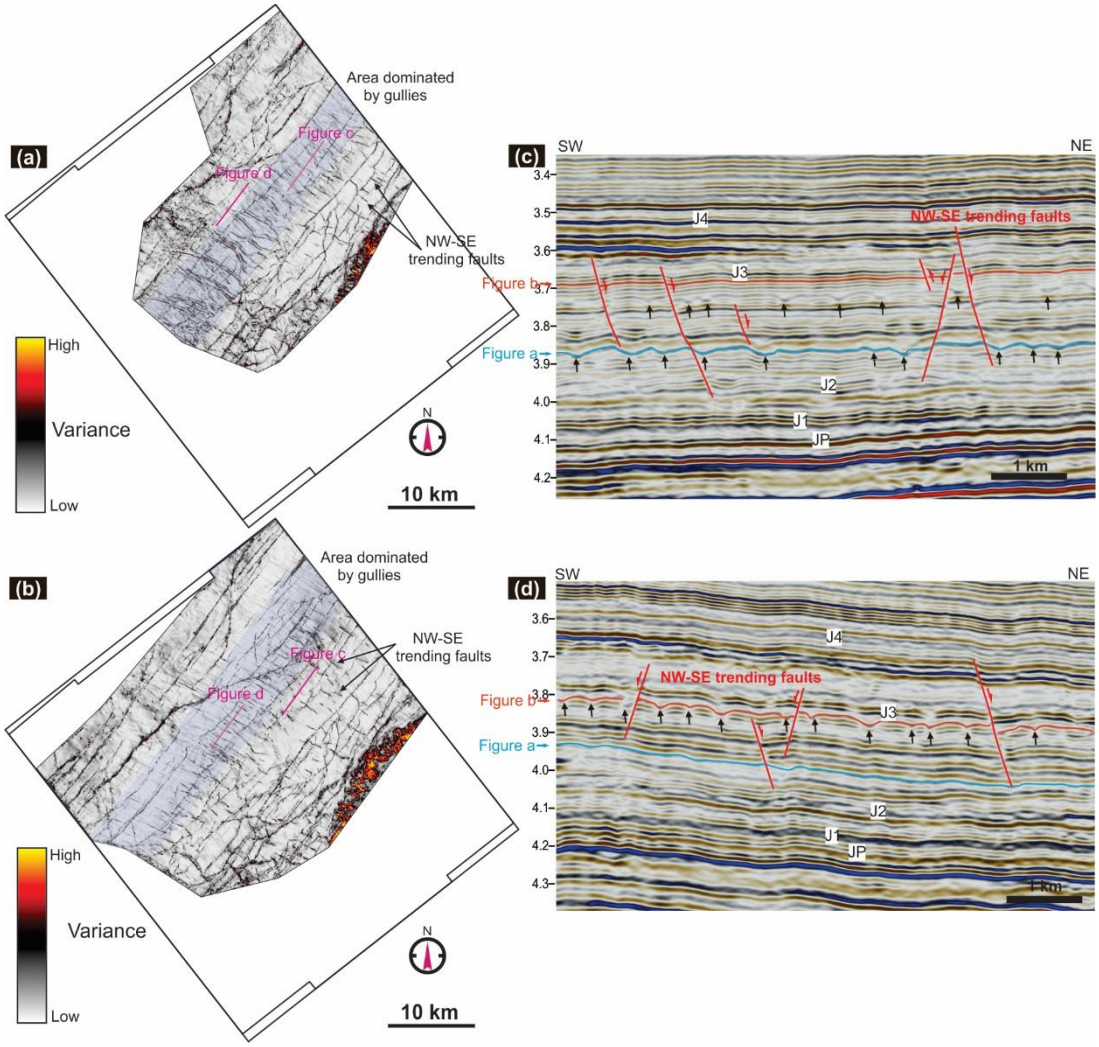

Figure 6-18. Variance attribute maps (a, b) and seismic sections (c, d) showing NW-SE trending gullies with low-amplitude infills (Seismic Facies VI) and NW-SE trending segmented Jurassic normal faults within the succession. The Jurassic normal faults, in some cases, overlap the gullies. The gullies are distinguished from the faults by their paired escarpments on the variance map.

6.3.5 Submarine Gullies

The interpreted gullies identified on northeast Exmouth Plateau (WA484P-3D) are distinguished from the submarine channels by their straight geometry and NW-SE strike (Figure 6-18a, b, 6-19a). The gullies were only developed in association with clinoformal front sets (SF III), and are present at multiple stratigraphic levels within Unit 3 (J2-J3) and Unit 4 (J3-J4) (Figure 6-18c, d). They extend up to 10 km with a width of 300 m and a depth of 20 ms TWT (32 m). The earliest gullies are slightly younger than the submarine channels. The positions where these gullies were developed shifted to the northwest consistently with the basinward accretion of the clinoforms (from figure 6-18a, to figure 6-18 b, then figure 6-19a). The gullies can be infilled by low amplitude muds (SF X) (Figure 6-18c, d) or high-amplitude sands (SF XI) (Figure 6-19a, b). For the gullies formed at the same time, the amplitudes of the infills are consistent from upslope to downslope (e.g., all gullies in Figure 6-18a have only low-amplitude infills; all gullies in Figure 6-19a have only high-amplitude infills). This is different from the submarine channels with low-amplitude infills upslope and high-amplitude infills downslope (Figure 6-17).

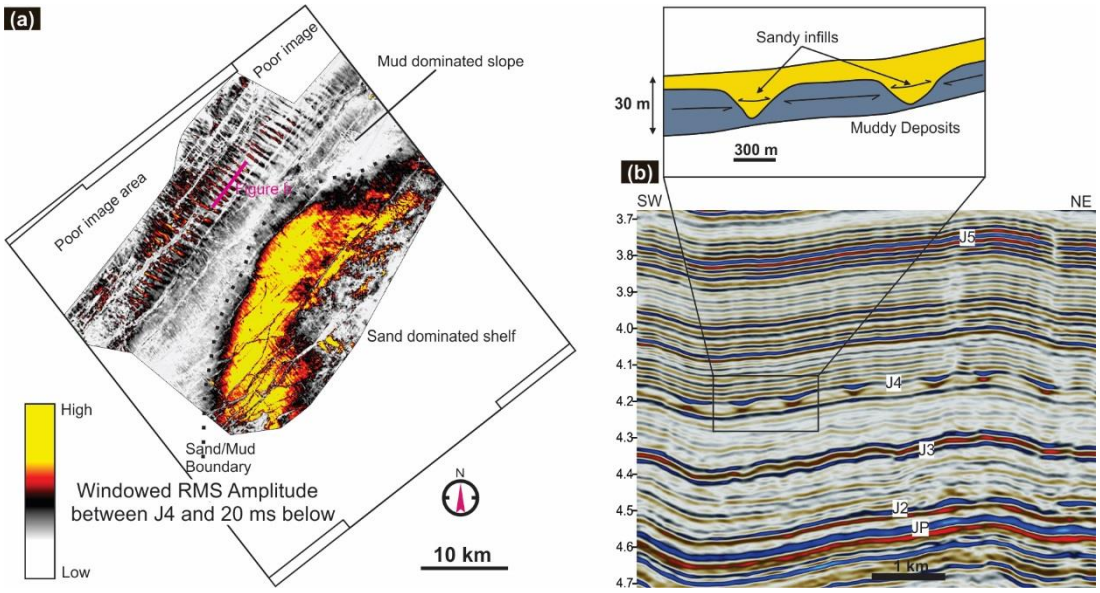

Figure 6-19. Windowed RMS amplitude surface map (a), seismic section and schematic illustration (b) the NW-SE trending gullies with high-amplitude infills (Seismic Facies VII). The gullies were developed on a mud dominated slope which is flanked by a sand dominated shelf.

6.3.6 Slump Complexes

The slump complexes (SF VIII) are interpreted in both the Rowley Sub-basin and northeast Exmouth Plateau. In Rowley Sub-basin, the slumps are observed in the lowermost part of the fluviodeltaic-related succession, which is associated with the slope-basin facies (SF III-IV) (LJ2-LJ3) in the distal area on the southwest flank of the northwest-trending arch (Figure 6-20). On the RMS amplitude map, the slumps show multiple high-amplitude stripes that have

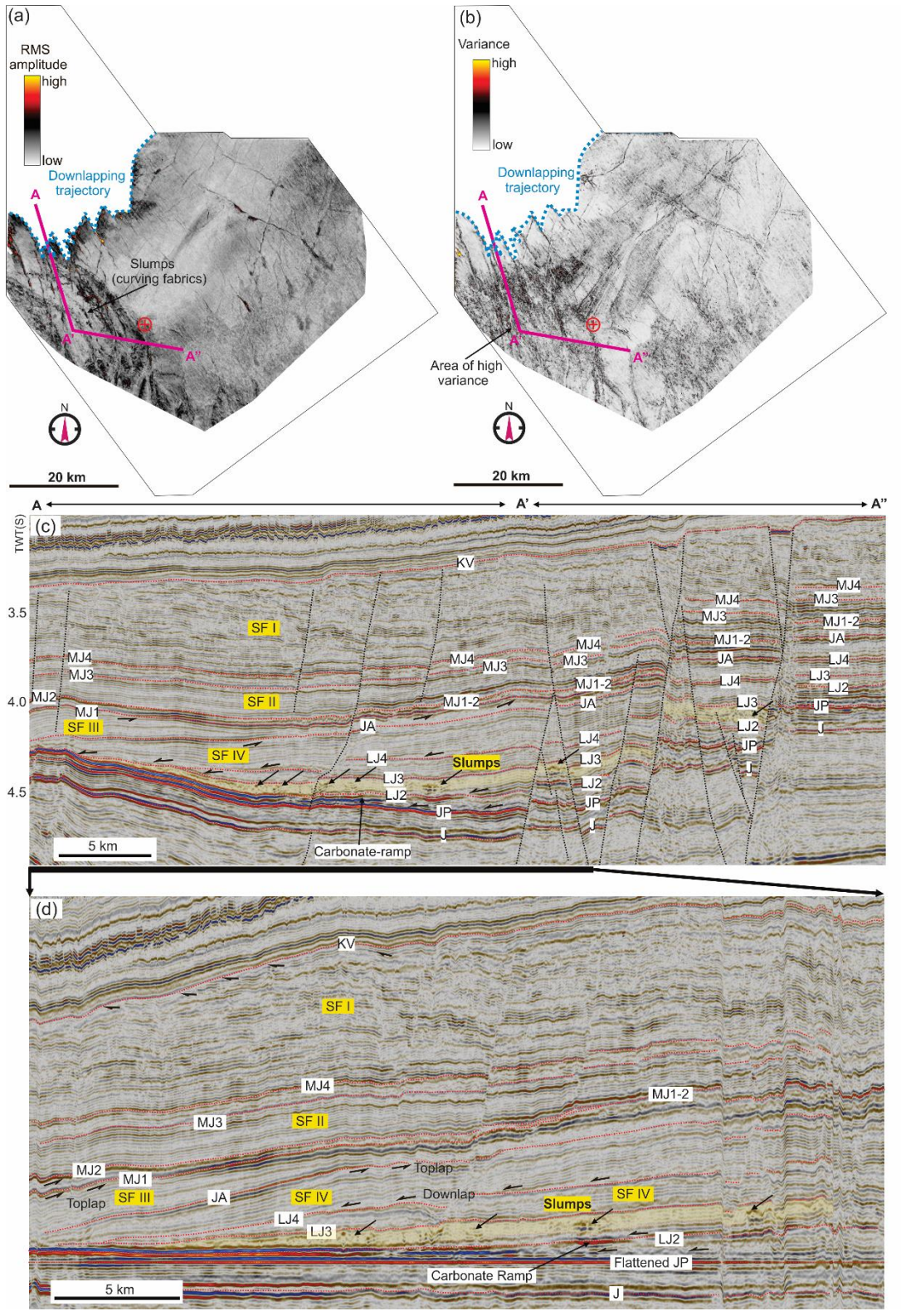

Figure 6-20. Lower Jurassic slump complexes that are shown on RMS amplitude (a) and variance (b) map of 10 ms below LJ3 and an arbitrary seismic section (a, b [flattened on JP]). The slump complexes are present on the southwestern flank of the northwest-southeast trending arch and characterized by disintegrated low-amplitude reflections incorporating isolated high-amplitude dots. These high-amplitude dots exhibit concave-towards-southwest geometries on the RMS amplitude. On variance map, the curving fabrics are less prominent and the influenced area is internally chaotic.

concave-towards-southwest listric geometry, which are alternating with areas of low amplitude (Figure 6-20a). This is consistent with section view of the slumps as highly disintegrated low-amplitude reflections containing isolated high-amplitude segments (Figure 6-20c, d). On variance map, the limits of the slumps are ambiguous and the slump-influenced area is characterized by high variance (Figure 6-19b).

On northeast Exmouth Plateau, the slump complexes observed were presumably much later. They are present at multiple levels within Unit 5 (J4-J5) and Unit 6 (J5-J6), which are dominated by medium-amplitude clinoformal topsets (SF II, Figure 6-21). They are made up of around 30-50 ms (47-79 m) of highly disrupted reflections. The amplitudes of the slump complexes are close to that of undeformed sediments below and above (Figure 6-21b, c), which suggests the slump complexes are derived from autochthonous sediments and subjected to little transportation. The slump complexes occupy an area of approximately 10×10 km, with poorly defined boundaries (Figure 6-21a). NW-SE trending fabrics are interpreted, and could represent the scour marks on the basal shear surfaces.

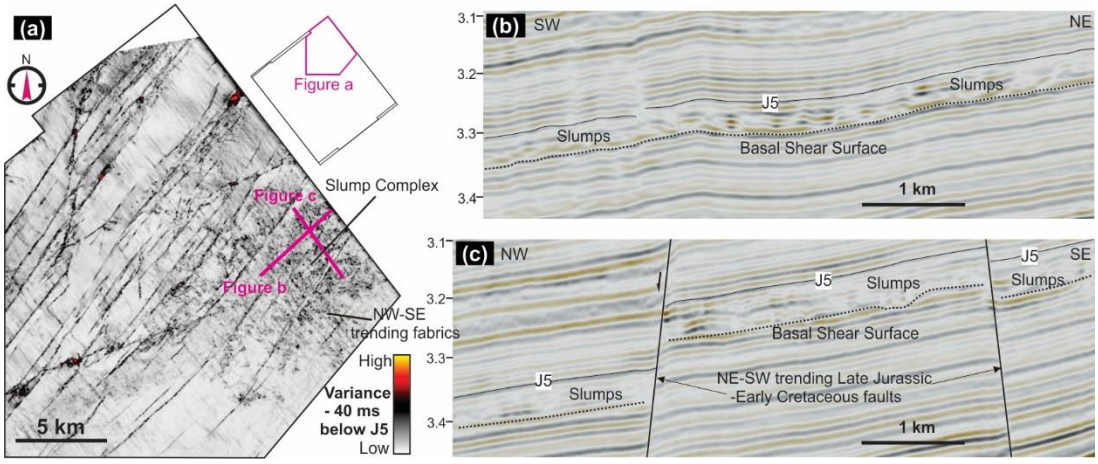

Figure 6-21. Slump complexes interpreted within the succession (Seismic Facies VIII) shown on variance attribute map (a) and on seismic sections (b).

6.3.7 Syn-tectonic Canyons

Several large-scale canyons (SF IX) are interpreted on the top of the Jurassic fluviodeltaic-related succession on northeast Exmouth Plateau. They were developed in areas of high geological relief, e.g., the Emu Fault System and the steeply NW-dipping Northern Slope (Figure 6-22a, b, c). Four major canyons were developed on the Northern Slope and strike northwesterly (Canyon 1-4, Figure 6-22c, d). A large number of relatively small canyons were developed between the major canyons and the sidewalls of large canyons, forming tree-branch-like morphology. These canyons terminate down-dip against a northeast- trending Late Jurassic to Early Cretaceous fault (FG 4a), which suggests they were developed

simultaneously with the fault activity. The cross-section profiles of the canyons have varied depth/width ratios and are filled with post-tectonic sediments (Figure 6-22d).

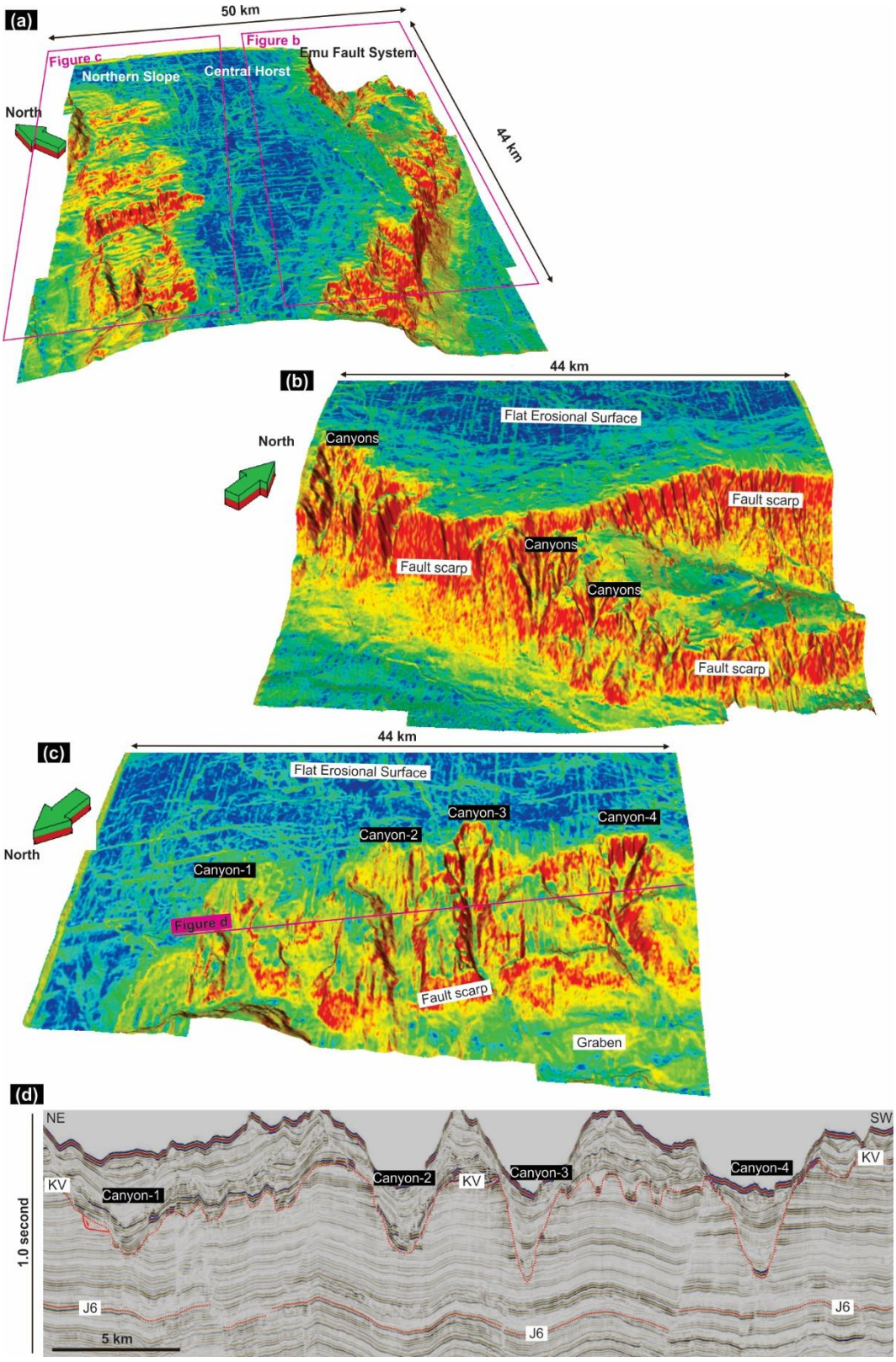

Figure 6-22. Oblique views of edge-detection attribute map of the Valanginian Unconformity (KV)(a, b, c) and a seismic section showing the syn-tectonic (Oxfordian-Valanginian) canyons developed on northeast Exmouth Plateau. The canyons were developed in areas of high geological relief, Northern Slope and Emu Fault System.

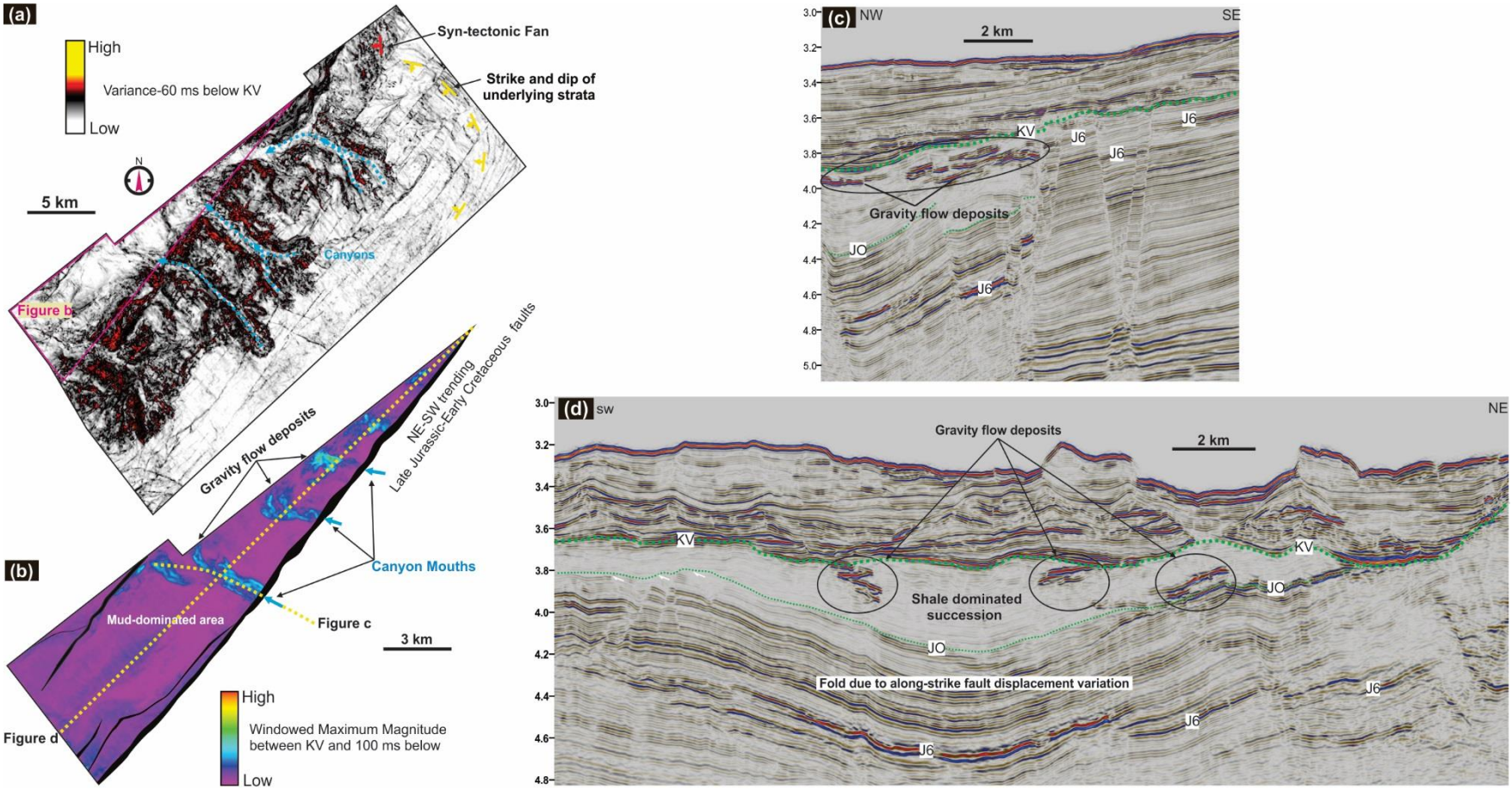

Figure 6-23. Variance extracted from 60 ms TWT below the Valanginian Unconformity (a) and windowed maximum magnitude between the Valanginian Unconformity and 100 ms below (b) showing large syn-tectonic canyons and canyon derived gravity flow deposits on the Northern Slope, northeast Exmouth Plateau (WA484P-3D). Seismic section views of the gravity flow deposits are shown (along the axis, d; perpendicular to the axes, e)

6.3.8 Syn-tectonic canyon-derived gravity flow deposits

The canyon-derived gravity flow deposits (SF XIV) are identified within the syn-tectonic marine shale dominated graben on the Northern Slope of the northeast Exmouth Plateau (WA484P-3D)(Figure 6-11). In plan view, the gravity flow deposits exhibit elongate shapes (1-1.5 km wide, 3-4 km long) with NW-SE axes and terminate against the hanging wall of a graben-boundary fault (Figure 6-23a, b). Interestingly, the foresaid canyons' mouths, namely, the points where canyons terminate at the footwall of the graben boundary fault, correspond to the locations of these gravity flow deposits (Figure 6-23a, b). This suggests that these deposits are genetically related to the canyon development. They consist of incongruous high-amplitude reflections that are incorporated into low amplitude to transparent packages (Figure 6-23c, d). These high-amplitude reflections display a discordant nature to some extent, which is demonstrated by the zigzag aggradation style, abrupt lateral termination and crosscutting relationship with the host strata (6-23c, d). This suggests that there may be a component of subsequent remobilisation and sand injection (see Discussion for details).

6.3.9 Syn-tectonic Fan

The syn-tectonic fan lobe (SF XV) is identified in the syn-tectonic succession in one of the northeast- trending mini-graben on the Northern Slope, northeast Exmouth Plateau (WA484P-3D)(Figure 6-11, 6-24). It consists of a package of discontinuous, alternating high- and low-amplitude reflections. A general clinoform-like internal architecture can be recognized. It is truncated by the Valanginian Unconformity (KV) and is unconformably lying on the Oxfordian Unconformity (JO) (Figure 6-24c, d). The fan lobe is situated in a syncline caused by along-strike variation in fault displacement (Figure 6-24d). It extends up to 9 km along the graben axis and has a maximum thickness of 260 ms TWT (410 m). N-S trending fabrics are revealed by a high-quality variance slice through the fan lobe (Figure 6-24a), and suggest the fan prograded towards the west (Figure 6-24d). The underlying Jurassic succession was deformed into a broad syncline due to the deformation during Oxfordian-Valanginian (Figure 6-24a). The RMS amplitude attribute suggests strong heterogeneity within the fan, which illustrates its likely rapid accumulation (Figure 6-24b).

6.3.10 Fault-controlled Sheet-like bodies

In the southwestern area of the Rowley Sub-basin (Curt 3D) where the syn-tectonic succession (JO-KV) is absent, the major unconformity (KV), which represents a hiatus from Oxfordian to Valanginian, show high reflection strengths in the northwest trending fault (FG 4c) bounded grabens/half grabens (Figure 6-12b, c). Seismic characteristics suggest that these sheet-like bodies are formed by materials that are harder than background sediments.

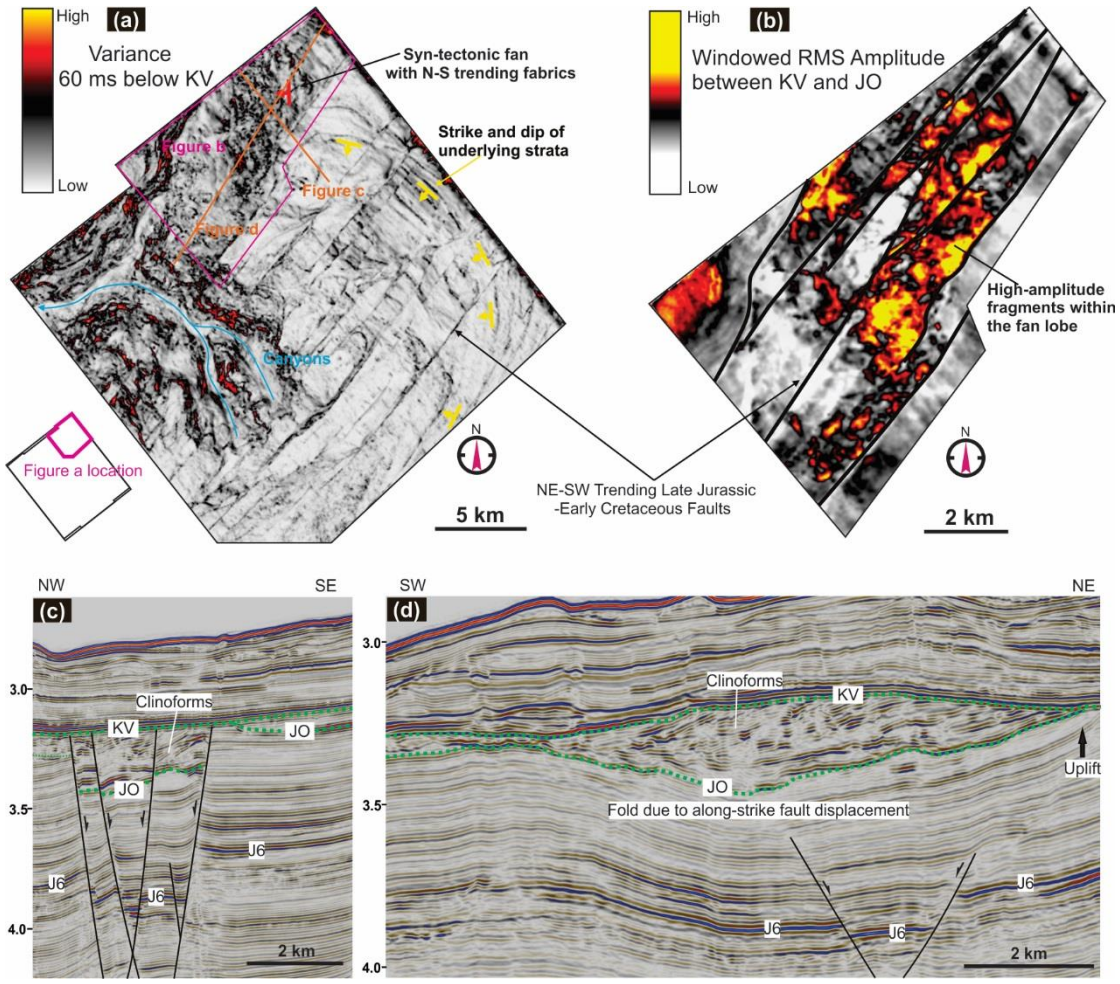

Figure 6-24. A syn-tectonic fan complex shown on variance map (a), windowed RMS amplitude map (b) and seismic sections (c, d). JO= Oxfordian Unconformity; KV= Valanginian Unconformity.

6.4 Discussion

This section will discuss the implications of the seismic facies, stratigraphic architecture and geomorphology for understanding the basin development, sediment filling, chronostratigraphic framework, governing processes of the key depositional elements and the role of relative sea-level and sediment supply.

Legendre Delta

The Pliensbachian-Oxfordian sequence was previously named the Legendre Delta, which includes the Murat, Athol and Legendre Formations (Bradshaw et al., 1988; Bradshaw et al., 1998; Longley et al., 2002). However, due to limited data, published studies on its internal architecture and development are rare. This study suggests that "delta", which usually refers to the deposits formed when a river enters an steady water body, is an inappropriate terminology for the system because 1) the fluviodeltaic plain (SF I) laterally extends over hundreds of kilometres and consists of a large number of channels (e.g., Figure 6-13c, d, 6-15e, f) and single delta cannot be recognized; 2) the sediments were transported tens of

kilometres into the ocean (relative to shoreline), forming a shelf-slope-basin clinoform system (e.g., Figure 6-3, 6-4, 6-15). Shelf-margin systems are normally treated as independent depositional system (relative to fluviodeltaic systems), despite the sediments can be fed by rivers. In this study, we use "fluvial-marine shelf system" for the Early-Middle Jurassic Legendre Delta succession (JP-JO), to emphasis the fact it has a fluvial origin but is more than just a fluvial/deltaic system.

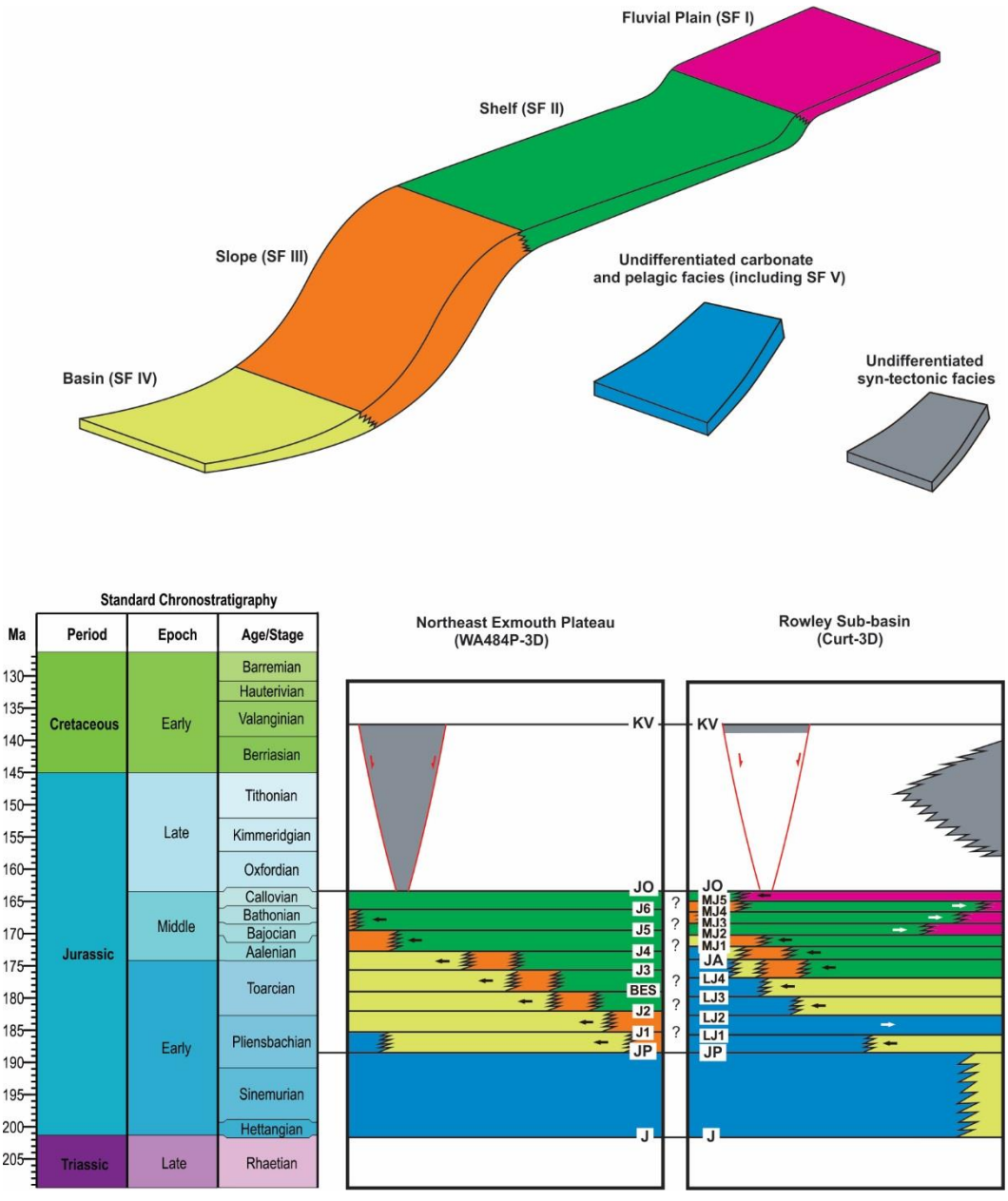

Figure 6-25. Schematic geometric model of the primary seismic facies (SF I, II, III, IV, V) defined in this study (upper) and stratigraphic frameworks established from the two 3D seismic surveys (Lower)

Chronostratigraphic Framework: Rowley Sub-basin vs northeast Exmouth Plateau

Due to the lack of wells on northeast Exmouth Plateau, a detailed chronostratigraphic framework is very difficult to establish for the fluvial-marine shelf succession. Comparing the

facies and stratigraphic architecture between the Rowley Sub-basin (Curt-3D) and the northeast Exmouth Plateau (WA484P), both similarities and differences are revealed (Figure 6-25). The two sub-basins both present a shelf-slope-basin system, which represent the subaqueous component of the fluviodeltaic-related system. However, its subaerial counterpart, the fluviodeltaic plain, is only present in the Rowley Sub-basin (succession from MJ2 to JO). This is likely because the northeast Exmouth Plateau (WA484P-3D) is relatively more distal than the Rowley Sub-basin (Curt-3D)(as suggested by the palaeogeography map in Figure 6-1) and the fluviodeltaic plain might not have reached the northeast Exmouth Plateau and/or the strong erosion of the northeast Exmouth Plateau (up to 2360 m of erosion on the Central Horst, northeast Exmouth Plateau) totally removed the fluvial succession (Figure 4-4, 6-2, 6-11). A retrogradation is observed in association with succession from MJ2 to MJ4 in the Rowley Sub-basin (e.g., Figure 6-4, 6-25). On the northeast Exmouth Plateau, the shelf-slope-basin system shows no landward pull-back. Controlled by relative sea-level and/or sediment supply, retrogradation should be a regionally recorded event. This inconsistency is also interpreted as a result of the significant erosion of the upper part of fluviodeltaic-related succession on the northeast Exmouth Plateau (Figure 4-4, 6-2, 6-11).

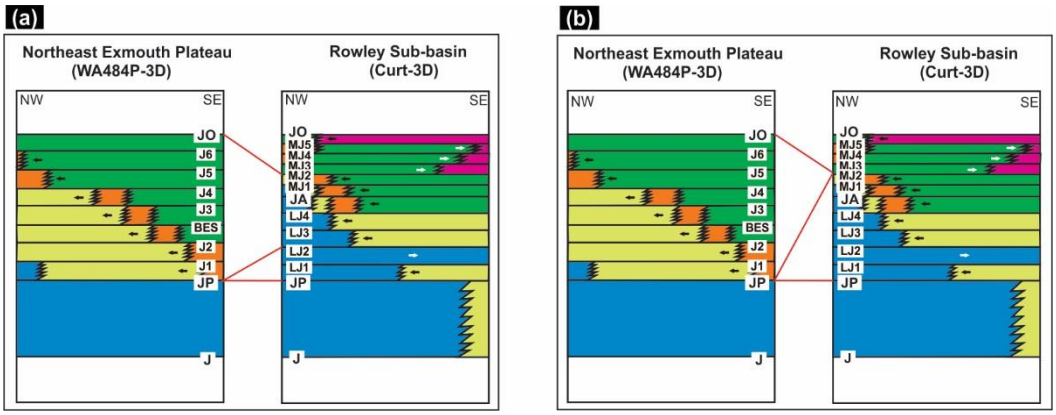

Figure 6-26. Two scenarios (a, overlapping model; b, continuous model) of stratigraphic framework correlation between the Rowley Sub-basin and the northeast Exmouth Plateau.

The interval LJ1-LJ2 in the Rowley Sub-basin yielded a carbonate shelf-ramp system (Figure 6-4b, 6-25), which suggests a temporal transgression and/or decrease of sediment inputs. However, on northeast Exmouth Plateau, no equivalent transgression is observed on the seismic (Figure 6-25). This is likely because there was very limited siliciclastic sediment inputs to the more distal northeast Exmouth Plateau (WA484P-3D) and the transgression event is difficult to separate from the underlying Pliensbachian maximum flooding surface.

The comparison of the two sub-basins suggests the succession on northeast Exmouth Plateau only records a small proportion of the story as the Rowley Sub-basin revealed. Two scenarios are highly possible: (1) the progradational sequences (J1-J6) on northeast Exmouth Plateau (WA484P-3D) overlaps the progradational phase (LJ2-MJ2) in the Rowley Sub-basin, and

the JP surface on northeast Exmouth Plateau represents a highly condensed succession that is equivalent to JP-LJ2 succession in the Rowley Sub-basin (overlapping model, Figure 6-26a). The erosive surface, J4 ES on northeast Exmouth Plateau, if it represents a tectonic event or sediment bypass on the shelf, is likely to correspond to either Aalenian horizon (JA) or MJ1 erosive surface in the Rowley Sub-basin; (2) Given that northeast Exmouth Plateau is presumably situated in more distal area of the system than the Rowley Sub-basin, the northeast Exmouth Plateau succession (J1-J6) can correspond to a continuous progradation of the system following the LJ2-MJ2 progradation and predating the retrogradation in MJ3-MJ5 in the Rowley Sub-basin (continuous model, Figure 6-26b). In this case, the JP surface on northeast Exmouth Plateau represents the time span from JP-MJ2 and the J4 ES should postdate both JA and MJ1 erosive surfaces in the Rowley Sub-basin.

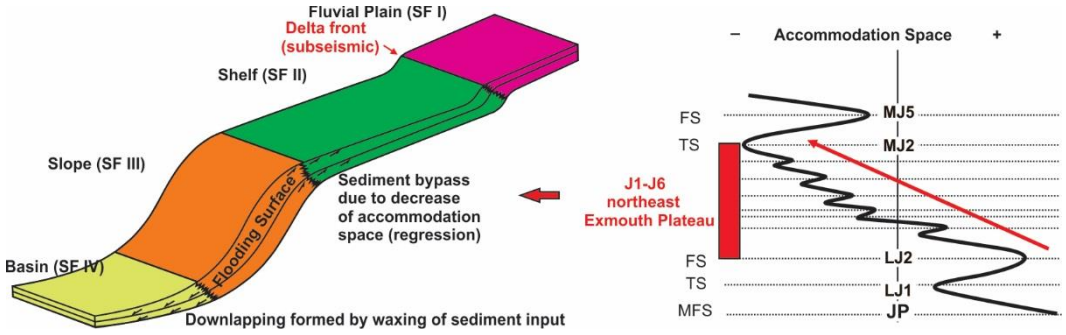

Figure 6-27. Schematic illustration of the maximum flooding surface bounded para-sequences interpreted in this study (left) and accommodation space change curves interpreted from the seismic stratigraphic and facies architecture (right). The figure shows a major phase of long-term stable / falling stage (e.g., J1-J6, northeast Exmouth Plateau), which consists of multiple short-term sea-level fluctuation and/or sediment waning-waxing

Submarine Channels: Relative Sea-level and Sediment Supply

In both sub-basins, downlapping is commonly associated with the horizons interpreted, but only present downslope and in the basin (JP, LJ2, LJ3, LJ4 and JA in the Rowley Sub-basin, Figure 6-3, 6-4; JP, J1, J2, J3, BES on northeast Exmouth Plateau, Figure 6-2, 6-8). It means the seismic units defined by these surfaces are equivalent to the maximum flooding surface bounded para-sequences (Galloway, 1989)(Figure 6-27). The flat shelf-edge trajectory on the northeast Exmouth Plateau suggests the succession (J1-J6) was formed during a constant basinward accretion (Figure 6-8c), which was likely a result of long-term stable or falling sea-level (Helland‐Hansen and Hampson, 2009). The flooding surface bounded para-sequences suggests multi-cyclic short-term waxing and waning of sediment inputs and/or short-term sea-level fluctuation. Each of the flooding surfaces recorded the waning of the sediment input and/or short-term transgression, which was followed by a waxing stage of sediment inputs and/or short-term regression. The strong sediment bypass on the shelf edge is likely a result of the waxing of the sediment input (Figure 6-27). The channelized sediment gravity flow is associated with one of the maximum flooding surfaces (BES, Figure 6-2, 6-8b, c), suggesting

that the development of the slope channels, no matter when it started, ended with a waning stage of sediment supply. The waxing of mud-prone sediments after the channel abandonment formed the downlaps on the channelized surfaces and their equivalent gravity flow deposits. Channel levees, which are normally a result of subaqueous channel overspill events and developed in association with channels formed by multiple cycles of waxing and waning of sediments supply, are not present at the channel margin. This may be related to the low sediment input and relatively short-lived channel development.

Clinoform Genesis

Clinoforms have been widely discussed in literature with respects to their characteristics, genesis and implications for reservoir prediction (Helland‐Hansen and Hampson, 2009; Helland-Hansen et al., 2012; Patruno et al., 2015a; Patruno et al., 2015b). The genesis of clinoforms usually includes both subaerial and subaqueous environment. Subaerial clinoforms, also named shoreline clinoforms, are formed where a river fed sediment reached a steady water body and are equivalent to deltas. They are normally characterized by a scale of tens of meters height and an oblique cross-section geometry with fluvial dominated topset (Patruno et al., 2015a). In this study, the fluviodeltaic plain consists of a wide area (over hundreds of kilometers) that is made up of fluvial channel belts, which supply sediments into the basin. A delta, which normally refers to a single river fed sediment accumulation, does not exist. If they do, they are usually sub-seismic (Patruno et al., 2015b). Subaqueous clinoforms are divided into three different categories: 1) subaqueous delta-scale clinoforms (height of several tens of meters), which are developed in high-energy deltaic margins where the topset-foreset rollover of these clinoforms is laterally separated from shoreline (compound delta clinoforms, see Patruno et al. (2015a) for details); 2) shelf-slope-basin clinoforms (height usually of several hundred meters), which formed as a result of shelf-slope accretion (Helland‐Hansen and Hampson, 2009), and 3) continental slope clinoforms (height up to several kilometers), which is a function of continental margin slope evolution.

The evidence that led to the interpretation of a shelf-slope-basin system (SF II, III, IV) in this study includes: 1) distributary fluvial channels, the most diagnostic features for subaerial delta plains, were not developed within the topset of the clinoforms (Shelf, SFII)(e,g., Figure 6-15); 2) the clinoforms show a vertical scale of several hundreds of meters (e.g., Figure 6-8c) and fundamentally differ from the subaerial clinoforms and the subaqueous delta-scale clinoforms, which are usually of the order of tens of meters (Helland‐Hansen and Hampson, 2009; Patruno et al., 2015a); 3) their sigmoidal cross-section geometry differs from the oblique geometry of most delta-scale clinoforms.

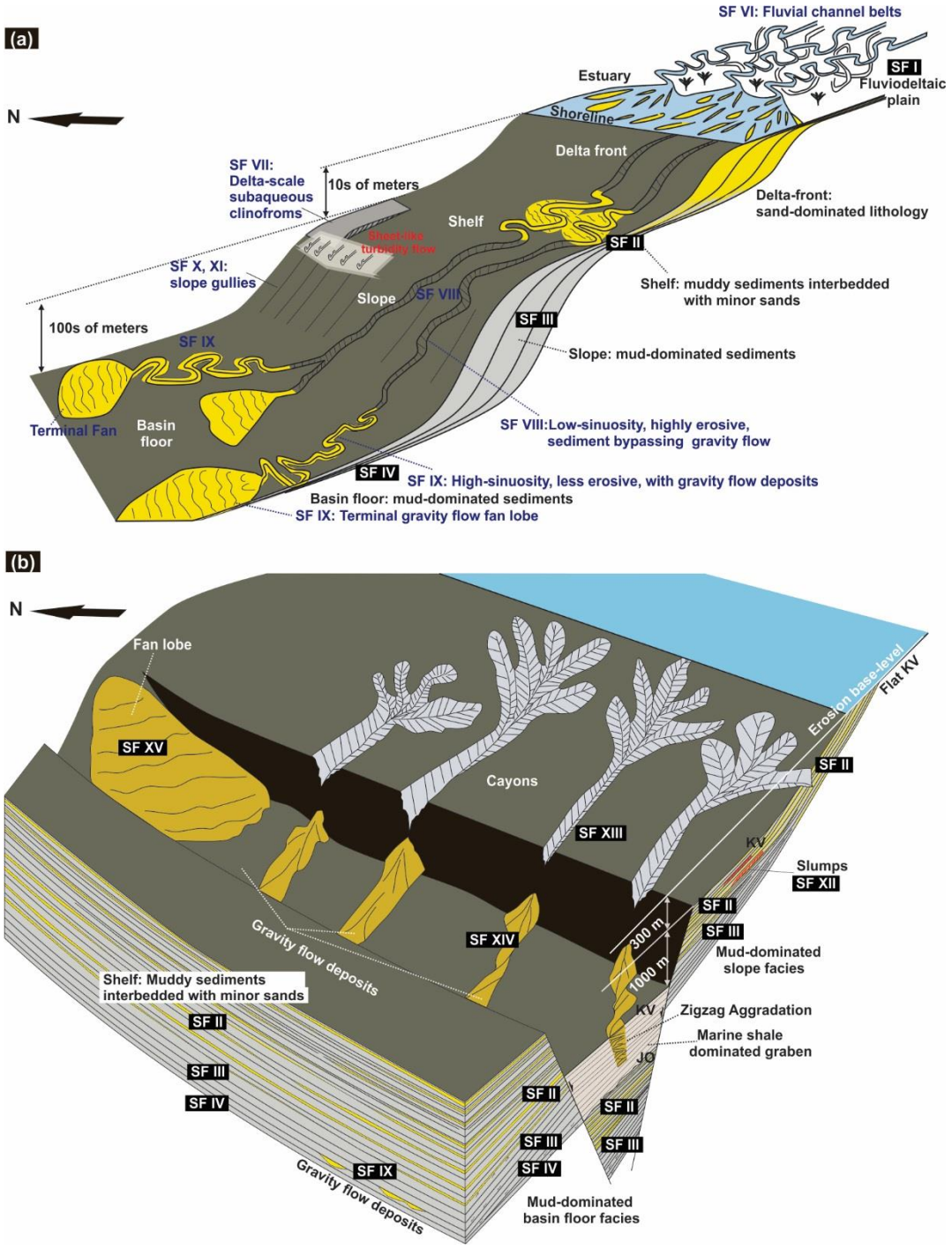

Figure 6-28. Schematic integrated three-dimensional depositional models of the WA484P-3D area based on the interpretation of the seismic facies and geomorphology. (a) Fluvial channel belts (SF VI) developed in the fluviodeltaic plain (SF I) in the Rowley Sub-basin and delta-scale subaqueous clinoforms (SF VII), subaqueous channels (SF VIII), gravity flow deposits (SF IX) and gullies (SF X, XI) developed in association with the shelf-slope-basin system (SF II, III, IV) on northeast Exmouth Plateau. (b) Canyons (SF XIII), canyon derived gravity flow deposits (SF XIV) and a fan lobe (SF XV) developed in a marine shale dominated graben during the subsequent rift tectonics; a flat erosion surface (KV, Valanginian Unconformity) formed at the erosion base level (near sea level) during this period; the slumps (SF XII) formed in association with the shelf facies (SF II) prior to the rift break-up

The interpretation of the subaqueous delta-scale clinoforms (SF VII) is based on the fact that their tens of meters scale is consistent with delta-scale clinoforms and fluvial channels are not associated with the clinoforms, which ruled out subaerial clinoforms (Figure 6-16, 6-28a).

Lithology Prediction

Lithology information of the fluviodeltaic-related succession (JP-JO) was previously known only from the Huntsman-1 (Figure 6-3c). The detailed interpretation of seismic facies, stratigraphic architecture and geomorphology provides a powerful tool to predict the temporal and spatial litho-facies changes, which is crucial for reservoir prediction. In Huntsman-1, the upper part of the succession, which is dominated by the fluviodeltaic plain facies (SF I), is comprised of coarse sand dominated deposits interbedded with siltstone, claystone and traces of lithic fragment and carbonaceous specks (Sturrock, 2007). It is consistent with the presence of numerous channels which transported massive sands that were presumably deposited as channel bars. The channels show low-amplitude geomorphology, which suggest they are likely infilled by muddy sediment during flooding events. The high-amplitude patches in the fluviodeltaic plain may represent highly vegetated areas which were subsequently turned into peat (Figure 6-14). The seismic morphology is similar to many other fluviodeltaic plain that are characterized by mud-infilled meandering channels. However, due to the limitation of seismic resolution, details of litho-facies distribution within the fluviodeltaic plain is difficult to constrain.

The subaerial to subaqueous transition, namely, shoreline delta, is not recognized from the seismic data. The fluviodeltaic plain changed into a wide shelf without any dipping reflections (subaerial delta front)(e.g., Figure 6-3, 6-4). It may suggest the scale (height) of the subaerial delta cannot be resolved by seismic or delta fronts were not developed associated with the system. By analogue, the areas where fluvial rivers meet the shoreline are places where large amount of river sands are dumped, therefore, reservoir-prone lithology is likely to be developed (Figure 6-28a).

Deposition at marine shelf-slope settings is usually dominated by fine-grained sediments deposition when the shoreline is situated at some distance or fluviodeltaic sediment flux is weak. In Huntsman-1, the slope and basin faices (SF III, IV) are equivalent to the marine shale dominated Murat and Athol Formation (Figure 6-3c). It is inferred that the lower part of the succession, which is dominated by low-amplitude basin and slope facies (SF III, IV)(e.g., Figure 6-2, 6-3, 6-4) were formed by mud-prone sediments (Figure 6-28a). For the topsets (shelf facies, SF II), more medium-high amplitude reflections alternate with low-amplitude reflections, which is indicative of the physical property contrasts of the sediments (Figure 6-2). The Huntsman-1 well suggests the shelf facies consists of mud-prone sediments interbedded with sands. This is indicative of episodic sand flux alternating with the draping of mud onto the shelf (e.g., Figure 6-15b, d and Figure 6-19a depict mud-dominated slope and sand dominated shelf; Figure 6-15f reveals a mud-dominated shelf).

Submarine Channels: Sediment Gravity Flow

The seismic geomorphology of the submarine channels on the slope suggests that the sinuosity, degree of erosion, and the type of infilling sediments were controlled by the steepness of the shelf slope. On the steep slope, submarine channels have low sinuosity and are highly erosive, and characterized by sediment gravity flow bypass (Figure 6-17). The channels become more sinuous, less erosive to the gently dipping downslope, and gravity flow bypass effects decrease as high-amplitude gravity flow deposits are present within the channel meanders. At the frontal area on the flat basin floor, high-amplitude terminal fan lobes are developed (Figure 6-28a). This study depicted a channel system that incorporates two end-member sub-marine channel systems: 1) low-sinuosity, high-gradient, bypassing gravity-flow system; 2) high-sinuosity, low-gradient, depositional gravity-flow system, which makes a useful predictive model for submarine channels in similar slope settings where data quality and coverage are limited. The channel sinuosity downslope variation confirms that the primary controlling factor for submarine channel sinuosity is slope-gradient (Clark et al., 1992). The trend that channel infills change from non-gravity flow deposits to gravity flow deposits downslope is consistent with the conclusion that submarine gravity flows change from completely bypassing flow to partially bypassing flow and then to depositional flow in the down-stream direction of submarine channels (Figure 6-28a) (Stevenson et al., 2015). The downslope change of the degree of erosion, indicate the trend of channel development to reach an equilibrium adjustment profile (Pirmez et al., 2000; Adeogba et al., 2005). High-degree erosion is more likely to occur in high-density turbidity flow than in highly cohesive debris flow (Mulder and Alexander, 2001). The decrease of erosion downslope may also suggest the evolution of sediment gravity flow from a fractional flow (e.g., turbidity flow) to cohesive flow (e.g., debris flow) in the flow direction, because the eroded muds from the slope merged into the flow and increased cohesion (Haughton et al., 2009).

Gullies on the Slope

Gullies are present within the slope facies at multiple stratigraphic levels, which indicate the governing process is common and could be intrinsic to the shelf slope (Figures 6-18, 6-19). It is interesting that the two type of gullies interpreted in this study, mud-rich (SF VI) and sand-rich (SF VII), show many similarities: 1) they are relatively straight and evenly spaced; 2) they developed no slumps at the heads and fan lobes at the toes; 3) their formation is transient (only associated with single reflections), thus they are not aggradational; 4) no levees were developed and their infills show no downslope change (e.g., amplitude) (Figure 6-18, 6-19). These similarities suggest, the two types of gullies are likely to share the same genesis. The straight geometry, spacing and uniform infills of the gullies make them different from similar morphological features that were predominantly controlled by point-conduit sand-prone

gravity flows, which show variable geometries, infills, spacing and sectional profiles (e.g., previously mentioned submarine channels). Dilute, sheet-like, mud-prone turbidity currents are believed to be able to create the straight and regularly spaced gullies because they can differentially erode the underlying slope due to autogenic slope instability variations and perturbation in turbidity flows (Izumi, 2004; Hall et al., 2008). Many gullies identified in different slope settings show similar geomorphology to gullies in this study and are interpreted to be formed by sheet like flows, such as turbidity and dense water flows (Hall et al., 2008; Jobe et al., 2011; Micallef and Mountjoy, 2011; Lonergan et al., 2013; Shumaker et al., 2017). Hence, it is likely the gullies are erosional troughs that were formed by similar sheet-like flows and draped by subsequent mud- or sand-prone sediments, depending on sand inputs, sea-level and current activities (Figure 6-28a). However, it remains a question that the gullies in this study have a non-aggradational nature, which suggests the primary causes was short-lived and episodic, while other reported gullies are usually aggradational and are sustained for a relatively long duration.

Slump Triggering Mechanism

Slumps are normally triggered by processes that generate driving forces and/or reduce the shear strength of the sediment (Lee et al., 2007). The driving forces includes seismic activity and slope steepening, both of which mainly result from tectonics, e.g., salt diapirism, faulting, uplifting. The reduction of shear strength, however, is related to many causes, e.g., rapid sedimentation, fluid overpressure in association with hydrocarbon generation and expulsion, and gas seepage and migration. In this study, the slumps interpreted in two locations may have different triggering causes. In Rowley Sub-basin, the slumps are associated with the basin facies (SF IV). Their presence on the flank of the northwest-trending Huntsman Arch and sliding-away from the arch axis suggest they were triggered by the arch formation (Figure 6-20). On northeast Exmouth Plateau, slumps are associated with the upper part of the succession, shelf facies (SF I), which usually indicate a low gradient (<<1°) (Figure 6-21). They were not developed within the lower part, slope facies (SF II), which have much steeper gradient (1°-4°). It suggests the primary triggering mechanisms only exerted an influence in the area at a late stage. Fault activities are constrained to the interval from Oxfordian-Valanginian in the area, which ruled out fault related steepening as a triggering mechanism. However, the intensified activity of large remote faults before rift-break up (e.g., faults in the Northern Carnarvon Basin) (Black et al., 2017), could potentially generate seismic activity and trigger the slumps in the study area. Other mechanism such as fluid overpressure, hydrocarbon generation and gas seepage, etc., could also potentially contribute to slump development.

Syn-tectonic Erosion and Sedimentation

Erosion associated with tectonic movement exerted a dominant influence on the preservation of the pre-tectonic succession. The syn-tectonic canyons interpreted on the northeast Exmouth Plateau (WA484P-3D) reveal that during active rifting, canyon development was a major mechanism for erosion (Figure 6-22, 6-28b). In the study area, the canyons on the Northern Slope have caused around 300 ms TWT (473 m) incision of the pre-tectonic fluviodeltaic-related sediments. The canyons were developed in areas of high relief, e.g., the Emu Fault System and the steeply northwest- dipping Northern Slope (Figure 6-22), and thus were likely governed by mass wasting processes (material moving downslope as a mass by gravity). The erosion by canyons differs from the erosion that was responsible for approximately 2360 m of thickness reduction and the formation of the flat Valanginian Unconformity on the Central Horst, northeast Exmouth Plateau (Figure 6-8a, 6-22) and in the outboard part of Rowley Sub-basin (Figure 4-2). Based on the "peneplain theory"(Davis, 1902; Phillips, 2002), a low-relief erosional surface that truncates all underlying rocks of different resistances represents erosion near base level/sea level. This indicates that the Central Horst on the northeast Exmouth Plateau and the outboard area of the Rowley Sub-basin were positioned close to sea level, potentially for a relatively long duration during rifting, thus the canyons on the Northern Slope and at Emu Fault System are likely submarine (Figure 6-28b). However, a short-lived local subaerial environment is possible in the early stage of the rift tectonics because the outboard part of the North West Shelf underwent a major uplifting and tilting, e.g., the formation of the Wombat Plateau and rift shoulder in the Rowley Sub-basin (Von Rad et al., 1992; Smith et al., 1999).

The canyon-derived gravity flow deposits (SF XIV) are interesting features. The locations of the high-amplitude bodies coinciding with the canyon months demonstrate they are deposits derived from the canyons (Figure 6-23, 6-28b). Hence, gravity flows should be principally responsible for their formation. It is possible that the zigzag-style aggradation were formed by multiple episodes of the gravity flows. The sharp angles between the high-amplitude reflections suggests abrupt changes of depositional base orientations, which in this case, most likely indicates episodic activities of the graben boundary faults (multiple fault slip events). However, the surrounding low-amplitude package seems internally conformable, and angular geometries (e.g., onlapping) are not seen (or they are not resolved because of their low-amplitude nature) (Figure 6-23). This may suggest there is no such abrupt base orientation change. In this regard, the zigzag pattern of the reflections, together with some other crosscutting reflections suggests there are intrusive component associated with them. Sand remobilisation or injection, which have been widely reported to be associated with gravity flow sandy deposits, are likely the causes of the intrusive features (Lonergan et al., 2000; Hurst et al., 2005; Szarawarska et al., 2010; Hurst et al., 2011). The rapidly deposited gravity

flow sediments could fluidize and inject into the host shale in a crosscutting manner. Typical geometries for sand injection, such as saucer-shape section profile and circular plan view, as reported in literature (Huuse et al., 2010; Szarawarska et al., 2010; Hurst and Vigorito, 2017), are not seen. Their elongate shapes in map view show strong alignment with the gravity flow direction (Figure 6-23b, 6-28b). These features suggest, sand injection, if it occurred, was very limited. An igneous origin can be excluded because of the absence of features, such as igneous bodies rooted lower in the succession, intrusions along with fault planes, hydrothermal vents and so on, despite the fact that extensive igneous intrusions, which were developed during the rifting in Oxfordian-Valanginian, have been reported in the southern part of the Northern Carnarvon Basin (McClay et al., 2013; Rohrman, 2013).

The syn-tectonic fan lobe (SF XV, Figure 6-24) on the northeast Exmouth Plateau could also represent a rapidly accumulated alluvial/submarine fan that was fed by the eroded sediments. However, an igneous genesis such as a lava flow cannot be ruled out. Similarly, the sheet-like bodies (SF XVI, Figure 6-12) in the Rowley Sub-basin show strong control of the northwest- trending faults (FG 4c), suggesting they are either syn-kinematics sediments that were derived from the tectonic erosion or igneous sills/flows as illustrated by McClay et al. (2013) in the southern part of Northern Carnarvon Basin.

Implications for Petroleum Exploration

Previous exploration in the area was mainly focused on the middle-upper Jurassic Legendre Formation, which was deposited in association with costal/fluvial plain of the Legendre Delta. The Lower Jurassic Murat Formation and Athol Formation were previously thought to be source rock units with little reservoir potential, because they are marine shale dominated and represent the distal area of the Legendre Delta (Edwards and Zumberge, 2005). The interpretation of channelized gravity flow deposits (SF VIII, IX, Figure 6-17) in this succession indicate that sands from the fluviodeltaic plain were transported by submarine channels across the shelf and slope, to basin floor in the early Jurassic. Highly erosive and bypassing gravity flows in submarine channels are usually high-density sand-prone gravity flows (McHargue et al., 2011). The upslope high-degree erosion and sediment bypass suggest that the downslope gravity flow deposits are sand-rich. Numerous analogs show that high-amplitude infills of sinuous deep-water channels normally contain reservoir-prone lithology and reservoirs in such cases are highly complex and heterogeneous, due to, e.g., the lack of connectivity between channels and the partitioning of sand bodies (Kolla et al., 2001; Saller et al., 2004; Cross et al., 2009). The gravity flow deposits developed within the sinuous channel segments and the terminal fans, are very likely reservoir facies. Their complexities and heterogeneities can exist due to: 1) mud-prone sediment eroded upslope merged into gravity flow, which increased flow cohesion and formed muddy debrites downslope, as

discussed by in extensive literature (Talling et al., 2007; Haughton et al., 2009; Talling et al., 2012); 2) sand bodies in the system lack connectivity, because the channel system was short-lived and shows lack of lateral amalgamation and vertical aggradation.

For the shelf margin clinoform system, the shelf that is adjacent to the fluviodeltaic plain, may contain a large volume of sand-rich sediments, which are normally good locations for reservoir facies. For the outer shelf, reservoir-prone lithology may develop, a result of episodic increased sand inputs. The extensive fluviodeltaic plain in the Rowley Sub-basin is the most likely locations of sandy lithology because of sand deposition in the fluvial channels.

The syn-tectonic canyon-derived gravity flow deposits (SF XIV) in a marine shale dominated graben during Oxfordian-Valanginian could form an effective source-reservoir-seal combination. The synchronous succession in Barrow-Dampier-Beagle Sub-basins consists of syn-rift turbidity and debris flow reservoirs containing large volumes of hydrocarbon that was partially sourced from the synchronous marine shale (Vincent and Tilbury, 1988; Osborne, 1994; Longley et al., 2002).

7 TECTONOSTRATIGRAPHIC EVOLUTION

This chapter presents an integrated basin evolution model for the study area, based on the results of the analysis of the structural architecture and the depositional system. For the Palaeozoic-Triassic, the details of the depositional system are not investigated due to data limitations, thus only the tectonic evolution is presented. For the Jurassic-Early Cretaceous, the depositional system is investigated, thus an integrated tectonostratigraphic evolution is presented.

7.1 Palaeozoic Tectonic Evolution

7.1.1 Carboniferous-Permian Rifting

The two perpendicular Palaeozoic rift system, the northwest- trending Devonian-Permian rift system and the northeast- trending Carboniferous-Permian rift system, are interpreted to have exerted an influence in the study area, which is demonstrated by the presence of the Palaeozoic faults (FG 1) and the architecture of the Mesozoic rift-related structures which suggest the control of pre-existing structures. Northwest- trending Palaeozoic faults are present on the southern flank of the Bedout Sub-basin and represent the extension of the Palaeozoic rift structures associated with the Canning Basin. Northeast- and north- trending Palaeozoic faults are present on the edge of the Lambert Shelf and on the Bedout High, and are equivalent to the northeast- to north- trending Palaeozoic structures in the Northern Carnarvon Basin (Sholl Island fault system, Flinders fault system and Mermaid fault system). In the outboard areas where Palaeozoic succession has poor imaging, both northeast- and northwest- trending Palaeozoic faults are conjectured to be present and exerted controls on the development of the northeast- trending Mesozoic faults, e,g., Whitetail faults system and northwest- trending structures in the Rowley Sub-basin, respectively (Figure 5-1). Due to the lack of constrains on stratigraphic ages, the exact timing of both the northeast- and northwest- trending Palaeozoic faults are difficult to resolve. The syn-kinematic growth wedges is top bounded by a prominent unconformity within the upper part of the Palaeozoic succession (estimated Early Permian [EP]). This is different from the Mermaid Fault in the Northern Carnarvon Basin, whose growth wedge is top bounded by the base of Triassic (McHarg et al., 2018). It could suggest that the Palaeozoic rift structures have different ages in the two basins. Alternatively, a subsequent uplift and erosion event in the Northern Carnarvon Basin (e.g., Bedout Movement?) could have removed the Upper Permian post-rift succession and led to Triassic sediment directly overlying the Palaeozoic growth wedge, as demonstrated in Figure 5-2d.

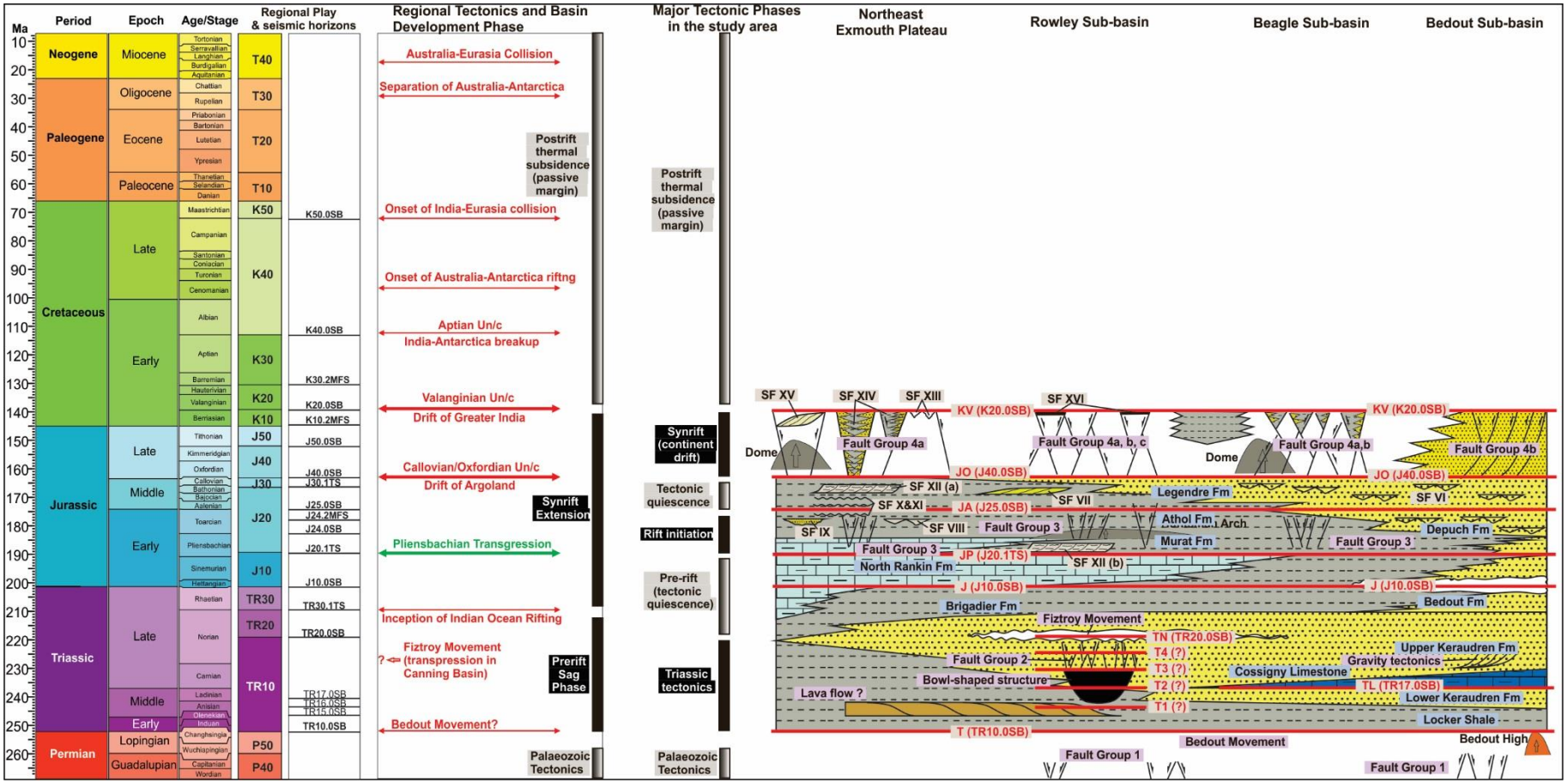

Figure 7-1. An integrated tectonostratigraphic evolution model, showing the chronostartigraphy, structures and depositional elements of the study area

7.1.2 Latest Permian Uplift and Erosion

In the latest Permian, the study area experienced a period of uplift and erosion (Bedout Movement), which led to the formation of the Bedout High and widespread erosion of the upper part of the Permian succession at the flanks of the Bedout High (Figure 5-2d, 5-13c), on the edge of the Lambert Shelf (Figure 5-2c) and in the outer Rowley Sub-basin (Figure 5-8e). This latest Permian event also laid the foundation for the Triassic basin architecture and geometry, including the westerly dipping embayment of the Bedout-Beagle Sub-basins and the open northwest- dipping Rowley Sub-basin. Regionally, the latest Permian Bedout Movement was rarely reported, which is mostly attributable to the deep burial of the Palaeozoic succession. As mentioned above, the prominent base of Triassic unconformity in the Northern Carnarvon Basin may at least partially contributed by the Bedout Movement.

7.2 Triassic Tectonic Evolution

In the Triassic, several tectonic events took places in the study area. From oldest to youngest, they include 1) lava flows that formed progradational clinoforms (T-T1), 2) the formation of the bowl-shaped structure (T1-T3), which may represent a caldera, 3) a major extensional event in the period of T3-T4 that formed a population of Triassic faults (FG 2), 4) a period of differential uplift and erosion in the Norian (TN, Fitzroy Movement), 5) gravity tectonics (through the Triassic?) (Figure 7-1).

7.2.1 Lava flow (T-T1)

The genesis of the clinoforms in the lower part of the Triassic succession in the Rowley Sub-basin has been interpreted as the latest Permian-earliest Triassic carbonate shelf-ramp system, which is purely based on the seismic facies and regional stratigraphic correlation (Paschke et al., 2018). However, the results of newest well constrained seismic interpretation suggests it is a progradational system formed by lava flows in the Early-Middle Triassic (MacNeill et al., 2018). This study does not provide any investigation of the architecture of this clinoform system, thus no conclusion is made. However, based on the stratigraphic relationship (the top of the clinoforms is defined as T1) (Figure 4-2), it was formed prior to other Triassic structures.

7.2.2 Formation of bowl-like structure (T1-T3)

The bowl-shaped structure in the outboard of the Rowley Sub-basin is interpreted to be formed during a period of T1-T3, which postdates the previously mentioned lava flows. It is characterized by ring-like and rounded intrusive features associated with the central materials on the “bowl floor”, which may represent igneous intrusions (Figure 5-21). In this case, it likely represents a caldera. Similar structures are rarely reported on the North West Shelf, and the genesis of this structure is uncertain.

7.2.3 Extension (T3-T4)

A major phase of extension took place in the period of T3-T4 and produced a large population of Triassic faults (FG 2). The development of these Triassic faults, in the southwest of the Rowley Sub-basin, were controlled by the pre-existing bowl-like structure and form curved patterns (Figure 5-3). In the northeast of the Rowley Sub-basin, they consist of two sets of northeast- trending faults that are soft linked with a set of west-northwest- trending faults (Figure 5-4), which suggests an oblique extension on the pre-existing structures (presumably Palaeozoic structures). Given that Triassic faults that are reported in the Browse Basin are mainly northeast- trending (Struckmeyer et al., 1998; MacNeill et al., 2018), a northwest-directed extension was likely to be responsible for the formation of the Triassic faults (FG 2) in the Rowley Sub-basin.

7.2.4 Differential uplift and erosion (Norian, Fitzroy Movement?)

In the Norian, a phase of differential uplift occurred in the study area. This event produced a wide northwest- trending high across the study area, including the northeast Exmouth Plateau, the Thouin Graben, southwest of the Rowley Sub-basin, the Bedout High and the Broome Platform (Figure 4-6a). The upper Triassic succession (presumably the upper part of the Mungaroo Formation equivalent) was significantly eroded on this northwest- trending high, forming a prominent angular unconformity in the study area (TN). The northwest trend and the nature of uplift and erosion, are consistent with the transpressional Fitzroy Movement in the onshore Canning Basin. However, typical transpression related structures, e.g., en echelon folds and flower structures, are not interpreted in the study area. The Triassic faults (FG 2) that were formed during T3-T4, were reactivated during this event (Figure 5-3).

7.2.5 Gravity tectonics (through the Triassic?)

In the Bedout Sub-basin, a large population of north-trending, west-dipping and large-displacement faults are interpreted to be developed in the Triassic. They display listric geometry and have consistent syn-sedimentary growth in the Triassic (Figure 5-13). These faults are conjectured to be at least partially controlled by gravity tectonics, which is attributed to the west-dipping detachment (Locker Shale), the embayment topography and the fluviodeltaic deposition background (Keraudren Formation).

7.3 Jurassic-Early Cretaceous Tectonostratigraphic Evolution

7.3.1 Early Jurassic carbonate dominated marine depositional system (Tectonically quiescent) (J-JP)

In the Northern Carnarvon Basin, the Early Jurassic (J-JP) is part of the syn-rift phase. However, the study area was tectonically quiescent in the Early Jurassic (J-JP) (Figure 7-1).

The deposition of carbonate-dominated Rankin Formation formed a northwesterly thinning sedimentary sheet.

7.3.2 Early-Middle Jurassic fluviodeltaic-related system (rift initiation-tectonically quiescence) (JP-JO)

In the Early-Middle Jurassic, the fluviodeltaic-related system (previous known Legendre Delta) was developed. Tectonically, the study area had experienced two phases: 1) Early (-Middle) Jurassic rift initiation and 2) Middle Jurassic (pre-Oxfordian) tectonic quiescence (Figure 7-1).

(1) Rift initiation phase

The rift processes in the study area initiated in the Early Jurassic. The structural development associated with the rift initiation includes the formation of the highly segmented Early Jurassic faults (FG 3), the northwest- plunging Huntsman Arch and the differential uplift and erosion in the northern Beagle Sub-basin. The rift initiation was likely related to the extension associated with east- directed Greater India drifting, which is demonstrated by the north-trending Early (-Middle) Jurassic faults (FG 3) in the Beagle Sub-basin (Figure 5-5) and outer Rowley Sub-basin (Figure 5-8). The structural development during the rift initiation was also controlled by pre-existing structures. The northwest- trending Early Jurassic faults (FG 3) on the northeast Exmouth Plateau (Figure 5-6) and southwest flank of the Rowley Sub-basin (Figure 5-7), the northwest- plunging Huntsman Arch (Figure 5-20) and the linear Early Jurassic uplift and erosion (Figure 5-5b, 5-9d) in the northern Beagle Sub-basin, all suggest that the underlying northwest- trending Triassic high and/or potential Palaeozoic structures exerted a dominant control on the structural grains.

The exact timing of the rift initiation is not fully controlled, due to the lack of a prominent unconformity across the study area. The only Early Jurassic angular unconformity, which was associated with the linear uplift and erosion in the northern Beagle Sub-basin (Figure 5-5b), is interpreted to correspond to the Pliensbachian horizon (JP). The Pliensbachian horizon (JP), for most of the study area, is interpreted as maximum flooding surface. The Early Jurassic faults (FG 3) in different sub-basins seemingly have slight different ages. In the northern Beagle Sub-basin (Figure 5-5), southwest of the Rowley Sub-basin (Figure 5-7) and on the northeast Exmouth Plateau (Figure 5-6), they have their upper tips located at or slightly above the Pliensbachian horizon, suggesting an Early Jurassic age. In the outer Rowley Sub-basin (Baxter-3D), they terminated at an intra-Middle Jurassic horizon (above JA) (Figure 5-8), thus have a Middle Jurassic age. The extent of the rift initiation also remains enigmatic, as Early Jurassic faults have not been recognized in the large northeast area of the Rowley Sub-basin (Curt-3D). Based on these observations, in conjunction with the fact that rift initiation in the

Northern Carnarvon Basin was in the Late Triassic, it is likely that the rift initiation on the North West Shelf has a northeasterly younging direction, and its influences attenuated in the similar direction and faded away in the northeast of the Rowley Sub-basin.

In the Middle Jurassic, after rift initiation and prior to the Argoland breakup in the Oxdordian, the study area experienced a period of tectonic quiescence (Figure 7-1).

(2) Development of a large fluviodeltaic-related system

A long-term phase of falling (or slightly stable) sea-level started simultaneously with the rift initiation since the Pliensbachian (JP), which led to the progradation of a large fluviodeltaic-related system. The sediments input by this system formed a northwest-progradational clastic shelf-slope clinoformal system (hundreds of meters high) in the Rowley Sub-basin (Curt-3D) and on the northeast Exmouth Plateau (WA484P-3D). Both of the two areas, from older to younger, underwent basin floor, shelf margin slope, marine shelf and fluviodeltaic plain deposition (Figure 6-2, 6-3). In the Rowley Sub-basin, a temporal transgression in the Early Jurassic formed a carbonate shelf ramp system, which is incorporated into a clastic shelf-slope-basin system. On the northeast Exmouth Plateau, the fluviodeltaic plain is absent, which is attributed to the erosion associated with the subsequent rift tectonics.

The early-stage deposition of the fluviodeltaic-related system was influenced by the rift initiation. The stratigraphic architecture of the Lower Jurassic shelf-slope succession was controlled by the Huntsman Arch in the southwest of Rowley Sub-basin and displays concave-outboard thickness contours (Figure 6-9).

Several types of depositional elements were formed in association with the development of the fluviodeltaic-related system, including: 1) a large population of channels associated with the fluviodeltaic plain in the Rowley Sub-basin, 2) a set of Middle Jurassic delta-scale subaqueous clinoforms developed at the shelf-slope transition in the Rowley Sub-basin, 3) two submarine channels developed on the slope and their associated gravity flow deposits in the basin, which are identified on the northeast Exmouth Plateau, 4) sands/muds filled slope gullies that were developed at multiple stratigraphic levels on the northeast Exmouth Plateau, 5) the Huntsman Arch controlled Lower Jurassic slumps developed in the Rowley Sub-basin and trigger-unknown shelf slumps on the northeast Exmouth Plateau (Figure 7-1).

The shelf-slope succession consists of several maximum flooding surface bounded parasequences, which suggests that the fluviodeltaic-related system was associated with multi-cyclic short-term waxing and waning of sediment inputs and/or short-term sea-level fluctuation. Each of the flooding surfaces recorded the waning of the sediment input and/or short-term transgression. The following waxing stage of sediment inputs and/or short-term

regression formed a strong sediment bypass on the shelf-slope transition and downlapping downslope and in the basin.

7.3.3 (Middle?) Late Jurassic-Early Cretaceous syn-extension system (continental drift) (JO-KV)

The period of Oxfordian-Valanginian was tectonically active for the region of North West Shelf. In the Oxfordian, Argoland started to drift in a northwest direction and formed the Argo Abyssal Plain. In the Valanginian, the Greater India-Australia breakup took place in an east-west direction. The extension associated with these two tectonic episodes formed the majority of the rift-related structures in the study area.

In the Bedout Sub-basin and central Beagle Sub-basin (Beagle-3D), north- trending faults (FG 4b) and the associated large rollover anticlines were formed in the Oxfordian, as a result of the reactivation of the Triassic gravity faults. Some of north- trending faults sustained their activities until the Valanginian.

In northern Beagle Sub-basin (CanningTQ-3D), the north- trending Early Jurassic faults (FG 3) formed in the rift initiation were reactivated and developed into larger faults of the same trends (FG 4c), forming a series of north- trending horsts and grabens. Simultaneous, a large population of the northeast- trending faults (FG 4a) were formed. These two sets of faults cut the area into rhombic-shaped compartments (Figure 5-9). A proportion of the northeast- (FG 4a) and north- (FG 4b) trending faults were active during the period of the Oxfordian-Valanginian.

On the northeast Exmouth Plateau (WA484P-3D), a large population of northeast- trending faults (FG 4a, Figure 5-11) were initially formed as a result of the northwest- directed extension generated by the Argoland drift, and most of them continued activities during the Oxfordian-Valanginian, due to extension of Greater India rifting.

In the southwest of the Rowley Sub-basin, the extension that was probably associated with the Greater India drifting reactivated the northwest- trending pre-existing structures in the area and formed a large number of northwest- trending faults (FG 4c) (Figure 5-16). Simultaneously, a small number of northeast- trending faults (FG 4a) were developed, which was likely related to the Argoland drifting (Figure 5-1). Due to the lack of sys-tectonic succession (JO-KV) in area, the timing of these faults are not well constrained. Comparing with faults in adjacent areas, -Oxfordian and Oxfordian-Valanginian are presumably the two age components.

Further to the northeast and the outboard of the Rowley Sub-basin, structures formed in this period are dominated by north-trending faults (FG 4b) (Figure 5-1). The development of these

north-trending faults in the northeast of the Rowley Sub-basin were restricted to the Oxfordian (Figure 5-15c), which are distinguished from their counterparts in other parts of the study area, which show both -Oxfordian and Oxfordian-Valanginian activities.

Several circular domes and elongate uplifts were developed in the period of Oxfordian-Valanginian, which was likely controlled by magma upwelling processes (Figure 5-18, 5-19).

Most of the study area in the outboard underwent significant erosion during the rift processes. On the northeast Exmouth Plateau (WA484P-3D), more than 2 km of the upper part of the fluviodeltaic-related succession was eroded on the central horst and formed a peneplaned unconformity (Figure 5-11, 6-2, 6-11). These eroded sediments were transported and re-deposited in the adjacent northeast- trending grabens on the Northern Slope. Several large-scale canyons, canyon-derived gravity flow deposits and a syn-tectonic fan lobe were developed (Figure 6-22, 6-23, 6-24). The syn-tectonic succession (JO-KV) is missing in the southwest of Rowley Sub-basin (Curt-3D), and several fault controlled seismically hard sheet-like bodies are present (6-12). Towards the northeast, the syn-tectonic succession is characterized by a northwesterly thickening wedge that consists of parallel low-amplitude reflections, which shows little syn-sedimentary faulting.

8 CONCLUSIONS

This study presents a comprehensive investigation into the tectonostratigraphic evolution of the Roebuck Basin and the northeast area of the Northern Carnarvon Basin. It has revealed a highly complex structural architecture that was a result of multiple tectonic events in the Palaeozoic, Triassic, Early Jurassic and Late Jurassic-Early Cretaceous. The main conclusions that can be drawn include:

(1) Both northwest- and northeast- trending rift structures were developed in the area, presumably in the Carboniferous-Early Permian.

(2) The latest Permian Bedout Movement in the area is characterized differential uplift and erosion, forming a prominent unconformity.

(3) The study area was tectonically active in the Triassic. From older to younger, structural development in the Triassic includes lava flows, formation of a bowl-shaped structure (a potential caldera), extensional faulting and differential uplift and erosion.

(4) The Early Jurassic was the rift initiation phase, which finally led to the India-Australia breakup in the Late Jurassic-Early Cretaceous. Structures formed during this phase include north- and northwest- trending small and segmented faults and the northwest-trending Huntsman Arch.

(5) The study area experienced a period of quiescence in the Middle Jurassic prior to the Oxfordian.

(6) In the Oxfordian, the northwest- directed Argoland drift presumably generated a population of northeast- trending ~Oxfordian faults. Interestingly, a large population north- trending faults were developed simultaneously.

(7) Both northeast- and north- trending ~Oxfordian faults were partially reactivated during the Oxfordian-Valanginian, under the extension associated with the east-directed India-Australia breakup.

(8) A population of northwest- trending faults were formed presumably during the Oxfordian-Valanginian, which was a result of oblique extension on the pre-existing northwest- trending structural fabrics.

(9) Several dome structures were formed during the Oxfordian-Valanginian and were potentially a result of magma upwelling.

(10) During the Pliensbachian-Oxfordian, a generally northwesterly progradational fluvial-marine shelf system was formed. It consists of a wide fluviodeltaic plain inputting sediments basinward, forming a set of shelf-slope-basin clinoforms.

(11) The early-stage deposition of shelf-slope succession was influenced by the rift initiation.

(12) Fluvial channel belts, delta-scale subaqueous clinoforms, submarine channels and associated gravity flows deposits, slope gullies and slump complexes are the major depositional elements that were developed in association with the fluvial-marine shelf system.

(13) During the rift tectonics in Oxfordian-Valanginian, the upper part of the fluvial-marine shelf succession was significantly eroded. The eroded sediments were transported through large subaqueous canyons and re-deposited as gravity flow deposits in the adjacent marine shale dominated grabens.

8.1 Recommendations for Future Work

The major findings of this study not only advance the understanding of the basin development history of the study area but also make clear a few potential research topics for the future.

(1) This study presents a Palaeozoic rift system, which is top bounded by a prominent unconformity (estimated in Early Permian age). In addition, a prominent base Triassic unconformity is also interpreted. In the south part of the Northern Carnarvon Basin, similar rift structures are top bounded by the base Triassic unconformity (McHarg et al., 2018). A detailed stratigraphic correlation from the Northern Carnarvon Basin to the Roebuck Basin along the edge of the Pilbara

Craton can better constrain the timing of the Palaeozoic rift and reveal the relationship between the Palaeozoic rifting and the Bedout Movement.

(2) The Triassic tectonics, from a regional context, is still mysterious. It is hoped that more studies that focus on the Triassic tectonics across the North West Shelf, can establish links to the Triassic structures interpreted in the study area, which can provide a better understanding of the regional Triassic tectonics.

(3) This study has revealed a northeast- younging and weakening direction of the rift initiation from the Northern Carnarvon Basin to the Roebuck Basin. The rift initiation in the Browse Basin and Bonaparte Basin remains unclear.

(4) There is still a large area that is not covered by 3D seismic surveys in the study area, structural interpretation of any 3D seismic data sets released in the future can reduce the uncertainties of the interpretation.

(5) Any additional data in the future, especially well constrains, are extremely useful for addressing the uncertainties of the interpretation and understanding the genesis of the irregular structures, e.g., bowl-shaped structure, syn-tectonic fan lobe and sheet-like bodies.

(6) The four circular domes seemingly form a chain. Do they suggest a hotspot, just as the Hawaii Island chain does?

9 REFERENCES

Adamson, K., S. Lang, N. Marshall, R. Seggie, N. Adamson, and K. Bann, 2013, Understanding the Late Triassic Mungaroo and Brigadier Deltas of the Northern Carnarvon Basin, North West Shelf, Australia, *in* M. Keep and S.J. Moss, ed., The Sedimentary Basins of Western Australia 4: Proceedings PESA Symposium, Perth, WA.

Adeogba, A. A., T. R. McHargue, and S. A. Graham, 2005, Transient fan architecture and depositional controls from near-surface 3-D seismic data, Niger Delta continental slope: AAPG bulletin, v. 89, p. 627-643.

AGSO Group, 1994, Deep reflections on the North West Shelf: changing perceptions of basin formation, *in* Purcell P.G. and R.R., ed., The Sedimentary Basins of Western Australia: Proceedings of the Western Australian Basins Symposium, Perth, WA, p. 63-76.

Al-Hinaai, J., and J. Redfern, 2014, The late Carboniferous basal Grant Group unconformity, Canning Basin, Australia: A complex surface recording glacial tectonic and halotectonic processes: Australian Journal of Earth Sciences, v. 61, p. 703-717.

Baillie, P., C. M. Powell, Z. Li, and A. Ryall, 1994, The tectonic framework of Western Australia's Neoproterozoic to Recent sedimentary basins, *in* Purcell P.G. and R.R., ed., The Sedimentary Basins of Western Australia: Proceedings of the Petroleum Exploration Society of Australia Symposium, Perth, WA, p. 62.

Bentley, J., 1988, The Candace Terrace-a geological perspective, *in* Purcell P.G. and R.R., ed., The North West Shelf, Australia: Proceedings of Petroleum Exploration Society Australia Symposium, Perth.

Black, M., K. McCormack, C. Elders, and D. Robertson, 2017, Extensional fault evolution within the Exmouth Sub-basin, North West Shelf, Australia: Marine and Petroleum Geology, v. 85, p. 301-315.

Bradshaw, J., J. Sayers, M. Bradshaw, R. Kneale, C. Ford, L. Spencer, and M. Lisk, 1998, Palaeogeography and its impact on the petroleum systems of the North West Shelf, Australia, *in* Purcell P.G. and R.R., ed., The Sedimentary Basins of Western Australia 2: Proceedings of Petroleum Exploration Society of Australia Symposium, Perth, WA, p. 95-121.

Bradshaw, M., A. Yeates, R. Beynon, A. Brakel, R. Langford, J. Totterdell, and M. Yeung, 1988, Palaeogeographic evolution of the North West Shelf Region, *in* Purcell P.G. and R.R., ed., The North West Shelf, Australia: Proceedings of Petroleum Exploration Society Australia Symposium, Perth, p. 29-54.

Carnarvon Petroleum Ltd, 2018, Dorado Contingent Resources, https://www.carnarvon.com.au/.

Cartwright, J., D. James, and A. Bolton, 2003, The genesis of polygonal fault systems: a review: Geological Society, London, Special Publications, v. 216, p. 223-243.

Clark, J., N. Kenyon, and K. Pickering, 1992, Quantitative analysis of the geometry of submarine channels: implications for the classification of submarine fans: Geology, v. 20, p. 633-636.

Colwell, J., and H. Stagg, 1994, Structure of the Offshore Canning Basin: First impressions from the new regional seep-seismic data set: the sedimentary basins of Western Australia: Proceedings of Petroleum Exploration society Australia symposium, Perth, p. 757-768.

Cross, N. E., A. Cunningham, R. J. Cook, A. Taha, E. Esmaie, and N. El Swidan, 2009, Three-dimensional seismic geomorphology of a deep-water slope-channel system: The Sequoia field, offshore west Nile Delta, Egypt: AAPG bulletin, v. 93, p. 1063-1086.

Davies, R. J., and M. T. Ireland, 2011, Initiation and propagation of polygonal fault arrays by thermally triggered volume reduction reactions in siliceous sediment: Marine Geology, v. 289, p. 150-158.

Davis, W. M., 1902, Baselevel, grade and peneplain: The Journal of Geology, v. 10, p. 77-111.

Edwards, D., and J. Zumberge, 2005, The Oils of Western Australia II: Regional Petroleum Geochemistry and Correlation of Crude Oils and Condensates from Western Australia and Papua New Guinea, Geoscience Australia. Retrieved August 12, 2017 from https://data.gov.au/dataset/305d506f-cfa3-4792-b1af-3ad14bc70b6c.

Elders, C., S. McHarg, and A. I'Anson, 2016, Fault Geometry and Deformation History, Northern Carnarvon Basin: ASEG Extended Abstracts, v. 2016, p. 1-3.

Ercole, C., L. Gibbons, and K. Ghori, 2003, Prospects and leads, central Canning Basin, Western Australia, Petroleum Division, Department of Industry and Resources, Western Australia, from http://www.dmp.wa.gov.au.

Forman, D. J., D. W. Wales, and R. V. Burne, 1981, Geological evolution of the Canning Basin, Western Australia, *in* G.M.Bladon, ed., Department of National Development and Energy, Bereau of Mineral Resources, Geology and Geophysics, Bulletin 210, Canberra, Australian Government Pub. Service.

Frankowicz, E., and K. McClay, 2010, Extensional fault segmentation and linkages, Bonaparte Basin, outer North west shelf, Australia: AAPG bulletin, v. 94, p. 977-1010.

Fullerton, L. G., W. W. Sager, and D. W. Handschumacher, 1989, Late Jurassic - Early Cretaceous evolution of the eastern Indian Ocean adjacent to northwest Australia: Journal of Geophysical Research: Solid Earth, v. 94, p. 2937-2953.

Galloway, W. E., 1989, Genetic stratigraphic sequences in basin analysis I: architecture and genesis of flooding-surface bounded depositional units: AAPG bulletin, v. 73, p. 125-142.

Gartrell, A., J. Torres, M. Dixon, and M. Keep, 2016, Mesozoic rift onset and its impact on the sequence stratigraphic architecture of the Northern Carnarvon Basin: The APPEA Journal, v. 56, p. 143-158.

Gibbons, A. D., 2012, Regional plate tectonic reconstructions of the Indian Ocean, PhD Thesis, University of Sydney.

Gibbons, A. D., U. Barckhausen, P. den Bogaard, K. Hoernle, R. Werner, J. M. Whittaker, and R. D. Müller, 2012, Constraining the Jurassic extent of Greater India: Tectonic evolution of the West Australian margin: Geochemistry, Geophysics, Geosystems, v. 13, p. Q05W13.

Gorter, J., 1996, Speculation on the origin of the Bedout High—a large circular structure of pre-Mesozoic age in the offshore Canning Basin, Western Australia: PESA News, p. 32-33.

Gorter, J., P. Jones, R. Nicoll, and C. Golding, 2005, A reappraisal of the Carboniferous stratigraphy and the petroleum potential of the southeastern Bonaparte Basin (Petrel Sub-basin), northwestern Australia: The APPEA Journal, v. 45, p. 275-296.

Goulty, N., 2008, Geomechanics of polygonal fault systems: a review: Petroleum Geoscience, v. 14, p. 389-397.

Gradstein, F., and J. Ludden, 1992, Radiometric age determinations for basement from Sites 765 and 766, Argo Abyssal Plain and northwestern Australian margin: Proceedings of the ocean drilling program, Scientific Results, p. 557-559.

Gunn, P., 1988, Bonaparte Basin: evolution and structural framework, *in* Purcell P.G. and R.R., ed., The North West Shelf, Australia: Proceedings of Petroleum Exploration Society Australia Symposium, Perth.

Haig, D. W., E. McCartain, A. J. Mory, G. Borges, V. I. Davydov, M. Dixon, A. Ernst, S. Groflin, E. Håkansson, and M. Keep, 2014, Postglacial Early Permian (late Sakmarian–early Artinskian) shallow-marine carbonate deposition along a 2000km transect from Timor to west Australia: Palaeogeography, Palaeoclimatology, Palaeoecology, v. 409, p. 180-204.

Harrowfield, M., G. R. Holdgate, C. J. Wilson, and S. McLoughlin, 2005, Tectonic significance of the Lambert Graben, East Antarctica: reconstructing the Gondwanan rift: Geology, v. 33, p. 197-200.

Haughton, P., C. Davis, W. McCaffrey, and S. Barker, 2009, Hybrid sediment gravity flow deposits–classification, origin and significance: Marine and petroleum geology, v. 26, p. 1900-1918.

Helland-Hansen, W., R. J. Steel, and T. O. Sømme, 2012, Shelf genesis revisited: Journal of Sedimentary Research, v. 82, p. 133-148.

Helland‐Hansen, W., and G. Hampson, 2009, Trajectory analysis: concepts and applications: Basin Research, v. 21, p. 454-483.

Hocking, R. M., 2008, Paleozoic Geology of the Canning Basin: A Field Guide, Department of Industry and Resources, from http://www.dmp.wa.gov.au/Geological-Survey/Premium-GSWA-Publications-1537.aspx.

Hocking, R. M., A. J. Mory, and I. R. Williams, 1994, An atlas of Neoproterozoic and Phanerozoic basins of Western Australia: The Sedimentary Basins of Western Australia: Proceedings of the Petroleum Exploration Society of Australia Symposium, Perth, p. 21-43.

Horstman, E., and P. Purcell, 1988, The offshore Canning Basin-a review: The North West Shelf, Australia: Proceedings of the Petroleum Exploration Society of Australia, Perth, p. 253-257.

Hurst, A., J. Cartwright, D. Duranti, M. Huuse, and M. Nelson, 2005, Sand injectites: an emerging global play in deep-water clastic environments: Geological Society, London, Petroleum Geology Conference series, p. 133-144.

Hurst, A., A. Scott, and M. Vigorito, 2011, Physical characteristics of sand injectites: Earth-Science Reviews, v. 106, p. 215-246.

Hurst, A., and M. Vigorito, 2017, Saucer-shaped sandstone intrusions: An underplayed reservoir target: AAPG Bulletin, v. 101, p. 625-633.

Huuse, M., C. A. L. Jackson, P. Van Rensbergen, R. J. Davies, P. B. Flemings, and R. J. Dixon, 2010, Subsurface sediment remobilization and fluid flow in sedimentary basins: an overview: Basin Research, v. 22, p. 342-360.

Iasky, R. P., A. Mory, K. Ghori, and S. Shevchenko, 1998a, Structure and petroleum potential of the southern Merlinleigh Sub-basin, Carnarvon Basin, Western Australia, v. 61, p. 63.

Iasky, R. P., A. J. Mory, and S. I. Shevchenko, 1998b, A structural interpretation of the Gascoyne Platform, southern Carnarvon Basin, WA: Geological Survey of Western Australia Perth, v. 61, p. 589-598.

Jackson, M., J. Kennard, and M. Moffat, 1993, Canning Basin project Stage 1, Lennard Shelf: Explanatory notes and map folios: Australian Geological Survey Organisation Record, v. 1.

Jitmahantakul, S., and K. McClay, 2013, Late Triassic – Mid-Jurassic to Neogene Extensional Fault Systems in the Exmouth Sub-Basin, Northern Carnarvon Basin, North West Shelf, Western Australia, *in* Keep M. and Moss S.J., ed., The sedimentary basins of Western Australia IV: Proceedings of the Petroleum Exploration Society of Australia Symposium: Perth, Petroleum Exploration Society of Western Australia, Perth, WA, p. 1-22.

Keep, M., A. Bishop, and I. Longley, 2000, Neogene wrench reactivation of the Barcoo Sub-basin, northwest Australia: implications for Neogene tectonics of the northern Australian margin: Petroleum Geoscience, v. 6, p. 211-220.

Keep, M., M. Harrowfield, and W. Crowe, 2007, The Neogene tectonic history of the North West Shelf, Australia*: Exploration Geophysics, v. 38, p. 151-174.

Kennard, J., M. Jackson, K. Romine, R. Shaw, and P. Southgate, 1994, Depositional sequences and associated petroleum systems of the Canning Basin, WA: The Sedimentary Basins of Western Australia: Proceedings of the Western Australian Basins Symposium, Perth, WA, PESA, p. 657-676.

Kolla, V., P. Bourges, J.-M. Urruty, and P. Safa, 2001, Evolution of deep-water Tertiary sinuous channels offshore Angola (west Africa) and implications for reservoir architecture: AAPG bulletin, v. 85, p. 1373-1405.

Langhi, L., and G. D. Borel, 2005, Influence of the Neotethys rifting on the development of the Dampier Sub-basin (North West Shelf of Australia), highlighted by subsidence modelling: Tectonophysics, v. 397, p. 93-111.

Lech, M. E., 2013, New Observations of the Post-Triassic Succession in the Central Beagle Sub-basin, Northern Carnarvon Basin, North West Shelf, Australia: The Sedimentary Basins of Western Australia IV: Proceedings of the Petroleum Exploration Society of Australia Symposium, Perth, WA, p. 24.

Lee, H. J., J. Locat, P. Desgagnés, J. D. Parsons, B. G. McAdoo, D. L. Orange, P. Puig, F. L. Wong, P. Dartnell, and E. Boulanger, 2007, Submarine mass movements on continental margins: Continental margin sedimentation: from sediment transport to sequence stratigraphy, p. 213-274.

Lipski, P., 1994, Structural framework and depositional history of the Bedout and Rowley Sub-basins: the sedimentary basins of Western Australia. Proceedings of the West Australian basins symposium, Petroleum Exploration society of Australia, Perth, p. 14-17.

Lonergan, L., N. Lee, H. D. Johnson, J. A. Cartwright, and R. J. Jolly, 2000, Remobilisation and injection in deepwater depositional systems: Implications for reservoir architecture and prediction, *in* Weimer P., Slatt R.M., Coleman J., Rosen N.C., Nelson H., Bouma A.H., Styzen M.J. and Lawrence D.T., ed., GCSSEPM Foundation 20th Annual Research Conference Deep-Water Reservoirs of the World, Houston, p. 515-532.

Longley, I., C. Buessenschuett, L. Clydsdale, C. Cubitt, R. Davis, M. Johnson, N. Marshall, A. Murray, R. Somerville, and T. Spry, 2002, The North West Shelf of Australia–a Woodside perspective, *in* M. Keep and S.J. Moss, ed., The Sedimentary Basins of Western Australia 3: Proceedings of the Petroleum Exploration Society of Australia Symposium, Perth, WA, p. 27-88.

MacNeill, M., N. Marshall, and C. McNamara, 2018, New Insights into a major Early-Middle Triassic Rift Episode in the NW Shelf of Australia: ASEG Extended Abstracts, v. 2018, p. 1-5.

Marshall, N., and S. Lang, 2013, A new sequence stratigraphic framework for the North West Shelf, Australia, *in* M. Keep and S.J. Moss, ed., The Sedimentary Basins of Western Australia 4: Proceedings PESA Symposium, Perth, WA, p. 1-32.

McClay, K., N. Scarselli, and S. Jitmahantakul, 2013, Igneous intrusions in the Carnarvon Basin, NW Shelf, Australia, *in* M. Keep and S.J. Moss, ed., The sedimentary basins of Western Australia IV: Proceedings of the Petroleum Exploration Society of Australia Symposium: Perth, Petroleum Exploration Society of Western Australia, Perth, WA, p. 1-20.

McCormack, K., and K. McClay, 2013, Structural architecture of the Gorgon Platform, North West Shelf, Australia, *in* M. Keep and S.J. Moss, ed., The Sedimentary Basins of Western Australia IV: Proceedings of the Petroleum Exploration Society of Australia Symposium, Perth, WA, p. 1-24.

McCormack, K., and K. McClay, 2018, Orthorhombic faulting in the Beagle Sub-basin, North West Shelf, Australia: Geological Society, London, Special Publications, v. 476, p. SP476. 3.

McGee, R., J. Goodall, and S. Molyneux, 2017, A re-evaluation of the Lower to Middle Triassic on the Candace Terrace, Northern Carnarvon Basin: The APPEA Journal, v. 57, p. 263-276.

McHarg, S., A. I'Anson, and C. Elders, 2018, The Permian and Carboniferous extensional history of the Northern Carnarvon Basin and its influence on Mesozoic extension: ASEG Extended Abstracts, v. 2018, p. 1-8.

McHargue, T., M. J. Pyrcz, M. D. Sullivan, J. Clark, A. Fildani, B. Romans, J. Covault, M. Levy, H. Posamentier, and N. Drinkwater, 2011, Architecture of turbidite channel systems on the continental slope: patterns and predictions: Marine and Petroleum Geology, v. 28, p. 728-743.

Metcalfe, I., 1999, Gondwana dispersion and Asian accretion: an overview: Gondwana dispersion and Asian accretion, p. 9-28.

Metcalfe, I., 2013, Gondwana dispersion and Asian accretion: tectonic and palaeogeographic evolution of eastern Tethys: Journal of Asian Earth Sciences, v. 66, p. 1-33.

Molyneux, S., J. Goodall, R. McGee, G. Mills, and B. Hartung-Kagi, 2016, Observations on the Lower Triassic petroleum prospectivity of the offshore Carnarvon and Roebuck basins: The APPEA Journal, v. 56, p. 173-202.

Mory, A., J. Redfern, and J. Martin, 2008, A review of Permian–Carboniferous glacial deposits in Western Australia: Geological Society of America Special Papers, v. 441, p. 29-40.

Mulder, T., and J. Alexander, 2001, The physical character of subaqueous sedimentary density flows and their deposits: Sedimentology, v. 48, p. 269-299.

Müller, R., A. Goncharov, and A. Kritski, 2005, Geophysical evaluation of the enigmatic Bedout basement high, offshore northwestern Australia: Earth and Planetary Science Letters, v. 237, p. 264-284.

Nicoll, R. S., J. R. Laurie, A. P. Kelman, D. J. Mantle, P. W. Haines, A. J. Mory, and R. M. Hocking, 2009, Canning Basin Biozonation and Stratigraphy: Geoscience Australia.

Nosiara, M., and J. Groombridge, 1983, La Grange-1 Well Completion Report-Interpretative Data, *in* W. A. Department of Mines and Petroleum, ed., Petroleum & Geothermal

Information Management System, from https://wapims.dmp.wa.gov.au/WAPIMS/Search/WellDetails

O'Halloran, G., C. Paschke, C. Dempsey, C. Hurren, R. Scott, and G. Liu, 2018, Evolution of "Tres Hombres"-A Mid-crustal Dome Structure within the Jurassic Northern Beagle Sub-basin Western Australia: An Integrated Geophysical Investigation: ASEG Extended Abstracts, v. 2018, p. 1-6.

Osborne, D., 1994, Nebo oil discovery, Beagle Sub-basin, *in* Purcell P.G. and R.R., ed., The sedimentary basins of Western Australia: West Australian Basins Symposium, Perth WA, p. 653-654.

Paschke, C., G. O'Halloran, and C. Dempsey, 2018, Interpretation of a Permian conjugate basin margin preserved on the outer Northwest Shelf of Australia: ASEG Extended Abstracts, v. 2018, p. 1-8.

Patruno, S., G. J. Hampson, and C. A. Jackson, 2015a, Quantitative characterisation of deltaic and subaqueous clinoforms: Earth-Science Reviews, v. 142, p. 79-119.

Patruno, S., G. J. Hampson, C. A. L. Jackson, and T. Dreyer, 2015b, Clinoform geometry, geomorphology, facies character and stratigraphic architecture of a sand‐rich subaqueous delta: Jurassic Sognefjord Formation, offshore Norway: Sedimentology, v. 62, p. 350-388.

Phillips, J. D., 2002, Erosion, isostatic response, and the missing peneplains: Geomorphology, v. 45, p. 225-241.

Pirmez, C., R. Beaubouef, S. Friedmann, and D. Mohrig, 2000, Equilibrium profile and baselevel in submarine channels: examples from Late Pleistocene systems and implications for the architecture of deepwater reservoirs: Global deep-water reservoirs: Gulf Coast Section SEPM Foundation 20th Annual Bob F. Perkins Research Conference, p. 782-805.

Powell, C. M., S. Roots, and J. Veevers, 1988, Pre-breakup continental extension in East Gondwanaland and the early opening of the eastern Indian Ocean: Tectonophysics, v. 155, p. 261-283.

Ramsay, D., and N. Exon, 1994, Structure and tectonic history of the northern Exmouth Plateau and Rowley Terrace: outer North West Shelf: Journal of Australian Geology and Geophysics, v. 15, p. 55-70.

Rattigan, J., 1967, Fold and fracture patterns resulting from basement wrenching in the Fitzroy Depression, Western Australia, Proceedings-Australasian Institute of Mining and Metallurgy, Melbourne, p. 17-22.

Reeckmann, S., and A. Mebberson, 1984, Igneous intrusions in the north-west Canning Basin and their impact on oil exploration: The Canning Basin, WA, p. 389-399.

Renne, P. R., H. J. Melosh, K. A. Farley, W. U. Reimold, C. Koeberl, M. R. Rampino, S. P. Kelly, and B. A. Ivanov, 2004, Is Bedout an impact crater? Take 2: Science, v. 306, p. 610-611.

Rohrman, M., 2013, Intrusive large igneous provinces below sedimentary basins: An example from the Exmouth Plateau (NW Australia): Journal of Geophysical Research: Solid Earth, v. 118, p. 4477-4487.

Saller, A. H., J. T. Noah, A. P. Ruzuar, and R. Schneider, 2004, Linked lowstand delta to basin-floor fan deposition, offshore Indonesia: An analog for deep-water reservoir systems: AAPG bulletin, v. 88, p. 21-46.

Saqab, M. M., and J. Bourget, 2015, Structural style in a young flexure-induced oblique extensional system, north-western Bonaparte Basin, Australia: Journal of Structural Geology, v. 77, p. 239-259.

Shaw, R. D., M. J. Sexton, and I. Zeilinger, 1994, The tectonic framework of the Canning Basin, WA, including 1: 2 million structural elements map of the Canning Basin, Australian Geological Survey Organisation Record 1994/48, 89p.

Smith, J. G., 1968, Tectonics of the Fitzroy wrench trough, Western Australia: American Journal of Science, v. 266, p. 766-776.

Smith, S., P. Tingate, C. Griffiths, and J. Hull, 1999, Petroleum systems and frontiers-The structural development and petroleum potential of the Roebuck Basin: APPEA Journal-Australian Petroleum Production and Exploration Association, v. 39, p. 364-385.

Smith, S. A., 1999, The Phanerozoic basin-fill history of the Roebuck Basin, PhD Thesis, University of Adelaide.

Stagg, H., and J. Colwell, 1994, The structural foundations of the Northern Carnarvon Basin: The sedimentary basins of Western Australia: Proceedings of Petroleum Exploration Society of Australia Symposium, Perth, p. 349-365.

Stevenson, C. J., C. A.-L. Jackson, D. M. Hodgson, S. M. Hubbard, and J. T. Eggenhuisen, 2015, Deep-water sediment bypass: Journal of Sedimentary Research, v. 85, p. 1058-1081.

Struckmeyer, H. I., K. Baxter, J. E. Blevin, and D. L. Cathro, 1997, Palaeozoic rift basin evolution in the Browse Basin, Northwest Shelf: Petroleum Exploration Society of Australia, v. 27, p. 62.

Struckmeyer, H. I., J. E. Blevin, J. Sayers, J. M. Totterdell, K. Baxter, D. L. Cathro, P. Purcell, and R. Purcell, 1998, Structural evolution of the Browse Basin, North West Shelf: new concepts from deep-seismic data: The Sedimentary Basins of Western Australia 2: Proceedings of the Petroleum Exploration Society of Australia Symposium, Perth, p. 345-367.

Sturrock, V., 2007, Huntsman 1 Well Completion Report-Interpretative Data, *in* W. A. Department of Mines and Petroleum, ed., Petroleum & Geothermal Information Management System. Retrieved September 12, 2017, from https://wapims.dmp.wa.gov.au/WAPIMS/Search/WellDetails

Szarawarska, E., M. Huuse, A. Hurst, W. De Boer, L. Lu, S. Molyneux, and P. Rawlinson, 2010, Three-dimensional seismic characterisation of large-scale sandstone intrusions in the lower Palaeogene of the North Sea: completely injected vs. in situ remobilised sandbodies: Basin Research, v. 22, p. 517-532.

Talling, P. J., L. A. Amy, and R. B. Wynn, 2007, New insight into the evolution of large‐volume turbidity currents: comparison of turbidite shape and previous modelling results: Sedimentology, v. 54, p. 737-769.

Talling, P. J., D. G. Masson, E. J. Sumner, and G. Malgesini, 2012, Subaqueous sediment density flows: Depositional processes and deposit types: Sedimentology, v. 59, p. 1937-2003.

Totterdell, J. M., L. Hall, T. Hashimoto, K. Owen, and M. T. Bradshaw, 2014, Petroleum Geology Inventory of Australia's Offshore Frontier Basins, Reccord 2014/09, Geoscience Australia, Canberra, from http://dx.doi.org/10.11636/Record.2014.009.

Vincent, P., and L. Tilbury, 1988, Gas and Oil Fields of the Rankin Trend and Northern Barrow-Dampier Sub-Basin, *in* Purcell P.G. and R.R., ed., The North West Shelf,

Australia: Proceedings of Petroleum Exploration Society Australia Symposium, Perth, p. 341-369.

Von Rad, U., N. F. Exon, and B. U. Haq, 1992, Rift-to-Drift History of the Wombat Plateau, North West Australia: Triassic to Tertiary Leg 122 Results: Proceedings of the Ocean Drilling Program, Scientific Result, v. 122, p. 765-800.

Wales, D., and D. Forman, 1981, Geological evolution of the Canning Basin, Western Australia, *in* G.M.Bladon, ed., Department of National Development and Energy, Bereau of Mineral Resources, Geology and Geophysics, Bulletin 210, Canberra, Australian Government Pub. Service.

Watterson, J., J. Walsh, A. Nicol, P. Nell, and P. Bretan, 2000, Geometry and origin of a polygonal fault system: Journal of the Geological Society, v. 157, p. 151-162.

Yeates, A., M. Bradshaw, J. Dickins, A. Brakel, N. Exon, R. Langford, S. Mulholland, J. Totterdell, and M. Yeung, 1987, The Westralian superbasin: an Australian link with Tethys: International symposium on Shallow Tethys 2, p. 199-213.

Zhan, Y., and A. Mory, 2013, Structural interpretation of the northern Canning Basin, western Australia, *in* M. Keep and S.J. Moss, ed., The Sedimentary Basins of Western Australia 4: Proceedings PESA Symposium, Perth, WA.